VOLUME 49, NUMBER 10

October, 1961

published monthly by The Institute of Radio Engineers, Inc.

Proceedings of the IRE®

contents

COVER

A single-sideband system that is compatible with AM was modulated by white noise to produce this panoramic picture. It shows how the spectrum is confined essentially within the lower sideband. The system is described on page 1503.

published monthly by The Institute of Radio Engineers, Inc.

Proceedings of the IRE®

continued

PROCEEDINGS OF THE IRE, published monthly by The Institute of Radio Engineers, Inc., at 1 East 79 Street, New York 21, N. Y. Manuscripts should be submitted in triplicate to the Editorial Department. Correspondence column items should not exceed four double-spaced pages (illustrations count as one-half page each). Responsibility for contents of papers published rests upon the authors, and not the IRE or its members. All republication rights, including translations, are reserved by the IRE and granted only on request. Abstracting is permitted with mention of source.

Thirty days advance notice is required for change of address. Price per copy: members of the Institute of Radio Engineers, one additional copy $1.25; non-members $2.25. Yearly subscription price: to members $9.00, one additional subscription $13.50; to non-members in United States, Canada, and U. S. Possessions $18.00; to non-members in foreign countries $19.00. Second-class postage paid at Menasha, Wisconsin, under the act of March 3, 1879. Acceptance for mailing at a special rate of postage is provided for in the act of February 28, 1925, embodied in Paragraph 4, Section 412, P. L. and R., authorized October 26, 1927. Printed in U.S.A.

October, 1961
Vol. 49 No. 10

Proceedings of the IRE

Poles and Zeros

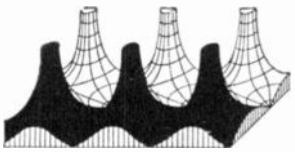

E&A-ECPD. These symbols stand for the Education and Accreditation Committee of the Engineers Council for Professional Development. In July, 1961, Poles and Zeros announced IRE's membership in ECPD and discussed briefly the ECPD committee structure. The Education and Accreditation Committee is of such significance that it seemed appropriate to single it out for detailed discussion on this page. In order to provide the most accurate and precise information about the committee, the Editor invited the committee's chairman to prepare a statement descriptive of its activities for Poles and Zeros.

Newman A. Hall, Chairman of the Department of Mechanical Engineering at Yale University, is the Chairman of the ECPD E&A Committee, and he has graciously accepted the Editor's invitation to prepare for IRE readers the story of the responsibilities and activities of his committee. For the material to follow, IRE and the Editor express their thanks to Professor Hall.

"The addition of the IRE as one of the constituent members of ECDP brings with it the obligation and opportunity to participate in one of its most significant activities, the Education and Accreditation Committee. In the total responsibility of ECPD in the professional development of the engineer, this committee plays the central role of maintaining contact with the institutions which provide the formal education of the engineer. It has the responsibility of speaking for the profession in matters of educational standards and of developing and administering criteria so that a reliable and meaningful program of accreditation of engineering schools can be carried forward.

"The establishment of accreditation criteria and an associated inspection program for engineering schools was one of the earliest formal programs of ECPD. The basic criteria were agreed upon in 1933 and, during the period 1936 to 1938, the initial program of accreditation was completed. During the war, the inspections of curricula were largely suspended and, on resumption afterwards, it was observed that a much more adequate base for conducting accreditation was needed. While the earlier Hammond Reports of 1940 and 1944 on the aims of engineering curricula led the way for changes which were taking place, a more extensive review was in order. Consequently, following a 1951 ECPD recommendation, ASEE instituted a study which resulted in the 1955 report on The Evaluation of Engineering Education. With this available, ECPD adopted in 1955 a set of additional criteria for accreditation which, together with the original bases, have since guided the recommendations of the Education and Accreditation Committee. These standards which the committee administers are designed to accommodate and encourage flexibility and creative development in engineering education, yet they are sufficiently incisive to insure that minimum requirements are significant.

"The membership of the Education and Accreditation Committee is representative of all the constituent societies of ECPD, including IRE. Great care is taken not only to insure that the committee is broadly familiar with various technical fields of engineering, but more significantly, that the individual members may be in a position, on the basis of their own experience in engineering education and good judgment, to counsel educational institutions wisely. Members in all cases are selected from individuals who have had experience as inspectors on accreditation teams, and it is the responsibility of each constituent society to insure that an adequate corps of representative, well-informed inspectors is available to the committee.

"Each accreditation inspection is organized by a member of the E&A Committee who serves as chairman. He is responsible for making arrangements with the institution, selecting inspectors from approved lists, supervising the inspection, including various conferences with administrative officials, and assembling and transmitting reports and recommendations to the E&A Committee for action. The final accreditation decision is made by ECPD itself, giving due consideration to the recommendations of the E&A Committee.

"A responsibility is accepted, not only to insure that minimum standards are maintained by the engineering schools, but increasingly in recent years there has been an effort to provide constructive assistance to the institutions in their constant efforts to improve the quality of their educational program. With the introduction of new principles and concepts into engineering practice, and with new proven methods of training engineers always becoming available, this service can be one of the most important provided by the committee.

"In order for such broad services to be possible, a very close relation must be maintained between the constituent societies and the committees. This is accomplished very effectively by the informal contacts provided by the membership of the committee in the several societies. Generally, the members are selected from those already very active in education and society affairs.

"With the addition of new organizations to ECPD, the scope of responsibility is broadened. The increased diversity in technical areas and operating levels in the engineering team effort constantly enlarges the area of concern. The goal of the committee is to effectively encompass all of these demands and to provide the maximum service to the profession."

—F. H., Jr.

Daniel E. Noble

Director, 1961

Daniel E. Noble (A'25–SM'44–F'47) was born in Naugatuck, Conn., on October 4, 1901. He graduated from Connecticut State College, Storrs, and supplemented his studies with additional work at Harvard Summer School and at M.I.T., both at Cambridge, Mass. An honorary D.Sc. degree was conferred upon him in 1957 by Arizona State College at Tempe. He taught mathematics and electrical engineering subjects for seventeen years before he joined Motorola, Inc. in 1940, as Director of Research. Before leaving the University of Connecticut, he pioneered FM radio broadcast and mobile radio development work and, as consultant to the Connecticut State Police, he was responsible for the design and development of the first statewide two-way mobile radio communications state police system and the first FM system. With Motorola, he advanced over the years to General Manager of the Communications and Electronics Division, to Vice President and Director of the corporation, and, finally, to his present assignment as Director and Executive Vice President in charge of the three Motorola Divisions dealing with communications, semiconductor and military electronics products. While Manager of the Communications Division of Motorola, he directed the development of equipment improvements which paced the universal changeover of land mobile radio systems from AM to FM. He particularly emphasized engineering effort directed to the solution of the problems related to the need for substantial increases in the efficiency of spectrum utilization.

With the announcement of the invention of the junction transistor, his interest turned to the semiconductor and solid state electronics fields as the most promising areas for corporate expansion. He initiated programs of transistor circuitry research and transistor applications in the Communications and Military Electronics Divisions, and established the corporate semiconductor research organization, which was later expanded into the Motorola Semiconductor Products Division. He also organized the Solid State Electronics Department which extended the research into the areas of specialized solid state devices, integrated circuits, and informational processing and controls.

Mr. Noble has served either as Chairman or as a member of many industry and professional technical and advisory committees, including the Radio Technical Planning Board (Chairman of Panel 13), and the National Color Television Systems Committee. He holds three patents on electronic devices, and he has published technical articles and papers dealing with the general problems relating to the development of effective and reliable equipment. He is a member of the Board of Directors of Arizona State University Foundation, and Chairman of the Foundation Advisory Committee on Engineering and Science Education. He is also a member of the Army Scientific Advisory Panel.

Scanning the Issue

Time-Varying Networks, I (Zadeh, p. 1488)—It has been the practice of the PROCEEDINGS to publish from time to time review and tutorial articles by leading authorities on subjects in which important progress has recently been made. Earlier this year the Editorial Board of the IRE set into motion a program for stepping up the frequency with which these articles appear. This paper was suggested for this program by the Professional Group on Circuit Theory and represents the first fruit of the Editorial Board's efforts. It deals with a subject about which very little was written prior to 1950. The past decade, however, has seen a host of technological developments that have given rise to problems involving the analysis and synthesis of time-varying systems. By way of example one could mention the advent of Wiener's theory, missile guidance techniques, parametric amplification, scatter communication, detection of fluctuating targets, communication via satellites, and many more. Presented here is Part I of an excellent two-part survey of some of the significant and lesser known contributions to time-varying-network theory that have been made in the U. S. and abroad during the past ten years.

Compatible Single Sideband (Kahn, p. 1503)—Due to the ever-increasing congestion of the radio frequency spectrum there has been widespread interest in recent years in single-sideband communication techniques. Indeed, interest in SSB reached such a level that the PROCEEDINGS devoted a special issue to the subject in December, 1956. Meanwhile, in August of that year, a new SSB system was quietly being installed at the U. S. Voice of America station in Munich, Germany. The new system was unique in that it did not require special SSB receivers. The broadcasts could be satisfactorily received with conventional AM broadcast receivers. In the five years that have intervened, the Compatible Single Sideband (CSSB) system has been the center of considerable controversy—controversy that has reached the pages of the PROCEEDINGS on two occasions. Questions were raised as to whether a CSSB wave with a distortion-free envelope could reproduce speech and music with adequate fidelity without generating an appreciable amount of undesired sideband radiation. These discussions arose largely because the full details of the system had never been disclosed for proprietary reasons. In the meantime, the CSSB system was installed and tested at five AM broadcast stations in the U. S. as well as at various government and aeronautical installations in a number of countries. The author has now set down a detailed description, explanation, and experimental evaluation of the CSSB system. This paper, then, represents an eagerly awaited first public disclosure of an important new single-sideband system that has been the subject of much interest and discussion among a wide circle of engineers in the broadcast and communications field.

Magnetic Circuits Employing Ceramic Magnets (Helmer, p. 1528)—Ceramic magnets are characterized by the fact that they have a fixed magnetization and a permeability equal approximately to that of free space. These properties lead to an interesting simplification of the field equations, a simplification which makes it readily possible for a device designer to design magnetic circuits to his own specifications rather than relying on a magnet manufacturer for the design. The author analyzes several types of magnetic circuits, including novel ceramic-steel and ceramic-iron configurations, and develops a method of optimizing their design. The paper could well be called semitutorial since, in addition to formulating design criteria, it brings a not-well-understood subject within ready grasp of applications people.

Electron-Trigonometry—A New Tool for Electron-Optical Design (Schlesinger, p. 1538)—The designing of an electron-optical system is basically a problem of predicting the size and position of electron images. Unfortunately, in most situations of practical interest it is not a problem that can be readily described or easily and directly solved mathematically. The designer, therefore, usually must resort to indirect analog techniques or tedious graphical methods of tracing principal trajectories, or analyze the problem with a computer in a way that, while it gives a specific answer, provides no insight into design relationships. In this paper the author develops a new method in which axial potential distributions of an electron-optical system are approximated by segments that are either linear or parabolic. This approach reduces the problem to trigonometric relationships that are not only simpler to handle but more direct than present methods of analysis. Moreover, the method lends itself well to programming for a digital computer. The wide application of electron optics today makes this a noteworthy contribution to the art.

A New FM-AM Method of Compression, Expansion, and Multiplication (Aiken and Süsskind, p. 1550)—This brief paper describes a novel method of combining two signals in such a way that the dynamic range of the first signal is expanded or compressed by the second. The technique has particular application to controlling the average levels of audio, radio or television signals. However, it may also find other interesting uses where modulation with separated components is involved, for example, as a multiplier in analog computers.

IRE Recommended Practices on Audio and Electroacoustics: Loudspeaker Measurements (p. 1553)—This document, drawn up by the Audio and Electroacoustics Committee of the IRE, defines terms associated with loudspeakers and their testing, recommends various methods of testing, and indicates preferred methods of presenting information regarding their characteristics. Included are methods of measuring reference pressure response, rating efficiency, directional properties, nonlinear distortion, and power capacity rating.

Coincidence Techniques for Radar Receivers Employing a Double-Threshold Method of Detection (Endresen and Hedemark, p. 1561)—The authors propose that the well-known double threshold radar detection technique requiring m or more detections in n consecutive trials be replaced by a video coincidence technique in which m or more consecutive *pairs* (or triples) of detections are required in n consecutive trials before saying that a target is present. The significance of requiring that the detections be clustered in groups of two or three is that this clustering is exactly what one expects when a true target appears and, on the other hand, is not at all characteristic of independent and random noise pulses which give rise to false alarms. Mathematical formulas are developed to determine how much is gained in terms of reducing false alarm probabilities and what price is paid in terms of reducing the detection range. The answers to these questions and the proposed coincidence technique itself will be of substantial interest to those concerned with suppressing pulse-type interference in radar systems.

Time-Varying Networks, I*

L. A. ZADEH†, FELLOW, IRE

Summary—**This paper presents an analysis of some of the significant developments in time-varying network theory which have taken place during the past decade, with the emphasis placed on three topics: 1) characterization of time-varying networks, and in particular, transition from the impulsive response to the differential equation; 2) the problem of factorization, with emphasis on the contributions of Darlington, Batkov and Paul Levy; and 3) randomly-varying systems and, in particular, the question of stability of discrete-time systems of this type. The identification problem, the analysis of periodically-varying systems, the synthesis problem, and the filtering and prediction of nonstationary processes will be treated in Part II, to be published later.**

THIS PAPER is primarily concerned with developments in time-varying-network theory which have taken place during the past decade. A survey paper by Bennett [1] provides a brief discussion of the developments prior to 1950.

The past ten years have witnessed a rapid growth of interest in time-varying networks as well as a marked shift in emphasis brought about by the advent of such new areas of research as missile guidance, detection of fluctuating targets, propagation through randomly-varying media, communication via satellites, parametric amplification, etc. Furthermore, the availability of machine computers has made, and is making, a profound impact on the whole process of constructing a model of a physical system and subjecting it to mathematical analysis, as well as on the reverse process of synthesizing a system from components having known characteristics. One consequence of the advent of machine computers is the growth in importance of the so-called identification problem, which, roughly speaking, is concerned with the determination of the characteristics of a given black box, based upon the observation of its external behavior. This stems from the fact that, with the aid of machine computers, the analysis of a system comprised of elements having known characteristics no longer presents essential difficulties. Thus the outstanding problem becomes that of identification, which in any case is a basic prerequisite to the analysis of a system by either machine computer or analytical means.

This paper is not purported to be an exhaustive survey. Rather, its limited aim is to present a connected and not too superficial account of some of the significant and lesser known contributions to time-varying-network theory made during the past ten years. Because of limitations on space, the paper is in two parts. Part I deals with the problem of transition from one mode of characterization to another, the so-called factorization problem, and with randomly-varying systems. The identification problem, the analysis of periodically-varying systems, the synthesis problem, the stability problem, the filtering and prediction of nonstationary processes, the resolution into elementary time functions and miscellaneous contributions will be treated in Part II, to be published later.

It should be noted, in the following exposition, that the amount of space devoted to a particular contribution is not necessarily a measure of its significance. As a general rule, the contributions which are well known or have appeared in widely available journals are referred to very briefly, while the results which appeared in unpublished reports or foreign publications are discussed in greater detail.

I. Characterization

It has long been known that the relation between the input and output of a time-varying system can be expressed in a variety of ways other than those based on the use of differential equations. Yet it was—and to some extent still is—standard practice to employ almost exclusively the differential-equation representation for the purpose of relating the input to the output, either directly or through the state variable.

It is largely during the past decade that a need for a wider variety of alternative representations became definitely established and their potentialities as well as limitations became more clearly understood. The reason for this development is twofold: first, it was found that many of the time-varying models of such systems as randomly-varying media, fluctuating targets, etc., cannot be characterized in terms of ordinary differential equations of finite order. Second, it became clear that in many of the problems of optimization, identification, detection, filtering, etc., it is much more convenient to use a representation tailored to the characteristics of a particular class of systems than to use an "all-purpose" representation involving a differential equation or a set of differential equations relating the input to the output.

In speaking of the modes of characterization other than those based on the use of differential equations, what we have in mind are the techniques centering on the resolution of input time functions into a family of "elementary signals" such as delta functions, exponentials, etc. If the responses of the system to such elementary signals can be determined, then the response to

* Received by the IRE, June 23, 1961; revised manuscript receiver, July 31, 1961. This work was supported in part by the Natl. Sci. Found. under Grant G-9106; it was presented at the Symposium on Time-Varying Networks, 1961 IRE International Convention, New York, N. Y.

† Dept. of Elec. Engrg., University of California, Berkeley, Calif.

an arbitrary input can be determined by superposition. In this way, the problem of finding the response to a given input is reduced to a large number of simple problems, each involving the determination of the response of the system to a particular elementary signal.

Before proceeding to discuss some of the contributions to the characterization of time-varying systems, it would be helpful to summarize some of the well-known facts pertaining to the technique of resolving the input and output into elementary signals. (For a more detailed discussion, see Huggins [19], Laning and Battin [16], Gerardi [12], and Zadeh [2].)

Resolution into Delta Functions

In this case, the family of elementary signals has the form $\{\delta(t-\xi),\ -\infty<\xi<\infty,\ -\infty<t<\infty\}$ where $\delta(t-\xi)$ denotes a unit impulse occurring at time ξ, with ξ ranging over the interval $(-\infty, \infty)$. Assuming, for simplicity, that the system has a single input u and a single output y, and that it is initially at rest, the relation between the input and output can be written as

$$y(t) = \int_{-\infty}^{\infty} h(t, \xi)u(\xi)d\xi \tag{1}$$

where $h(t, \xi)$ is called the *impulsive* (or impulse) *response* of the system and is defined as the response of the system at rest to $\delta(t-\xi)$. If a system is *nonanticipative* (*i.e.*, if, for all t, $y(t)$ is independent of the values of the input for times greater than t), then $h(t, \xi) \equiv 0$ for $t<\xi$ and the upper limit in (1) can be replaced by t. (For a discussion of the relationship between the impulsive response and Green's function, see Miller [3] and Zadeh [4].)

Resolution into Exponential Functions

Here, the elementary signals are of the form $\{e^{j\omega t},\ -\infty<\omega<\infty,\ -\infty<t<\infty\}$ or more generally $\{e^{st},\ s\in C\}$ where C is a Bromwich-Wagner contour in the s plane. In terms of such signals, a system B is characterized by its frequency-response function $H(j\omega, t)$, which is defined as

$$H(j\omega, t) = \frac{\text{response of } B \text{ to } e^{j\omega t}}{e^{j\omega t}}. \tag{2}$$

The time-varying frequency-response function $H(j\omega, t)$ constitutes a natural generalization of $H(j\omega)$—the frequency-response function of a time-invariant system. If the system is initially at rest and the Fourier transform of the input u is denoted by $U(j\omega)$, the expression for the output at time t, $y(t)$, in terms of $H(j\omega, t)$ and $U(j\omega)$ is

$$y(t) = \frac{1}{2\pi}\int_{-\infty}^{\infty} H(j\omega, t)U(j\omega)e^{j\omega t}d\omega. \tag{3}$$

General Relations for Resolution into Elementary Time Functions

If a family of time functions $\{k(t, \lambda)\}$, with λ taking values on some contour C in the λ plane and t ranging over a finite or infinite interval T, form a basis for the input and output spaces of a system B [in the sense that the $k(t, \lambda)$ and C are such that any signal in the input or the output space of B can be resolved into the $k(t, \lambda)$], then an input u can be expressed as

$$u(t) = \int_C k(t, \lambda)U(\lambda)d\lambda, \qquad t \in T, \tag{4}$$

where $U(\lambda)$ is an integral transform of u given formally by

$$U(\lambda) = \int_{-\infty}^{\infty} k^{-1}(\lambda, t)u(t)dt. \tag{5}$$

In this relation, the kernel $k^{-1}(\lambda, t)$ is inverse to $k(t, \lambda)$ in the sense that

$$\int_C k(t, \lambda)k^{-1}(\lambda, \xi)d\lambda = \delta(t-\xi), \qquad t, \xi \in T. \tag{6}$$

B is characterized by its responses to the $k(t, \lambda)$, $\lambda \in C$. Thus, if the response of B to $k(t, \lambda)$ is denoted by $K(t, \lambda)$, then the response of B to u (with B initially at rest) can be written as:

$$y(t) = \int_C K(t, \lambda)U(\lambda)d\lambda. \tag{7}$$

Eqs. (1) and (3) are special cases of this relation corresponding to $k(t, \lambda) = \delta(t-\lambda)$ and $k(t, \lambda) = e^{j\lambda t}/2\pi j$, respectively.

Resolution into Eigenfunctions

A function $k(t, \lambda)$, $t \in T$, is an eigenfunction of B if the response of B to $k(t, \lambda)$ (with B initially at rest) is of the form: constant (depending on λ) times $k(t, \lambda)$. If B has a set of eigenfunctions $\{k(t, \lambda), \lambda \in C\}$ which can be used as a basis for the input and output spaces of B, then the input-output relationship of B can be expressed in the simple form

$$Y(\lambda) = R(\lambda)U(\lambda) \tag{8}$$

where $R(\lambda)$ is the response function of B

$$R(\lambda) = \frac{\text{response of } B \text{ to } k(t, \lambda)}{k(t, \lambda)} \tag{9}$$

and $U(\lambda)$ and $Y(\lambda)$ are the integral transforms of u and y, respectively; *i.e.*,

$$U(\lambda) = \int_T k^{-1}(\lambda, t)u(t)dt \tag{10}$$

and

$$Y(\lambda) = \int_T k^{-1}(\lambda, t)y(t)dt. \tag{11}$$

It can be shown readily that if a system is time-invariant and homogeneous (in the sense that if u is any input in the input space of B, then for all real constants k, the response of B to ku is k times the response of B to u), then the functions $\{e^{j\omega t},\ -\infty<\omega<\infty,$

$-\infty < t < \infty\}$ constitute an eigenfunction set for B. (Note that B need not be linear.) It is in this sense that the exponential functions $\{e^{j\omega t}\}$ constitute a "natural" set of elementary time functions for linear time-invariant systems.

This concludes our brief review of the terminology and basic relations pertaining to the characterization of linear systems in terms of their responses to elementary time functions.

II. Transitions Between Different Modes of Characterization

In dealing with time-varying systems, one frequently encounters a situation where a system B is characterized in a given way W, and it is desired—for one reason or another—to characterize B in a particular way W^* which is different from W. For example, B might be initially characterized[1] by a differential equation of the form

$$a_n(t)\frac{d^n y}{dt^n} + \cdots + a_0(t)y = b_m(t)\frac{d^m u}{dt^m} + \cdots + b_0(t)u, \quad (12)$$

or more compactly

$$L(p, t)y = M(p, t)u, \qquad p = \frac{d}{dt}$$

where

$$L(p, t) = \sum_{i=1}^{n} a_i(t)p^i$$

$$M(p, t) = \sum_{j=1}^{m} b_j(t)p^j$$

and the $a_i(t)$ and $b_j(t)$ are given functions of time. The desired characterization of B is:

$$y(t) = \int_{-\infty}^{\infty} h(t, \xi)u(\xi)d\xi \quad (13)$$

where $h(t, \xi)$ is the impulsive response of B. Here, the problem is that of solving the differential equation

$$(a_n(t)p^n + \cdots + a_0(t))h(t, \xi) = (b_m(t)p^m + \cdots + b_0(t))\delta(t - \xi) \quad (14)$$

subject to the initial condition

$$\frac{\partial^\nu h(t, \xi)}{\partial t^\nu}\Bigg]_{t=\xi-} = 0, \qquad \nu = 0, 1, \cdots, n-1.$$

(For a more detailed discussion of this and related problems, see Borsky [6], Solodov [5], and Zadeh [4].

[1] It is generally unrecognized that a differential equation such as (12) does not characterize a system uniquely unless it is tacitly understood that the system must be nonanticipative. More specifically, (12) defines $n+1$ nonequivalent systems of which one is nonanticipative, one is purely anticipative, and the rest operate on both the past and the future of the input.

Usually, the problem is to pass from an implicit characterization employing differential operators to an explicit characterization involving such functions as the impulsive response, frequency-response function, etc. In some cases, however, one is faced with a converse problem, namely, that of passing from, say, the impulsive response to the differential equation. This may happen, for example, when it is desired to simulate a system on an analog computer which is designed to handle differential equations.

An interesting special case of the latter type of problem was considered by White [7]. Specifically, White considers the case where one is given the eigenfunction set $\{k(t, \lambda)\}$ of an undetermined differential operator $L(p, t)$ which admits a representation of the form

$$L(p, t) = \sum_{\nu}\sum_{\mu} l_{\nu\mu}t^{\nu+\mu}p^\nu \quad (15)$$

where the $l_{\nu\mu}$ are unknown constants, and ν and μ range over integers. Furthermore, it is assumed that $k(t, \lambda)$ can be expanded as a power series in λt,

$$k(t, \lambda) = \sum_{n=0}^{\infty} k_n(\lambda t)^n, \quad (16)$$

and that the response function $R(\lambda)$ can likewise be expanded as

$$R(\lambda) = \sum_{s} h_s\lambda^s, \quad (17)$$

where the coefficients h_s may be adjusted to yield a simple solution to the problem if one exists.

Formally, the problem is solved by substituting (12)–(14) in

$$L(p, t)k(t, \lambda) = R(\lambda)k(t, \lambda), \quad (18)$$

and equating the coefficients of the like powers of λ and t. This yields a set of equations

$$\sum_{\nu} l_{\nu,-\mu}\frac{n!}{(n-\nu)!} = h_\mu\frac{k_{n-\mu}}{k_n}, \quad (19)$$

which may be solved for the $l_{\nu\mu}$ (if a solution exists).

For example,

$$k(t, \lambda) = J_0(\lambda t) \qquad (\textit{B}\text{essel function}) \quad (20)$$

$$= \sum_{n=0}^{\infty}(-1)^{n/2}\frac{(\lambda t)^n}{2^n[(n/2)!]^2} \qquad n = 0, 2, 4, \cdots. \quad (21)$$

In this case, it is expedient to set $h_2 = -1$, $h_0 = h_1 = h_3 = \cdots = 0$. Then

$$\sum_{\nu} l_{\nu,-\mu}\frac{n!}{(n-\nu)!} = -1[-4(n/2)^2], \quad (22)$$

or

$$+l_{0,-2} + l_{1,-2}n + l_{2,-2}n(n-1) + \cdots = n^2 \quad (23)$$

from which it follows that

$$l_{1,-2} = 1, \qquad l_{2,-2} = 1, \qquad \text{all other } l_{\nu\mu} = 0.$$

Thus, the desired operator is

$$L(p, t) = p^2 + \frac{1}{t} p. \tag{24}$$

The relation given by (19) can readily be extended to the case where $k(t, \lambda)$ admits a more general representation of the form

$$k(t, \lambda) = \sum_n \sum_m k_{nm} \lambda^n t^m. \tag{25}$$

Then (19) becomes

$$\sum_m \sum_\nu k_{nm} l_{\nu,\mu-m} \frac{m!}{(m-\nu)!} = \sum_m h_{n-m} k_{m\mu}, \tag{26}$$

which, for the special case of (16), reduces to (19).

If the eigenfunction set is identified with the functions $\{t^{-\lambda}, 0 < t < \infty\}$, with λ taking values on a Bromwich-Wagner contour in the λ plane, then the differential operators relating y to u assume the form

$$(a_n t^n p^n + a_{n-1} t^{n-1} p^{n-1} + \cdots + a_0) y = (b_m t^m p^m + \cdots + b_0) u, \tag{27}$$

where the a's and b's are constants. Networks described by equations of this form have been studied by Aseltine [8], Aseltine and Trautman [9], Davis [10], Ho and Davis [11], Gerardi [12], and others, and are referred to in the literature as the Euler-Cauchy networks. In effect, such networks can be obtained from time-invariant networks by the transformation of time-scale $t \rightarrow -\log t$. Based on this observation, it can readily be shown that the impulsive response of a nonanticipative Euler-Cauchy network is of the form

$$h(t, \xi) = 1(t - \xi) \frac{1}{t} g\left(\frac{t}{\xi}\right) \tag{28}$$

where $g(t-\xi)$ is the impulsive response of the time-invariant network from which the Euler-Cauchy network is derived.

If $k(t, \lambda)$ is identified with $1/(2\pi j)(t^{-\lambda})$, then the inverse kernel is given by

$$k^{-1}(\lambda, t) = t^{\lambda - 1}, \qquad 0 \leq t < \infty. \tag{29}$$

Thus, the resolution of a signal $u(t \geq 0)$ into the $k(t, \lambda)$ assumes the form

$$u(t) = \frac{1}{2\pi j} \int_C t^{-\lambda} U(\lambda) d\lambda \tag{30}$$

and

$$U(\lambda) = \int_0^\infty u(t) t^{\lambda - 1} d\lambda \tag{31}$$

where $U(\lambda)$ is the Mellin transform of u. In some cases, it is more convenient to employ a modified Mellin transform of u which is related to (31) by the translation $t \rightarrow t + a$, where a is a constant. Such transforms have been used for illustrative purposes by Davis [10]. More recently, Peschon [13] has found a useful application for modified Mellin transforms in final value control problems.

An interesting idea which was motivated by the work of Aseltine and Trautman is contained in the paper by Davis [10] cited above. Specifically, let

$$L = a_1(t) p + a_0(t) \tag{32}$$

be a first-order differential operator and let $k(t, \lambda)$ and $k^{-1}(t, \lambda)$ be, respectively, the solutions of

$$Ly = \lambda y, \qquad y(0) = 1 \tag{33}$$

and

$$L^* y = \lambda y, \qquad y(0) = 1 \tag{34}$$

where

$$L^* = -p a_1(t) + a_0(t) \tag{35}$$

is the adjoint[2] of L. Then the kernels $k(t, \lambda)$ and $k^{-1}(\lambda, t)$ are inverse to one another in the sense of (6), and, under mildly restrictive conditions, one can write

$$U(\lambda) = \int_0^\infty k^{-1}(t, \lambda) u(t) dt \tag{36}$$

and

$$u(t) = \frac{1}{2\pi j} \int_C k(t, \lambda) U(\lambda) d\lambda. \tag{37}$$

Now, given a time-invariant network N, one can transform it into a time-varying network N^* by replacing each unit inductor (which corresponds to the operator p) with a network l corresponding to operator L, and replacing each unit capacitor with a network l' corresponding to the operator L^{-1} (inverse of L), leaving all resistances unchanged. The networks l and l' corresponding to L and L^{-1}, respectively, are described by the voltage-current relations $v = Li$ and $i = Lv$. Thus, l' can be obtained from l by dualization. Clearly, if a network function associated with time-invariant N is a function $H(s)$ of complex-frequency s, then the corresponding response function for time-varying N^* will be $H(\lambda)$, with λ being the parameter entering into $k(t, \lambda)$. In this way, one can derive from a prototype time-invariant network N a wide variety of time-varying networks N^* which are described by the same equations

[2] The adjoint of a differential operator

$$L = \sum_n a_n(t) p^n$$

is defined as

$$L^* = \sum_n (-1)^n p^n a_n(t),$$

where $p^n a_n(t)$ signifies that p^n operates on the product of $a_n(t)$ and the operand; *e.g.*, $(pa_1(t) + a_0(t))u(t)$ means $d/(dt)(a_1(t)u(t)) + a_0(t)u(t)$. For a more detailed discussion see, for instance, Ince [14], Friedman [15], and Laning and Battin [16]. It should be noted, alternatively, that the adjoint of a system B with impulsive response $h(t, \xi)$ can be defined as a system B^* whose impulsive response $h^*(t, \xi)$ is $h(\xi, t)$, *i.e.*, $h^*(t, \xi) \equiv h(\xi, t)$. With this as the starting point, it is a simple matter to show that if B is characterized by the differential equation $Ly = u$, then B^* is characterized by the differential equation $L^* y = u$, where L^* is the adjoint of L in the sense defined above. However, if B is characterized by $Ly = Mu$, then, except in special cases, the characterizing equation for B *is not* $L^* y = M^* u$.

in terms of λ as N is in terms of s. In effect, Davis' method amounts to an extension of the familiar frequency-transformation technique (see Laurent [17], Bode [17a], and Zadeh [17b]), to time-varying networks. More recently, somewhat overlapping results have been obtained independently by Wattenburg [18].

There are several other contributions, notably by Huggins [19], Lai [20], Gerlach [21], Narendra [22], and others, which are concerned with various techniques of resolution of time functions into elementary signals. These contributions will be discussed in Part II of the paper.

Transition from Impulsive Response to the Differential Equation

The problem of finding the differential equation of a system which is characterized by its impulsive response arises in situations where it is simpler to simulate or synthesize a system in terms of its differential equations rather than its impulsive response. It arises also in connection with the so-called factorization problem which is discussed in Section III of this paper.

This problem was first formulated and partially solved by Batkov [23]. Batkov's approach is based on the well-known fact (see, for instance, Coddington and Levinson [24], and Miller [3]) that the impulsive response of a system characterized by the differential equation

$$Ly = (a_n(t)p^n + \cdots + a_0(t))y(t) = u(t) \tag{38}$$

has the form

$$h(t, \xi) = 1(t - \xi) \sum_{\nu=1}^{n} \psi_i(t)\psi_i^*(\xi) \tag{39}$$

where the $\psi_i(t)$ are any n linearly independent solutions of the homogeneous equation $Ly=0$ and the $\psi_i^*(t)$ are n linearly independent solutions of the adjoint equation

$$L^*y = ((-1)p^n a_n(t) + \cdots + a_0(t))y(t) = 0. \tag{40}$$

The $\psi_i^*(t)$ can be expressed in terms of the $\psi_i(t)$ by solving the system of n linear equations in the $\psi_i^*(\xi)$

$$\left.\frac{\partial^k h(t, \xi)}{\partial t^k}\right]_{t=\xi} = 0, \qquad k = 0, 1, \cdots, n-2 \tag{41}$$

$$\left.\frac{\partial^{n-1} h(t, \xi)}{\partial t^{n-1}}\right]_{t=\xi} = \frac{1}{a_n(\xi)}. \tag{42}$$

Another well-known fact is that the operator L can readily be constructed from the knowledge of the $\psi_i(t)$. Specifically (see, for example, Ince [14]), one can write

$$Ly = \begin{vmatrix} \psi_1(t) & \cdots & \psi_n(t) & y(t) \\ \psi_1^{(1)}(t) & \cdots & \psi_n^{(1)}(t) & y^{(1)}(t) \\ \cdots & & & \\ \psi_1^{(n)}(t) & & \psi_n^{(n)}(t) & y^{(n)}(t) \end{vmatrix}. \tag{43}$$

Thus, if $h(t, \xi)$ is given in the form (39) and it is known that the system is characterizable in the form (1), then L can be obtained at once from (43). Far less trivial is the more general case where the differential equation characterizing the system is of the form $Ly = Mu$ or, more explicitly,

$$[a_n(t)p^n + \cdots + a_0(t)]y = [b_m(t)p^m + \cdots + b_0(t)]u, \tag{44}$$

where $m < n$ and the $a_i(t)$ and $b_j(t)$ are initially unknown coefficients.[3] In this case, the impulsive response reads

$$h(t, \xi) = 1(t - \xi) \sum_{i=1}^{n} \psi_i(t)\theta_i(\xi) \tag{45}$$

where the $\psi_i(t)$, $i = 1, \cdots, n$ are n linearly independent solutions of $Ly=0$ and the $\theta_i(t)$, $i = 1, \cdots, n$, are given by

$$\theta_i(t) = M^*[\psi_i^*(t)], \qquad i = 1, \cdots, n, \tag{46}$$

where the $\psi_i^*(t)$ are n linearly independent solutions of the adjoint equation $L^*y=0$ (satisfying [41] and [42]) and M^* is the adjoint of M. If $h(t, \xi)$ is given in this form, then from (45) one can find the $\psi_i(t)$ and $\theta_i(t)$. Once the $\psi_i(t)$ are known, it is a relatively simple matter to determine the $\psi_i^*(t)$.[4] Thus, the problem reduces to finding M^* from (46). On writing

$$M^* = b_m^*(t)p^m + \cdots + b_0^*(t) \tag{47}$$

where the $b_i^*(t)$ are undetermined coefficients, (46) yields a set of n simultaneous equations in the $b_i^*(t)$

$$\theta_i(t) = \sum_{k=0}^{n-1} b_k^*(t)\psi_i^{*(k)}(t), \qquad i = 1, \cdots, n. \tag{48}$$

Once these n equations are solved for the $m+1$ coefficients $b_k^*(t)$ in M^*, M can be found from the relation between a differential operator and its adjoint.[2] This completes the determination of L and M in (44) from the knowledge of $h(t, \xi)$.

It is simpler and frequently more effective to derive from $h(t, \xi)$, not a single differential equation of the form $Ly = Mu$, but a system of n first-order differential equations of the form

$$\dot{x}(t) = A(t)x(t) + B(t)u(t) \tag{49}$$

together with the expression for the output

$$y(t) = \alpha_1(t)x_1(t) + \cdots + \alpha_n(t)x_n(t) + \beta_0(t)u(t) + \cdots + \beta_{m-n}(t)u^{(m-n)}(t) \tag{50}$$

[3] The procedure for finding the operator M given in Batkov's paper is somewhat less straightforward than that given here.

[4] See Ince [14], p. 124.

where $\mathbf{x}(t)=(x_1(t), \cdots, x_n(t))$ is a state vector, $\boldsymbol{A}(t)$ and $\boldsymbol{B}(t)$ are matrices, and the $\alpha_i(t)$ and $\beta_k(t)$ are scalar coefficients. These equations constitute a very useful mode of characterization of a system and will be referred to as its state equations. For a homogeneous equation $Ly=0$, the state equation $\dot{\mathbf{x}}=\boldsymbol{A}\mathbf{x}$ is simply a normal form of $Ly=0$ (see, for instance, Ince [14]). Equations of the form (49) and (50) have been employed extensively in analytical dynamics and, more recently, in the theory of automatic control.

We shall discuss briefly three problems arising in connection with the state equations of a system: first, the problem of obtaining the representation (49) and (50) from $h(t, \xi)$; second, the problem of obtaining (49) and (50) from $Ly=mu$; and third, the problem of obtaining (49) and (50) directly from the structure of a time-varying network.

Batkov [23] and, somewhat earlier, Darlington [25] have indicated how the first two of these problems can be solved. As for the third problem, Kinarawala [26] has shown how one can adapt Bashkow's A-matrix technique [27] to time-varying networks and thereby obtain (49) for any $R(t)L(t)C(t)$ network without the necessity of performing differentiations or integrations on the loop or node equations of the network.

The basic idea behind the methods of Darlington and Batkov is closely related to the partial-fractions technique of Lur'e [28][5] for casting into the diagonal or, more generally, the Jordan canonical form, the dynamical equations of the linear part of a nonlinear system. Specifically, we observe that each term in the expression for $h(t, \xi)$

$$h(t, \xi) = 1(t-\xi)\sum_{i=1}^{n}\psi_i(t)\theta_i(\xi) \tag{51}$$

can be identified with the impulsive response of a first-order system. Thus, we can write

$$y(t) = x_1(t) + \cdots + x_n(t) \tag{52}$$

where $x_i(t)$ is defined by

$$x_i(t) = \int_{-\infty}^{t}\psi_i(t)\theta_i(\xi)u(\xi)d\xi. \tag{53}$$

Differentiating both sides of (53), we get

$$\dot{x}_i(t) = \psi_i(t)\theta_i(t)u(t) + \int_{-\infty}^{t}\dot{\psi}_i(t)\theta_i(\xi)u(\xi)d\xi \tag{54}$$

which can be written as

$$\dot{x}_i(t) = \frac{\dot{\psi}_i(t)}{\psi_i(t)}x_i(t) + \psi_i(t)\theta_i(t)u(t), \quad i=1, \cdots, n. \tag{55}$$

These equations, together with (52), form the state equations for the system, with

$$A = \begin{bmatrix} \dot{\psi}_1/\psi_1 & 0 & 0 & \cdot & 0 \\ 0 & \dot{\psi}_2/\psi_2 & 0 & \cdot & 0 \\ 0 & 0 & 0 & \cdot & \dot{\psi}_n/\psi_n \end{bmatrix},$$

$$B = \begin{bmatrix} \psi_1\theta_1 \\ \psi_2\theta_2 \\ \psi_n\theta_n \end{bmatrix} \tag{56}$$

and $\alpha_1=\cdots=\alpha_n=1$, $\beta_0=\cdots=\beta_{m-n}=0$ (assuming that $m<n$). The main advantage of this technique is that it yields a diagonal A matrix.[6]

The same idea can be used to derive an analog of the partial-fractions expansion for time-varying networks. As an illustration, consider a second-order system characterized by a single differential equation

$$(p^2 + a_1(t)p + a_0(t))y = (b_1(t)p + b_0(t))u \tag{57}$$

and let ψ_1 and ψ_2 be any two linearly independent solutions of $(p^2+a_1(t)p+a_0(t))y=0$. Then, on denoting $\dot{\psi}_1/\psi_1$ by λ_1, $\dot{\psi}_2/\psi_2$ by λ_2, and using the results just described, we can write (with the dependence of x_1, λ_1, ψ_1, etc., on t implied but not exhibited explicitly)

$$\dot{x}_1 = \lambda_1 x_1 + \psi_1\theta_1 u \tag{58}$$

$$\dot{x}_2 = \lambda_2 x_2 + \psi_2\theta_2 u \tag{59}$$

$$y = x_1 + x_2 \tag{60}$$

which is equivalent to expressing y in the form

$$y = [(p-\lambda_1)^{-1}\psi_1\theta_1]u + [(p-\lambda_2)^{-1}\psi_2\theta_2]u \tag{61}$$

where $(p-\lambda_1)^{-1}$ and $(p-\lambda_2)^{-1}$ denote the operators inverse to $p-\lambda_1$ and $p-\lambda_2$, respectively. In effect, this amounts to the partial-fractions expansion

$$(p^2 + a_1p + a_0)^{-1}(b_1p + b_0) = (p-\lambda_1)^{-1}\psi_1\theta_1 + (p-\lambda_2)^{-1}\psi_2\theta_2 \tag{62}$$

where, to recapitulate, ψ_1, ψ_2 are two linearly independent solutions of $(p^2+a_1p+a_0)y=0$

$$\lambda_1 = \dot{\psi}_1/\psi_1, \qquad \lambda_2 = \dot{\psi}_2/\psi_2 \tag{63}$$

$$\theta_1 = (-pb_1 + b_0)\psi_1^*, \qquad \theta_2 = (-pb_1 + b_0)\psi_2^* \tag{64}$$

and ψ_1^* and ψ_2^* are two linearly independent solutions of the adjoint equation $L^*y=(p^2-pa_1+a_0)y=0$ (satisfying [41] and [42]).

Partial-fractions expansions of this type and their application to the analysis and synthesis of time-varying networks have their origin in the work of Darlington [25], [29], [30].

[5] See also B. V. Bulgakov, "On normal coordinates," *Prikl. Mat. i Meh.*, vol. 10, no. 2, pp. 273–290; 1946.

[6] This technique results in a diagonal A even in the case of a time-invariant system whose characteristics equation $L(p)=0$ has repeated roots. However, the price for this is that one or more of the elements of A are functions of time rather than constants. If it is required that the elements of A be constants, then A can always be put into the Jordan canonical form but not, in general, the diagonal form.

The methods described above furnish a straightforward way for effecting a transition from a single differential equation

$$Ly = u, \qquad (L \text{ of order } n) \tag{65}$$

to the state equations

$$\dot{x} = Ax + Bu, \qquad A \text{ diagonal} \tag{66}$$

$$y = \alpha_1 x_1 + \cdots + \alpha_n x_n \tag{67}$$

provided one knows a set of n linearly independent solutions of the homogeneous equation $Ly=0$. Note that if A is not required to be diagonal, then the transition can be effected in conventional ways without the knowledge of solutions of $Ly=0$.

From (66) and (67), one can pass to a more explicit characterization

$$x(t) = G(t, t_0)x(t_0) + \int_{t_0}^{t} G(t, \xi)Bu(\xi)d\xi \tag{68}$$

$$y = \alpha_1 x_1 + \cdots + \alpha_n x_n \tag{69}$$

by using the standard form of solution of the vector equation (66). (See, for instance, Coddington and Levinson [24] and Laning and Battin [16].) The $n \times n$ matrix $G(t, t_0)$ appearing in (68) has as its ith column $(i=1, \cdots, n)$ the functions $\psi_i(t, t_0)$, $\psi_i^{(1)}(t, t_0)$, $\cdots$, $\psi^{(n-1)}(t, t_0)$ where $\psi_i(t, t_0)$ is the solution of $Ly=0$ which satisfies the initial conditions

$$\frac{\partial \psi_i^{(k)}(t, t_0)}{\partial t^k}\Bigg]_{t=t_0} = 0$$

for $k \neq i-1$ (with k ranging over the set $0, \cdots, n-1$) and

$$\frac{\partial \psi_i^{(k)}(t, t_0)}{\partial t^k}\Bigg]_{t=t_0} = 1$$

for $k=i-1$. $G(t, t_0)$ is known by a variety of names of which the *transition matrix* is the more frequently used in engineering literature. (For a more detailed discussion of the properties of $G(t, t_0)$, see, for instance, Laning and Battin [34] and Kalman and Bertram [35].)

Now suppose that one does not know a set of n linearly independent solutions of $Ly=0$ or $\dot{x}=Ax$. In these circumstances, there is no general way of passing from (65) or (66) to (68). However, there are special cases for which $G(t, t_0)$ can readily be found. One such case has been discussed by Gauthier [36] and independently by Kinarawala [26]. Specifically, this is the case where, as in the constant coefficient case, $G(t, t_0)$ can be expressed as

$$G(t, t_0) = \exp - \int_{t_0}^{t} A(\xi)d\xi. \tag{70}$$

It is easy to show that $G(t, t_0)$ can be written in this form if, and only if, the matrices $A(t)$ and $\int_{t_0} A(\xi)d\xi$ commute, *i.e.*,

$$A(t)\int_{t_0}^{t} A(\xi)d\xi \equiv \left(\int_{t_0}^{t} A(\xi)d\xi\right)A(t). \tag{71}$$

We turn next to an important problem on which the techniques discussed in this section have a significant bearing. This is the problem of factorization.

III. Problem of Factorization

In dealing with stationary as well as nonstationary time series and, more particularly, with problems of prediction, detection and filtering, it is frequently expedient to employ so-called spectrum-shaping techniques which allow one to modify at will the spectral density and the correlation function of a random process. The spectrum-shaping technique was first used by Bode and Shannon [31] and independently by Zadeh and Ragazzini [32]. Its extension to time-varying systems was given by Laning and Battin [16] and Miller and Zadeh [33].

In the case of nonstationary processes, a typical problem in spectrum shaping is the following. Given a nonstationary process $\{u(t), -\infty < t < \infty\}$ with covariance function $R(t, \tau)$, find a linear network B such that the covariance function of the process resulting from acting on $\{u\}$ with B is $\delta(t-\tau)$ (or, more generally, a linear combination of δ functions of various orders). In other words, we wish to find a B such that $\{y(t), -\infty < t < \infty\}$, where $y=Bu$, has white spectrum. Furthermore, we wish to characterize B by a single differential equation.

This problem has an important bearing on the solution of an integral equation which is encountered very frequently in the prediction, detection and filtering of nonstationary processes. The equation in question reads

$$f(t) = \int_{a}^{b} R(t, \tau)x(\tau)d\tau, \qquad a \leq t \leq b \tag{72}$$

where $R(t, \tau)$ is a covariance function, $f(t)$ is a given function on $[a, b]$, and $x(t)$ is an unknown function. It is easy to show (see, for instance, Miller and Zadeh [33]) that the solution of this equation can be reduced to the factorization of $R(t, \tau)$. In this connection, it is of interest to note that the methods given by Laning and Battin [16], Zadeh and Miller [33], Shinbrot [37], [38], Pugachev [39], [40], and others, for the solution of this equation are either explicitly based on the factorization of $R(t, \tau)$ or make an implicit use of it.

For our purposes, it will be somewhat more convenient to discuss a converse problem, namely, that of finding a spectrum-shaping network B such that the covariance

function of the process resulting from acting with B on white noise is $R(t, \tau)$. If the impulsive response of B is denoted by $h(t, \xi)$, then it is easy to verify that

$$R(t, \tau) = \int_{-\infty}^{\infty} h(t, \xi)h(\tau, \xi)d\xi. \tag{73}$$

Thus, in this case the factorization problem becomes that of solving the integral equation (73) for $h(t, \xi)$. [Note that if $h(t, \xi)$ is assumed to be nonanticipative, then the upper limit in (73) becomes Min (t, τ).]

If B is characterizable by a differential equation of order n, then its impulsive response is of the form (45)

$$h(t, \xi) = 1(t - \xi) \sum_{i=1}^{n} \psi_i(t)\theta_i(\xi) \tag{74}$$

where the meaning of the ψ_i and θ_i was discussed previously. On substituting this expression into (73), one gets, after some straightforward manipulations

$$R(t, \tau) = \sum_{i=1}^{n} \psi_i(t)\gamma_i(\tau), \qquad t > \tau \tag{75}$$

$$= \sum_{i=1}^{n} \psi_i(\tau)\gamma_i(t), \qquad t < \tau \tag{76}$$

where

$$\gamma_i(t) = \sum_{j=1}^{n} \psi_j(t) \int_{-\infty}^{t} \theta_i(\xi)\theta_j(\xi)d\xi, i = 1, \cdots, n.$$

Thus, if $R(t, \tau)$ is given in this form, then the problem of finding the differential equation can be solved by first finding $h(t, \xi)$ [based on (74)–(76)] and then using $h(t, \xi)$ to determine the differential equation by the techniques described in the preceding section. Essentially, this approach to the determination of the spectrum-shaping network was developed by Darlington [29] and, independently, by Batkov [41]. Darlington, in particular, has considered the questions of existence and uniqueness of a nonanticipative (physically realizable) impulsive response $h(t, \xi)$ satisfying the integral euqation (73). However, neither Darlington nor Batkov have proved that any given real-valued covariance function (satisfying the conditions of symmetry and positive definiteness) can be expressed in the form (73), with $h(t, \xi)$ being a real-valued function vanishing for $\xi > t$.

As is well known for the time-invariant case, a rational spectral-density function $S(\omega)$ [$S(\omega)$ = Fourier transform of $R(t)$, with $R(t) = R(t, 0)$ = autocorrelation function] can be expressed in an infinity of ways as a product of factors $H_1(j\omega)$ and $H_2(j\omega)$

$$S(\omega) = H_1(j\omega)H_2(j\omega) \tag{76a}$$

if no restrictions are imposed on $H_1(j\omega)$ and $H_2(j\omega)$ other than that H_1 and H_2 be rational and real functions of $j\omega$. However, if 1) $H_1(j\omega)$ is required to be minimum phase (no poles or zeros in the right-half plane), which is equivalent to requiring that the impulsive responses $h_1(t)$ and $h_1^{-1}(t)$, corresponding to $H_1(j\omega)$ and $1/H_1(j\omega)$, respectively (h_1 = inverse Fourier transform of H_1, h_1^{-1} = inverse Fourier transform of H_1^{-1}), be nonanticipative, and 2) $H_2(j\omega)$ is required to be maximum phase (no poles or zeros in the left-half plane), which is equivalent to requiring that h_2 and h_2^{-1} be purely anticipative, *i.e.*, $h_2(t) = h_2^{-1}(t) = 0$ for $t > 0$, then the factorization (76a) is essentially unique.

Now in the time-varying case, the algebraic decomposition (76a) which corresponds to the convolution

$$R(t) = \int_{-\infty}^{\infty} h_1(t - \xi)h_2(\xi)d\xi \tag{76b}$$

is replaced by

$$R(t, \tau) = \int_{-\infty}^{\infty} h_1(t, \xi)h_2(\xi, \tau)d\xi \tag{76c}$$

which is the composition[7] of impulsive responses h_1 and h_2. Equivalently, (76c) may be written as

$$R(t, \tau) = \int_{-\infty}^{\infty} h_1(t, \xi)h_2^*(\tau, \xi)d\xi \tag{76d}$$

where h_2^* is the adjoint of h_2 [*i.e.*, $h_2^*(t, \xi) = h_2(\xi, t)$].[2] Thus, in the time-varying case, the algebraic problem of decomposition of $S(\omega)$ into two factors $H_1(j\omega)$ and $H_2(j\omega)$ satisfying 1) and 2) becomes that of solving the integral equation (76c) for h_1 and h_2, under the condition that $h_1(t, \xi)$ and $h_1^{-1}(t, \xi)$ vanish for $t < \xi$, and $h_2(t, \xi)$ and $h_2^{-1}(t, \xi)$ vanish for $t > \xi$.

If h_1 and h_2 satisfy these conditions and $R(t, \tau)$ is symmetric in its arguments [which in the stationary case corresponds to the condition that $S(\omega)$ is an even function of ω], then $h_1 = h_2^*$ and (76d) becomes

$$R(t, \tau) = \int_{-\infty}^{\text{Min}(t,\tau)} h(t, \xi)h^*(\xi, \tau)d\xi \tag{76e}$$

which is equivalent to (73). Now if: a) $h(t, \xi)$ is regarded as the impulsive response of a system characterized by a differential equation

$$Ly = Mu \tag{76f}$$

in which L and M are undetermined differential operators, and b) $R(t, \xi)$ is given in the form (75), (76), then by using the techniques of Darlington and Batkov it is

[7] The composition of $h_1(t, \xi)$ and $h_2(t, \xi)$ is defined as

$$h_3(t, \xi) = \int_{-\infty}^{\infty} h_1(t, \lambda)h_2(\lambda, \xi)d\lambda.$$

Essentially, if B_i is a system whose impulsive response is $h_i (i = 1, 2, 3)$, then h_3 is the impulsive response of B_1B_2, that is, the tandem combination of B_1 and B_2, with B_1 operating on the output of B_2.

a relatively simple matter to determine L. The determination of M, however, reduces to a problem for which neither Darlington nor Batkov give explicit solutions except in certain special cases. Specifically, the problem is that of finding a representation for a given self-adjoint differential operator $K(K=K^*)$ in the form

$$K = M(p, t)M^*(p, t) \tag{76g}$$

where the product should be understood in the operator sense. In the time-invariant case, this problem reduces to the straightforward algebraic problem of factoring an even polynomial in p into the product of two real polynomials which are complex conjugates of one another. In the time-varying case, M and M^* can readily be determined if one knows a set of basis functions[8] for K (which is analogous to knowing the zeros of K in the time-invariant case). Unfortunately, the assumption that K is a differential operator with a known set of basis functions is rarely satisfied in practice.

A different and more general approach to the factorization problem was developed by Levy in a series of papers [42a]–[42c] dealing with the theory of Wiener processes.[9] A fairly detailed exposition of those aspects of Levy's method which are relevant to the factorization problem are contained in the appendix of Batkov's paper [41]. Briefly, let $\eta(t, \tau)$ and $\beta(\theta, \lambda)$ denote the expressions appearing on the right side of (77) and (78):

$$\eta(t, \tau) = \frac{\dfrac{\partial^{2n-2m}R(t, \tau)}{\partial t^{n-m}\partial \tau^{n-m}}}{\left.\dfrac{\partial^{n-m}h(t, \lambda)}{\partial t^{n-m-1}}\right]_{\lambda=t} \left.\dfrac{\partial^{n-m-1}h(t, \lambda)}{\partial t^{n-m-1}}\right]_{\lambda=\tau}} \tag{77}$$

$$\beta(\theta, \lambda) = \frac{\dfrac{\partial^{n-m}h(\theta, \lambda)}{\partial \theta^{n-m}}}{\left.\dfrac{\partial^{n-m-1}h(\theta, \lambda)}{\partial \theta^{n-m-1}}\right]_{\lambda=\theta}}, \qquad \theta > \lambda \tag{78}$$

it is easy to verify that $\beta(t, \xi)$ satisfies a Volterra equation of the second kind

$$\eta(t, \tau) = \int_0^t \beta(t, \lambda)\beta(\tau, \lambda)d\lambda + \beta(t, \tau), \qquad t < \tau. \tag{79}$$

The resolvent of this equation, $\alpha(t, \xi)$, is by definition a function satisfying the integral equation

$$\beta(t, \xi) = \alpha(t, \xi) + \int_0^t \beta(\lambda, \xi)\alpha(t, \lambda)d\lambda. \tag{80}$$

From this and the preceding equations, it can be deduced that $\alpha(t, \xi)$ satisfies a Fredholm integral equation of the second kind

$$\alpha(t, \xi) = \eta(t, \xi) - \int_0^t \eta(\lambda, \xi)\alpha(t, \lambda)d\lambda, \qquad t > \xi. \tag{81}$$

Now the function $\eta(t, \xi)$ in (81) can be expressed explicitly in terms of $R(t, \tau)$ and its derivatives by expressing the two factors in the denominator of $\eta(t, \xi)$ [see (77)] in terms of $R(t, \tau)$. For example,

$$\left.\frac{\partial^{n-m-1}h(\theta, \lambda)}{\partial \theta^{n-m-1}}\right]_{\lambda=\theta} = \sqrt{(-1)^{n-m-1}R_{2n-2m-1}(\theta, \theta)}. \tag{82}$$

Thus, (81) can be solved, in principle, for $\alpha(t, \xi)$ in terms of $\eta(t, \xi)$. Then, knowing $\alpha(t, \xi)$, one can determine $\beta(t, \xi)$ from (80). Finally, $h(t, \tau)$ is found from the relation (note the interchange in arguments in h)

$$h(\tau, t) = \gamma(t, \tau) - \int_0^t \alpha(t, \lambda)\gamma(\lambda, \tau)d\lambda, \qquad t < \tau \tag{83}$$

where

$$\gamma(t, \tau) = \frac{\dfrac{\partial^{n-m}R(t, \tau)}{\partial t^{n-m}}}{\left.\dfrac{\partial^{n-m-1}h(t, \lambda)}{\partial t^{n-m-1}}\right]_{\lambda=t}}, \qquad t < \tau \tag{84}$$

and the denominator of $\gamma(t, \tau)$ is expressible in terms of $R(t, \tau)$ in the manner cited previously. In summary, by the use of this technique, the solution of the integral equation (73) for $h(t, \xi)$ is reduced to the considerably simpler problem of solving the Fredholm equation (81) for $\alpha(t, \lambda)$.

The problem of factorization is encountered also in the analysis of multipath communication systems [43], [44], where it leads to integral equations of the form (73) defined on a finite interval. Such equations have been discussed by Kailath [43] and Middleton [44].

IV. Randomly-Varying Systems

Linear randomly-varying systems play an important role in problems encountered in the study of such varied phenomena as propagation through time-varying media, reflection from fluctuating targets, turbulence, scattering, amplitude and phase modulation, magnetohydrodynamics and plasma.

Despite their importance, few if any attempts at studying the behavior of randomly-varying systems on a theoretical level were made prior to 1950. The papers published since then deal almost entirely with systems in which the random variations in parameters are stationary. This restriction is an essential one, since from a statistical viewpoint a stationary randomly-varying system behaves in some respects like a time-

[8] The basis functions of a differential operator L of order n are any n linearly independent solutions of the differential equation $Lu=0$.

[9] A Wiener process is the integral of white noise, with the limits of integration being 0 and t.

invariant system. For example, if one is observing the input and output of a time-varying black box B and it is not known whether B is linear or nonlinear, then there is no way of deciding between the two alternatives if B is nonstationary. On the other hand, if B is stationary, then it can be shown that B is linear if it has the following extended superposition property. Let $\{u(t), -\infty < t < \infty\}$ and $\{v(t), -\infty < t < \infty\}$ be two independent stationary processes which are independent also of the random processes governing the behavior of B. Let $R_u(\tau)$ and $R_v(\tau)$ be the correlation functions of the processes resulting from operating with B on the $\{u\}$ and $\{v\}$ processes, respectively. Let $R_{\alpha u+\beta v}(\tau)$ be the correlation function of the process resulting from operating with B on the process $\{\alpha u+\beta v\}$, where α and β are arbitrary real constants. If

$$R_{\alpha u+\beta v}(\tau) = \alpha^2 R_u(\tau) + \beta^2 R_v(\tau) \tag{85}$$

for all α, β, $\{u\}$ and $\{v\}$, then we shall say that B has the superposition property for correlation functions. Clearly, any stationary linear system will have this property, and the converse can also be demonstrated to be true. Consequently, (85) can be used as a basis for determining whether B is linear or nonlinear by observing the input and output of B over periods of time sufficiently long to enable the observer to obtain accurate estimates of the correlation functions involved in (85). It is tacitly understood, of course, that B is such that in the absence of input its state reverts to the ground (unexcited) state as $t \to \infty$.

The correlation function of the output y of a stationary system B which is subjected to a stationary input process $\{u\}$ can be conveniently expressed in terms of the correlation function of B. Specifically, the correlation function of a stationary randomly-varying system B is defined as follows (see Zadeh [45], [46]):

$$R(j\omega, \tau) = E\{H(j\omega, t)H(-j\omega, t+\tau)\} \tag{86}$$

where $H(j\omega, t)$ is the frequency-response function of B, and E denotes the expectation operator. (It is understood that, for each real ω, $\{H(j\omega, t), -\infty < t < \infty\}$ is a stationary random process.)

If $\{u(t)\}$ and $\{H(j\omega, t)\}$ are independent, then it can readily be shown that the correlation function of the output process, $R_y(\tau)$, is related to $R(j\omega, \tau)$ and the correlation function of the input process $R_u(\tau)$ through

$$R_y(\tau) = \frac{1}{2\pi}\int_{-\infty}^{\infty} R(j\omega, \tau)F\{R_u(\tau)\}e^{j\omega\tau}d\omega \tag{87}$$

where $F\{R_u(\tau)\}$ is the Fourier transform of the input correlation function. This relation is of the same form as the equation expressing the output of a time-varying network with frequency-response function $R(j\omega, \tau)$, with the input being $R_u(\tau)$. [Compare (3).] Relations of the form (87) have been applied by Bugnolo [47], [48] to the analysis of scattering by randomly-varying media.

In the special but significant case of a system characterized by an input-output relationship of the form

$$y(t) = u(t - \alpha(t)) \tag{88}$$

the frequency-response function reads

$$H(j\omega, t) = e^{-j\omega\alpha(t)} \tag{89}$$

where $\alpha(t)$ plays the role of a variable time delay. If $\{\alpha(t)\}$ is assumed to be a stationary Gaussian process, then the expression for $R(j\omega, \tau)$ is

$$R(j\omega, \tau) = \exp\{\omega^2[R(\tau) - R(0)]\} \tag{90}$$

where $R(\tau)$ is the correlation function of $\{\alpha(t)\}$. This result was extended by Price [50] to systems for which $H(j\omega, t)$ is of the form

$$H(j\omega, t) = \sum_i a_i e^{j\omega\alpha_i(t)} \tag{91}$$

where the $\{\alpha_i(t)\}$ are independent stationary Gaussian processes. Such systems are encountered in connection with the detection of fluctuating targets—a subject that is discussed at length by Price [51] and Price and Green [52]. A more detailed account of the results obtained by Price, Price and Green, Kailath [52], [53], and others, in connection with the identification of randomly-varying systems will be presented in Part II of this paper.

Although the correlation function $R(j\omega, \tau)$ of a stationary randomly-varying system B, or more generally, the function $R(j\omega, j\omega', \tau)$

$$R(j\omega, j\omega', \tau) = E\{H(j\omega, t)H(j\omega', t+\tau)\} \tag{92}$$

which is the expectation of the product of $H(j\omega, t)$ and $H(j\omega', t+\tau)$, conveys considerable information concerning the statistical characteristics of B, its application is limited to those systems which are characterized by their frequency-response functions. If—as is frequently the case—B is characterized by a differential equation with randomly-varying coefficients, then it is generally simpler to employ more direct techniques for studying the behavior of B in statistical terms. For example, if in

$$a_n(t)\frac{d^n y}{dt^n} + \cdots + a_0(t)y = u(t) \tag{93}$$

each $a_i(t)$ can be expressed as

$$a_i(t) = \bar{a}_i(t) + \epsilon_i(t) \tag{94}$$

where $\bar{a}_i(t)$ is the expected value of $a_i(t)$, and $\epsilon_i(t)$ is in some suitable sense small compared with $\bar{a}_i(t)$, then (93) can be solved by the usual perturbation techniques, with y expressed as the sum of a nonrandom term and

a random term due to the $\epsilon_i(t)$. [$u(t)$ is assumed to be nonrandom.] This approach and elaborations on it have been employed by, among others, Sverdrup [54], Bugnolo [47], [48], and Janos [55]. The key assumption in Janos' work, which was motivated by applications to the multipath problem, is that the coefficients $a_i(t)$ are stationary and stationarily correlated Gaussian processes. In Bugnolo's work, the perturbation technique is used mainly to yield an approximation to the correlation function of a system comprising a randomly-varying propagation medium.

An important problem in the case of a stationary randomly-varying system whose output is a nonstationary process (*e.g.*, due to the effect of initial conditions and/or the application of a nonstationary input) is that of determining the asymptotic behavior of various moments of the output as $t \to \infty$. The analysis of a first-order system

$$\dot{y} + a(t)y = u(t), \tag{95}$$

in which $a(t)$ is a randomly-varying coefficient and u is a nonrandom input, was carried out by Rosenbloom [56] for the case where $\{a(t)\}$ is a Gaussian process, not necessarily stationary. Rosenbloom considered the question of stability of such systems and noted, in particular, that under certain conditions the unit step response of a first-order randomly-varying system can tend to 1 in probability, and yet the mean value of the response may approach $-\infty$ as $t \to \infty$.

A more general analysis of first-order systems in which both $\{a\}$ and $\{u\}$ are stationary and stationarily correlated Gaussian processes was given by Tikhonov [57]. An interesting feature of Tikhonov's method is a simple and yet highly effective artifice for avoiding the difficulties arising out of the dependence of $\{a(t)\}$ and $\{u(t)\}$ processes. Specifically, the general solution of (95) reads

$$y(t) = y(t_0) \exp\left\{-\int_{t_0}^{t} a(\lambda)d\lambda\right\} + \int_{t_0}^{t} d\xi \exp\left\{-\int_{\xi}^{t} a(\lambda)d\lambda\right\} u(\xi). \tag{96}$$

In this form, the calculation of various moments of $y(t)$ is complicated by the fact that the second term on the right involves the product of

$$\exp\left\{-\int_{\xi}^{t} a(\lambda)d\lambda\right\}$$

and $u(\xi)$. These two processes are not independent and, furthermore,

$$\left\{\exp\left\{-\int_{\xi}^{t} a(\lambda)\right\}d\lambda\right\}$$

is not a Gaussian process.

As noted by Tikhonov, this apparent difficulty can be resolved by writing (96) as

$$y(t) = y(t_0) \exp\left\{-\int_{t_0}^{t} a(\lambda)d\lambda\right\} - \frac{\partial}{\partial\gamma}\left[\int_{t_0}^{t} \exp\left\{-\int_{\xi}^{t} ((\lambda)d\lambda\right\} e^{-\gamma u(\xi)}d\xi\right]_{\gamma=0} \tag{97}$$

where γ is a dummy parameter. In this expression, the product of

$$\exp\left\{-\int_{t_0}^{t} a(\lambda)d\lambda\right\}$$

and $u(\xi)$ is replaced by

$$\exp\left\{-\int_{\xi}^{t} a(\lambda)d\lambda - \gamma u(\xi)\right\},$$

which is much easier to deal with. By using this artifice, Tikhonov succeeded in obtaining an explicit expression for the correlation function of $\{y(t)\}$, which enabled him to study the asymptotic behavior of the expectation of $y(t)$ and the variance of $y(t)$ for large t.

For higher-order systems, concrete results concerning the mean-square stability were obtained by Samuels and Eringen [58], [59]. In particular, for a system of the form

$$Ly + \alpha_k(t)\frac{d^k y}{dt^k} = u(t) \tag{98}$$

in which L is a differential operator with constant coefficients, α_k is a randomly-varying parameter with correlation function $\delta(\tau)$, and u is a randomly-varying input, Samuels and Eringen obtained an explicit expression for the expectation $E\{y^2(t)\}$ as a function of t. This permitted them to determine if a system of the type under consideration is stable in mean square, that is, if

$$\lim_{t\to\infty} E\{y^2(t)\} < M,$$

where M is a finite constant. Similar results have been derived independently by Bergen [60].

On a more general level, an extension of Lyapounov's second method to randomly-varying, not necessarily linear, systems was made by Bertram and Sarachik [61]. Essentially, Bertram and Sarachik extended to systems characterized by vector differential equations of the form

$$\dot{\mathbf{x}} = f(\mathbf{x}, \omega, t) \tag{99}$$

where ω denotes an element of a probability space Ω, the basic notions of stability, asymptotic stability, asymptotic stability in the large, etc., and derived sufficient conditions *a la* Lyapounov for various types of stability. For example, the equilibrium solution

$x \equiv 0$ of (99) is said to be stable in the mean if for any $\epsilon > 0$, t_0 exists a $\delta(\epsilon, t_0) > 0$ such that for any initial x (at $t = t_0$) satisfying $\|x(t_0)\| < \delta(\epsilon, t_0)$ ($\|x\|$ denotes the norm of x), the expectation $E\{\|x(t)\|\}$ is smaller than ϵ for all $t \geq t_0$. Then—in a way paralleling that used in the second method of Lyapounov—it can be shown that if there exists a Lyapounov function $V(x, t)$ defined on the state space such that

1) $V(x, t) = 0$ for all t.
2) $V(x, t)$ is continuous in both x and t and the first partial derivatives in these variables exist.
3) For all x in the state space, $V(x, t) \geq \alpha \|x\|$ for some fixed $\alpha > 0$.
4) $E\{dV(x, t)/dt\} \leq 0$ along a solution.

Then the solution $x(t) \equiv 0$ is stable in the mean.

Unfortunately, this and related results do not provide an effective means of determining whether a given randomly-varying system is stable or unstable, since there are no general techniques for finding a Lyapounov function for a given time-varying, much less randomly-varying, system.

Indeed, the only fairly general type of randomly-varying system for which effective stability criteria have been developed is the *piecewise constant* system characterized by differential equations of the form

$$\dot{x} = A_k x, \qquad t_{k-1} \leq t < t_k, \qquad k = 1, 2, \cdots, \tag{100}$$

where x denotes the state vector, A_k is a constant matrix, and either the A_k or the t_k or both are random variables, with the A_k ranging over a finite set of constant matrices. Various special cases of such systems were studied by Bellman [62], Bellman, Harris, and Shapiro [63], Karlin [64], Kalman [65], Bergen [66], and Bharucha [67].

The principal contribution to the stability theory of such systems was made by Bellman, who was the first to point out that the Kronecker product of matrices furnishes a natural way for attacking the problem of stability of systems of this type. Specifically, Bellman considered the asymptotic behavior of products of matrices of the form

$$\boldsymbol{X}_N = \boldsymbol{Z}_N \boldsymbol{Z}_{N-1} \cdots \boldsymbol{Z}_1 \tag{101}$$

where $\boldsymbol{Z}_i$, $i = 1, 2, \cdots, N$, are the elements of a sequence of independent, identically-distributed random matrices. For simplicity, the $\boldsymbol{Z}_i$ are assumed to range over two fixed 2×2 matrices $\boldsymbol{A}$ and $\boldsymbol{B}$, with $\Pr\{\boldsymbol{Z}_i = \boldsymbol{A}\} = \Pr\{\boldsymbol{Z}_i = \boldsymbol{B}\} = 1/2$.

In effect, the case considered by Bellman is the discrete-time version of (100), with $t_k = k$. Thus,

$$x_k = \boldsymbol{Z}_k x_{k-1}, \qquad k = 1, 2, \cdots, \tag{102}$$

and

$$x_N = (\boldsymbol{Z}_N \cdots \boldsymbol{Z}_1) x_0. \tag{103}$$

If the two components of x_N are denoted by x_{1N} and x_{2N}, and the norm of x is defined by

$$\|x\| = x_1^2 + x_2^2,$$

then

$$\|x_N\|^2 = x_0' \boldsymbol{Z}_1' \cdots \boldsymbol{Z}_N' \boldsymbol{Z}_N \cdots \boldsymbol{Z}_1 x_0 \tag{104}$$

where the prime signifies transposition. We are interested in the behavior of the expected value of $\|x_N\|^2$ as $N \to \infty$.

The expected value of $\|x_N\|^2$ could readily be found from (104) if the $\boldsymbol{Z}_i$ commuted with one another and their transposes, for (104) could then be written as

$$\|x_N\|^2 = x_0' \boldsymbol{Z}_1' \boldsymbol{Z}_1 \boldsymbol{Z}_2' \boldsymbol{Z}_2 \cdots \boldsymbol{Z}_N' \boldsymbol{Z}_N x_0, \tag{105}$$

and, on taking the expectation of both sides of (105), we would have

$$E\|x_N\|^2 = x_0' [E(\boldsymbol{Z}_1' \boldsymbol{Z}_1)]^N x_0 \tag{106}$$

since $E(\boldsymbol{Z}_1' \boldsymbol{Z}_1) = E(\boldsymbol{Z}_2' \boldsymbol{Z}_2) = \cdots = E(\boldsymbol{Z}_N' \boldsymbol{Z}_N)$, and the $\boldsymbol{Z}_i$ are mutually independent. Unfortunately, the $\boldsymbol{Z}_i$, in general, do not commute and as a consequence the expectation of $\|x\|^2$ cannot be obtained in the simple fashion of (105) and (106).

To circumvent this difficulty, Bellman employed the notion of the Kronecker product (see, for instance, MacDuffie [68]), which is defined by the relation

$$A \otimes B = \begin{bmatrix} a_{11} b_{11} & a_{11} b_{12} & a_{12} b_{11} & a_{12} b_{12} \\ a_{11} b_{21} & a_{11} b_{22} & a_{12} b_{21} & a_{12} b_{22} \\ a_{21} b_{11} & a_{21} b_{12} & a_{22} b_{11} & a_{22} b_{12} \\ a_{21} b_{21} & a_{21} b_{22} & a_{22} b_{21} & a_{22} b_{22} \end{bmatrix} \tag{107}$$

where A and B are, for simplicity, taken to be 2×2 matrices with elements a_{ij} and b_{ij}, respectively. Similarly, the nth Kronecker power of A is defined as

$$A_{[n]} = A \otimes A \otimes \cdots \otimes A. \tag{108}$$

Thus, the second power of a column 2-vector x is given by

$$\begin{bmatrix} x_1 \\ x_2 \end{bmatrix}_{[2]} = \begin{bmatrix} x_1^2 \\ x_1 x_2 \\ x_2 x_1 \\ x_2^2 \end{bmatrix}. \tag{109}$$

A key property of the Kronecker powers of a matrix is expressed by the following identity.

$$AB_{[m]} = A_{[m]} B_{[m]} \tag{110}$$

which means that the mth Kronecker power of the product of A and B is the product of mth Kronecker powers of A and B. Based on this identity, we can derive from

$$x_k = Zk x_{k-1}, \qquad k = 1, 2, \cdots, N \tag{111}$$

the relation

$$x_{k[2]} = Z_{k[2]}x_{k-1[2]}, \qquad k = 1, \cdots, N \tag{112}$$

and hence,

$$x_{N[2]} = Z_{N[2]}Z_{N-1[2]} \cdots Z_{1[2]}x_{0[2]}. \tag{113}$$

Now we can take the expectation of both sides of (113) without the problems which were encountered in (104) as a result of the noncommutativity of the Z_i. Thus, we obtain

$$E\{x_{N[2]}\} = [E\{Z_{1[2]}\}]^N E\{x_{0[2]}\}. \tag{114}$$

Comparing $x_{N[2]}$ with $\|x\|^2$, it is clear that if $x_{N[2]} \to 0$ as $N \to \infty$, so does $\|x\|^2$, and vice versa. Consequently, the stability in the mean of the system described by (102) is governed by the behavior of $[E\{Z_{1[2]}\}]^N$ as $N \to \infty$. Specifically, if the eigenvalues of the matrix $E\{Z_{1[2]}\}$ lie inside the unit circle, then $E\{x_{N[2]}\} \to 0$ as $N \to \infty$ (assuming that $Ex_{0[2]} < \infty$), and hence, the system is asymptotically stable in the large (in the mean norm). If one or more eigenvalues lie outside the unit circle, the system is unstable in the mean norm. These and other cases are discussed in greater detail by Bharucha [67].

The case where the t_k are random variables with the $t_k - t_{k-1}$, $k = 1, 2, \cdots$, being mutually independent random variables, was first studied by Kalman [69]. Kalman, too, used Kronecker powers of matrices, but his formulas are somewhat complicated by the fact that they relate the expected value of $\|x_N\|^2$ to x_0, rather than the expected value of $x_{N[2]}$ to that of $x_{0[2]}$, as in (114).

The foregoing discussion dealt with the case of free (unforced) systems, that is, systems subjected to zero input. For forced systems, Kalman showed that if the input is bounded, then the response is bounded (in mean square) if and only if the system is stable in the mean square.

Another theorem relating the stability of the free system to the boundedness of the response to bounded inputs was given by Bharucha [69]. Bharucha's theorem is essentially an extension to randomly-varying systems of a theorem due to Perron [70] and Malkin [71]. The statement of Malkin's theorem is as follows: consider a system B characterized by the vector equation

$$\dot{x} = A(t)x + u \tag{115}$$

where x is the state vector, u is the input vector, and $A(t)$ is a bounded ($\|A(t)\| \leq M < \infty$), $0 \leq t < \infty$) and continuous matrix. Then the response of B to any bounded input is bounded if, and only if, there exist positive numbers α and β such that the norm of every solution $x(t)$ of the free system

$$\dot{x} = A(t)x, \tag{116}$$

satisfies the inequality

$$\|x(t)\| \leq \alpha e^{-\beta(t-t_0)}\|x(t_0)\|, \qquad 0 \leq t_0 < t < \infty. \tag{117}$$

In the case of a randomly-varying system, $\{A(t)\}$ is a random process. For such systems, Bharucha shows that if:

1) $\sup_t \|A(t)\|$ is almost surely bounded, and $A(t)$ is almost surely continuous.
2) $E\|G(t, \xi)\| \leq \alpha e^{-\beta(t-\xi)}$, $\alpha \geq 0$, $\beta > 0$ where $G(t, \xi)$ is the transition matrix of (115).
3) The input process is bounded and independent of $\{A(t)\}$, then $\sup_t E\|x(t))\|$ is bounded for every bounded $\|x(t_0)\|$.

In the analyses of the stability in the mean of systems defined by (102), it is usually assumed that the Z_i form a sequence of independent random matrices. This assumption is much too restrictive for many practical purposes. For example, in the case of discrete channels with fading, the successive Z_i have a high degree of dependence. As an approximation to systems of this type, it is natural to assume that the Z_i form a Markov process. The stability in the mean square of such systems was studied by Bharucha, but little if anything is known concerning their behavior when subjected to random inputs.

Acknowledgment

The author is indebted to S. Darlington, C. Desoer, E. Kuh, T. Kailath, R. Price, B. Friedland, D. Bugnolo, B. Bharucha, C. Galtieri, B. Whalen, and C. Süsskind for supplying him with references and sharing their knowledge of various facets of time-varying-network theory.

References

[1] W. R. Bennett, "A general review of linear varying parameter and non-linear circuit analysis." PROC. IRE, vol. 38, pp. 259–263; March, 1950.
[2] L. A. Zadeh, "A general theory of linear signal transmission systems," *J. Franklin Inst.*, vol. 253, pp. 293–312; April, 1952.
[3] K. S. Miller, "Properties of impulsive responses and Green's functions," IRE TRANS. ON CIRCUIT THEORY, vol. CT-2, pp. 26–31; March, 1955.
[4] L. A. Zadeh, "The determination of the impulsive response of variable networks," *J. Appl. Phys.*, vol. 21, pp. 642–645; July, 1950.
[5] A. V. Solodov, "On the transformation of initial conditions on the output of a linear time-varying system into an equivalent input signal," *Avtomat. i Telemekh.*, vol. 19, no. 7, pp. 654–660; 1958.
[6] V. Borsky, "On the properties of impulsive response of varying-parameter systems," *Avtomat. i Telemekh.*, vol. 20, no. 7, pp. 848–855; 1959.
[7] W. D. White, private communication; March 26, 1952.
[8] J. Aseltine, "Transforms for Linear Time-Varying Systems," Dept. of Engrg., University of California, Los Angeles, Tech. Rept. No. 52–1; January, 1952. Also in *J. Appl. Phys.*, vol. 25, pp. 761–764; June, 1954.
[9] —— and D. Trautman, "Transforms for Linear Time-Varying Network Functions," presented at the IRE Natl. Convention, New York, N. Y.; March 3–5, 1952.
[10] H. Davis, "The Analysis and Synthesis of a Class of Linear Time-Varying Networks," Dept. of Engrg., University of California, Los Angeles, Network Res. Bull. No. 7; June, 1953.
[11] E. C. Ho and H. Davis, "Generalized Operational Calculus for Time-Varying Networks," Dept. of Engrg., University of California, Los Angeles, Rept. No. 54-71; July, 1954.
[12] F. R. Gerardi, "Application of Mellin and Hankel transforms to networks with time-varying parameters," IRE TRANS. ON CIRCUIT THEORY, vol. CT-6, pp. 197–208; June, 1959.

[13] J. Peschon, "A Modified Form of the Mellin Transform and its Application to the Optimum Final Value Control Problem," Stanford Electronics Labs., Stanford University, Stanford, Calif., Tech. Rept. No. 2102-1; November, 1959.
[14] E. L. Ince, "Ordinary Differential Equations," Dover Publications, Inc., New York, N. Y.
[15] B. Friedman, "Principles and Techniques of Applied Mathematics," John Wiley and Sons, Inc., New York, N. Y.; 1956.
[16] J. H. Laning and R. H. Battin, "Random Processes in Automatic Control," McGraw-Hill Book Co., Inc., New York, N. Y.; 1956.
[17] T. Laurent, "Transformation frequentielle des lignes artificielles correctrices d'affaiblissement," *Ericsson Technics*, vol. 3, no. 2, pp. 15–25; 1935.
[17a] H. W. Bode, "Network Analysis and Feedback Amplifier Design," D. Van Nostrand Co., Inc., New York, N. Y.; 1945.
[17b] L. A. Zadeh, "Band-pass low-pass transformation in variable networks," PROC. IRE, vol. 38, pp. 1339–1341; November, 1950
[18] W. H. Wattenburg, "Transform Methods and Time-Varying Systems," Electronics Res. Lab., University of California, Berkeley, Rept. No. 321; September 23, 1960.
[19] W. H. Huggins, "Representation and Analysis of Signals, Part 1," The Johns Hopkins University, Baltimore, Md., Rept. No. AFCRC TR-57-357; September, 1957.
[20] D. C. Lai, "Representation and Analysis of Signals—Signal Space Concepts and Dirac's Notation, Part VI," The Johns Hopkins University, Baltimore, Md., Rept. No. AFCRC-TN-60-167; January, 1960.
[21] A. A. Gerlach, "A time-variable transform and its application to spectral analysis," IRE TRANS. ON CIRCUIT THEORY, vol. CT-2, pp. 22–25; March, 1955.
[22] K. S. Narendra, "Integral Transforms for a Class of Time Varying Linear Systems," Cruft Lab., Harvard University, Cambridge, Mass., Tech. Rept. No. 330; October, 1960.
[23] A. M. Batkov, "On the problem of synthesis of linear dynamic systems with variable parameters," *Avtomat. i Telemekh.*, vol. 19, no. 1, pp. 49–54; 1958.
[24] E. A. Coddington and N. Levinson, "Theory of Ordinary Differential Equations," McGraw-Hill Book Co., Inc., New York, N. Y.; 1955.
[25] S. Darlington, "An introduction to time-variable networks," *Proc. Symp. on Circuit Analysis*, University of Illinois, Urbana; 1955.
[26] B. K. Kinarawala, "Analysis of time-varying networks," 1961 IRE INTERNATIONAL CONVENTION RECORD, pt. 4, pp. 268–276.
[27] T. Bashkow, "The *A* matrix, new network description," IRE TRANS. ON CIRCUIT THEORY, vol. CT-4, pp. 117–119; September, 1957.
[28] A. I. Lur'e, "Some Nonlinear Problems in the Theory of Automatic Control," Gos. Izdat. Tekh. Teor. Lit., Moscow, USSR; 1951. (English translation by Ministry of Supply, London, Eng.; 1957.)
[29] S. Darlington, "Nonstationary smoothing and prediction using network theory concepts," IRE TRANS. ON CIRCUIT THEORY (special suppl.), vol. CT-6, pp. 1–11; May, 1959.
[30] ——, "Time-variable transducers," *Proc. PIB Symp. on Active Networks and Feedback Systems*, Polytechnic Institute of Brooklyn, N. Y., April, 1960.
[31] H. W. Bode and C. E. Shannon, "A simplified derivation of linear least-squares smoothing and prediction theory," PROC. IRE, vol. 38, pp. 417–425; April, 1950.
[32] L. A. Zadeh and J. R. Ragazzini, "An extension of Wiener's theory of prediction," *J. Appl. Phys.*, vol. 21, pp. 645–655; July, 1950.
[33] K. S. Miller and L. A. Zadeh, "Solution of an integral equation occurring in the theories of prediction and detection," IRE TRANS. ON INFORMATION THEORY, vol. IT-2, pp. 72–75; June, 1956.
[34] J. H. Laning and R. H. Battin, "An application of analog computers to the statistical analysis of time-variable networks," IRE TRANS. ON CIRCUIT THEORY, vol. CT-2, pp. 44–49; March, 1955.
[35] R. E. Kalman and J. E. Bertram, "General synthesis procedure for computer control of single and multi-loop linear systems," *Trans. AIEE*, vol. 77 (*Application and Industry*, no. 11), pp. 602–609; 1958.
[36] L. Gauthier, "Note sur un casse-pipes," *Societe d'Electronique et d'Automatisme*, Publication No. 319; February 18, 1954.
[37] M. Shinbrot, "On the integral equation occurring in optimization theory with nonstationary inputs," *J. Math. and Phys.*, vol. 36, pp. 121–129; July, 1957.
[38] ——, "A generalization of a method for the solution of the integral equation arising in optimization of time-varying linear systems with nonstationary inputs," IRE TRANS. ON INFORMATION THEORY, vol. IT-3, pp. 220–224; December, 1957.
[39] V. S. Pugachev, "A method of solving the basic integral equation of statistical theory of optimum systems in finite form," *Prikl. Mat. i Mekh.*, vol. 23, no. 1, pp. 3–14; 1959.
[40] ——, "Theory of Random Functions and its Application to Problems of Automatic Control," Fizmatgiz, Moscow, USSR, 2nd ed.; 1960.
[41] A. M. Batkov, "An extension of the method of shaping filters to nonstationary random processes," *Avtomat. i Telemekh.*, vol. 20, no. 8, pp. 1081–1094; 1959.
[42a] P. Levy, "Integration d'une equation integrale non lineaire," *Compt. rend. acad. sci.*, vol. 242, no. 10, pp. 1252–1255; 1956.
[42b] ——, "Random functions: general theory with special reference to Laplacian random functions," *University of California Publ. in Statistics*, vol. 1, pp. 331–390; March, 1953.
[42c] ——, "A special problem of Brownian motion and a general theory of Gaussian random functions," *Proc. 3rd Berkeley Symp. on Problems and Statistics*, Univ. of Calif. Press, Berkeley, vol. 2, pp. 133–175; 1956.
[43] T. Kailath, "Solution of an integral equation occurring in multipath communication problems," IRE TRANS. ON INFORMATION THEORY (Correspondence), vol. IT-6, p. 412; June, 1960.
[44] D. Middleton, "On the detection of stochastic signals in additive normal noise—Part I," IRE TRANS. ON INFORMATION THEORY, vol. IT-3, pp. 86–121; June, 1957.
[45] L. A. Zadeh, "Correlation functions and power spectra in variable networks," PROC. IRE, vol. 38, pp. 1342–1345; November, 1950.
[46] ——, "On a class of stochastic operators," *J. Math. and Phys.*, vol. 32, pp. 48–53; April, 1953.
[47] D. S. Bugnolo, "Correlation functions and power spectra of radio links affected by random dielectric noise," IRE TRANS. ON ANTENNAS AND PROPAGATION, vol. AP-7, pp. 137–141; April, 1959.
[48] ——, "Transport equation for the spectral density of a multipath scattered electromagnetic field," *J. Appl. Phys.*, vol. 31, pp. 1176–1182; July, 1960.
[49] L. A. Zadeh, "Correlation functions and spectra of phase- and delay-modulated signals," PROC. IRE, vol. 39, pp. 425–428; April, 1951.
[50] R. Price, "Statistical Theory Applied to Communication Through Multipath Disturbances," Res. Lab. of Electronics, Mass. Inst. Tech., Cambridge, Tech. Rept. No. 266; September, 1953.
[51] —— and P. E. Green, Jr., "Signal Processing in Radar Astronomy—Communication via Fluctuating Multipath Media," Mass. Inst. Tech., Lincoln Lab., Lexington, Tech. Rept. No. 234; October, 1960.
[52] T. Kailath, "Sampling Models for Linear Time-Variant Filters," Research Lab. of Electronics, Mass. Inst. Tech., Cambridge, Tech. Rept. No. 352; May, 1959.
[53] ——, "Correlation detection of signals perturbed by a random channel," IRE TRANS. ON INFORMATION THEORY, vol. IT-6, pp. 361–366; June, 1960.
[54] M. Sundstrom, "Some statistical problems in the theory of servomechanisms," *Arkiv. Mat.*, vol. 2, pp. 139–246; 1952.
[55] W. Janos, "On Estimating the Solution to a Class of Multipath Problems," presented at URSI Fall Meeting, Boulder, Colo.; December 13, 1960.
[56] A. Rosenbloom, "Analysis of linear systems with randomly time-varying parameters," *Proc. of PIB Symp. on Information Networks*, Polytechnic Institute of Brooklyn, N. Y., pp. 145–153; 1954.
[57] V. I. Tikhonov, "The effect of fluctuations on simplest parametric systems," *Avtomat. i Telemekh.*, vol. 19, no. 8, pp. 717–724; 1958.
[58] J. C. Samuels and A. C. Eringen, "On stochastic linear systems," *J. Math. and Phys.*, vol. 28, pp. 83–103; July, 1959.
[59] J. C. Samuels, "On the mean square stability of random linear systems," IRE TRANS. ON CIRCUIT THEORY (special suppl.), vol. CT-6, pp. 248–259; May, 1959.
[60] A. R. Bergen, "Random Linear Systems: A Special Case," AIEE Paper No. 61-72; February, 1961.
[61] J. E. Bertram and P. E. Sarachik, "Stability of circuits with randomly time-varying parameters," IRE TRANS. ON CIRCUIT THEORY (special suppl.), vol. CT-6, pp. 260–270; May, 1959.
[62] R. Bellman, "Limit theorems for non-commutative operations, I," *Duke Math. J.*, vol. 21, pp. 491–500; September, 1954.
[63] R. Bellman, *et al.*, "Studies in Functional Equations Occurring in Decision Processes," The RAND Corp., Santa Monica, Calif., Paper No. 382; 1952.
[64] S. Karlin, "A Mathematical Treatment of Learning Models," The RAND Corp., Santa Monica, Calif., Res. Memo No. 921; 1952.
[65] R. E. Kalman, "Analysis and Synthesis of Linear Systems Operating on Randomly Sampled Data," Ph.D. dissertation, Columbia University, New York, N. Y.; August 10, 1957.

[66] A. R. Bergen, "Stability of systems with randomly time-varying parameters," IRE TRANS. ON AUTOMATIC CONTROL, vol. AC-5, pp. 265–269; September, 1960.
[67] B. Bharucha, "Stability of Random Linear Systems with Markov Parameters, I," Electronics Res. Lab., Dept. of Elec. Engrg., University of California, Berkeley, Rept. No. 289; June, 1960.
[68] C. C. MacDuffie, "The Theory of Matrices," Chelsea Publishing Co., New York, N. Y.; 1956.
[69] B. Bharucha, "On the Stability of Random Systems," Ph.D. dissertation, Dept. of Elec. Engrg., University of California, Berkeley; June, 1961.
[70] O. Perron, "The stability problem in differential equations," *Math. Z.*, vol. 32, no. 5, pp. 703–728; 1930. (See also no. 3, pp. 465–473.)
[71] I. G. Malkin, *Sbornik Nauch Trudov Kazan*, Aviatzinova Inst., no. 3, 1935; no. 7, 1937. (Available in English as *Am. Math. Soc. Trans.*, no. 20; 1950.

ADDITIONAL PAPERS

[72] B. S. Tsybakov, "The capacity of multipath channels," *Radiotekh. i Electron.*, vol. 4, no. 9, pp. 1427–1433; 1959.
[73] A. Rosenbloom, *et al.*, "Analysis of linear systems with randomly varying inputs and parameters," 1955 IRE CONVENTION RECORD, pt. 4, pp. 106–118.
[74] D. Mintzer, "Wave propagation in a randomly inhomogeneous medium," *J. Acoust. Soc. Am.*, vol. 25, pt. 1, pp. 922–927, September, 1953; vol. 25, pt. 2, pp. 1107–1110, November, 1953; vol. 26, pp. 186–190, March, 1954.
[75] L. E. Franks and I. W. Sandberg, "An alternative approach to the realization of network transfer functions: the N-path filter," *Bell Sys. Tech. J.*, vol. 39, pp. 1321–1350; September, 1960.
[76] R. E. Kalman, "A new approach to linear filtering and prediction problems," *J. Basic Engrg.*, vol. 82D, pp. 35–45; March, 1960.
[77] I. A. Boguslavskii, "On the filtering of a class of non-stationary random processes," *Avtomat. i Telemekh.*, vol. 20, no. 6, pp. 708–720; 1959.
[78] Ya. N. Roitenberg, "A method for the construction of Lyapounov functions for linear systems with variable coefficients," *Prikl. Mat. i Mekh.*, vol. 22, No. 2, pp. 167–172; 1958.
[79] R. E. Bellman, "Stability Theory of Differential Equations," McGraw-Hill Book Co., Inc., New York, N. Y.; 1953.
[80] A. N. Sklarevitch, "On the representation of a time-varying differential operator-polynomial as a sum of time-invariant operators," *Avtomat. i Telemekh.*, vol. 22, no. 3, pp. 297–305; 1961.
[81] D. I. Gladkov, "On the synthesis of linear automatic control systems," *Avtomat. i Telemekh.*, vol. 22, no. 3, pp. 306–313; 1961.
[82] ——, "Synthesis of linear time-varying dynamical systems," *Publ. Zhukovski VVIA Inst.*, no. 753, 1959.
[83] A. V. Solodov, "Statistical analysis of non-stationary processes in linear systems by the use of inverse simulating devices," *Avtomat. i Telemekh.*, vol. 19, no. 4, pp. 312–324; 1958.
[83a] P. S. Matveyev, "The determination of optimal impulse response functions in the presence of internal noise," *Avtomat. i Telemekh.*, vol. 21, pp. 286–292; March, 1960.
[83b] V. S. Baranova and A. A. Pervozvanskii, "Parametric phenomena in simplest continuous extremal control systems," *Avtomat. i Telemekh.*, vol. 21, pp. 1250–1253; September, 1960.
[83c] E. A. Barbasin, "On the estimation of maximum deviation from a prescribed trajectory," *Avtomat. i Telemekh.*, vol. 21, pp. 1341–1351, October, 1960. (Also pp. 941–950; July, 1960.)
[83d] B. E. Rudnitskii, "The determination of transfer functions of some time-varying systems," *Avtomat. i Telemekh.*, vol. 21, pp. 1565–1575; December, 1960.
[83e] Ts. G. Litovtchenko, "Analytical solution of linear equations describing a class of dynamic systems with time-varying parameters," *Avtomat. i Telemekh.*, vol. 22, pp. 457–465; April, 1961.
[84] J. B. Cruz and M. E. Van Valkenburg, "The synthesis of models for time-varying linear systems," *Proc. PIB Symp. on Active Networks and Feedback Systems*, Polytechnic Institute of Brooklyn, N. Y.; April, 1960.
[85] J. R. MacDonald and D. E. Edmonson, "Exact solution of a time-varying capacitance problem," PROC. IRE, vol. 49, pp. 453–466; February, 1961.
[86] A. D. Wheelon, "Radio wave scattering by tropospheric irregularities," *J. Res. NBS*, vol. 63D, pp. 205–233; September–October, 1959.
[87] R. A. Silverman, "Locally Stationary Random Processes," Inst. of Math. Sci., New York, N. Y., Res. Rept. No. MME-2; April, 1957.
[88] A. V. Solodov, "Elements of the theory of linear systems with varying parameters," *Publ. Dzerzhinsky AIA Inst.*; 1958.
[89] S. Hayashi and H. Nishihara, "New Method of Analysis of Interrupted Electric Circuits of the Third Genus, with its Application to Harmonic Producer Circuits," Engrg. Res. Inst., Kyoto University, Kyoto, Japan, Tech. Rept. No. 15; December, 1953.
[90] T. Watanabe, "Introduction of the translational operator in frequency domain and treatment of certain linear differential equations, I, II," *Mem. Coll. Sci., Univ. Kyoto*, vol. 28, no. 4; 1958.
[91] T. Kasami and H. Ozaki, "Periodically variable linear networks," *J. Inst. Elec. Commun. Engrs. Japan*, vol. 43, pp. 590–597; May, 1960.
[92] Yu. M. Kozlov, "On the design of follower systems with self-regulating parameters," *Bull. Acad. Sci. USSR, Energetics and Automation*, no. 2, pp. 65–70; March–April, 1959.
[93] B. E. Keiser, "The linear input-controlled variable-pass network," IRE TRANS. ON INFORMATION THEORY, vol. IT-1, pp. 34–39; March, 1955.
[94] A. M. Batkov and V. V. Solodovnikov, "On a method of determination of optimal characteristics of a class of self-adjusting systems," *Avtomat. i Telemekh.*, vol. 18, no. 5, pp. 377–391; 1957.
[95] E. Henze, "Abriss einer Verallgemeinerten Filtertheorie," *Arch. elekt. Übertragung*, vol. 10, no. 12, pp. 541–551; 1956.
[96] R. C. Booton, "An optimization theory for time-varying linear systems with nonstationary statistical inputs," PROC. IRE, vol. 40, pp. 977–981; August, 1952.
[97] M. Morduchow and L. Galowin, "On double-pulse stability criteria with damping," *Quart. Appl. Math.*, vol. 10, pp. 17–23; April, 1952.
[98] L. A. Pipes, "Analysis of linear time-varying circuits by the Brillouin-Wentzel-Kramers method," *Commun. and Electronics*, Paper 54–183; March, 1954.
[99] ——, "Matrix analysis of linear time-varying circuits," *J. Appl. Phys.*, vol. 25, pp. 1179–1185; September, 1954.
[100] C. P. Gadsden, "An electrical network with varying parameters," *Quart. Appl. Math.*, vol. 8, pp. 199–205; July, 1950.
[101] W. J. Duncan, "Solution of ordinary linear differential equations with variable coefficients by impulsive admittances," *Quart. J. Mech. and Appl. Math.*, vol. 6, pt. 1, pp. 122–127; month, 1953.
[102] B. Friedland, "Time-varying sampled-data systems," *Proc. 2nd Midwest Symp. on Circuit Theory*, Michigan State University, East Lansing, December 3–4, 1956.
[103] ——, "A technique for the analysis of time-varying sampled-data systems," *Trans. AIEE*, vol. 73 (*Applications and Industry*), pp. 407–414; January, 1957.
[104] ——, "Time-varying analysis of a guidance system," *Trans. AIEE*, vol. 75 (*Applications and Industry*), pp. 75–81; May, 1958.
[105] ——, "Filtering and prediction of nonstationary sampled-data," *Inform. and Control*, vol. 1, pp. 297–313; December, 1958.
[106] ——, "Sampled-data control systems containing periodically varying members," *Proc. of Congress of Internatl. Federation of Automatic Control*, Moscow, USSR; June, 1960.
[107] L. A. Zadeh, "Frequency analysis of variable networks," PROC. IRE, vol. 38, pp. 291–299; March, 1950.
[108] ——, "Circuit analysis of linear varying-parameter networks," *J. Appl. Phys.*, vol. 21, pp. 1171–1177; November, 1950.
[109] ——, "On stability of linear varying-parameter systems," *J. Appl. Phys.*, vol. 22, pp. 402–405; April, 1951.
[110] ——, "Initial conditions in linear varying-parameter systems," *J. Appl. Phys.*, vol. 22, pp. 782–786; June, 1951.
[111] ——, "Time-dependent heaviside operators," *J. Math. and Phys.*, vol. 30, pp. 73–78; July, 1951.
[112] ——, "Applications of time-variable network theory," *Proc. Symp. on Circuit Analysis*, University of Illinois, Urbana, pp. 6.1–6.14; 1955.
[113] D. B. Duncan, "Response of linear time-dependent systems to random inputs," *J. Appl. Phys.*, vol. 24, pp. 609–611; May, 1953.
[114] G. W. Johnson and F. G. Kilmer, "Integral Transforms for Algebraic Analysis and Design of a Class of Linear-Variable and Adaptive Control Systems," IRE Paper No. 60AC-10; September, 1960.
[115] J. S. Bendat, "Exact integral equation solutions and synthesis for a large class of optimum time variable linear filters," IRE TRANS. ON INFORMATION THEORY, vol. IT-3, pp. 71–80; March, 1957.
[116] J. A. Aseltine, "A transform method for linear time-varying systems," *J. Appl. Phys.*, vol. 25, pp. 761–764; June, 1954.
[117] J. M. Manley, "Some properties of time-varying networks," IRE TRANS. on CIRCUIT THEORY, vol. CT-7, pp. 69–78; August, 1960.
[118] A. L. Bolle, "Application of complex symbolism to linear variable networks," IRE TRANS. on CIRCUIT THEORY, vol. CT-2, pp. 32–35; March, 1955.

[119] A. H. Koschmann, "Time-varying filters for nonstationary signals on a finite interval," 1955 IRE CONVENTION RECORD, pt. 4, pp. 102–106.
[120] I. Matyash, "Methods of analog computer solution of linear differential equations with variable coefficients," *Avtomat. i Telemekh.*, vol. 20, pp. 813–821; July, 1959.
[121] J. A. Aseltine and R. R. Favreau, "Weighting functions for time-varying feedback systems," PROC. IRE, vol. 42, pp. 1559–1564; October, 1954.
[122] G. P. Tartakowskii, "Application of simulation in analyzing linear pulse systems with variable parameters," *Avtomat. i Telemekh.*, vol. 20, pp. 559–566; May, 1959.
[123] ——, "Time and frequency characteristics of linear pulse systems with variable parameters," *Radiotekh. i Elektron.*, vol. 1, no. 12; 1956.
[124] S. V. Mal'chikov, "On the synthesis of linear automatic control systems with variable parameters," *Avtomat. i Telemekh.*, vol. 20, pp. 1543–1549; December, 1959.
[125] C. A. Desoer, "Steady-state transmission through a linear network containing a single time-varying element," IRE TRANS. ON CIRCUIT THEORY, vol. CT-6, pp. 244–252; September, 1959.
[126] J. B. Cruz, Jr., "A generalization of the impulse train approximation for time-varying linear system synthesis in the time domain," IRE TRANS. ON CIRCUIT THEORY, vol. CT-6, pp. 393–394; December, 1959.
[127] B. J. Leon, "A frequency-domain theory for parametric networks," IRE TRANS. ON CIRCUIT THEORY, vol. CT-7, pp. 321–329; September, 1960.
[128] W. R. Bennett, "Steady-state transmission through networks containing periodically operated switches," IRE TRANS. ON CIRCUIT THEORY, vol. CT-2, pp. 17–21; March, 1955.
[129] A. Fettweis, "Steady-state analysis of circuits containing a periodically-operated switch," IRE TRANS. ON CIRCUIT THEORY, vol. CT-6, pp. 252–260; September, 1959.
[130] C. A. Desoer, "A network containing a periodically operated switch solved by successive approximations," *Bell Sys. Tech. J.*, vol. 36, pp. 1403–1428; November, 1957.
[131] L. A. Pipes, "Four methods for the analysis of time-variable circuits," IRE TRANS. ON CIRCUIT THEORY, vol. CT-2, pp. 4–12; March, 1955.
[132] J. Brodin, "Analysis of time-dependent linear networks," IRE TRANS. ON CIRCUIT THEORY, vol. CT-2, pp. 12–16; March, 1955.
[133] M. C. Herrero, "Resonance phenomena in time-varying circuits," IRE TRANS. ON CIRCUIT THEORY, vol. CT-2, pp. 35–41; March, 1955.
[134] H. C. Hsieh, "On the Optimum Synthesis of Discrete Multipole Filters with Random and Non-Random Inputs," Dept. of Engrg., University of California, Los Angeles, Rept. No. 60-106; December, 1960.
[135] E. B. Stear and A. R. Stubberud, "Nonstationary Signal Flow Graph Theory," Dept. of Engrg., University of California, Los Angeles, Rept. No. 60-64; November, 1960.
[136] V. Doležal, "On the application of operators in the theory of linear dynamical systems," *Aplikace Matematiky* (Prague), no. 1, pp. 36–67; 1961.
[137] U. P. Leonov, "On an approximate method of synthesis of optimal linear systems for the extraction of a useful signal in noise," *Automat. i Telemekh.*, vol. 20, pp. 1071–1080; August, 1959.
[138] S. Duinker, "General properties of frequency converting networks," *Philips Res. Repts.*, vol. 13, pp. 37–38, February; pp. 101–148, April, 1958.

Compatible Single Sideband*

LEONARD R. KAHN†, SENIOR MEMBER, IRE

Summary—**A compatible single-sideband (CSSB) wave is a new type of modulated wave which is compatible with existing AM receivers. Spectrum analysis and measurement indicate that if the CSSB system is applied to a conventional AM broadcast transmitter, a desired-to-undesired sideband ratio of slightly better than 30 db will be achieved under normal modulation conditions. Also described is a beat frequency problem which introduces a special type of undesired sideband component. This component falls extremely close to the carrier and should not be present during the vast majority of program conditions. Thus, the technique meets the requirement of theoretically distortion-free envelope characteristics with a good desired-to-undesired sideband ratio.**

Measurements are described which show the advantages of the system. It appears that the main advantage of the technique is to reduce co- and adjacent-channel interference effects. CSSB also provides a higher fidelity signal when received by conventional inexpensive broadcast receivers. The on-the-air tests indicated good listener acceptance of the new system.

The system also appears to have applications in communications service where cost and size bar the use of conventional sideband techniques. The technique does not suffer from Doppler shift difficulties.

* Received by the IRE, June 16, 1961; revised manuscript received, August 7, 1961.
† Kahn Research Laboratories, Inc., Freeport, Long Island, N. Y.

INTRODUCTION

THE FACT that there is a severe shortage of spectrum space available to the broadcaster and to the high-frequency communicator has been stressed in a number of persuasive papers.[1,2]

One method of greatly easing this critical shortage is the use of the SSB. The number of SSB transmitters in operation has greatly increased during the past decade because of this serious spectrum shortage and because of a number of other operational advantages of SSB. However, there are many services that cannot justify the expense and complexity of conventional SSB equipment. These services include broadcasting and many mobile communication systems. The purpose of this paper is to describe a new type of SSB wave called compatible single sideband (CSSB), which appears to be

[1] D. G. Fink, "Danger! The radio spectrum is bursting at seams," *J. Franklin Inst.*, vol. 261, pp. 477–493; May, 1956.
[2] G. Jacobs and E. T. Martin, "The dwindling high-frequency spectrum," 1961 IRE INTERNATIONAL CONVENTION RECORD, pt. 8, pp. 179–195. (To be published in IRE TRANS. ON COMMUNICATIONS SYSTEMS.)

suitable for broadcasting and most mobile communications systems.

The CSSB technique discussed in this paper has recently been defined by the CCIR in the following manner: "A single-sideband transmission is considered to be compatible if it can be received on the existing conventional double-sideband receivers without any modifications whatsoever and with satisfactory quality of reception."[3]

The main advantage of CSSB over conventional SSB operation is that it may be received on the millions of conventional receivers presently in service in homes and vehicles. Equipment has been manufactured for adapting existing transmitters, and extensive tests have been run to prove that this system is completely compatible with AM transmitters as well as with AM receivers.

It might be best, right at the outset, to stress the point that the CSSB system is an altogether different system from the one proposed by the author for conventional SSB communications, that is, the envelope elimination and restoration (EER) SSB system.[4,5] The EER system, though compatible with existing class-C AM transmitters, requires the use of conventional SSB receivers and may not be received without distortion on AM receivers. The EER system was introduced in 1952 and now enjoys considerable commercial application in standard point-to-point long distance circuits.

Over the years there have been constant efforts to reduce co- and adjacent-channel interference by the use of SSB in the broadcast field. The methods proposed, while ingenious, have not received commercial acceptance. Early attempts in Great Britain and the Netherlands[6,7] suggested that double-sideband transmission be utilized for low audio-frequency components and SSB transmission be used for high audio-frequency components. Those systems depended upon the fact that, at high frequencies, only low percentages of modulation are required. Therefore, conventional SSB waves would be acceptable because, at low percentages of modulation, a conventional full carrier sideband has relatively low envelope distortion. These systems, however, do not reduce greatly co-channel interference and require replacement of many existing transmitters. Because of these limitations, these systems have not gained favor.

Recently, there have been Russian publications[8,9] indicating that intensive research has been conducted in the USSR on this same problem. They call their system "optimum modulation" but it appears that the sideband rejection of this technique is small and there is a relatively high degree of envelope distortion. It is interesting to note that Kliagin[9] provides a detailed analysis of what he calls a "Kahn transmitter." The curve of the PM wave of such a transmitter is shown in his Fig. 3. On this same figure a curve for a perfect system (but one undiscovered by Kliagin) is provided and this curve is very similar to the one described in the following discussion of the actual CSSB system.

A recent article[10] in these PROCEEDINGS described a CSSB technique developed at the University of Calcutta. The technique developed by Chakrabarti was used several years ago by this author but, because of the complexity of the equipment required for synthesizing the desired type of wave, Chakrabarti's procedure is in some respects less satisfactory than the method disclosed in this paper. It is, however, quite interesting to note that appreciable advances are being made independently at a number of research organizations throughout the world.

The first installation of equipment utilizing the CSSB technique described here was made in August, 1956, at the U. S. Voice of America megawatt station in Munich, Germany. This equipment utilized a simplified CSSB technique.

I. Problems of Utilizing the Conventional SSB Full Carrier System in AM Broadcasting Service

The reader may wonder why a SSB plus full carrier wave is not acceptable for transmission to conventional AM receivers. This section describes in some detail the reason why such two-spectral component waves are not acceptable for broadcast and high-quality AM reception.

The envelope of a carrier plus only one sideband component wave is highly distorted at high percentages of modulation. Actually, when the sideband approaches the level of the carrier, the envelope distortion is approximately 24 per cent.

Figs. 1 and 2 are curves indicating distortion for conventional SSB waves. They are taken from the section on CSSB of the *N.1B Handbook* written by Harmon.[11] Fig. 1 shows the envelope function for a carrier plus SSB wave. This would be the waveshape produced at the output of a diode demodulator or any other "linear" detector in the conventional AM receiver. It should be noted that the distortion is very noticeable at high percentages of modulation.

[3] "Resolutions, Questions, and Study Programmes," Vol. 2, CCIR, 9th Plenary Assembly, Los Angeles, Calif., pp. 165–166; 1959.
[4] L. R. Kahn, "Single-sideband transmission by envelope elimination and restoration," PROC. IRE, vol. 40, pp. 803–806; July, 1952.
[5] L. R. Kahn, "Comparison of linear single-sideband transmitters with envelope elimination and restoration single-sideband transmitters," PROC. IRE, vol. 44 pp. 1706–1712; December, 1956.
[6] P. P. Eckersley, "Asymmetric-sideband broadcasting," PROC. IRE, vol. 16, pp 1041–1092; September, 1938.
[7] N. Koomans, "Asymmetric-sideband broadcasting," PROC. IRE, vol. 27, pp. 687–690; November, 1939.
[8] S. I. Tetal'baum and Iu. G. Grinevich, "Description of the results of experimental examination of the basic principle of the theory of optimal amplitude-phase modulation," *Radiotekhnika* (*Moscow*), vol. 12; December, 1957.
[9] L. E. Kliagin, "Spectrum analysis in amplitude-phase modulation," *Radiotekhnika* (*Moscow*), vol. 15, pp. 67–73; August, 1960.
[10] R. M. Golden, M. R. Schroeder and N. B. Chakrabarti, "Discussion of 'combined AM and PM for a One-Sided Spectrum'," PROC. IRE, vol. 49, pp. 1094–1095; June, 1961.
[11] R. N. Harmon, "Experience with CSSB at KDKA," in "National Association of Broadcasters Engineering Handbook," A. P. Walker, Ed., McGraw-Hill Book Co., Inc., New York, N. Y., pp. 8-41 to 8-52; 1960.

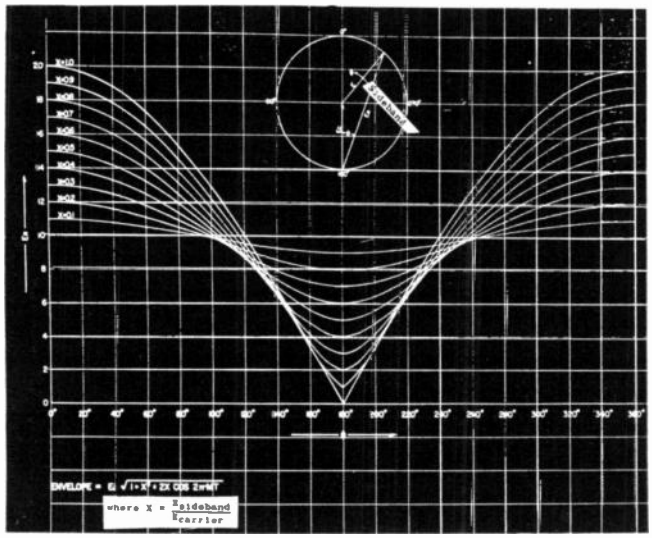

Fig. 1—Envelope wave shape of two-element carrier plus SSB wave for various ratios of sideband-to-carrier.

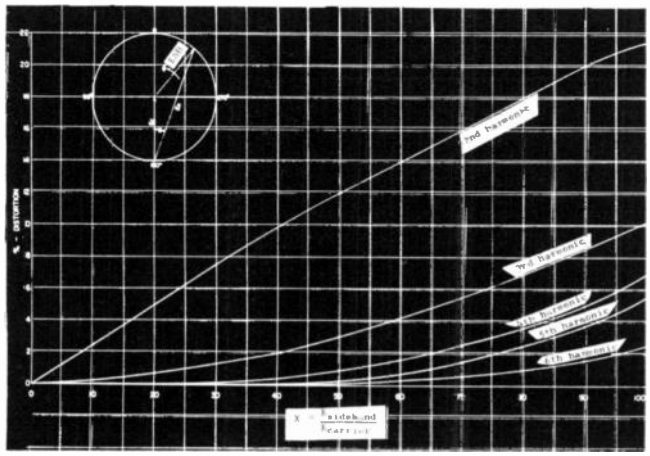

Fig. 2—Fourier series components of two-element envelope wave-shape for various ratios of sideband-to-carrier level.

Fig. 2 shows the results of a Fourier series analysis of the envelope function which was shown in Fig. 1. As mentioned before, the total harmonic distortion is approximately 24 per cent when the sideband level equals the carrier level.

Such distortion is obviously unacceptable for broadcast service and would seriously degrade even conventional communications systems. Also, it may be seen that, since the distortion accounts for much of the negative modulation swing, complete 100 per cent modulation cannot be achieved. Because of this, the maximum modulation value is equivalent to only 67 per cent of the average value of the wave. In addition, there is a severe "carrier shift;" that is, the average value of the modulated wave varies with modulation and this would slightly disturb the AVC operation of the receiver. Thus, we see that a conventional SSB wave is not suitable for high-quality broadcast use.

II. Practical Background Considerations

In analyzing any new system that claims to be compatible with existing equipment, it is necessary to understand fully the characteristics of the "existing" equipment. Careful study and experimentation with existing AM transmitters reveals that almost all AM broadcast transmitters and the vast majority of communciation transmitters are perfectly suitable for CSSB service. Generally, the transmitters are considerably better in terms of frequency response and distortion than the associated receivers. The reason for this is that the cost of the transmitter is less severely limited because generally the number of receivers far exceeds the number of transmitters. Thus, the limitation as to quality of the CSSB system, as well as the conventional AM system, is due to receiver limitations.

A number of surveys have shown that the conventional AM receiver designed for broadcast operation is severely restricted in bandwidth. A recent survey reported by a noted pioneer in radio and television research, R. B. Dome of the General Electric Company, indicated that the average broadcast receiver's bandwidth is exceedingly narrow. Dome's survey is concluded as follows:

> The 6 db bandwidths of 135 broadcast receivers indicate that some 50% of the receivers had a total IF bandwidth of less than 7.5 kc which is equivalent to less than 3.75 kc audio response at the −6 db point when conventional AM signals are received. He also reported that 79% of the receivers tested ran less than 9.5 kc total bandwidth, thus producing a high frequency −6 db cutoff point of 4.75 kc for conventional AM reception. Furthermore, his studies showed that only 9% of the receivers had a −6 db audio response to a double-sideband AM wave of 5.75 kc or higher.

It is interesting to note that these figures appear to correlate fairly well with figures provided by the British.[12]

The reason for this poor receiver frequency response is the necessity to compromise between adjacent channel interference rejection and good fidelity. Also, in inexpensive receiver design, the number of tuned circuits and IF transformers must be minimized; therefore, the shape factor of the selectivity curve generally leaves much to be desired. Fig. 3 shows an over-all fidelity characteristic of a typical home receiver of recent design.

The second basic practical fact that must be considered in an analysis of the CSSB system is the type of message to be transmitted. The CSSB system has been proposed for broadcast service and voice communications. Therefore, it is important to consider the characteristics of voice and musical waves.

It is well known that voice and musical waves are wideband signals in the sense that they cover many octaves. *However, the energy density is much higher at the*

[12] E. K. Sanderman, "Radio Engineering," Chapman and Hall Ltd., London, England, vol. 2, p. 101; 1953. See the list of characteristics of commercial receivers. Sanderman reports that the −3 db high-frequency audio cutoff point of typical sets were 1.6 kc, 3.7 kc, 3.4 kc, 5.2 kc, and 2 kc.

moderately low frequencies than at the high audio frequencies. But, even though there is a relatively small amount of energy in, say, the 3- to 5-kc range, such frequencies cannot be eliminated without loss of intelligibility. This is especially true under poor signal-to-noise ratio reception conditions. A curve has been published[13] showing the frequency characteristics of a typical musical wave; a curve showing the cumulative characteristic derived from this work is shown in Fig. 4. (A further discussion concerning typical spectra will be found in Section VII.)

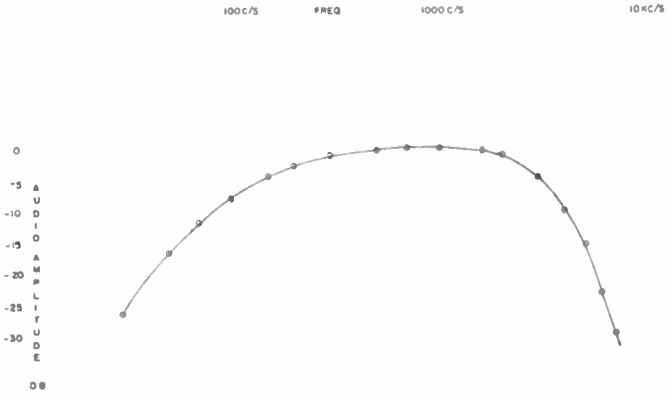

Fig. 3—Frequency response of typical broadcast receiver, RCA Model 9-C-7-EE.

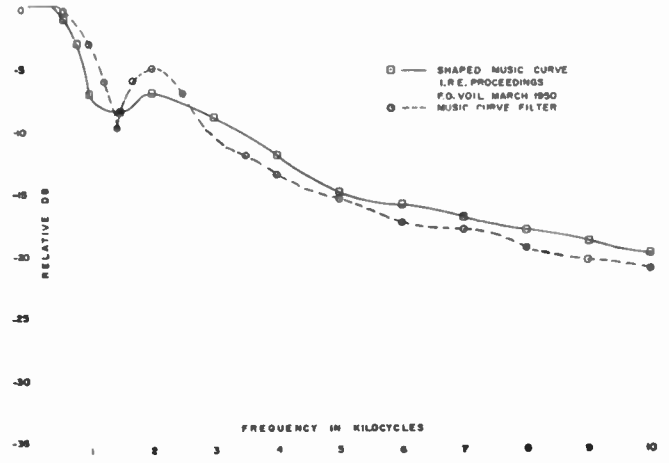

Fig. 4—Voice and music spectrum curve.

III. Basic Structure of the CSSB Wave

A perfect CSSB wave would have the following characteristics:

1) an envelope which reproduces the input modulating wave without nonlinear distortion.
2) a spectrum characteristic limited to a band extending from one side of the carrier and having a bandwidth equal to the highest audio frequency of the modulating signal.

[13] V. O. Voil, "Some problems of disk recording for broadcasting purposes," Proc. IRE, vol. 38, pp. 233–238; March, 1950.

It will be seen in the following discussion that the simultaneous satisfaction of both specifications is contradictive. But, from a practical standpoint, a very close approximation to both specifications can be and has been accomplished.

For broadcast applications, the first specification, the theoretically distortion-free envelope, is paramount. Therefore, some small liberties must be taken with the second specification. In other words, by insisting upon a theoretically distortion-free enevelope, some undesired sideband radiation is produced. However, this undesired radiation is relatively small and the wave is quite suitable for the applications indicated.

A SSB wave is a hybrid modulated wave. That is, SSB waves have both AM components and PM components. Thus, in order to describe an SSB wave, one must define the PM function as well as the AM function.

In the case of CSSB, we assume that the envelope is theoretically free of distortion. Thus, if a sine wave is fed to a perfect CSSB transmitter, the envelope of the radiated waves has a perfect sinusoidal shape. The other defining function of this hybrid modulated wave is the PM component, and research on the CSSB system centered upon the quest for an appropriate PM function. *What was desired was a PM wave that, when amplitude-modulated by the input signal, would concentrate the energy of the total wave in one sideband.* It will be seen that the PM wave is a nonlinear function of the input wave. The procedure used in deriving this PM wave will be described later.

In order to obtain the desired low distortion envelope function for large modulation percentages by a single tone, it is necessary to have at least three spectrum components. This, of course, is true for conventional AM where three components (carrier plus symmetrical upper and lower sidebands) are transmitted when a sinusoidal wave is used to modulate the transmitter. In the AM case, the carrier is located in the center of the spectrum and is surrounded by the upper and lower sideband components.

In the case of CSSB, the carrier is on one side of the wave and first- and second-order sideband components *are both on one side of the carrier.* These three components are necessary at high percentages of modulation but, as will be shown later, at low percentages of modulation only a carrier and a first-order sideband component are required. *Since the high-frequency components of speech and music have relatively small amplitudes, these high-frequency components require only one sideband plus the carrier, and the bandwidth of the CSSB signal can be made approximately equal to the bandwidth of the audio modulating signal.*

Since the procedure used in developing the CSSB system was relatively involved, it might be advantageous to describe briefly the steps taken in performing this work. First of all, analysis was performed on various three-element waves in order to determine the optimum component relationship of a three-element wave. *This*

three-element wave was used as a mathematical "model" for determining the structure of an actual CSSB wave for the case of single-tone modulation.

It might be questioned why the three-element "model" wave was not used as the actual wave. The reason is two-fold: First, such a wave, with the proper component phase and amplitude relationships, would be quite difficult to generate. Second, the three-element model has an inherent envelope distortion of almost 5 per cent. Because the derived CSSB wave is theoretically free of envelope distortion, and in practice has approximately only 1 per cent distortion, the derived system is actually an improvement on the mathematical model.

Once the desired relative amplitudes of the components were determined, it was necessary to calculate the PM component of this three-element mathematical model wave. After the PM component was derived, comparison was made between the PM characteristics of various *two-element carrier-plus-sideband waves* and the desired PM component. Two-element waves were considered because they are simple to produce. Study proved that the summation of the PM components of two different two-element waves closely approximated the desired three-element PM component.

A spectrum analysis was then performed showing that the synthetic PM component, when amplitude-modulated by a perfect sine wave function, would have satisfactory spectrum characteristics. At this point, experimental work was performed to ascertain the actual operating characteristics.

IV. Discussion of Three-Element CSSB Mathematical "Model" Wave and Means for Approximation

From the above discussion of a SSB full-carrier wave, we see that a two-component wave has an envelope function that would be highly distorted and unacceptable as a true compatible system. Therefore, it is necessary to transmit additional components in order to make the wave compatible with conventional AM receivers. In practice, one additional sideband component placed in the desired sideband and separated from the carrier by two times the frequency of a sinusoidal modulation is all that is necessary to make the wave compatible.

Fig. 5 shows the amount of envelope distortion at maximum percentage modulation of a three-element wave for various ratios of second-order sideband component. It is assumed that sinusoidal modulation is used and that the carrier level is varied so that the sum of the carrier plus the second-order sideband just equals the amplitude of the unmodulated carrier. A study of this curve indicates that the distortion varies from zero, at a ratio of 0.5, to about 24 per cent distortion at zero ratio of second-order to first-order sideband voltage. Of course, the 24 per cent envelope distortion figure occurs at the limiting situation where the signal degenerates into a two-element wave.

As mentioned above, the amplitude of the carrier frequency component in this three-element model wave equals the difference between unmodulated carrier amplitude and the second-order sideband component amplitude. Thus, in the 0.5 ratio, 100 per cent single-tone modulation case, the carrier level equals the amplitude of the second-order sideband, and except for a frequency shift, it is the same as a conventional 100 per cent modulated AM wave. The difference is that the carrier is at one side of the spectrum of the wave, instead of in the center as in conventional AM (see Fig. 6).

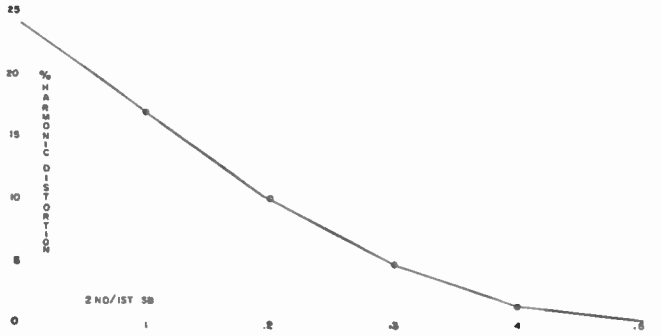

Fig. 5—Total harmonic distortion for three-element CSSB "model" wave as a function of the ratio of the second-order sideband to the first-order sideband at maximum modulation.

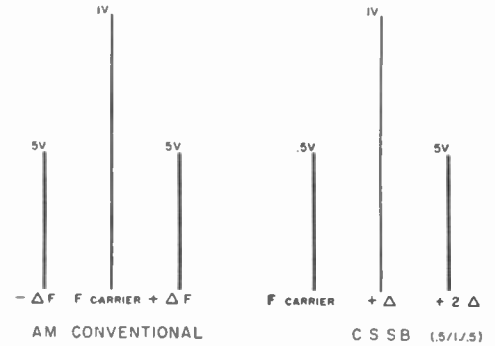

Fig. 6—Spectrum diagram of conventional AM wave and CSSB wave having 0.5 to 1 to 0.5 ratio of carrier to first-order sideband to second-order sideband.

Even though the 0.5-ratio model would appear to be the best choice because of the absence of envelope distortion, other requirements help to determine the choice. These other problems necessitate a lower ratio of second-order sideband to first-order sideband. If two audio signal tones of approximately equal amplitude are fed to the input of the CSSB transmitter, an undesired sideband radiation is produced. In this case, a lower ratio of second- to first-order sideband is preferred, and as will be shown later, a ratio of approximately 0.3 appears to be an acceptable compromise choice.

Another reason for using the carrier/first sideband/second sideband ratio of 0.7/1/0.3 is that at lower percentages of modulation the bandwidth of the signal must not increase. If a larger second-order component were used at maximum modulation, this would not be

true, and the undesired components would be excessive at lower percentages of modulation.

Thus, the three-element mathematical model of a CSSB wave may be described as follows:

$$e = E_{\text{carrier}}[(1 - 0.3m^2)\cos w_c t + m\cos(w_c + w_{Af})t + 0.3m^2\cos(w_c + 2w_{Af})t], \quad (1)$$

where

E_{carrier} = carrier voltage when modulation is absent,
m = envelope modulation factor,
w_c = angular velocity of carrier,
w_{Af} = angular velocity of tone modulation.

At low percentages of modulation, (1) indicates that the second-order component is very small. This can be seen by studying Figs. 1 and 2, which indicate that at low percentage modulation the envelope distortion of a conventional carrier plus a sideband two-element wave is small. Therefore, the requirement of a second-order term decreases as the percentage modulation decreases (see Fig. 7).

Eq. (1) shows that the first-order sideband is a linear function of percentage modulation and that the second-order sideband follows a squared function of percentage modulation. The carrier amplitude at low percentage modulation equals the average amplitude of the wave and gradually decreases as the modulation level increases. Though the model only provides approximate relationships, it appears to fit practical situations quite well, and it has been helpful in deriving some of the techniques used.

It should be stressed that the average amplitude of the actual CSSB wave is constant and does not shift with percentage modulation. In other words, no "carrier shift" is created when CSSB is used. Of course, if the transmitter produces distortion with attendant carrier shift when transmitting conventional amplitude signals, it will produce the same carrier shift when the CSSB system is used.

It should be further stressed that in the actual CSSB system, the mechanism for producing the envelope function is such that theoretically the system is completely free of envelope distortion, and is in that respect superior to the mathematical three-element model. Therefore, assuming a receiver having perfect characteristics, the entire system would be completely free of any harmonic or intermodulation distortion. In practice, measurements at a number of stations show that the total harmonic envelope distortion of the transmitter plus CSSB adapter is within 1 per cent of the distortion of the transmitter.

We have shown that at low percentage modulations only a carrier plus SSB is transmitted. Since the higher frequency components of voice and musical waves are generally of very low amplitude, the spectrum requirement for such an SSB wave is approximately equal to the audio bandwidth, and a wave closely approximating the bandwidth of conventional SSB is generated. When low-frequency high-amplitude signals are transmitted, the second-order sideband is required. But because this second-order sideband falls well within the bandwidth of the signal, it does not increase the bandwidth of the signal but merely increases the density of the spectrum of the wave.

Fig. 7 shows the manner in which the first-order and second-order sidebands vary with percentage modulation, assuming the model defined in (1). We note that, below 30 per cent modulation, the second-order sideband is more than 30 db below the carrier level. This is the reason the spectrum is maintained essentially equal to the audio bandwidth of the modulation.

Fig. 8 was derived from Fig. 7 by utilizing the frequency characteristic of music as illustrated in Fig. 4. The frequency axis indicates the frequency of the component being considered. Thus, at 5 kc one sees that the first-order sideband is 15 db below the amplitude of the low-frequency reference. A 2.5-kc signal produces the second-order component which would appear at 5 kc, and which is 25 db below the low-frequency reference and 10 db below the 5-kc first-order sideband. In addition, the effect of the sideband filter used in this system is shown cutting off the wave sharply above 8 kc. Fig. 8 shows that the first-order sideband, except for the very edge, is considerably greater than the second-order sideband. *Therefore, the second-order sideband does not materially alter the bandwidth of the signal because the band is already occupied by the first-order sideband.* This con-

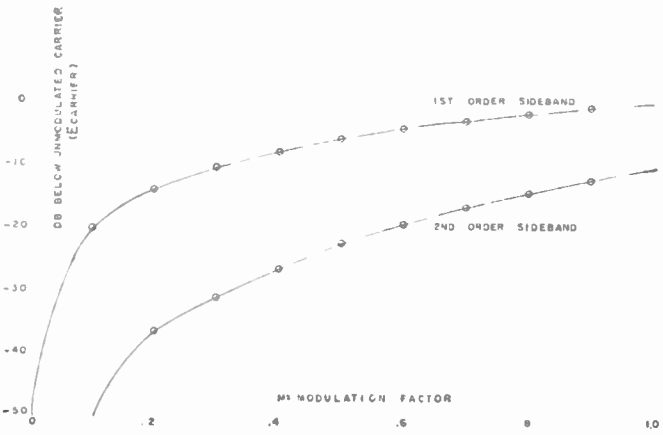

Fig. 7—Curve of amplitude of first-order and second-order sideband components for various amounts of modulation assuming "model" wave having carrier to first-order sideband to second-order sideband ratio of 0.7 to 1 to 0.3 at maximum modulation.

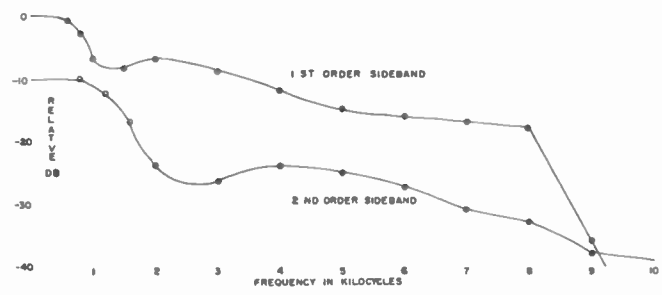

Fig. 8—Amplitude of first-order and second-order sideband components of "model" CSSB wave, assuming spectrum distribution of music shown in Fig. 4.

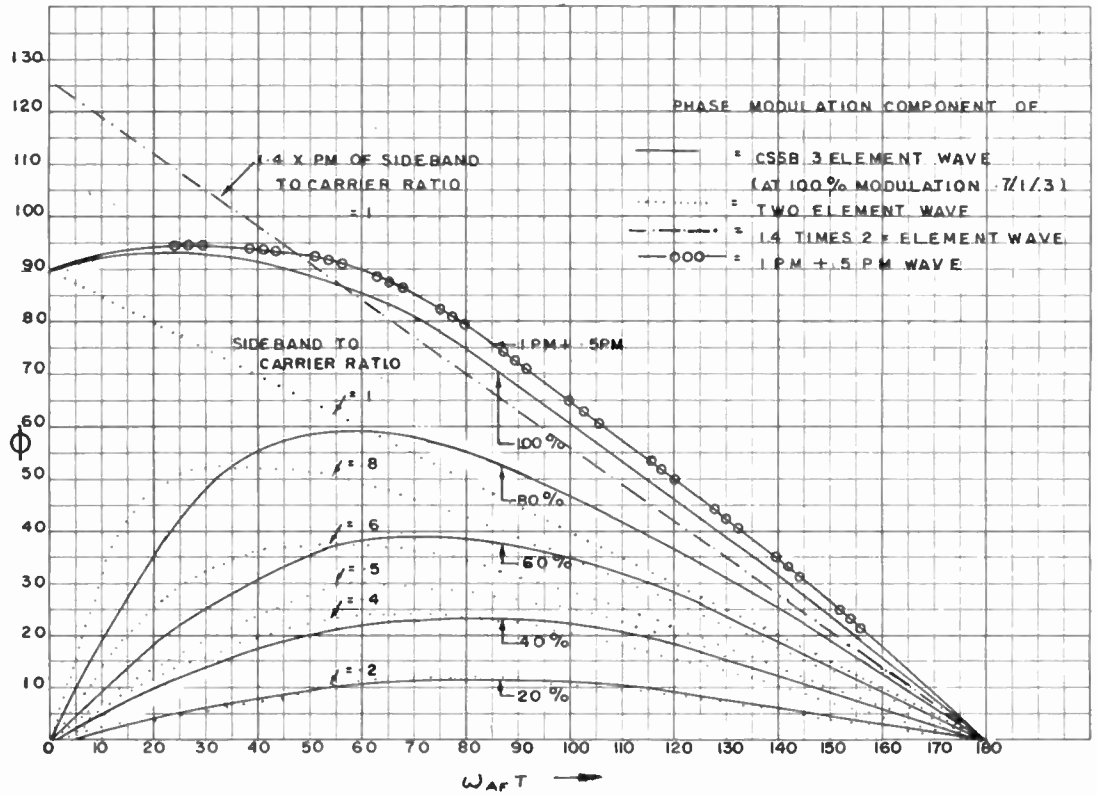

Fig. 9—Phase modulation component of CSSB "model" wave, also of two-element carrier plus sideband wave for various percentage modulation.

clusion is supported by extensive measurements which prove that the spectrum is merely made denser by the second-order sideband and does not increase the bandwidth appreciably over what a normal SSB system would require. It should be recalled that the fact that high-frequency music components are weak is also the basis for the use of pre-emphasis in FM broadcasting and disk recording.

Fig. 9 shows, among other things, a plot of the PM component of the three-element tone model wave having a carrier-to-first-order sideband-to-second-order sideband ratio of 0.7/1/0.3. It should be noted that in Fig. 9 a half cycle of the PM component is shown. This wave is an odd function about $t=0$, that is, $f(t)=-f(-t)$.

Fig. 9 also shows curves of the PM component of the model signal at low percentage modulation. Eq. (1) was used in calculating these curves.

The dotted curves shown in Fig. 9 represent the PM component of a two-element wave having a carrier-to-sideband ratio as indicated on the curve. It is seen that, except at very low percentages of modulation, the PM for the two-element case is considerably different from that for the desired CSSB case.

The phase-modulated wave produced by adding the PM component of a two-element wave having a carrier-to-sideband ratio of 1 to the PM component of a two-element wave having a carrier-to-sideband ratio of 0.5 closely approximates the PM component of the desired CSSB wave at 100 per cent modulation. At moderate percentages of modulation, the PM component of a two-element wave has too large an amount of phase swing for certain portions of the modulating cycle, and too small a phase swing at other segments of the modulating cycle. In order to satisfy this problem, nonlinear circuits were designed to produce a summation of two PM components, which closely approximate the PM component of the two- and three-element CSSB models.

For instance, at 60 per cent modulation, a sideband-to-carrier ratio of 0.5 would be added to one of about 0.1. Thus, by proper use of nonlinear curves a close fit can be obtained for various percentages of modulation. The panoramic pictures shown in Fig. 10 indicate that the technique used was successful in producing the proper PM component. Thus, this PM wave when amplitude modulated by a wave derived from the input wave produces the desired spectrum characteristic.

Fig. 10(a)–(o) (pp. 1510–1512) were made by taking panoramic pictures of a small laboratory CSSB transmitter. In taking the pictures in Fig. 10(a)–(l), this transmitter was modulated at various percentages of modulation with a 1000-cycle tone. The pictures indicate that the undesired sideband is approximately 33 db below the unmodulated carrier under the worst operational condition. Note that Fig. 20 (k) and (l) show the spectrum when the transmitter is over-modulated.

Fig. 10(m) shows the same laboratory transmitter 100 per cent modulated by white, or random, noise. Fig. 10(n) shows the spectrum for 100 per cent modulation of this transmitter by program material and Fig. 10(o) shows the effect of over-modulation; that is, on peaks the transmitter indicated 110 per cent modulation.

The problem of generating such a CSSB wave re-

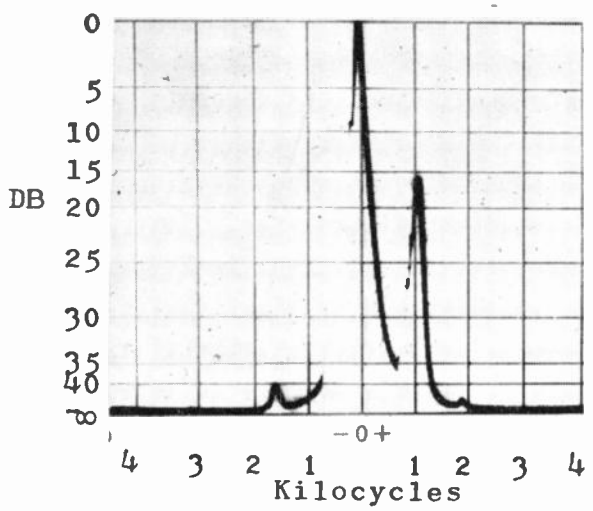

(a) Single tone, 10 per cent modulation

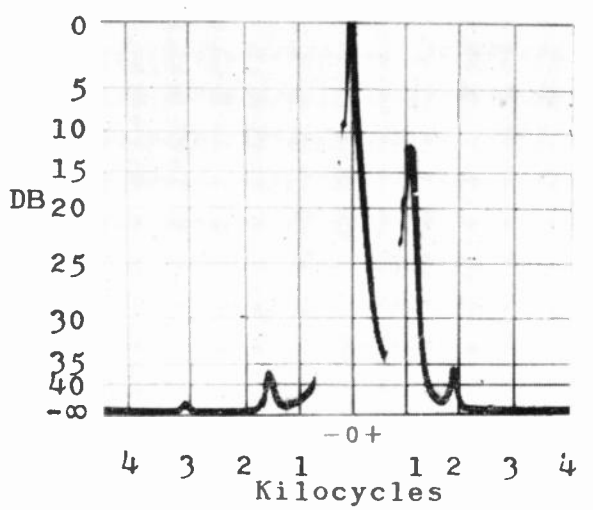

(b) Single tone, 20 per cent modulation

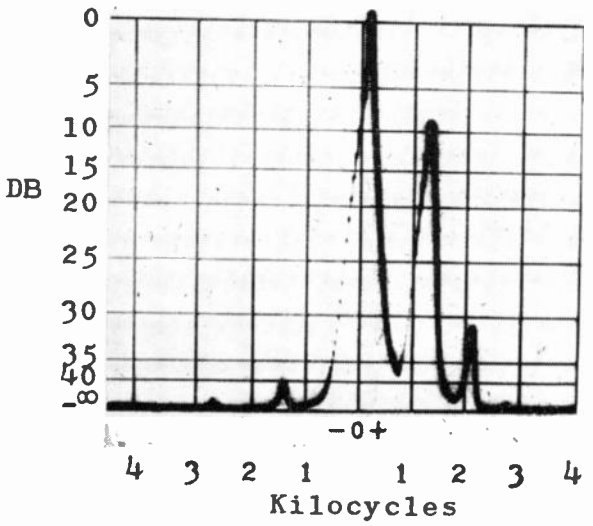

(c) Single tone, 30 per cent modulation

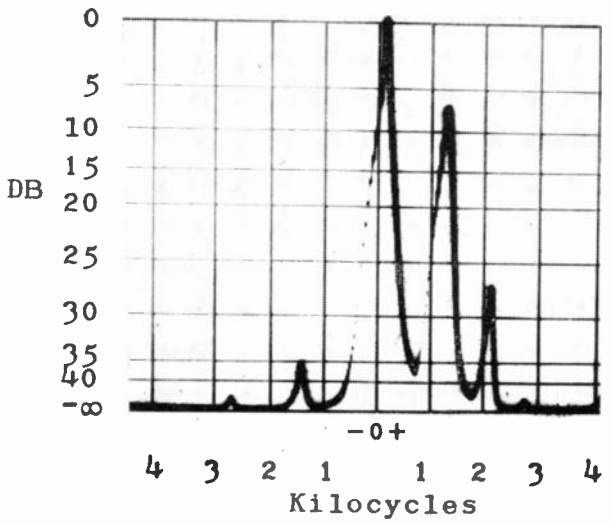

(d) Single tone, 40 per cent modulation

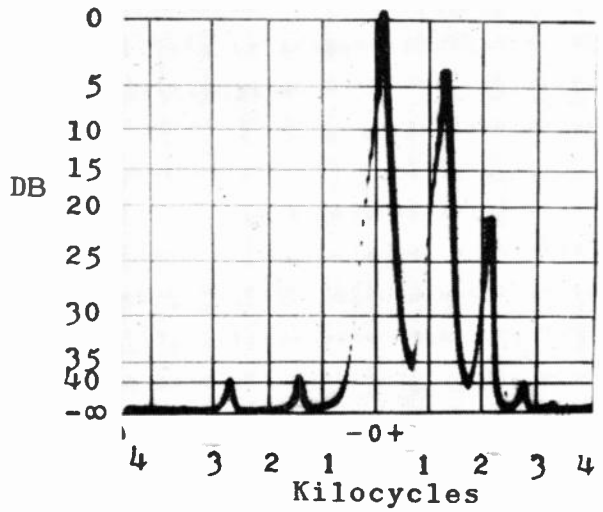

(e) Single tone, 55 per cent modulation

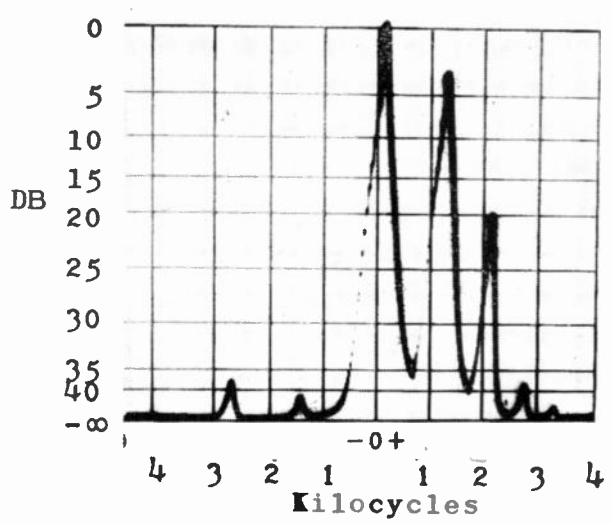

(f) Single tone, 60 per cent modulation

Fig. 10—Panoramic photographs of actual CSSB wave for various modulation conditions.

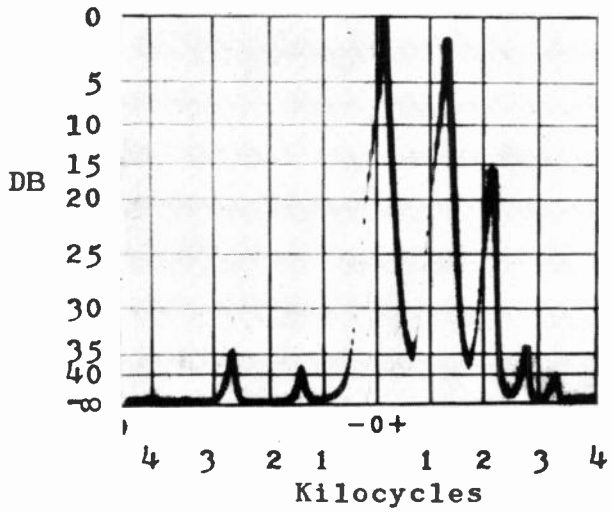

(g) Single tone, 70 per cent modulation

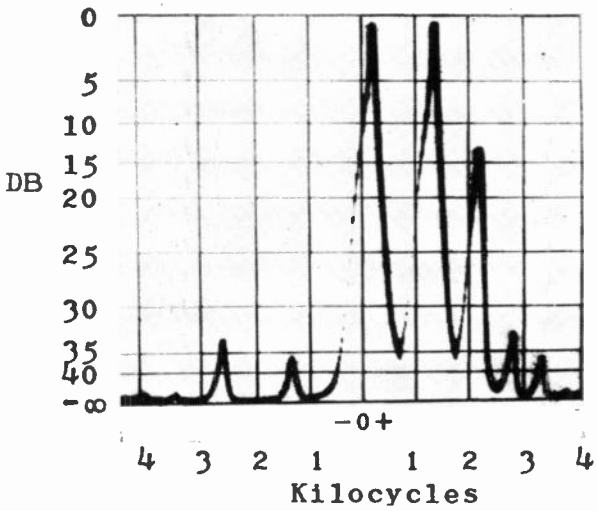

(h) Single tone, 80 per cent modulation

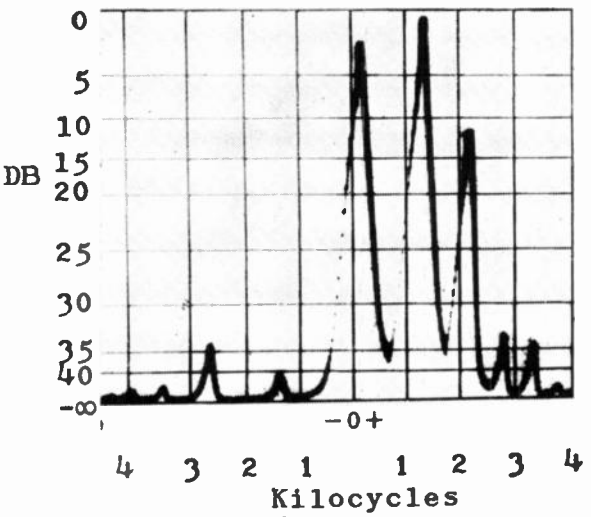

(i) Single tone, 90 per cent modulation

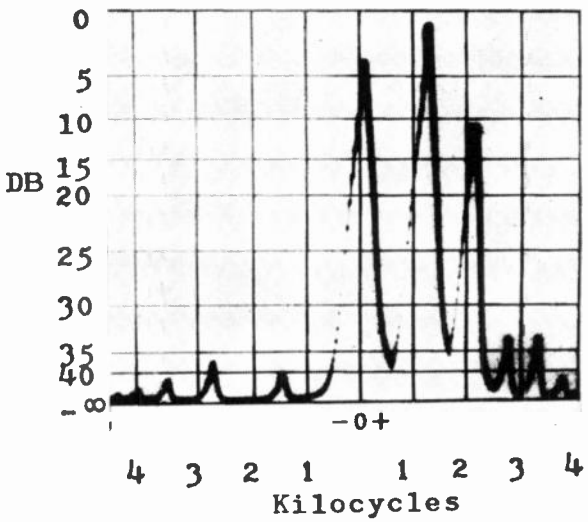

(j) Single tone, 100 per cent modulation

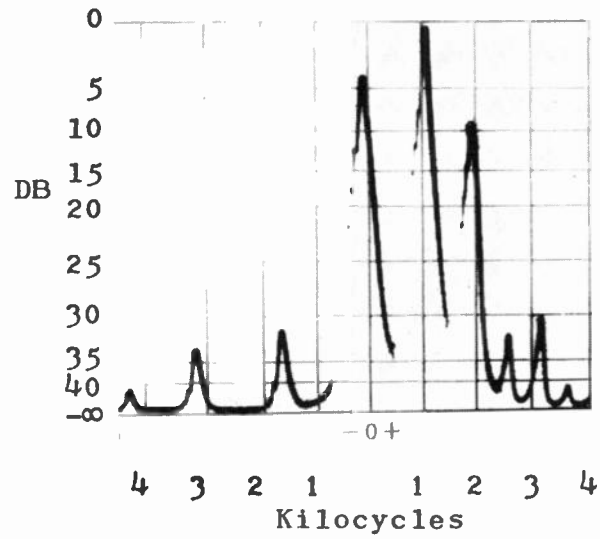

(k) Single tone, 110 per cent modulation

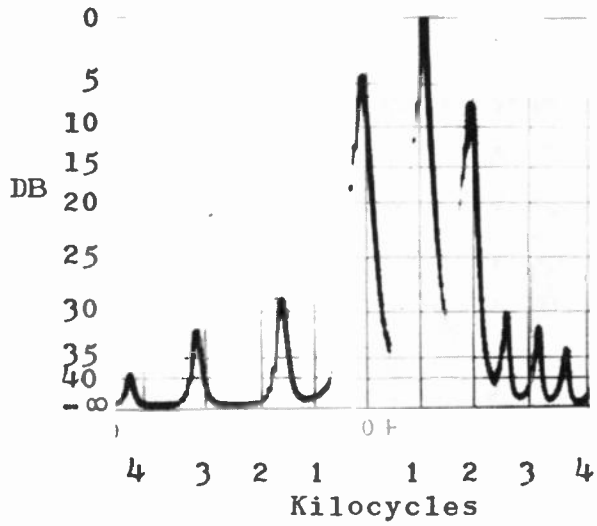

(l) Single tone, 120 per cent modulation

Fig. 10—(Continued)

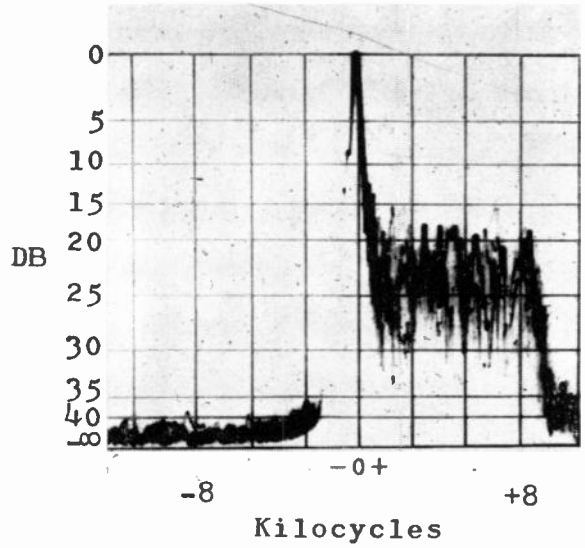

(m) 100 per cent white noise modulation

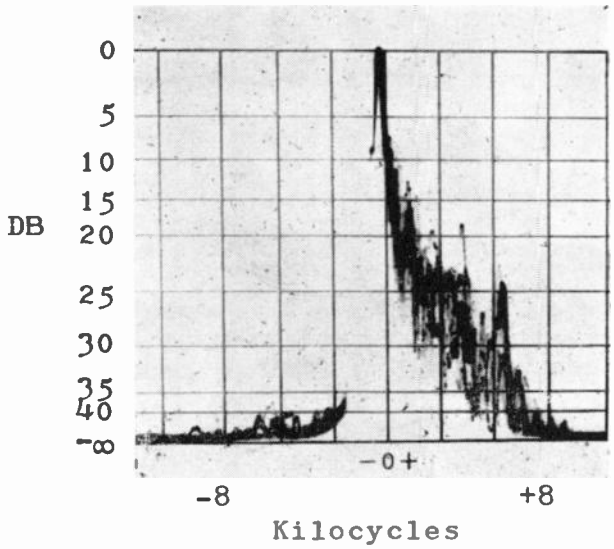

(n) 100 per cent program modulation

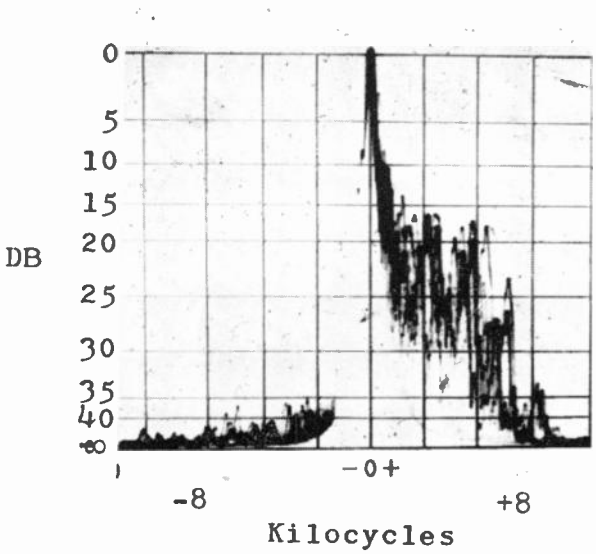

(o) 110 per cent program modulation

Fig. 10

solves itself into producing the desired PM. This can be done by a number of methods.

A CSSB technique (Fig. 11) which was extensively used in equipment produced by the Kahn Research Laboratories was to generate a normal SSB full carrier wave and pass this wave through a limiter in order to isolate the PM. The amount of PM can be shown to be insufficient by study of Fig. 5 from a previously published article[4] on the envelope elimination and restoration SSB system. (Also, see Fig. 9 of this paper.) Therefore, the amount of PM was multiplied by use of a harmonic multiplier and a frequency divider. The combination increased the PM by a factor of 1.4. Though this technique produced acceptable signals, it had one severe problem. It was very sensitive to overmodulation because the average frequency suddenly shifts when the sideband exceeds the amplitude of the carrier at the output of the SSB generator.

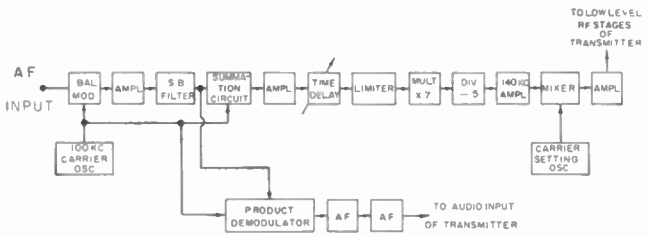

Fig. 11—Block diagram of CSSB system using 1.4 phase stretch circuit.

A more recent development resulted in the "1 PM plus 0.5 PM" system which takes considerable amounts of overmodulation. This system produces a wave having reasonably good sideband isolation during overmodulation periods and excellent sideband isolation during normal operation. This system is described in detail in Section V.

A special technique for communication purposes, which has some inherent envelope distortion but very low out-of-band radiation, has also been investigated but will not be discussed here.

V. Block Diagram of CSSB System Using 1 PM Plus 0.5 PM Technique

The block, shown in Fig. 12, indicates the procedure used to produce the desired CSSB wave by the new 1 PM plus 0.5 PM procedure. The SSB wave is generated in a conventional SSB generator utilizing a balanced modulator plus sideband filter. In the actual equipment, a high-selectivity crystal lattice network filter is utilized. The amplitude characteristic of this filter is such that the output is essentially flat from 50 cycles to 8000 cycles above the carrier frequency. The SSB wave, without carrier, is amplified and fed to a cathode follower. This cathode follower provides a low output impedance and is used to drive two nonlinear circuits which have similar, but not equal, nonlinear characteristics. Both nonlinear networks provide lower attenuation for high-amplitude wave levels than they do for

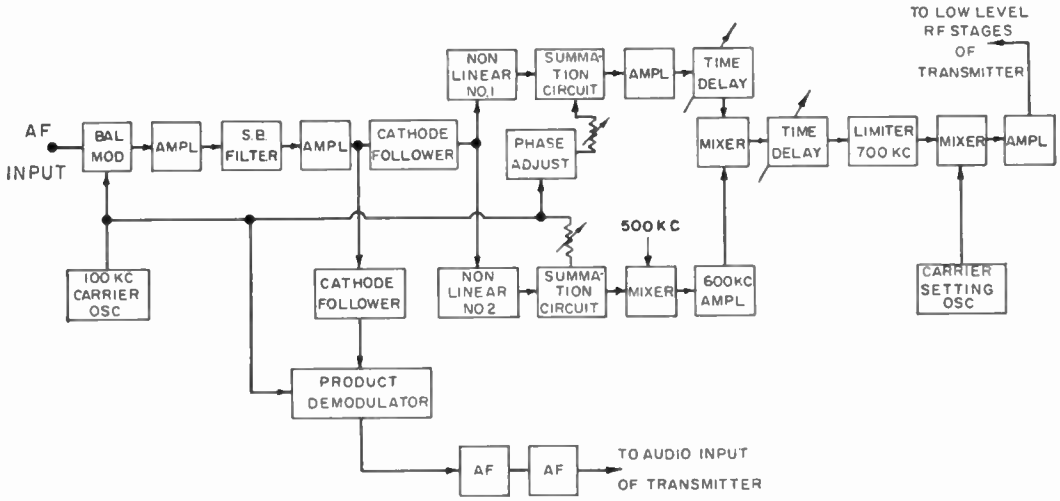

Fig. 12—Block diagram of CSSB system using 1 PM +0.5 PM technique.

low-amplitude waves. These networks are required because the amount of PM boost varies from about 1.5 at 100 per cent modulation to unity at very low percentages of modulation.

Nonlinear circuit No. 1 feeds a summation circuit in which the carrier is added to the sideband wave. The carrier is passed through a phase-shift circuit to align properly the phase relationship between the two paths. The carrier amplitude is such that when the input level is just sufficient to produce 100 per cent modulation, the carrier and the sideband are equal. This is required to produce the PM wave in Fig. 9 which is labeled "sideband-to-carrier ratio equals 1." The output of this summation circuit is amplified and fed through a time delay circuit. The time delay circuit is used to compensate for small difference in time delay between the 1 PM path and the 0.5 PM path. The output of the time delay circuit is fed to a mixer.

Now returning to the output of the cathode follower, it is seen that the cathode follower also drives nonlinear circuit No. 2. This nonlinear circuit feeds a second summation circuit in which the carrier at a level of twice the sideband level at maximum modulation is added to the sideband wave. Thus, the sideband-to-carrier ratio at 100 per cent modulation is 0.5. The output of the summation circuit feeds a mixer in which the wave is heterodyned, in this example, to 600 kc. The output of the 600-kc amplifier is fed to the mixer, in which it heterodynes with the 100-kc 1 PM wave and the mixer summation component 700 kc is selected.

The 700-kc component is phase-modulated by the sum of the PM of the two paths so that the PM equals 1 PM plus 0.5 PM at 100 per cent modulation. At very low percentages of modulation, the nonlinear circuits function so as to produce a PM component equal to that of carrier plus sideband wave, where the sideband-to-carrier ratio equals the percentage modulation. This PM is proper for minimizing the unwanted sideband, and it closely approximates the PM waveshapes of the three-element wave shown in Fig. 9. This combined AM and PM wave is then fed to a limiter in which the AM component of the wave is removed, producing a pure PM wave. The wave is then converted in frequency to a desired carrier frequency where it may be used to drive a class-C high-level, low-level, Doherty, Chireux, or Ampliphase type of transmitter.

In the transmitter, the 1 PM plus 0.5 PM wave is amplitude-modulated by a wave form that is derived from the SSB wave by demodulating that wave by the carrier in a product demodulator. Since a product demodulator may be used to produce a very low distortion audio wave when demodulating a conventional SSB wave, the envelope can be almost free of envelope nonlinear distortion. The reason for this rather complicated technique for deriving the AM component is that, while the original audio wave has all the desired spectrum components, the phase of these components is altered by the crystal filter in the SSB generator. Therefore, unless an elaborate compensating phase-shift network is used, such a wave would not have the proper phase characteristics for the desired envelope function.

Because the CSSB system described here is synthesized from PM and AM components, any type of AM transmitter now in current use may be adapted for CSSB use with little or no alteration of the transmitter.

VI. Spectrum Analysis of a CSSB Wave

Those familiar with modulation analysis techniques will recognize that a complete analysis of the spectrum characteristic of such a system is an extremely involved problem. The reasons for this are that the block diagram incorporates a number of nonlinear elements, and that PM is used with its infinite spectrum. Therefore, in the following analysis only the relatively simple case of single-tone modulation is discussed. *This analysis does not pretend to be complete, but is shown merely as an aid in understanding the system whereby the wave is generated* and because it was used in the original development of the system. Further analysis with different types of waveshapes would no doubt produce interesting results;

however, it is expected that such work would be quite difficult and laborious. Furthermore, the researcher must still face the problem of determining what is a "typical" waveshape, that is, one which will simulate voice and music. Because of the large number of voice and music waveshapes involved, such solutions would always be subject to question.

A most interesting technique[14] was utilized by Mertens of the European Broadcasting Union in analyzing CSSB. He used an analog computer and generated a large number of operating situations. Because full information had not been published on the CSSB system, Mertens recognized that the analysis was limited. It should be noted that the use of an analog computer on the full detailed block of this system would require considerable complexity.

The following describes the procedure used in determining the CSSB spectrum for a single tone modulating wave. Since the worst spurious radiation would generally occur at the maximum modulation, this is the condition assumed in the following analysis.

The spectrum of the amplitude-limited sum of two equal-amplitude sinusoids may be represented as follows:[5]

$$e_{\mathrm{pm}1/1} = \sum_{n=-\infty}^{n=\infty} A_n \cos (w_{c1} + nw_{Af})t \tag{2}$$

where w_{c1} is the angular velocity of the carrier frequency and w_{Af} is the angular velocity of the modulating audio tone.

$$\begin{aligned} A_0 &= +1 & A_{+1} &= -1/3 \\ A_{-1} &= +1 & A_{+2} &= +1/5 \\ A_{-2} &= -1/3 & A_{+3} &= -1/7 \\ A_{-3} &= +1/5 & A_{+4} &= +1/9 \\ A_{-4} &= -1/7 & & \text{etc.} \\ & \text{etc.} \end{aligned}$$

The amplitude of the components has been normalized so that the carrier-frequency component A_0 and the first-order lower-sideband component A_{-1} have unity amplitudes. It should be noted that it is assumed that the lower sideband was the desired sideband in the present case, although either sideband may have been considered in the analysis. Also, the instant of time chosen for $t=0$ is when the carrier and the lower sideband phasors are exactly in phase.

It is interesting to note that this spectrum is equivalent to that of a double-sideband suppressed-carrier signal in which the modulating signal is a square wave. The fundamental frequency component of the square wave would equal $w_{Af}/2$.

The spectrum of the PM component of an SSB wave having a sideband-to-carrier ratio of 0.5 may be represented as

$$e_{pm}1/0.5 = \sum_{m=-\infty}^{m=\infty} B_m \cos (w_{c2} + mw_{Af})t. \tag{3}$$

The value of B_m may be found in some very detailed tables calculated by Granlund[15] or by utilizing a technique described in a paper analyzing limiters.[16] The tuned circuits, in the plate circuit of the mixer, are tuned to a frequency which is the sum of the two input frequencies. Therefore, a wave is produced having a PM component equal to the sum of the PM component of the 1-to-1 sideband-to-carrier ratio signal plus the PM component of the 0.5-to-1 sideband-to-carrier ratio.

$$\begin{aligned} & e_{PM}\,1/1 \times e_{PM}1/0.5 \\ &= \sum_{n=-\infty}^{n=\infty} A_n \cos (w_{c1} + nw_{Af})t \times \sum_{m=-\infty}^{m=\infty} B_m \cos (w_{c2} + mw_{Af})t \\ &= \sum_{n=-\infty}^{n=\infty} \sum_{m=-\infty}^{m=\infty} A_n B_m (\cos w_{c1} + nw_{Af})t \times \cos (w_{c2} + mw_{Af})t \\ &= \sum_{n=-\infty}^{n=\infty} \sum_{m=-\infty}^{m=\infty} \frac{A_n B_m}{2} \cos [w_{c1} + w_{c2} + (n+m)w_{Af}]t \\ &\quad + \frac{A_n B_m}{2} \cos [w_{c1} - w_{c2} + (n-m)w_{Af}]t. \end{aligned} \tag{4}$$

Since the mixer output is filtered, only those components that fall close to the summation frequency of the two input frequencies, that is, $w_{c1}+w_{c2}$, are passed. Therefore, the second term of (4) may be ignored.

The chart in Fig. 13 indicates the procedure used in calculating the resultant PM spectrum. The top row indicates the PM spectrum of the two equal tone waves (1 PM), and the first left-hand column indicates the PM spectrum of the carrier-plus-half-amplitude-lower-sideband wave. The product of these spectrum components is shown in the center of the chart. (These figures were not multiplied by 0.5 as called for by the trigonometric identity, since we are only interested in relative values.) Each of these numbers contributes to its columns a final amplitude which is shown in the bottom row with the amplitude of the new frequency components. This wave centers around the sum frequency of the first carrier frequency and the second carrier frequency ($w_{c1}+w_{c2}$). For instance, if the third-order lower sideband were multiplied by the first-order upper sideband, the resulting frequency would be equal to the sum of the carrier frequencies minus twice the audio frequency. The products with appropriate signs are then summed and the resulting summation is the spectrum composition of the total PM wave. This is the PM spectrum which is amplitude-modulated in the associated transmitter.

Fig. 14 shows the effect of AM on the PM wave. The result of this calculation provides us with the spectrum

[14] H. Mertens, "A study by means of an analogue computer of the spectrum of CSSB modulation," *Eur. Broadcasting U. Rev.*, vol. 64, pp. 249–258; December, 1960.

[15] J. Granlund, "Interference in Frequency Modulation Reception," Research Lab. of Electronics, M.I.T., Cambridge, Mass., Tech. Rept. 42, pp. 29–48; January 20, 1949.

[16] L. R. Kahn, "Analysis of a limiter as a variable gain device," *Elec. Engr.*, vol. 72, pp. 1106–1109; December, 1953.

PM Component of Carrier plus equal SB wave	$\omega_{c1}-4\omega_{Af}$ −0.143 v	$\omega_{c1}-3\omega_{Af}$ +0.200	$\omega_{c1}-2\omega_{Af}$ −0.333	$\omega_{c1}-\omega_{Af}$ +1.0	ω_{c1} +1.0	$\omega_{c1}+\omega_{Af}$ −0.333	$\omega_{c1}+2\omega_{Af}$ +0.200	$\omega_{c1}+3\omega_{Af}$ −0.143	$\omega_{c1}+4\omega_{Af}$ +0.111
PM Spectrum of Carrier Plus Half Amplitude SB Wave									
$\omega_{c2}+6\omega_{Af}+0.0031$								+001	−001
$\omega_{c2}+5\omega_{Af}-0.0068$				+001	−001	+001	−001	+002	−007
$\omega_{c2}+4\omega_{Af}+0.0150$			−001	+002	−002	+003	−005	+015	+015
$\omega_{c2}+3\omega_{Af}-0.0345$		+003	−004	+005	−007	+011	−035	−035	+011
$\omega_{c2}+2\omega_{Af}+0.0834$	−008	+009	−012	+017	−028	+083	+083	−028	+017
$\omega_{c2}+\omega_{Af}-0.2252$	−025	+032	−045	+075	−225	−225	+075	−045	+032
$\omega_{c2}+0.9342$	−133	+187	−311	+934	+934	−311	+187	−133	+104
$\omega_{c2}-\omega_{Af}+0.2586$	+052	−086	+259	+259	−086	+052	−037	+029	−024
$-2\omega_{Af}-0.0335$	+011	−034	−034	+011	−007	+005	−004	+003	
$-3\omega_{Af}+0.0085$	+009	+009	−003	+002	−001	+001	−001		
$-4\omega_{Af}-0.0027$	−003	+001	−001						
	−097	+121	−152	+1.306	+577	−380	+262	−191	+147
	$-4\omega_{Af}$	$-3\omega_{Af}$	$-2\omega_{Af}$	$-\omega_{Af}$	$\omega_{c1}+\omega_{c2}$	$+\omega_{Af}$	$+2\omega_{Af}$	$+3\omega_{Af}$	

Fig. 13—Spectrum calculations for determining PM spectrum of 1 PM+0.5 PM system.

PM Component of 1 PM+0.5 PM	$-4\omega_{Af}$ −097	$-3\omega_{Af}$ +121	$-2\omega_{Af}$ −152	$-\omega_{Af}$ +1.306	$\omega_{c1}+\omega_{c2}$ +577	$+\omega_{Af}$ −380	$+2\omega_{Af}$ +262	$+3\omega_{Af}$ −191	$+4\omega_{Af}$ +147
Sideband Produced by Modulation of each PM Component by Sine Wave at 100 per cent Modulation	+038 +061	−049 −076	+061 +653	−0.076 +0.289	+653 −190	+289 +131	−190 −096	+131 +074	−096 −069
Spectrum Produced	+002	−004	+562	+1.519	+1.040	−040	−024	+014	−018
Spectrum Produced in db	−57.7	−51	−8.6 Second-Order Sideband	0 First-Order Sideband	−3.3 Carrier	−31.7	−36	−40.7	−38.6

Fig. 14—Spectrum calculations for CSSB system assuming perfect transmitter.

PM Component of 1 PM+0.5 PM	+075	$-4\omega_{Af}$ −097	$-3\omega_{Af}$ +121	$-2\omega_{Af}$ −152	$-\omega_{Af}$ +1.306	$\omega_{c1}+\omega_{c2}$ +577	$+\omega_{Af}$ −380	$+3\omega_{Af}$ +262	$+3\omega_{Af}$ −191	$+4\omega_{Af}$ +147
Sideband Produced by Sinusoidal 97 per cent AM of Each PM Component	−023 −047	+036 +059	−047 −074	+059 +633	−074 +280	+633 −184	+280 +127	−184 −093	+127 +071	−093
Sidebands Produced by 3 per cent AM Second Harmonic Distortion Wave of Each PM Component		+001 +002	−001 −020	+002 −008	−002 +006	+002 −004	−020 +003	−009 −002	+006 +002	−004
Spectrum Produced		+001	−021	+534	+1.516	+1.024	+010	−026	+015	
Spectrum Produced in db		−63	−37.1	−9 Second-Order Sideband	0 First-Order Sideband	−3.4 Carrier	−43.6	−35.4	−40.1	

Fig. 15—Spectrum calculations for CSSB system assuming transmitter having 3 per cent envelope distortion.

composition of the desired CSSB wave. Each of the PM spectrum components is assumed to be a carrier for the AM; therefore, two symmetrical sidebands spaced by the frequency of modulation are produced about each PM component. The summation of the sidebands produced by the AM and the PM spectrum is the spectrum of the desired-output wave. It should be noted that we have assumed, in this figure, that there was no envelope distortion present. Fig. 15 provides a similar analysis except for the assumption that the transmitter has 3 per cent second harmonic[17] envelope distortion.

We have assumed, in calculating the PM spectrum, that separate limiters were used in the 1 PM branch and

[17] The distortion figure of 3 per cent is based on the economic factors involved in high-powered transmitter design. Economic use of large tubes is necessary and therefore a small degree of emission limiting is generally experienced. This is the basis for the assumption that the second harmonic distortion is out of phase with the fundamental component during the positive modulation peak.

the 0.5 PM branch. Experiments were performed with this type of block diagram which proved that the same spectrum results whether the limiting is performed on the individual components or on the heterodyned wave. Of course, the analysis could have been performed by merely mixing the two waves and then determining the effect of limiting after the heterodyning process by use of a technique outlined in a previous paper.[16]

Another undesired sideband component is produced when more than a single tone is transmitted. The following analysis indicates the level of this component.

The level of the carrier component is a function of the audio input level. If two equal-amplitude tones, which have a combined peak level sufficient to cause 100 per cent modulation, are used to modulate the transmitter, the percentage of modulation will vary from 0 per cent to 100 per cent according to the phase relationship between the two modulation tones. When the two components are instantaneously out of phase their resultant is zero, and the instantaneous percentage modulation is zero per cent. At other times the two components add and the modulation reaches 100 per cent. Thus, the carrier amplitude (for the 0.7/1/0.3 carrier-to-sideband component ratio) shifts from 0.7 at 100 per cent modulation to 1 at zero per cent modulation. This variation in carrier level occurs at a rate equal to the beat frequency between the two modulation tones.

Of course, the variation in carrier amplitude is AM, and therefore two sidebands are generated. These components are each equal to $(1-0.7)/4$ E_{carrier} or 0.075 E_{carrier}. Thus, each of these components is a little over 23 db below the unmodulated carrier amplitude or 29 db below the peak envelope power level. One of these sidebands falls in the undesired sideband spectrum. As the two-tone audio wave decreases in amplitude, the undesired sideband component decreases. Also, as the two tones depart from amplitude equality the component decreases.

In practice, the spacing between two strong equal amplitude tones in speech and music normally is very small,[18] less than 100 or 200 cycles, and therefore the spurious components produced by this mechanism are very close to the carrier and should not increase the adjacent-channel interference to any great degree.

It should be stressed that while this spurious component is undesirable, it does not introduce envelope distortion and is not heard or measured when such a signal is received on an envelope detector. Actually, all of these spurious components are required if the envelope is to be free of distortion, and if the receiver eliminates these components some distortion will result. Fortunately, those components are extremely close to the carrier and, in practice, are passed by the receiver so that the envelope is relatively free of distortion.

[18] Harvey Fletcher, "Speech and Hearing," D. Van Nostrand Co., Inc., Princeton, N. J., 2nd ed.; 1953.

ADVANTAGES AND EXPERIMENTAL EVALUATION OF THE CSSB SYSTEM

One of the main applications of CSSB is in the field of AM broadcasting. Therefore, detailed measurements under broadcasting conditions are given below.

All the tests made were based on the original 1.4 phase stretch circuitry. From subsequent tests, it would appear that use of the new CSSB technique, 1 PM plus 0.5 PM, would provide additional advantages.

VII. "Shaped Noise" Evaluation Procedure

One of the basic problems in attempting a quantitative comparison of equipment developed for use in the transmission of voice and music is determination of a method for evaluating the effect of the characteristic spectrum distribution of the signal. Obviously, the use of a constant amplitude sine wave up to 15 kc would be unrealistic and would preclude acceptance of our present interference standards which allow 10-kc spacing of carriers. Therefore, it was felt that a new technique was required for proper comparison of CSSB with AM. The use of this technique has been favorably commented upon by one distinguished engineer,[19] and it may be useful for evaluation of other program-modulated signals.

This new technique might be called a "shaped noise" evaluation procedure. In carrying out this procedure, a filter was designed and built which has the musical energy frequency characteristic shown in Fig. 4. This filter was then fed white noise and the output was used in the evaluation tests. By this procedure, the statistical measurement problem was bypassed and one answer was accepted for this spectrum characteristic. Of course, the accuracy of the evaluation is largely dependent upon the shape of the curve used for shaping the noise. It should be mentioned that there is a heated controversy raging over the exact nature of the spectrum energy distribution of voice and music. Since our own tests are quite limited, we are forced to depend upon the authority of others.

It might be mentioned, furthermore, that one recent publication[20] questions the possibility of ever deriving a meaningful spectrum distribution curve. Thus, we see that this is not a simple matter; but neither is an evaluation simple which is made up of a large number of samples which may in themselves prove in the long run to be atypical. A study of various published spectrum diagrams relative to the peak values of *the total audio waves* indicates that the probability is extremely small that a component above 3 or 4 kc would have sufficient amplitude to produce a strong second-order sideband component (see Fig. 4).

[19] R. N. Harmon, "Reply Comments of Westinghouse Broadcasting Co., Inc.," FCC Docket No. 13596 (RM-156); January 13, 1961.

[20] J. G. McKnight, "The distribution of peak energy in recorded music, and its relation to magnetic recording systems," *J. Audio Engrg. Soc.*, vol. 7; April, 1959.

VIII. Signal-to-Noise Ratio and Frequency Response Comparison

In order to determine the amount of improvement in high-frequency response and signal-to-noise ratio of the CSSB system, consideration will be given first to the use of receivers having square top-selectivity characteristics. Later, measurements of conventional inexpensive broadcast receiver characteristics will be considered.

If a *perfect* AM receiver were used to receive a double-sideband AM wave, its pass band would have to be two times the highest audio frequency to be received. Thus, if an AM wave is modulated by components up to 10 kc, the IF and RF stages of the receiver should be 20 kc wide. For CSSB transmission, the bandwidth need only be 10 kc wide. Therefore, since random noise power is doubled when the bandwidth is doubled, the signal-to-noise ratio would be 3 db better for CSSB transmission. In the case of impulse noise, the noise power increases as a squared function of bandwidth. Therefore, there is a 6 db S/N ratio improvement for impulse noise when CSSB transmission is used.

It should be noted that these improvements in signal-to-noise ratios are for AM receivers with square top-selectivity characteristics, and the receivers in use today are far from perfect in regard to their selectivity characteristics. Actually, in practice these receivers are much narrower than they should be for double-sideband use for economic reasons; they therefore tend to destroy signal components that are important to speech intelligibility.

It becomes very difficult to specify signal-to-noise improvements when one considers the relative importance of different voice and music spectrum components. This is especially true in situations where the selectivity characteristic of the networks involved is rounded.

For instance, if a voice component at 3500 cycles is attenuated 7 db and a component at 2000 cycles is attenuated 1 db, then the signal-to-noise ratio for that 3500-cycle component would be reduced over the 2000-cycle tone by a factor of 6 db. Thus, the effective signal-to-noise ratio is a function of frequency response, and a single figure for signal-to-noise ratio cannot be easily derived. Therefore, no exact figure will be offered for the signal-to-noise improvement of CSSB, because the signal-to-noise ratio and the frequency response of the system are so closely related.

Except for the difference in bandwidth, the frequency response of the square selectivity curve AM receiver would be identical to that of a square selectivity curve CSSB receiver. Therefore, there would be no frequency response difference between the two systems when such receivers were used.

As noted above, the bandwidths of both domestic sets and foreign sets leave much to be desired. Actually, their poor high-frequency characteristics not only degrade the musical reproduction process but also reduce voice intelligibility. It has been pointed out[18] that loss of frequency response above 3000 cycles reduces the intelligibility of "s" sounds from 100 per cent to 40 per cent, the "th" sound from 100 per cent to 66 per cent, the "z" sound from 100 per cent to 80 per cent, and the "t" sound from 100 per cent to 81 per cent. These measurements were made under relatively good signal-to-noise conditions; it has been noted that under poor signal-to-noise conditions the loss of intelligibility due to reduced high-frequency response is even more severe. There is a noise-masking effect that further degrades intelligibility when high-frequency components are attenuated by the limited frequency response of the equipment.

The CSSB system, by improving the high-frequency response of the system, increases the area of good reception and especially benefits the fringe-area listener.

The over-all selectivity characteristic of a typical inexpensive table model receiver, shown in Fig. 3, indicates that the 3-db high-frequency audio cutoff is only 2.6 kc. Laboratory tests indicate that the receiver, when used for CSSB reception, may be detuned 2 or 3 kc, improving the high-frequency response. Figs. 16 and 17 confirm this improvement in high-frequency response.

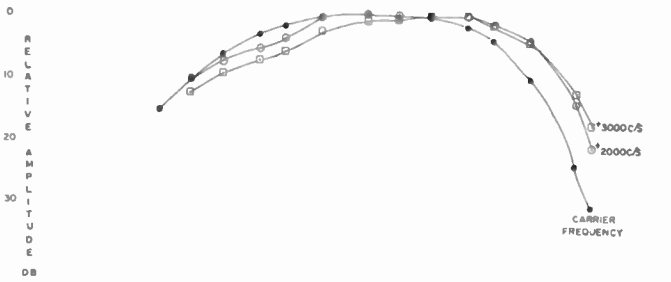

Fig. 16—Frequency of typical CSSB system as a function of receiver detuning. Logarithmic frequency scale.

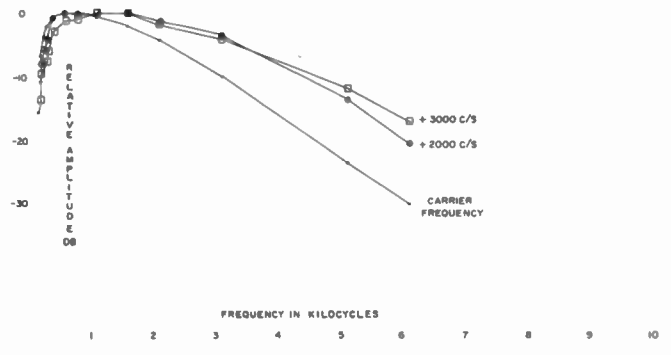

Fig. 17—Frequency response of typical CSSB system as a function of receiver detuning. Linear scale.

Both of these figures are plots of the over-all audio response of the receiver when tuned for AM (marked "carrier frequency" on the curve) or for CSSB with detuning of 2 and 3 kc. Fig. 17 is the same as Fig. 16 except that a linear plot which tends to emphasize the high-frequency characteristics of the response, is used instead of a logarithmic plot. The improved high-frequency response is especially noticeable in fringe-area listening where speech is unintelligible when AM is used.

It should also be noted that the amount of receiver detuning is a function of the signal-to-noise and signal-to-interference ratios. The smaller amount of detuning would occur when the receiver was operated under good signal-to-noise and interference situations. When the noise is high, or the interference is severe, the optimum amount of detuning increases. There are a number of reasons for this increase in allowable detuning.

The amount of detuning that the normal listener would tolerate is a function of the amount of distortion he hears. Under poor signal-to-noise situations, the noise masks distortion; therefore, the listener naturally tends to tune further from carrier in order to obtain increased volume and increased high-frequency response. This improved frequency response is extremely important under low signal-to-noise situations because the noise tends to mask the weak high-frequency sounds. Therefore, the average listener will, without being told, detune the receiver further in poor signal-to-noise situations than when the signal-to-noise is good.

IX. Co-Channel Interference

In considering co-channel interference, assume first the use of a receiver which has a perfectly flat pass band with an infinite cutoff slope IF/RF selectivity characteristic, and consider the case of two CSSB signals operating at the same carrier frequency but on opposite sidebands. Since a perfect receiver is considered, the crosstalk interference between these two co-channel stations would be equal to the undesired sideband radiation of the transmitter. Thus, if a 30-db desired-to-undesired sideband ratio were maintained at the transmitter, the isolation between the channels would be 30 db for equal signal strengths. If the geographical spacing provided additional isolation, then the isolation would, of course, be equal to 30 db plus the geographical isolation.

Consider the improvement that would be obtained when a CSSB signal operated simultaneously on the same channel as a conventional double-sideband AM signal. In this case, if the receivers had perfectly flat-top, sharp-sided selectivity characteristics, the double-sideband signal would be reduced by a factor of approximately 7 db when the CSSB wave was received. This loss is due in part to the fact that one of the sidebands of the interfering double-sideband signal is not accepted by the receiver and in part to the quadrature relationship between the carrier and remaining sideband. Therefore, the AM of the AM signal would be reduced to a little less than 50 per cent.

Listeners tuned to the double-sideband signal could, by using a perfect selectivity characteristic receiver, drop interference from the other station by 30 db. But, because his highly selective receiver would eliminate one of the desired sidebands, the desired modulation would be reduced by 7 db, and 11 per cent envelope distortion would be introduced (because of sideband wave). Thus, the AM wave listener would have a net gain in signal-to-interference ratio of 23 db, but at the same time considerable distortion would be introduced. Of course, he could still tune to the carrier and maintain the exact receiving conditions that existed when both stations were transmitting conventional double-sideband AM waves.

In practice, the listener automatically tunes his set to accommodate prevailing conditions. For instance, if his home is near the double-sideband AM station, he will normally tune to the carrier so as to receive the loudest signal. If, however, he lives near the interfering CSSB co-channel station, he will tune his set away from the sideband of the CSSB station so as to minimize interference. Thus, because the interfering station radiates only one sideband, the listener has the possibility of reducing interference by tuning away from the sideband used by the co-channel station. The CSSB signal listener can reduce interference effects by tuning away from the carrier and toward the desired sideband.

Some will question the ability of the average listener to optimize reception in this manner, but while every listener will not do this, most listeners, by tuning for the best sound, should approximate the desired result. This is especially true for listeners who live in areas where radio reception is poor, and are therefore accustomed to listening to marginal signals.

If both stations utilized the CSSB system and transmitted opposite sidebands, the greatest gain would be achieved. It should be noted that if the two CSSB co-channel stations transmit on the same sideband, there is neither improvement nor degradation in the interference situation. Of course, the other advantages of CSSB operation are still applicable.

The selectivity characteristics of common home receivers are, as mentioned above, far from perfect. (It should be noted that it is practical to make receivers with excellent selective characteristics which could provide almost the full interference improvement; however, in this study it is more important to consider sets now in use.) Actual laboratory tests which used conventional inexpensive receivers and which were made during the study of co-channel interference, verify the above conclusions. Figs. 18 and 19 show various conditions of co-channel interference under situations in which CSSB is used by the desired station or by both stations. A maximum gain of 10 to 15 db is indicated for the weak high AF components.

Another advantage of the CSSB signal is that it is slightly less sensitive to phase rotation of the carrier, especially at low percentages of modulation. This is because the other sideband is absent; therefore, since only two strong components are present at low percentages of modulation, the phase of the carrier does not influence the envelope waveshape for these low percentage modulation conditions. When the undesired signal has

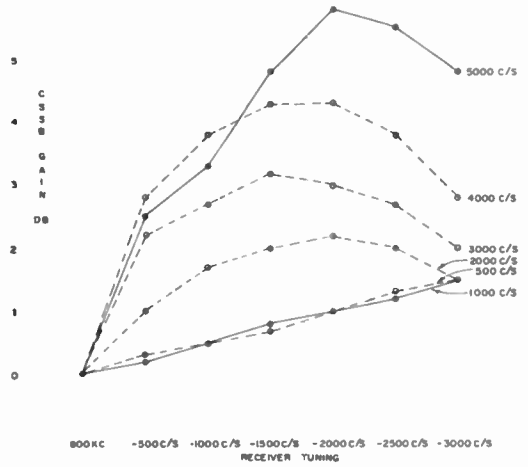

Fig. 18—Co-channel interference gain by use of CSSB as a function of receiver tuning. Transmitter creating interference operates AM, desired operates CSSB.

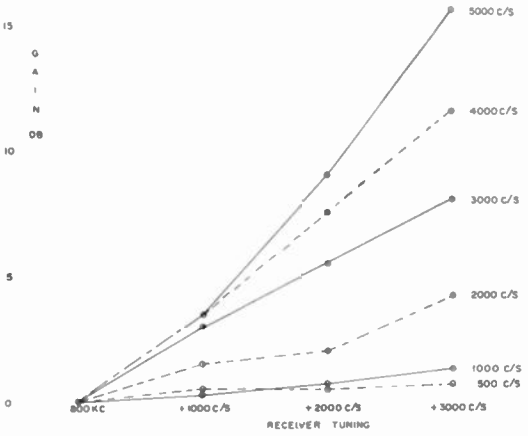

Fig. 19—Co-channel interference gain by use of CSSB as a function of receiver tuning. Transmitter creating interference and desired operates CSSB.

a carrier frequency approximately equal to that of the desired carrier frequency, the combined carriers will be phase modulated at a low-frequency beat-note rate. Because CSSB is less sensitive to phase discrepancies, it should be a little less sensitive to this form of carrier beating distortion.

X. Adjacent Channel Interference

In the following, it will be assumed that, except where noted, a 10-kc channel separation is used. The "shaped noise" technique, described above, was used throughout these measurements on adjacent channel interference. Tests with pure random noise modulation (up to 20 kc) indicate a much greater gain for CSSB; however, while strong high-frequency sounds are occasionally emitted, it is believed that the shaped noise test gives a far more realistic answer.

The four possible methods of arranging the sidebands between two interfering adjacent channel CSSB stations are shown in Fig. 20. Three of these arrangements ap-

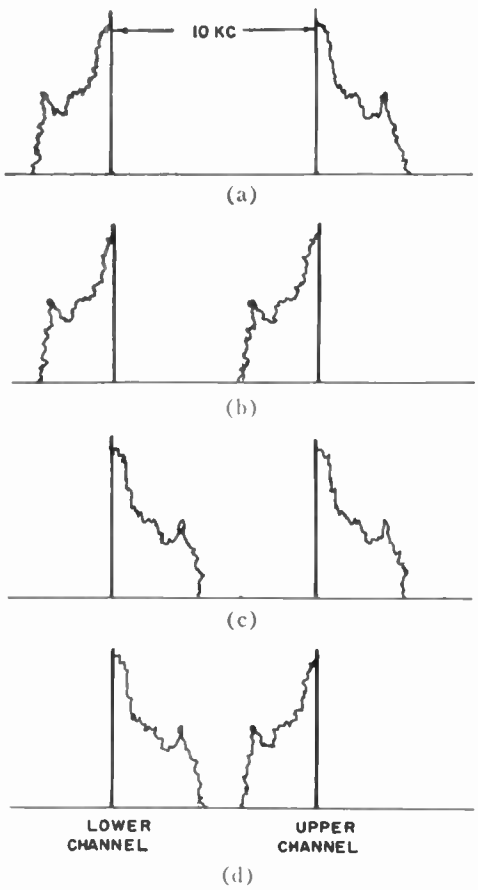

Fig. 20—Various conditions of adjacent channel interference.

pear to offer appreciable improvements in interference. The fourth would not greatly alter the interference situation by changing to CSSB operation.

In the first arrangement, Fig. 20(a), the higher frequency station utilizes the upper sideband and the lower frequency station takes the lower sideband. In this most favorable case, the nearest strong component would be at least 13 kc away from the center tuning point of the receiver. This 13-kc figure is arrived at by recognizing that the carriers are spaced by 10 kc and that the receiver, under strong interference conditions, would be tuned approximately 3 kc on the desired side. Fig. 21(b) shows actual measurements for this situation, and Fig. 21(a) shows the conventional AM situation which may be used for a comparison. It should be noted that detuning by 3000 cycles produces a gain for CSSB of 17 db. [See pp. 1520–1522 for Figs. 21(a)–(i).]

Fig. 20(b) shows the situation where both CSSB adjacent channel stations operate on the lower sideband. In this situation, the person listening to the lower frequency station would tune his receiver 3 kc below the carrier of that station. Therefore, the closest interference component would be approximately 5 kc from the center of the receiver's band pass. Fig. 21(c) indicates that under such conditions a gain of a little over 11 db would result.

Adjacent Channel Interference
As a Function of Tuning
Using RCA Model 9-C-7EE Receiver
KRL Stereo Adapter
KRL CSSB Adapter
Two Experimental 5 Watt Test Transmitters

Desired Interference

AM/AM

Desired—AM 20 per cent at 2000 cps
Interference—Shaped noise AM at 100 per cent
Carrier amplitudes at equality with 10 kc separation

Signal to Interference Ratio +18.0 db

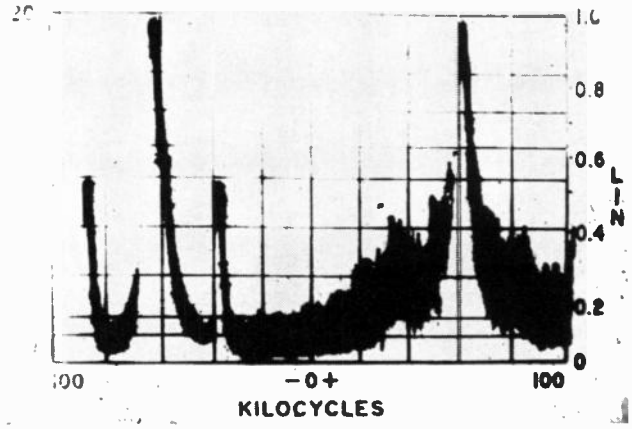

(a)

Lower Sideband/Lower Sideband

Desired—LSB 20 per cent modulation at 2000 cps
Interference—LSB shaped noise at 100 per cent modulation
Carrier amplitudes at equality with 10 kc separation

Receiver Tuning	Signal-to-Interference Ratio
Carrier	+19.5 db
−1000	+24.5 db
−2000	+27.5 db
−3000	+29.5 db

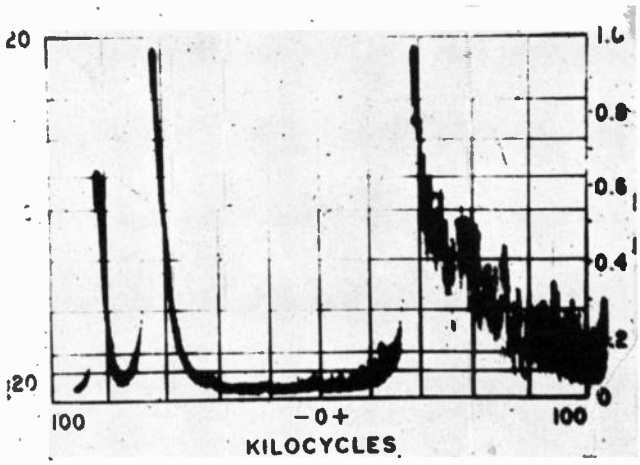

(b)

Lower Sideband/Upper Sideband

Desired—LSB 20 per cent modulation at 2000 cps
Interference—USB shaped noise at 100 per cent modulation
Carrier amplitudes at equality with 10 kc separation

Receiver Tuning	Signal-to-Interference Ratio
Carrier	+28.0 db
−1000	+31.5 db*
−2000	+33.5 db
−3000	+35.0 db*

* Measurement limited by ambient noise.

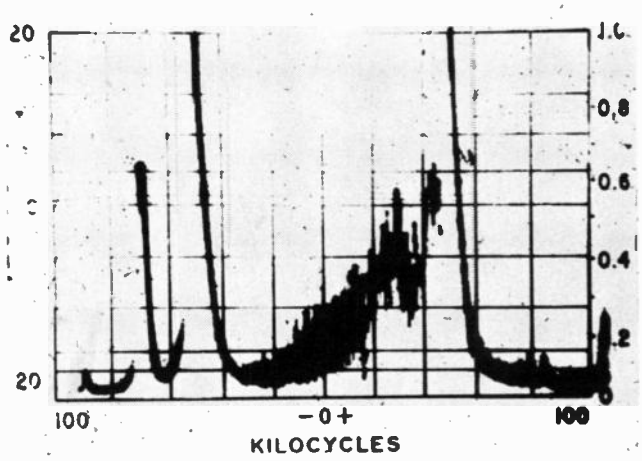

(c)

Fig. 21—Measurements for adjacent channel interference.

Adjacent Channel Interference

Using RCA Model 9-C-7EE Receiver
Measurements Signal Generator Model 65-B (as AM source)
KRL Stereo Adapter
KRL Compatible Adapter
Two Experimental 5 Watt Test Transmitters

Desired Interference

AM/AM

Desired—AM 30 per cent at 400 cps
Interference—Shaped noise AM at 100 per cent
Carrier amplitudes at equality with 10 kc separation

Signal to Interference Ratio +27.0 db

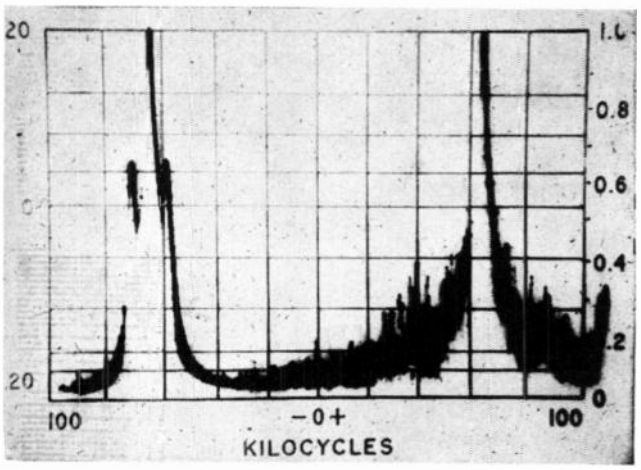

(d)

Upper Sideband/Upper Sideband

Desired—USB 30 per cent modulation at 400 cps
Interference—USB shaped noise at 100 per cent modulation
Carrier amplitudes at equality with 10 kc separation

Signal to Interference Ratio +37 db

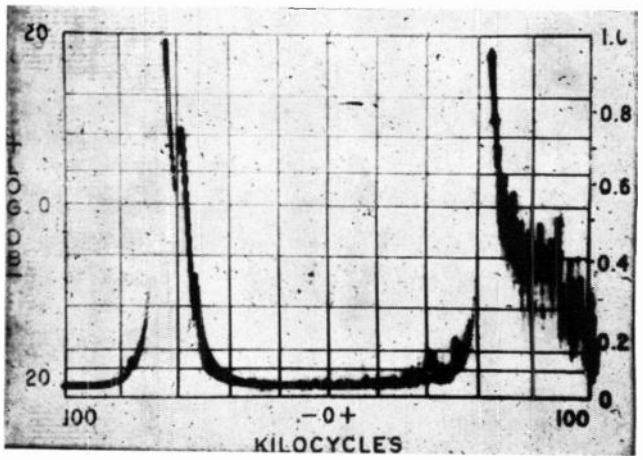

(e)

Upper Sideband/Lower Sideband

Desired—USB 30 per cent modulation at 400 cps
Interference—LSB shaped noise at 100 per cent modulation
Carrier amplitudes at equality with 10 kc separation

Signal to Interference Ratio +28 db

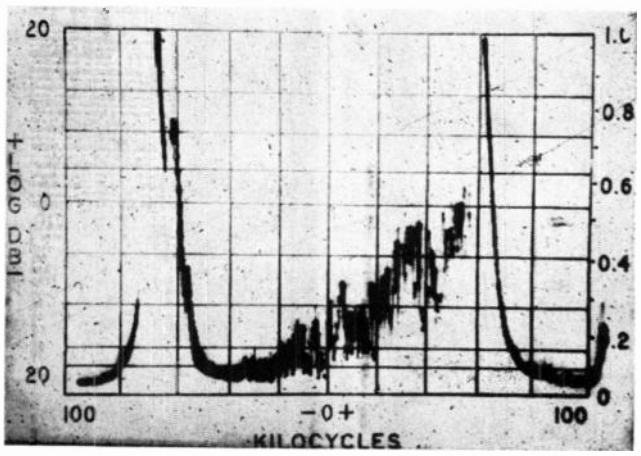

(f)

Fig. 21 (Continued)

Adjacent Channel Interference
Using RCA Model 9-C-7EE and RCA X1 Receivers
KRL Stereo Adapter
Experimental 5 Watt Test Transmitter (as CSSB source)
Measurements Signal Generator Model 65-B (as AM source)

Desired Interference

AM/AM

Desired—AM 30 per cent at 400 cps
Interference—Shaped noise AM at 100 per cent
Carrier amplitudes at equality with 10 kc separation
Interfering carrier amplitude 30 times desired with 20 kc separation

Signal to Interference Ratio

10 kc	9-C-7EE	+27.0 db
	RCA X1	+31.0 db
20 kc	9-C-7EE	+ 4.5 db
	RCA X1	+14.0 db

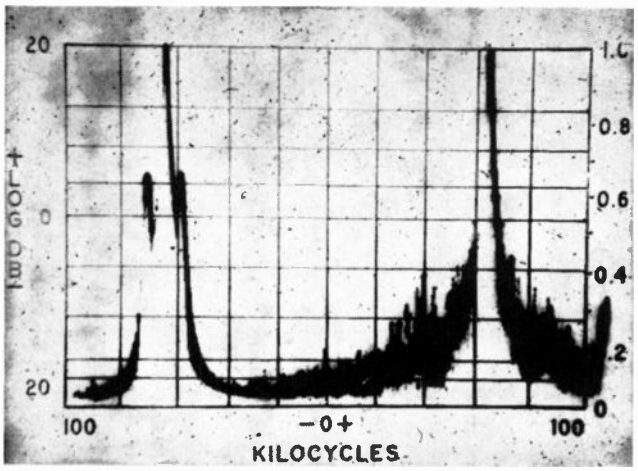

(g)

AM/Upper Sideband

Desired—AM 30 per cent at 400 cps
Interference—Shaped noise USB at 100 per cent modulation
Carrier amplitudes at equality with 10 kc separation

Signal to Interference Ratio

10 kc	9-C-7EE	+37 db
	RCA X1	+43 db*
20 kc	9-C-7EE	+33 db
	RCA X1	+44 db*

* limited by ambient noise

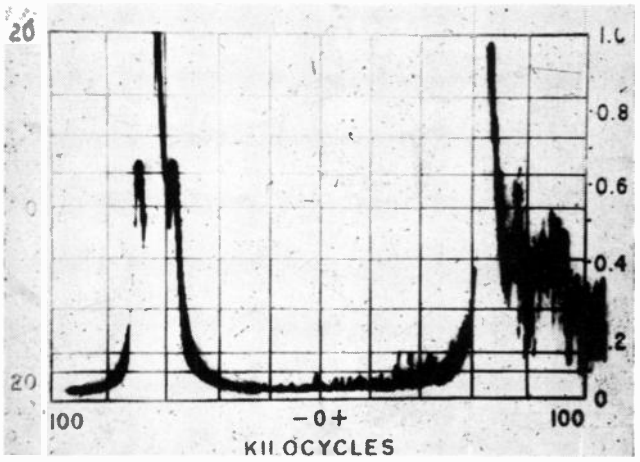

(h)

AM/Lower Sideband

Desired—AM 30 per cent at 400 cps
Interference—Shaped noise LSB at 100 per cent modulation
Carrier amplitudes at equality with 10 kc separation

Signal to Interference Ratio

10 kc	9-C-7EE	+28 db
	RCA X1	+35 db
20 kc	9-C-7EE	+33 db
	RCA X1	+44 db*

* limited by ambient noise

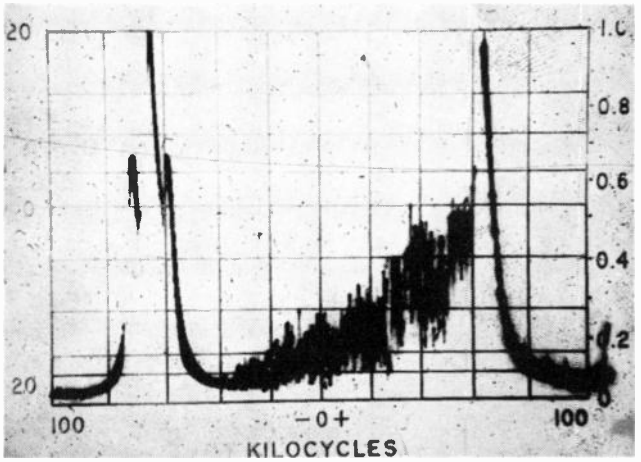

(i)

Fig. 21

In the next possible arrangement of sidebands, Fig. 20(c), the upper sideband is transmitted by both stations. In this instance, the person listening to the higher frequency station tunes his receiver approximately 3 kc above the carrier frequency, and the lower frequency station listener tunes his receiver to the carrier frequency. For the low-frequency listener, the nearest component would be 10 kc away from the center of the receiver's pass band. For the high-frequency listener, the nearest component would be some 5 kc away from the center tuning. The 5-kc figure is based upon the assumption that the listener will detune his receiver by 3 kc and that the crystal filter in the sideband transmitter adapter limits the strong signal components to 8 kc. The spectrogram shown in Fig. 21(e) provides measurements for this situation. The receiver is assumed to be tuned to the carrier of the low-frequency station and a gain of some 10 db over the AM situation has been measured. The case in which the listener tunes to the higher frequency station is not indicated in these figures but is identical to the spectrum situation shown in Fig. 21(c). In this case, a 1.5-db gain is provided when the receiver is tuned to the carrier, and over 11-db gain when the receiver is detuned 3 kc for best interference avoidance.

In the fourth situation, Fig. 20(d), the high-frequency station uses the lower sideband and the lower frequency station the upper sideband. This is the least desirable situation, and in this case the receivers should be tuned to the carriers for best reception in regions experiencing interference. The one advantage to the system is that the high-frequency components from the signal are restricted to 8 kc, whereas in present operation they are not restricted. There should be some improvements, therefore, in reception because of the foregoing factor. It is felt, however, that this advantage would be almost offset by the fact that the sideband level would be raised in both cases by 6 db. The spectrogram, Fig. 21(f), provides actual measurements for this situation, in which a small gain (1 db) was achieved for this CSSB situation over the conventional AM arrangement.

XI. Mixed CSSB and AM Transmission

It is obvious that, even if CSSB operation were accepted simultaneously in all countries, the transitio . to this form of operation would take many years; it is therefore very important to consider the situation of mixed CSSB-AM operation.

In the first case, assume that the sideband of the CSSB wave is away from the AM wave (if the CSSB were used by the lower frequency station, the lower sideband would be emitted; if it were used by the higher frequency station, the upper sideband would be emitted). The listener to the CSSB station, by detuning his receiver 3 kc, would gain approximately 7–10 db over AM operation. The AM station listener would achieve a gain of 10 to 12 db [see the spectrogram of Fig. 21(h)].

If the CSSB station picked the sideband closest to the AM wave, the CSSB signal listener would tune to the carrier, and there would be neither loss nor gain in interference. Also, the AM wave listener would have no real gain or loss in interference. The reason is that he would lose approximately 6 db because of the increased sideband levels from the CSSB signal, but would also gain, because the sideband components would be restricted and would not be closer than 2 kc to his carrier. Actual measurements [see Fig. 21(i)] indicate a 1 to 4 db gain for CSSB for 10 kc carrier separation.

XII. Detailed Consideration of Least Favorable Interference Situation for CSSB Operation

In proposing any new system, thorough consideration should be given to the least favorable operating situation, and for CSSB operation this would occur when the transmitted sideband was closest to the signal being disturbed. Even under this condition, there would be a small improvement over present AM operation for both stations' listeners.

The CSSB equipment specification limits the response to 8 kc. This specification was formulated because it is apparent from spectrum analysis of CSSB that some increase in interference for the worst condition can be expected in the absence of the 8-kc filter.

If one studies Fig. 16 or Fig. 17, it is apparent that an appreciable amount of high-frequency fall-off may occur in the CSSB transmission equipment while still providing improved over-all high-frequency audio characteristics.

Because of the 8-kc high-frequency response restriction, there is a gain of 1 to 4 db in the least desirable adjacent channel interference condition. [See Fig. 21(i).] As stated above, this is not a preferred condition of operation, and there is a much greater gain when the other sideband, the one farthest away from the station suffering interference, is used. However, there will necessarily be instances in which this condition will arise: thus the necessity for limiting the high-frequency response of the equipment.

With reference to measurements made on the interference characteristics of the CSSB system when the CSSB signal is spaced 20 kc from the desired signal, the improvement is quite substantial no matter which sideband is used by the CSSB broadcaster. For 20-kc adjacent channel interference, a gain of up to 28.5 to 30 db was measured over AM operation no matter which sideband was used. The reason for this gain is the use of the sharp sideband filter which insures that the bulk of the energy transmitted is restricted to a bandwidth of 8 kc. However, a note of caution is required. The interference characteristic for 20-kc carrier separation is extremely sensitive to the amount of high-frequency content in the modulating wave. Thus, since these measurements are highly dependent on the type of signal being transmitted, it is difficult to state unequivocally that in practice the full 20-kc separation gain will be achieved.

XIII. Television Receiver Radiation Interference Reduction

One of the most serious problems that presently faces the AM broadcaster is the interference produced by poorly shielded television receivers. This problem arises from the fact that most horizontal sweep frequency amplifiers have sufficient harmonic radiation to extend over the entire broadcast range and even up into the high-frequency range. This effect is similar to having some 68 high-powered broadcast stations covering the U. S. added to the broadcast band.

In 1958, questionnaires were sent by Kahn Research Laboratories, Inc., to some 1500 individuals in the New York City metropolitan and suburban area. The addresses were chosen by taking random columns from various telephone books. Ten replied that they did not have radio receivers, 205 stated that the television interference was not objectionable, and 211 said it was objectionable. Thus, over 50 per cent of those who actually answered the questionnaires indicated that they suffered from this type of interference. The importance of this problem has been confirmed by discussions with various broadcasters throughout the U. S. and Canada. One solution to this problem would be to provide better shielding in the television receiver, but this would increase the cost of the receiver. It would be unrealistic to expect that sets now in the hands of the public would be so altered.

The use of CSSB, however, does provide a solution to this problem for many broadcast channels. First of all, the very fact that CSSB increases the level of the high-frequency components of the desired signal should improve the signal-to-interference ratio. Also, by choosing the sideband away from the interference component, an appreciable gain can be achieved.

Fig. 22 is a chart which shows the frequency distribution of the television interference components. This chart was prepared by merely calculating the frequency of the harmonics of the 15.75-kc horizontal output frequency that fall in the broadcast band.

A study of this chart will show that in most cases an appreciable improvement can be achieved by selecting the proper sideband. For instance, if the station is operating on 1180 kc, it should select the lower sideband in order to reduce the television interference which falls at 1181.25 kc. The listener, by tuning his receiver for loudest sound, would reduce this form of interference.

In order to confirm these theoretical conclusions, various interference situations were checked with an average receiver tuned for optimum reception of CSSB when transmitting on the appropriate sideband for avoidance of this interference. (See Figs. 23 and 24.)

The various conditions of interference separation were investigated while varying the tuning of the receiver. It can be seen from Figs. 23 and 24 that the advantage is quite impressive (up to some 16 db) for large amounts of detuning and large separation of interference from the carrier.

Interference Frequency	*Interference Frequency*
551.25	1086.75
567	1102.5
582.75	1118.25
598.5	1134
614.25	1149.75
630	1165.5
645.75	1181.25
661.5 (42nd harmonic of 15.75 kc)	1197
677.25	1212.75
693	1228.5
708.75	1244.25
724.5	1260
740.2	1275.75
756	1291.5
771.75	1307.25
787.5	1323
803.25	1338.75
819	1354.5
834.75	1370.25
850.5	1386
866.25	1401.75
882	1417.5
897.75	1433.25
913.5	1449
929.25	1464.75
945	1480.5
960.75	1496.25
976.5	1512
992.25	1527.75
1008	1543.5
1023.75	1559.25
1039.5	1575
1055.25	1590.75
1071	1606.5 (102nd harmonic of 15.75 kc)

Fig. 22—Distribution of television interference in standard radio broadcast range.

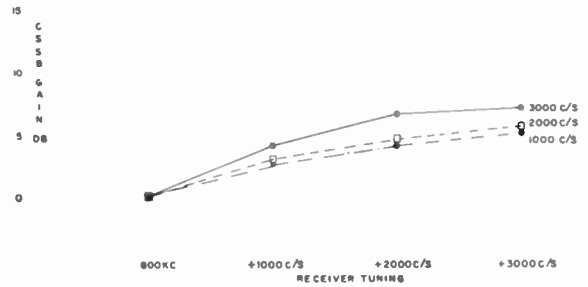

Fig. 23—CSSB gain in reducing TV interference as a function of receiver tuning. Desired modulation frequency 400 cycles. Curve markings indicate difference between carrier and interference frequencies.

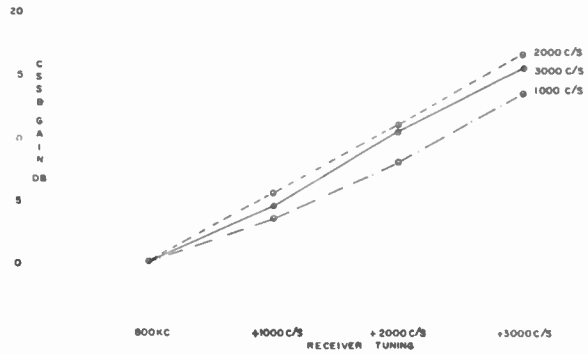

Fig. 24—CSSB gain in reducing TV interference as a function of receiver tuning. Desired modulation frequency 3000 cycles. Curve markings indicate difference between carrier and interference frequencies.

XIV. Reduction of Certain Types of Fading Distortion

Because of the lack of sensitivity to the phase of the carrier at low percentages of modulation, a reduction of fading distortion might be expected if CSSB were used. Laboratory tests, however, are unwieldy and inconclusive. Further proof would necessitate extensive field testing under actual broadcast operating conditions. It is therefore only possible to theorize that there may be some small advantage in the use of CSSB under fading distortion conditions.

XV. Measurements of Sensitivity of CSSB System to Receiver Tuning

One of the main questions that should be considered in evaluating the CSSB system is the question of sensitivity of the system to receiver tuning error.

Figs. 25–29 provide information regarding the tuning error sensitivity. Figs. 25–27 show total harmonic distortion of the entire system for two typical receivers when a 1000-cycle tone is used to modulate the CSSB transmitter, and its associated AM transmitter by 95 per cent. As a control for the test, a curve is provided showing the distortion produced when AM transmission is used. It should be stressed that in all cases over-all system distortion figures—that is, the distortion introduced by the CSSB adapter plus the transmitter and the associated receiver—are shown.

Fig. 26 shows a similar curve, but the equipment is modulated by 3 kc at 95 per cent modulation instead of by 1000 cycles. In all cases, the upper sideband is transmitted when the CSSB system is used. Fig. 27 shows

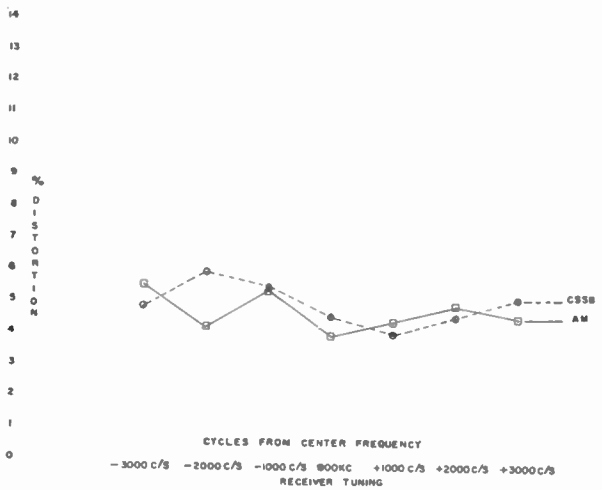

Fig. 25—Total harmonic distortion at output of receiver for AM and CSSB as a function of receiver tuning. Receiver used RCA Model X1. Modulation 1000 cycles (95 per cent).

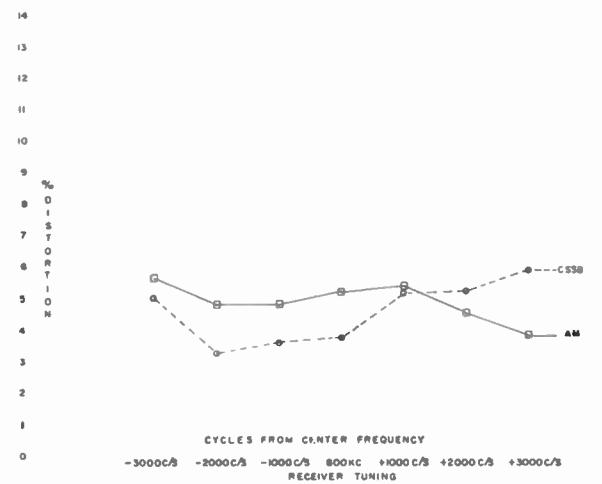

Fig. 26—Total harmonic distortion at output of receiver for AM and CSSB as a function of receiver tuning. Receiver used RCA Model X1. Modulation 3000 cycles (95 per cent).

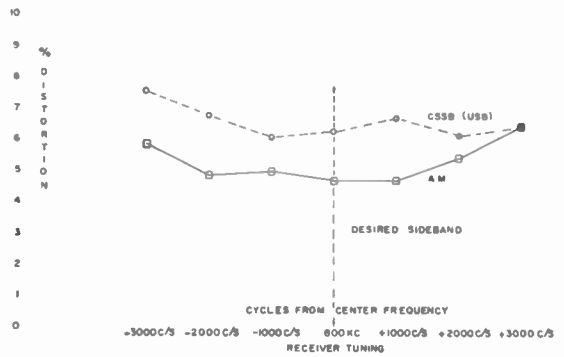

Fig. 27—Total harmonic distortion at output of receiver for AM and CSSB as a function of receiver tuning. Receiver used RCA Model 9C7EE. Modulation frequency used is 1000 cycles (95 per cent).

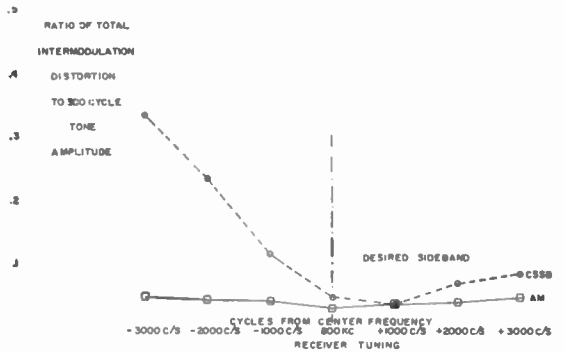

Fig. 28—Over-all system intermodulation distortion as function of receiver detuning. RCA Model X1. Modulation frequency 300 and 3000 cycles peak percentage modulation 85 per cent.

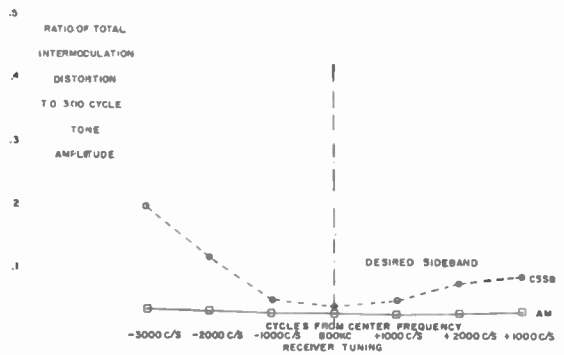

Fig. 29—Over-all system intermodulation distortion as function of receiver detuning. RCA Model 9C7EE. Modulation frequency 300 and 3000 cycles peak percentage modulation 85 per cent.

the harmonic distortion when a second receiver was tested.

Figs. 28 and 29 provide information regarding intermodulation distortion. A test signal was used which included a 300-cycle tone and a 3000-cycle tone, the 3000-cycle tone having one-fourth the amplitude of the 300-cycle tone. The peak modulation used for this test was 85 per cent.

These tests indicate that while the harmonic distortion of CSSB is quite low for a fair amount of detuning, the intermodulation distortion rapidly rises when one tunes to the attenuated sideband. It should be noted, however, that the listener would know that he was tuned to the incorrect sideband because the output level would be very low.

While these measurements indicate that the system may be less tolerant to incorrect tuning, an improperly tuned receiver is obvious to the listener because of the decreased volume. The incorrect tuning is easily and naturally corrected, and there is a compensating factor. By far the greatest trouble experienced by the public when tuning a receiver is caused by interference from adjacent or co-channel transmissions or from television receiver radiation interference. By reducing these difficulties, the system decreases the problem of tuning. Thus, it is felt that the sensitivity in tuning is more than compensated by the reduced difficulty in tuning for avoidance of interference.

XVI. Results of Limited On-the-Air Tests

A number of stations participated in tests of CSSB, including KDKA, Pittsburgh;[21] WGBB, Freeport, Long Island, N. Y.; WMGM, New York; WABC, New York; and WSM, Nashville. In addition, there are a number of U. S. Government and foreign stations in Europe, South America, and Asia, as well as in Canada, equipped for CSSB operation.

As to the increased level and improved fidelity, only one of the stations that conducted CSSB tests requested listener comments. This station was WGBB in Freeport, a 250-watt station (the only low-powered station which participated in these tests). According to their report, their solicitation resulted in the following listener comments:

Improved reception with CSSB	118,
No difference in signal	26,
Poorer reception with CSSB	7.

Some of the 118 favorable comments included: "better than ever," "very loud and clear," "no more interference from that Brooklyn station, now very clear even on my old radio," "previous to installation of new equipment we hadn't been getting WGBB clearly," "sound is much better, in fact I don't believe that it could be any better. I used to have trouble tuning in," "WGBB tone and fidelity has definitely been improved. Particularly noticeable in car radio on North Shore of Long Island where reception had previously been poor, or none at all."

At most of the CSSB experimental broadcast stations, the equipment achieved an average of 30 db of sideband rejection. These figures, for high-powered operation (many test stations operated at a 200 kw peak envelope power rating), compare quite favorably with standard high-power SSB transmitters. A number of different types of transmitters were used, including Doherty type, high-level, and low-level systems. At several of these stations, the equipment was used without readjustment for some three months of operation, and at the end of these test periods the sideband suppression still exceeded the 30-db figure. Thus, it is felt that satisfactory CSSB operation can be achieved with little required maintenance.[21] It should be noted that in all of these cases, the 1.4 phase stretch circuit was used, and it is felt that improved performance could be achieved by use of the newer and simpler 0.5 PM plus 1 PM circuit as this new circuit avoids the use of a critical frequency divider circuit and can also withstand reasonable amounts of overmodulation.

Tests to determine the suitability of CSSB transmission for aeronautical service were made by Aeronautical Radio, Inc., which is a communications company specializing in aeronautical mobile service. It is owned principally by the airlines. These tests, which ran approximately three months, transmitted CSSB from the Long Island, N. Y., ARINC station to conventional airborne AM receiving equipment flying in the Caribbean area, as well as to a military aircraft equipped with a suppressed carrier sideband receiver. The tests were quite successful and Aeronautical Radio has recommended CSSB as one of the four acceptable SSB techniques for ground-to-air and air-to-ground service.[22]

XVII. Summary of Advantages of the CSSB System

The advantages of the CSSB system over conventional amplitude modulation for broadcast service may be summarized as follows:

1) A signal-to-noise power gain for a *given audio fidelity*. This may be seen by recognizing the fact that the bandwidth of a receiver for CSSB need only be $\frac{1}{2}$ of that for AM. Therefore, white noise should be reduced by 3 db and impulse noise by

[21] Westinghouse reported to the Federal Communications Commission that not a single complaint of bad reception of any type was received from KDKA's transmissions on CSSB for a period of over five months.

The chief gain of using CSSB to KDKA is the reduction of adjacent channel interference between KDKA on 1020 kcs and WBZ in Boston on 1030 kcs. The removal of KDKA's upper side frequencies has relieved interference to WBZ's reception and the ability of receivers tuned to KDKA to tune slightly off resonance away from WBZ and toward the radiated lower sideband of KDKA has also given KDKA some additional immunity from WBZ.

In our experience with the Kahn adapter at KDKA it has been reliable, stable, and simple to operate.

We believe further experience will gain additional information which will probably show the Kahn adapter is most useful as an allocation tool.

[22] "Airborne HF SSB/AM System," ARINC Characteristic No. 533; February 15, 1960.

some 6 db. In practice, it appears that due to economics and the requirements for reduction of adjacent channel interference, the common broadcast receiver is actually more suitable for CSSB than for double-sideband AM reception.

2) Improved audio fidelity. Because, as mentioned above, the receivers are too narrow for AM, halving the bandwidth of the signal allows the higher frequency components to be passed, resulting in improved fidelity.
3) Reduction in co- and adjacent-channel interference: a) to the CSSB listener, and b) to the station which previously experienced interference from the station now using CSSB.
4) Provision of a means for reducing interference caused by improperly-shielded TV receivers and other devices, because, under many practical conditions, the station may choose the appropriate sideband to reduce the interference.
5) Possible reduction of selective fading distortion. There is very little evidence regarding this last advantage, and it is the author's feeling that this may turn out to be of relatively little importance in practice.

The advantages of CSSB for communications service are the same as above stated for broadcast service, plus the following:

1) In comparison with conventional SSB and in common with conventional AM, CSSB does not suffer from sensitivity to Doppler shift, because the carrier is transmitted.
2) CSSB can be used with existing receivers and generally with a much lower priced type of receiver than required for conventional SSB reception.
3) CSSB can enjoy full advantage of speech clipping[23,24] which provides some 6 to 9 db of gain and allows the equipment to be operated with less supervision. This is not true for conventional SSB.

On the other hand, in comparison with a fully implemented SSB system, CSSB is more sensitive to selective fading. Its main applications besides AM broadcasting appear to be in mobile telephone and other voice communications circuits where cost and equipment complexity are major factors.

[23] L. R. Kahn, "The use of speech clipping in single-sideband communications systems," PROC. IRE, vol. 45, pp. 1148–1149; August, 1957.
[24] W. Lyons, "SSB and ISB systems for long-distance radio telegraph," *Trans. AIEE*, vol. 46 (*Commun. and Electronics*), pp. 921–924; January, 1960.

Conclusions

Since, in the CSSB system, only the low-frequency voice and music components have sufficient amplitude to produce appreciable second-order sideband components, the bandwidth of the CSSB wave is essentially that of a conventional SSB wave.

Because this new type of wave occupies approximately one-half the bandwidth which an AM wave occupies, CSSB effectively reduces co- and adjacent-channel interference. Equipment was described which makes it possible to adapt conventional AM transmitters to this mode of operation. Measurements indicate that most of the theoretical advantages of this system are achieved in actual practice.

Acknowledgment

The development of the CSSB system has been an extremely long and involved project and the author wishes to acknowledge the assistance of many distinguished engineers.

First of all, the author would like to acknowledge the participation of his colleagues at Kahn Research Laboratories, including Lloyd A. Ottenberg, Robert C. Rogers, Heino L. Pull, Dr. Leonard O. Goldstone and Kenneth B. Boothe. In addition, he wishes to thank Ralph Harmon, George Hagerty, A. C. Goodnow and T. C. Kenney of the Westinghouse Broadcasting System; Gatien Dandois of the Canadian Broadcasting Company; William T. Carnes of Aeronautical Radio; Charles Affelder and Julius Ross of the United States Information Agency; Leucien E. Rawls, formerly of WSM; Arthur Gulbis of Radio Rumbos, Caracas, Venezuela; and Aurele Borsuirt of CJAD, Montreal, Quebec, Canada.

The author also wishes to thank a number of esteemed engineers who helped in reviewing this paper before submission and who made many suggestions for improving it: Prof. Walter Lyons, Harold A. Taylor and E. Williamson of RCA Communications; Dr. Elie J. Baghdady of Massachusetts Institute of Technology; Dr. William B. Jones of Georgia Institute of Technology; Dr. Mischa Schwartz and Martin R. Wohlers of Polytechnic Institute of Brooklyn; and Dr. John C. Hancock of Purdue University.

Magnetic Circuits Employing Ceramic Magnets*

J. C. HELMER†

Summary—Measurements of the field produced by a ceramic, brick-shaped magnet show that the assumption of fixed, uniform magnetization is a useful approximation to the physical state of the magnet. One consequence is that the magnetization is easily measured without disturbing the physical state of the magnet. Another consequence is that the incremental permeability of a ceramic magnet is approximately that of free space. This leads to a significant simplification in the equations describing the fields produced in magnetic circuits employing ceramic magnets. Several types of magnetic circuits are analyzed from this new point of view. A method of design optimization is developed which, in one particular case, violates the ancient criterion that the magnet operate at the point of maximum *BH* product. A generalized derivation of the *BH* energy theorem is given. The properties of steel magnets are contrasted with those of ceramic magnets. In an effort to make use of the leakage field of steel horseshoe magnets, a low-leakage ceramic-steel magnet is developed in which both magnetic materials operate at their respective points of maximum *BH* product. A method is described and analyzed by which the uniformity of the field produced by ceramic pole pieces is improved by covering the pole faces with thin sheets of iron.

I. Introduction

IT IS sometimes stated that the design of permanent magnet circuits is more of an art than a science. This statement applies particularly to circuits containing steel magnets. The situation is quite different when we consider the properties of ceramic magnets. Here we have a material with fixed magnetization and a permeability equal approximately to that of free space. The resulting simplification in the field equations has not been pointed out in the literature. A consequence of this simplification is that it is possible for a novice to build a circuit out of blocks of iron and precharged blocks of ceramic magnet and end up with a precalculated field. Therefore, it is the purpose of this paper to show that the design of ceramic, permanent magnet circuits is more of a science than an art.

An important consequence of the above remarks is that it is not necessary for the manufacturer of a device employing a ceramic permanent magnet to rely upon the magnet maker for the design of the magnetic circuit. Thus, the device designer may employ a unified approach which optimizes all properties of the device. This work has been motivated, in particular, by problems arising in the design of Vaclon®, high vacuum pumps which depend for their operation on strong, uniform, magnetic fields.

* Received by the IRE, May 8, 1961; revised manuscript received, July 12, 1961.

† Central Res. Dept., Varian Associates, Palo Alto, Calif.

II. The Theory of Permanent Magnet Circuits

A. The Field Potentials

Magnets are endowed with a magnetization M through which the fields they produce may be calculated. Depending on whether the source of M is in atomic currents or magnetic poles, we may have (in mks units) either

$$\boldsymbol{B} = \nabla \times \boldsymbol{A}, \qquad \boldsymbol{A} = \frac{\mu_0}{4\pi}\int \frac{\nabla \times \boldsymbol{M}}{r}\, dV \tag{1}$$

or

$$\boldsymbol{H} = -\nabla\Phi, \qquad \Phi = \frac{-1}{4\pi}\int \frac{\nabla\cdot\boldsymbol{M}}{r}\, dV, \tag{2}$$

where $\boldsymbol{A}$ is the vector potential resulting from a volume current density $i = \nabla\times M$, and Φ is the scalar potential resulting from a volume pole density $\rho = -\nabla\cdot M$.[1] Since free magnetic poles do not exist (?), some writers prefer on the grounds of physical reality to work with the vector potential $\boldsymbol{A}$. However, for a given volume distribution of $\boldsymbol{M}$, either potential produces the same results, and the choice of which potential to use is dictated by the nature of the problem. Permanent magnet circuits frequently employ bodies of material (iron) which have nearly infinite permeability relative to the other parts of the circuit. In such bodies the approximation $H=0$ is good and therefore the surface of such a body becomes an equiscalar potential. The fictitious magnetic poles move about on this surface in much the same way as electric charge on a conductor and the resulting field may be found by solution of Laplace's equation $\nabla^2\Phi = 0$ in the external space. For this reason the scalar potential Φ is most useful in determining the fields of permanent magnets.

For illustration, consider the example of a bar magnet with fixed, uniform magnetization, terminated on each end with an irregular blob of iron. Since the magnetization of the bar is fixed, the permeability of the bar is the same as that of free space. The magnetic field may be found by solving Laplace's equation subject to the condition that each blob of iron defines an equipotential surface. Afterwards the potential difference is adjusted so that the number of poles on the surface of each blob (including the surface in contact with the magnet) is the same as that which previously existed

[1] W. K. H. Panofsky and M. Phillips, "Classical Electricity and Magnetism," Addison-Wesley Publishing Co., Reading, Mass., ch. 8; 1955.

on the ends of the bar magnet. Or, in cgs units,

$$4\pi \int_{\text{magnet end}} \boldsymbol{M}\cdot d\boldsymbol{A} = \int_{\text{iron surface}} \boldsymbol{H}\cdot d\boldsymbol{S}. \qquad (3)$$

The concept of fixed magnetization applies particularly well to ceramic magnets. This concept may be applied to steel magnets if we also assign to them a relative permeability greater than unity, as determined approximately by the slope of the demagnetization curve for values of $\boldsymbol{H}$ between zero and the point of maximum energy product. In this case the behavior of the magnet is analagous to that of a dielectric with self-polarization, and the additional boundary defined by the surface of the permanent magnet greatly increases the difficulty of obtaining analytic solutions for the magnetic field.

B. The B·H Integral Theorem

Consider an arbitrarily selected volume V in a space throughout which $\nabla\cdot\boldsymbol{B}=0$ and $\nabla\times\boldsymbol{H}=0$. We will compute the $B\cdot H$ integral within this volume.

$$W_i = \int_V \boldsymbol{B}\cdot\boldsymbol{H}dV = -\int_V \boldsymbol{B}\cdot\nabla\Phi dV \qquad (4)$$

where Φ is the scalar potential for H.

Note, however, that

$$\nabla\cdot\boldsymbol{B}\Phi = \Phi\nabla\cdot\boldsymbol{B} + \boldsymbol{B}\cdot\nabla\Phi = \boldsymbol{B}\cdot\nabla\Phi. \qquad (5)$$

Then

$$W_i = -\int_V \nabla\cdot\boldsymbol{B}\Phi dv = -\int_S \Phi\boldsymbol{B}\cdot d\boldsymbol{S} \qquad (6)$$

where S is the surface of the volume in question and $d\boldsymbol{S}$ is a vector directed outward normally from this surface. We will compute now the $\boldsymbol{B}\cdot\boldsymbol{H}$ integral over all of the space outside of V. By the same argument we arrive at an expression of identical form

$$W_0 = -\int_S \Phi\boldsymbol{B}\cdot d\boldsymbol{S}_-, \qquad d\boldsymbol{S}_- = -d\boldsymbol{S}, \qquad (7)$$

where $d\boldsymbol{S}_-$ is a vector directed normally towards the interior of V. The integral over the boundary at infinity vanishes because at a sufficiently great distance r, the strongest type of field we can have is a dipole field whose strength goes as $1/r^3$. Then

$$\int \Phi|\,B|\,|\,dS| \sim \frac{1}{r} \to 0 \quad \text{as} \quad r\to\infty. \qquad (8)$$

Since Φ is single valued and $\boldsymbol{B}$ is continuous, we conclude that

$$-W_i = W_0. \qquad (9)$$

Therefore, the $\boldsymbol{B}\cdot\boldsymbol{H}$ integral within V is equal to minus the $\boldsymbol{B}\cdot\boldsymbol{H}$ integral outside of V. This can be only if $\boldsymbol{B}\cdot\boldsymbol{H}\equiv 0$ or if there is some region in which $\boldsymbol{B}$ and $\boldsymbol{H}$ components are oppositely directed. The interior of a magnet is such a region, as shown in Fig. 1.

The above integral theorem becomes useful when the surface S defines the boundary of a permanent magnet. Then the volume of the magnet is given by

$$V = \frac{W_0}{-(\boldsymbol{B}\cdot\boldsymbol{H})\ \text{average in magnet}}. \qquad (10)$$

For a given external-field energy the volume of magnetic material is minimized by maximizing the $-\boldsymbol{B}\cdot\boldsymbol{H}$ product in the magnet.

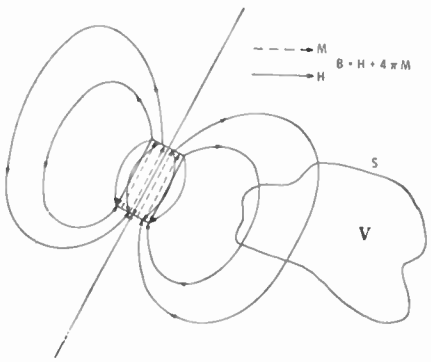

Fig. 1—Field of a permanent magnet.

Consider now a magnet with fixed, uniform magnetization in a uniform field H. We can write (in cgs units) $\boldsymbol{B}=\boldsymbol{B}_r+\boldsymbol{H}$, where $B_r=4\pi M$ is the magnetic remanence given by the value of B when $H=0$. Then

$$-\boldsymbol{B}\cdot\boldsymbol{H} = -(\boldsymbol{B}_r+\boldsymbol{H})\cdot\boldsymbol{H} = -B_rH\alpha - H^2, \qquad (11)$$

where α is the cosine of the angle between $\boldsymbol{B}_r$ and $\boldsymbol{H}$. Thus, the maximum value of $-(\boldsymbol{B}\cdot\boldsymbol{H})$ is obtained when

$$H = \frac{-B_r\alpha}{2}, \qquad -(\boldsymbol{B}\cdot\boldsymbol{H})_{\max} = \frac{B_r^2\alpha^2}{4}, \qquad (12)$$

and this, in turn, is maximized when $\alpha=-1$ so that $\boldsymbol{H}$ is antiparallel to $\boldsymbol{B}_r$. Thus, for a given external-field energy the volume of a ceramic magnet is minimized by designing the circuit so that within the magnet, H is antiparallel to M and has the value $H=B_r/2$. It may not always be possible to design the circuit so that the magnet operates in this way. If, as we shall see in Section IV, there are constraints which fix the cross section of the magnet, then the optimum point of operation is not at the point of maximum BH product.

In steel magnets the point of maximum BH product is set by the value of H at which severe demagnetization sets in. This may be seen in the demagnetization curves in Fig. 2. The demagnetization curves of magnets of equal maximum BH product are tangent to the same $BH=$const. curve. Thus, according to the BH energy theorem, there is not nearly as much difference in re-

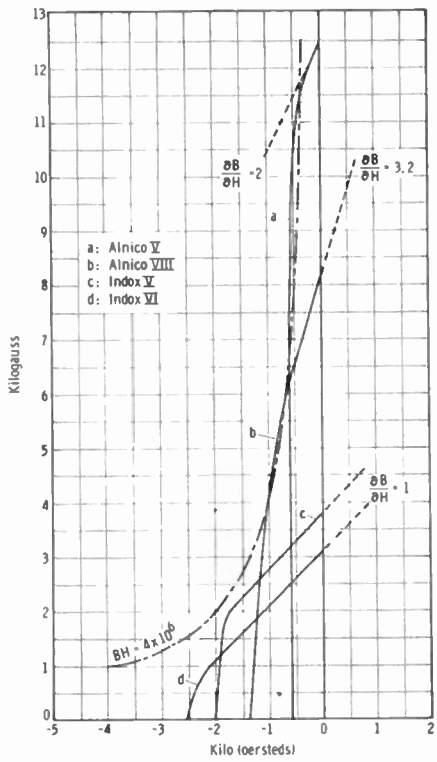

Fig. 2—Demagnetization curves.

quired volume between the ceramic and steel magnets as one might suppose from the difference in magnetic remanence.

C. *Efficiency*

Through (10) we may define the efficiency of a magnetic circuit as follows:

$$\text{Efficiency} = \frac{\text{measured gap energy} \times 2}{\text{magnet volume} \times (-B \cdot H)_{\max}}. \quad (13)$$

If in the gap energy we include only that part of the field which is useful, then (13) is a measure of the overall quality of the circuit. If in the gap energy we include the energy of leakage fields as well, then (13) is a measure of the efficiency of utilization of the permanent magnet material. It is difficult to estimate the leakage energy, although in certain simple geometries it is possible to use analytic methods.[2]

III. Ceramic Magnets

A. *Demagnetization Curves*

In Fig. 2 are shown the demagnetization curves for several types of magnetic materials supplied by the Indiana Steel Products Co. Two barium-ferrite ceramic magnets are shown, denoted by Indox V and VI. Over a wide range in H the demagnetization curves of the ceramic magnets are characterized by straight lines with slope $dB/dH \simeq 1$. If we plot $4\pi M = B - H$ against H, we get horizontal lines which show that the magnetization M is fixed and independent of H. Indox becomes demagnetized eventually, but this occurs beyond the point $H = -(B_r/2)$, so that over most of its working range it may be considered an ideal magnet. The incremental permeability of these magnets is given actually as approximately 1.05. This means that a demagnetizing field of strength $H = B_r/2$ will reduce the magnetization by about 2.5 per cent. The assumption of fixed magnetization, therefore, introduces a minimum error in the field calculations of about this size.

Ceramic magnets are frequently available in brick form, magnetized in a direction normal to one of the faces of the brick, as in Fig. 3. For uniform magnetization $\nabla \cdot \boldsymbol{M}$ is zero in the interior of the magnet, and is nonzero only at the faces normal to M. On these faces the divergence of $\boldsymbol{M}$ gives rise to a magnetic-pole density equal to M poles per unit area. The field arising from one surface layer alone is strong enough so that for Indox V the material just below the surface is on the verge of becoming demagnetized. This is seen by noting that the field adjacent to the surface layer, due to the surface layer alone is

$$H = -2\pi M = -\frac{B_r}{2}, \quad (14)$$

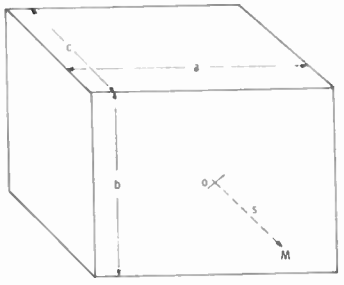

Fig. 3—Geometry of a brick-shaped magnet.

where B_r is the magnetic remanence. The presence of the opposite surface layer increases the internal demagnetizing field so that for samples such that $a, b \gg c$ in Fig. 3 the external field is cancelled and the internal field is $H = -B_r$. Such a condition will produce demagnetization in Indox V and VI magnets. This places restrictions on the dimensions of brick-shaped magnets if they are to be fully charged before being placed in the circuit. For instance, an Indox V magnet with dimensions $a = b = 3''$, $c = 2''$ became about 20 per cent demagnetized when separated into two pieces of dimensions $a = b = 3''$, $c = 1''$. To prevent demagnetization of Indox V, a practical rule is that c, the distance between pole faces, be at least two-thirds of the shortest face dimension. If this condition is not met, then the magnets may be charged in their circuit at a saturation flux density of 10,000 gauss.

[2] One reviewer suggests that the leakage energy may be obtained by subtracting the measured gap energy from the magnet energy.

B. Measurement of the Remanence of Ceramic Magnets

A method of measuring the remanence of a ceramic magnet is to measure the field strength along an axis s that passes through the center of the pole faces. For simple rectangular or cylindrical magnet geometries the field may be calculated and the remanence determined by matching the theoretical curve to the experimental points. This has been done for brick-shaped Indox V magnets with the following results.

The field due to one pole face of a brick-shaped magnet, as shown in Fig. 3 is given by

$$H = \frac{B_r}{4\pi}\int_{-b/2}^{b/2}\int_{-a/2}^{a/2}\frac{s\,dy\,dx}{(x^2+y^2+s^2)^{3/2}} = \frac{B_r}{\pi}\tan^{-1}\frac{ab}{2s(4s^2+a^2+b^2)^{1/2}}, \quad (15)$$

where a, b are the dimensions of the pole face, and s is the normal distance from the center of the pole face. If c is the face separation, then the total field is given by

$$H = \frac{B_r}{\pi}\left\{\tan^{-1}\frac{ab}{2s\sqrt{4s^2+a^2+b^2}} - \tan^{-1}\frac{ab}{2(s+c)\sqrt{4(s+c)^2+a^2+b^2}}\right\}. \quad (16)$$

The field at a distance s from one pole face on the axis of a *cylindrical* magnet, due to that pole face alone, is given by

$$H = \frac{B_r}{4\pi}\int_0^a \frac{2\pi s r\,dr}{(s^2+r^2)^{3/2}} = \frac{B_r}{2}\left(1-\frac{s}{(s^2+a^2)^{1/2}}\right). \quad (17)$$

where a is the radius of the cylinder.

In Figs. 4–6 are shown the results of measurement and calculation for three Indox V magnets of different dimensions. At distances greater than one inch from the pole face there is very precise agreement between theory and experiment. Thus, the remanence is quite accurately determined. Very close to the center of the pole face the field falls off somewhat below the calculated value. This indicates that the magnetization at the center of the block is a little below average.

One magnet was found in which the field strength at the face center was lower than the field strength a small distance from the face center. Measurements of total field strength along a perpendicular line through the axis at a constant distance from the face, as shown in Fig. 7, indicate that this effect is confined to a small region in the neighborhood of the face center. For this reason it is not a large source of error. In fact the field strengths obtained when these magnets are placed in circuits are close enough to the calculated values based on the measured remanence, that one suspects that the magnetization at the center has partly recovered itself

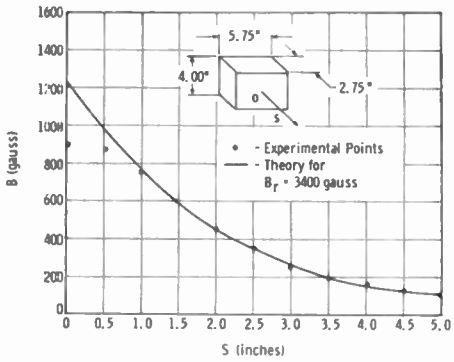

Fig. 4—Measured and calculated field of a ceramic magnet.

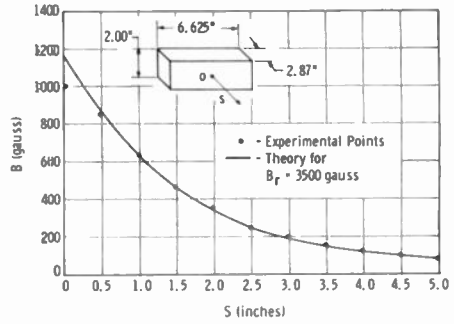

Fig. 5—Measured and calculated field of a ceramic magnet.

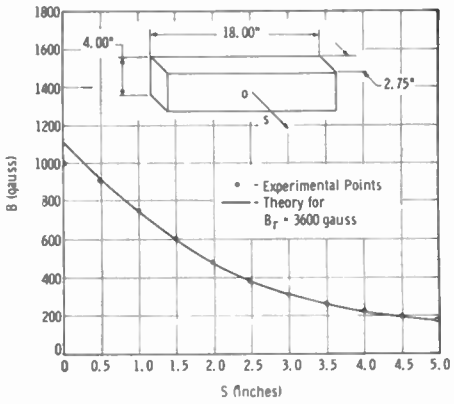

Fig. 6—Measured and calculated field of a ceramic magnet.

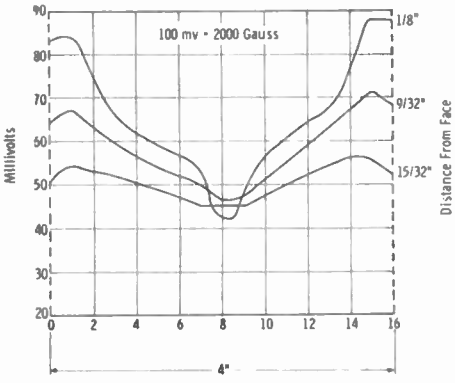

Fig. 7—Field profile on the face of a ceramic magnet.

under the influence of the new field distribution. The reason that an isolated magnet will become preferentially demagnetized at a face center is that the demagnetizing field of the opposite face is strongest at this point.

A feature of the theoretical field is that it falls off most rapidly close to the pole surface. This violates the intuitive conclusion, based on the behavior of fields adjacent to equipotential surfaces, that the slope of the field function in the normal direction at the surface should be zero. This conclusion is invalid because uniform charge surfaces are not equipotential surfaces. The behavior of fields close to uniform charge surfaces is clarified by the following argument. Consider the field component normal to the plane of a uniformly charged, planar surface of area A. The angle θ between the radius vector r, from an element of area dA on the surface to the field point, and the normal to the plane is the same as the angle between the radius vector r and the normal to dA, since dA is part of the plane. Thus, the normal field component is given by

$$H_n = \rho \int \frac{dA \cos\theta}{r^2} = \rho\Omega, \tag{18}$$

where $\rho = B_r/4\pi$ is the uniform charge density on the planar surface A and Ω is the solid angle subtended by the surface A at the field point. It is clear now that (15) and (17) are derived from solid-angle calculations. It is clear also that the solid angle Ω varies most rapidly with normal displacement adjacent to the charge plane.

IV. Magnetic Circuits Containing Ceramic Magnets

A. Field of a Magnet in a Long Cylindrical Armature

The field of two uniformly-magnetized ceramic pole pieces in a very long cylindrical armature, shown in Fig. 8(a), may be calculated exactly by image theory in two dimensions. Each line charge dq at radius r gives rise to an image charge $-dq$ in the same direction at radius $r' = R^2/r$, where $dq = B_r dx/2\pi$ and R is the inner radius of the armature. The field at the center is equal to twice the field produced by one pole face and its image alone. Thus, the field at the center is

$$H = 2\int_{-b}^{b} \frac{B_r dx}{2\pi} \cdot \frac{a}{\sqrt{a^2+x^2}} \cdot \left(\frac{1}{\sqrt{a^2+x^2}} - \frac{\sqrt{a^2+x^2}}{R^2} \right) \tag{19}$$

$$\therefore\ H = \frac{2B_r}{\pi} \left\{ \tan^{-1}\left(\frac{b}{a}\right) - \frac{ab}{R^2} \right\}. \tag{20}$$

It is evident that the term $\tan^{-1} b/a$ arises from the pole faces alone, while the term $-ab/R^2$ arises from the image charges. In many practical designs the image term may produce only a small correction so that a useful estimate of the field strength, representing an upper limit, is obtained by calculating the field due to the pole face charge alone. This is a particularly useful procedure when the armature is neither long nor cylindrical. For this reason it is of value to have on hand the field reduction factors H/B_r for square and strip pole faces, given respectively by the functions

$$\frac{2}{\pi} \tan^{-1} \frac{b^2}{a(a^2+2b^2)^{1/2}} \quad \text{and} \quad \frac{2}{\pi} \tan^{-1} \frac{b}{a}, \tag{21}$$

where b is the face width and a is the gap width.

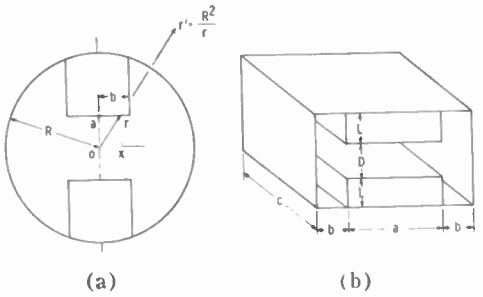

(a) (b)

Fig. 8—(a) Ceramic magnets in a cylindrical armature. (b) Ceramic magnets in a rectangular armature.

B. Field of a Ceramic Magnet in a Rectangular Armature (special case)

Thus far, we have considered magnet configurations which permit an exact field calculation to be made. An alternative approach, which forms the basis of magnetic-circuit engineering, is to make a guess at the shape of the magnetic field and then to apply the equations

$$\nabla \cdot \boldsymbol{B} = 0 \qquad \nabla \times \boldsymbol{H} = 0 \tag{22}$$

in order to determine the strength of the field. The first equation states that the magnetic induction is continuous, while the second equation states that the line integral of H around any closed path is zero.

The simplest case that may be analyzed is the case in which B is assumed to be uniform in the magnet and in the gap. This condition is met to a good approximation in the central field region of the circuit in Fig. 8(b), under the conditions $a, c \gg L, D$. Assuming that $H \simeq 0$ in the armature, we obtain the equations

$$H = B_r - H_m, \qquad DH = 2LH_m, \tag{23}$$

where H is the field strength in the gap and H_m is the field strength in the magnet. These equations have the solution

$$H = \frac{B_r}{1 + \dfrac{D}{2L}}. \tag{24}$$

The magnets operate at the point of maximum-energy product when $D = 2L$, that is the total magnet length is equal to the gap width. If, however, the magnet cross

section is fixed by the dimensions of the device, so that the magnet length is the only free variable, then different optimum dimensions are obtained. Considering the volume of the magnets plus the volume of the gap, the gap energy divided by this volume is given by

$$\frac{H^2Dac}{(D+2L)ac} = B_r^2 \frac{\left(2\frac{L}{D}\right)^2}{\left(1+\frac{2L}{D}\right)^3}. \qquad (25)$$

Thus, the useful magnetic energy per unit circuit volume is maximized when $L=D$, so that the total magnet length is equal to twice the gap width. This results in a field in the gap equal to $H=2(B_r/3)$, and a field in the magnet equal to $H_m=B_r/3$.

C. Iron Pole Faces

Ceramic pole pieces, as discussed in the previous sections, are quite effective in producing fields of about 2000 gauss along the magnetic axis. When we move away from the center of the field towards the gap edge we find that the field strength falls off gradually, starting about one gap width from the gap edge. At the intersection of the midplane between the pole faces and the gap edge the field strength will have dropped to about one-half of its value at the center. This "edge effect" may be calculated exactly for the case of two semi-infinite, uniform charge surfaces which are positioned relative to each other in the manner of condenser plates. These uniform charge surfaces represent the uniform pole distributions on the opposite faces of two semi-infinite, ceramic blocks. The field strength at the midplane is given then by

$$H = B_r\left(\frac{1}{2}+\frac{1}{\pi}\tan^{-1}\frac{2x}{a}\right), \qquad (26)$$

where a is the gap width and x is the horizontal distance between the gap edge and the field point, measured normal to the gap edge. This function is plotted in Fig. 9.

For applications requiring more uniform fields, the uniformity may be greatly improved by covering the ceramic pole faces with a thin sheet of iron. This frees the poles on the ceramic face and allows them to bunch up around the edges. In this way the field strength is raised near the edges and reduced near the center. The effectiveness of the pole redistribution in increasing field uniformity may be evaluated by the methods described in Section II-A. For this case we use the Schwarz transformation.[3]

$$dZ = \frac{(Z_1-1)(Z_1+1)}{Z_1}\,dZ_1. \qquad (27)$$

[3] Panofsky and Phillips, *op. cit.*, ch. 4.

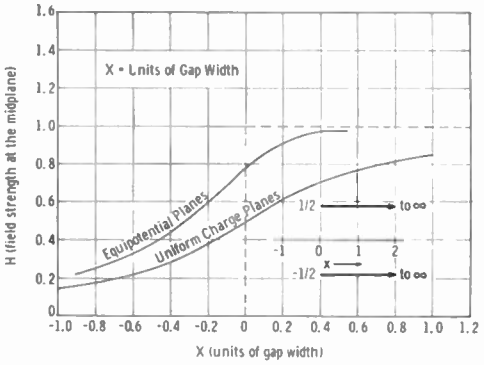

Fig. 9—Field strength near the edge of a magnetic gap.

This transformation bends the real axis in the Z_1 plane through an angle of $-\pi$ at $Z_1=\pm 1$ and through an angle of π at $Z_1=0$. In this way the real axis of the Z_1 plane becomes transformed into two semi-infinite, parallel lines in the Z plane, representing semi-infinite, parallel plates in two dimensions. The origin $Z_1=0$ is transformed to a point at infinity between the two plates, so that radial and azimuthal lines in the Z_1 plane represent lines of constant potential and constant stream in the Z plane. In this way the shape and strength of the field is determined for two semi-infinite, equipotential planes. The strength of the field at the midplane in the neighborhood of the gap edge is shown in Fig. 9. The addition of the iron pole faces produces a remarkable increase in field uniformity in comparison with the field due to ceramic pole faces. The fall-off in field strength near the edge does not begin until we are within 0.2 gap widths of the edge, and then on the midplane at the gap edge the field has dropped only to $\sim$0.8 of the central value.

Another aspect of the field related to its uniformity near the gap edge is its radius of curvature. The ratio of the gap width to the radius of curvature at the midplane is calculated in Fig. 10 for ceramic and iron pole faces. Again we see the effectiveness of the iron faces in increasing the field uniformity. The radius of curvature at the edge is on the order of the gap width.

The price of this increased field uniformity is a reduction in the useful energy contained in the gap. This arises because the total flux, including leakage, remains fixed. Then the bunching of the poles at the edges of the iron faces increases the amount of leakage flux at the expense of the flux inside the gap. An evaluation of this effect involves calculating the total energy in the gap for each case, and then comparing the two cases under the constraint that the total flux, including leakage, remains constant. This is a fairly difficult calculation which is easy to bypass with an experimental result. In Fig. 11 we show the measured field strength at the midplane between two ceramic pole pieces in a cylindrical armature. Although this is a three-dimensional rather

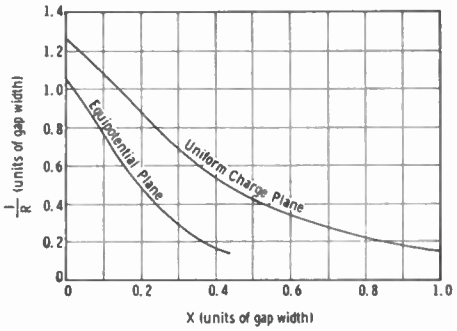

Fig. 10—Field curvature near the edge of a magnetic gap.

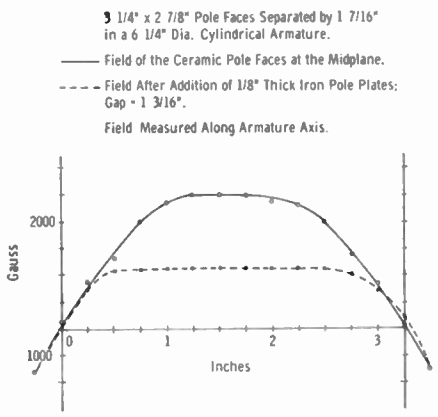

Fig. 11—Measured field strength in the plane of a magnetic gap.

than a two-dimensional configuration, we see that the two-dimensional calculations are quite successful in predicting the behavior of the field in the neighborhood of the gap edge. We note also that in spite of the fact that the addition of the iron pole faces has reduced the gap width, the field strength is substantially lower than that obtained with the bare ceramic pole faces. Thus, the addition of the iron pole faces causes a very substantial reduction in the useful energy contained in the gap.

It is not easy to calculate the field strength in the gap when the ceramic poles are faced with iron. However, the following approximate procedure has met with some success. We may consider the pole density as being almost uniform except at the gap edges where the density becomes infinite. Calculations indicate that over a considerable range of geometry the plates of non-uniform pole density may be replaced by fictitious plates of uniform pole density which extend beyond the real plates by an amount equal to ~0.4 gap widths. This tends to preserve the pole density at the center and the total flux. The equivalent uniform pole density is given by

$$M = \frac{B_r}{4\pi} \cdot \frac{A}{A + 0.4Cd}, \tag{28}$$

where A is the area of the real pole faces, C is the circumference of the pole face, and d is the gap width. With this value of M the field at the center is calculated for a uniform pole sheet which extends beyond the real faces by an amount $0.4d$. Once having the field at the center, we have it approximately everywhere by virtue of Fig. 9.

D. Field of a Magnet Between Two Rectangular Iron Plates

The results of the preceding section may be applied to the circuit of Fig. 12(a). We assume that the plates extend, in effect, a distance of about $0.4d$ beyond each edge. The field strength is accordingly given by (15) and (28).

$$H \simeq B_r \cdot \frac{A_m}{ab + 0.8(a+b)d} \cdot \frac{2}{\pi} \tan^{-1} \frac{a_1 b_1}{d\sqrt{d^2 + a_1^2 + b_1^2}}, \tag{29}$$

where A_m is the pole face area of the magnet, and $a_1 = a + 0.8d$, $b_1 = b + 0.8d$.

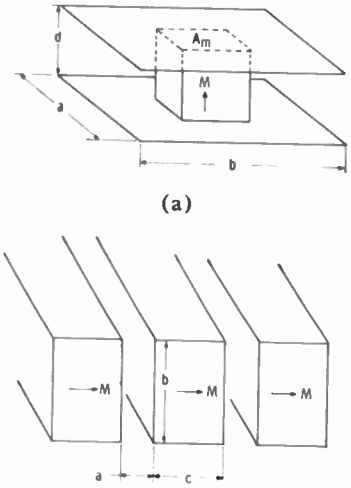

Fig. 12—(a) Magnet between iron planes. (b) A linear array of magnets.

E. Periodic Structures

The magnet for a high-speed VacIon® pump consists of a linear array of long rectangular ceramic bars, as shown in Fig. 12(b), magnetized to provide a high magnetic field between the bars. For an infinite array, the field at the center of a gap is given by

$$H = \frac{2B_r}{\pi} \sum_{n=0}^{\infty} \left(\tan^{-1} \frac{b}{(2n+1)a + 2nc} - \tan^{-1} \frac{b}{(2n+1)a + 2(n+1)c} \right). \tag{30}$$

The nth term in this summation represents the contribution to the field by a magnet bar whose nearest face is

a distance of $(2n+1)(a/2)+nc$ from the field point. It is of some interest to show that this summation reduces in the limit $b \gg a$, c to a simple circuit formula. For $b \gg c$, the term difference in the parenthesis reduces to

$$\frac{2\dfrac{c}{b}}{1+\left[\dfrac{(2n+1)a+2nc}{b}\right]^2}. \tag{31}$$

If we let

$$x = \frac{(2n+1)a+2nc}{b}$$

then for a unit change in n, the corresponding change Δx in x is given by

$$1 = \frac{b}{2(a+c)}\Delta x. \tag{32}$$

Consequently, the summation reduces to

$$H = \frac{2B_r}{\pi}\cdot\frac{c}{a+c}\int_0^\infty \frac{dx}{1+x^2} = B_r\frac{c}{a+c}. \tag{33}$$

Allowing for the change in notation we see that this is the same equation used in (24) for ceramic poles in a rectangular armature.

As before, the gap energy per unit circuit length may be maximized. This yields the same result, *i.e.*,

$$c = 2a.$$

Thus, the total magnet length per gap is equal to twice the gap width. This optimization calculation has been carried out numerically with (30) for $b/a = 3$. This yields again the result $c \simeq 2a$, and we conclude that the optimum dimensions are not very sensitive to the value of b. For low values of b/a, such as $b/a = 3$, the field strength must be calculated by summing up the individual terms in (30). The series converges fairly rapidly for dimensions near optimum although, in general, it is surprising how slowly the field from distant gaps falls off in two dimensions.

V. The Combination of Ceramic and Steel Magnets

A. Comparison of Steel and Ceramic Magnets

The most commonly used steel magnetic material is Alnico V, which has a much higher remanence than Indox V ceramic, and a much lower field strength at the point of maximum BH product. This is shown in Fig. 2. The resulting value of maximum BH product for Alnico V is about 1.6 times greater than that for Indox V ceramic. This means, according to (10), that it requires a smaller volume of Alnico than of Indox in order to energize a given gap. In practice this may not work out due to the fairly high-flux leakage from the steel magnet itself.

The consequence of the very high remanence of Alnico V is that only a small cross-sectional magnet area is required to obtain a high flux. On the other hand, the low coercive force results in a magnet element that is much longer than the gap spacing when high fields are required. Thus, steel magnets tend to be long and thin while ceramic magnets tend to be short and fat. The great virtue of a steel magnet is that the long, thin element can be cast into a horseshoe which surrounds the gap at a distance. A particular advantage of a ceramic magnet is that due to its very high coercive force it can be used directly in parallel with a high field gap.

B. The Wedge Magnet

The main factor limiting the efficiency of steel horseshoe magnets is the energy contained in the leakage fields in the interior of the horseshoe. The strength of the leakage field is frequently on the order of 1000 gauss and it would provide therefore a good working field for a ceramic magnet whose magnetization is oriented antiparallel to this field. The induction of the ceramic magnet would then be added to that of the steel magnet so that a gap of larger area may be energized. We can look at this another way and say that the relatively high permeability of the steel magnet tends to confine to its body the fields of the ceramic magnet and to direct them into the gap. Considerations of this kind have been employed by Glass[4] in the design of steel magnets for electron beam focusing.

We will inquire now as to what is the optimum configuration for a ceramic magnet encased by a steel magnet. We wish that all volume elements of the structure operate at the point of maximum BH product. Further consideration reveals that in two dimensions this condition is met in the structure of Fig. 13(a) if the correct values are chosen for the angles θ and ψ. The steel magnet is magnetized in the radial direction while the ceramic magnet is magnetized in the azimuthal direction (although in practice it would probably be magnetized normal to the x axis). As in Section IV-B we will assume that we know the shape of the field. Outside of the steel magnet the H-field lines are assumed to form circles with a common origin at the left-hand corner of the magnet. In the upper half plane the H field inside of the steel magnet is assumed to be directed radially towards the origin while the H field in the ceramic magnet is in the negative azimuthal direction. The lines of induction B flow through the ceramic magnet in the positive azimuthal direction and out through the steel arms in the positive radial direction to a load (a gap) which is not shown. The circular H field outside of the magnet is a leakage field which may be neglected (as we will do) if θ is small compared with 90°.

[4] M. S. Glass, "Appraisal of permanent magnet materials for magnetic focusing of electron beams," *J. Appl. Phys.*, vol. 29, p. 403; March, 1958.

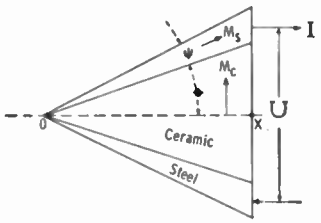

(a)

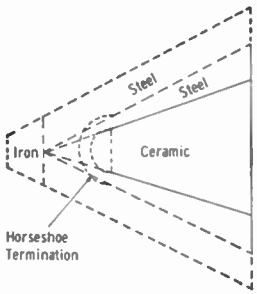

(b)

Fig. 13—(a) A combination ceramic-steel magnet. (b) Modifications.

Let B_c, H_c and B_s, H_s be the points of maximum energy product for the ceramic and steel magnets respectively. Then the angle θ is given by the equation $H_s x = H_c x\theta$ or

$$\theta = \frac{H_s}{H_c} \simeq \tfrac{1}{3} \text{ radian} \tag{35}$$

and ψ is given by the equation $B_c x = B_s x\psi$, or

$$\psi = \frac{B_c}{B_s} \simeq \tfrac{1}{6} \text{ radian}, \tag{36}$$

where the numerical values are given for the combination of Indox V and Alnico V. A wedge magnet of unit width and length x delivers a flux I and a potential U given by the equations

$$I = B_c x, \qquad U = 2H_s x. \tag{37}$$

This is a rather high-impedance output which may be suitable for electron beam focusing. The design may be modified for circular geometry in which the angle θ remains the same but the variation in thickness of the steel magnet is no longer linear with distance.

The impedance of a wedge magnet may be lowered, that is the flux may be increased, by adding a constant thickness of steel magnet to it. Also, the initial sharp corner may be avoided by starting out with a small horseshoe magnet as in Fig. 13(b).

VI. Conclusions

Measurements have been presented which show that the assumption of fixed magnetization is a useful approximation to the state of ceramic magnets. By means of this assumption a precise determination of remanence is made possible. Because of the fixed magnetization the field produced by isolated ceramic bars is easily computed, while the field due to ceramic magnets in an iron circuit may be calculated by image theory. It has been shown that by facing ceramic poles with a thin sheet of iron the field homogeneity is increased at the expense of reduced stored energy in the gap. A design optimization procedure has been found that violates in a specific case the ancient criterion that the magnet operate at the point of maximum BH product. An effort to make use of the leakage field from a steel horseshoe magnet has led to the design of a low-leakage ceramic-steel magnet in which both magnetic materials operate at their respective points of maximum BH product.

In applying the equations derived in this paper, the writer has been able to consistently predict field strengths within 10 per cent of their measured values. However, the ceramic-steel magnet has not been tested and so its actual performance must remain somewhat speculative.

Appendix

A. *Field of Two Equipotential Semi-Infinite Planes*

Integration of the Schwarz transformation

$$dZ = \frac{(Z_1 - a)(Z_1 + a)}{Z_1} dZ_1$$

yields

$$Z = \frac{Z_1^2}{2} - a^2 \ln Z_1 + C.$$

We want to evaluate C and a so that the real axis in the Z_1 plane transforms into two lines parallel to the x axis, which terminate on the y axis at points $0, \pm i/2$. Setting $\operatorname{Re} Z = 0$ and $Z_1 = \pm a$, gives

$$\operatorname{Re} C = -\frac{a^2}{2} + a^2 \ln a.$$

Then

$$Z = \tfrac{1}{2}(Z_1^2 - a^2) - a^2 \ln \frac{Z_1}{a} + C'.$$

Then setting $Z_1 = a$, $\operatorname{Im} Z = i/2$ and $Z_1 = -a$, $\operatorname{Im} Z = -(i/2)$ gives, respectively,

$$C' = \frac{i}{2}, \qquad a^2 = \frac{1}{\pi}.$$

Since lines in Z_1 of constant angle are potential lines, and lines of constant radius are stream lines, we let $Z_1/a = \exp C''(V + iU)$, where U and V are the potential and stream functions. When $U = 0$ we move along the line $Z = x, i/2$ and when $C''U = \pi$, we move along the line $Z = x, -i/2$. For a potential difference of unity

we chose $C''=\pi$. Thus, the complete transformation is

$$Z=\frac{1}{2\pi}\left[e^{2\pi V}(\cos 2\pi U+i\sin 2\pi U)-1\right]-V-iU+\frac{i}{2}.$$

The field strength at the midplane may be obtained by setting $U=\frac{1}{2}$ and plotting $\partial V/\partial x$ against x. This is done by a graphical procedure involving the equations for $U=\frac{1}{2}$

$$-x=\frac{1}{2\pi}(e^{2\pi V}+1)+V, \qquad \frac{-dx}{dV}=e^{2\pi V}+1.$$

The charge density on the planes can be obtained by setting $V=0$ and calculating dV/dx from the equation of x against V

$$-x=\frac{1}{2\pi}(1-e^{2\pi V})+V.$$

It is clear that on the plane $U=0$, the condition $V=0$ gives $x=0$ so that the zero reference point for the stream function is at the edge of the plane.

Acknowledgment

The author wishes to thank Dr. R. L. Jepsen for his many helpful criticisms of this work.

Bibliography

[1] J. J. Went, *et al.*, "Ferroxdure, a class of new permanent magnet materials," *Philips Tech. Rev.*, vol. 13, pp. 194–208; January, 1952.
[2] J. J. Went, *et al.*, "Hexagonal iron oxide powders as permanent materials," *Phys. Rev.*, vol. 86, p. 424; May 1, 1952.
[3] G. W. Rathenau, "Ferromagnetic properties of hexagonal iron-oxide compounds with and without preferred orientation," *Z. Phys.*, vol. 133, no. 1–2, pp. 250–260; 1952.
[4] A. L. Stuyts, *et al.*, "Preferred crystal orientation in ferromagnetic ceramics," *J. Appl. Phys.*, vol. 23, p. 1282; November, 1952.
[5] G. W. Rathenau, "Saturation and magnetization of hexagonal iron oxide compounds," *Rev. Mod. Phys.*, vol. 25, pp. 297–301; January, 1953.
[6] P. Rhodes and G. Rowlands, "Demagnetizing energies of uniformly magnetized rectangular blocks," *Proc. Leeds Phil. Lit. Soc., Sci. Sect.*, vol. 6, pp. 191–210; December, 1954.
[7] M. T. Weiss and P. W. Anderson, "Ferromagnetic resonance in Ferroxdure," *Phys. Rev.*, vol. 98, pp. 925–926; May 15, 1955.
[8] J. L. Symonds, "Methods of measuring strong magnetic fields," *Repts. Progr. Phys.*, vol. 18, pp. 83–126; 1955.
[9] V. I. Skobelkin and R. N. Solomko, "Magnetostatics with ferromagnets," *Soviet Phys. JETP*, vol. 1, pp. 370–374; September, 1955.
[10] K. J. Sixtus, *et al.*, "Investigations on barium ferrite magnets," *J. Appl. Phys.*, vol. 27, pp. 1051–1057; September, 1956.
[11] B. Kubota and C. Okazaki, "Multipolarization in the hexagonal barium iron oxide magnets," *J. Phys. Soc. Japan*, vol. 10, p. 723; August, 1955.
[12] G. Heimke, "Anomalous magnetic properties of barium ferrite as a function of sintering temperature," *Naturwissenschaften*, vol. 45, pp. 260–261; 1958.
[13] E. Schwabe, "Temperature dependence of the magnetic properties of barium ferrite," *Z. angew. Phys.*, vol. 9, pp. 183–187; April, 1957.
[14] W. E. Henry, "Magnetization studies and possible magnetic structure of barium ferrite III," *Phys. Rev.*, vol. 112, pp. 326–327; October 15, 1958.
[15] H. B. G. Casimir, *et al.*, "Report on some research in the field of magnetism at the Philips Laboratories," *J. Phys. Radium*, vol. 20, pp. 360–373; February–March, 1959.
[16] J. R. Feldmeier, "Microwave magnetrons," M.I.T. Rad. Lab. Ser., McGraw-Hill Book Co., Inc., New York, N. Y.; 1948. See especially ch. 13.
[17] E. M. Underhill, Ed., "Permanent Magnet Handbook," Crucible Steel Co. of America, Pittsburgh, Pa.; 1957.

Electron Trigonometry—A New Tool for Electron-Optical Design*

KURT SCHLESINGER†, FELLOW, IRE

Summary—**Electron-trigonometry is a new method to predict image formation in an electron-optical system, which may consist of one, or more, electron lenses of finite length, including electrostatic, magnetic or mixed lenses.**

Electron-trigonometry by-passes trajectory tracing and the determination of cardinal points. Instead, it provides immediate information about size and position of an electron image.

To analyze an electrostatic system by "electron-trigonometry," a given axial potential distribution is approximated by segments, which are either voltage-linear, or parabolic. These segments are joined together with continuity of function and slope. Linear sections are replaced by equivalent drift tubes whose lengths are scaled appropriately. Parabolic sections are shown to observe certain basic triangle rules about the sum of three phase angles of flight, which are specifically defined for object, image, and lens volume. Magnification and position of electron images are immediately known from these same phase angles. This includes both real and virtual images, and lenses of either polarity.

A system including magnetic lenses is similarly treated. Such fields are subdivided into segments where the magnetic field is replaced by its average value while the axis potential is either linear or parabolic.

As a test case, electron-trigonometry is applied to the well-known system of a two-cylinder, bi-potential lens. This is a double lens system whose axis potential distribution is not simple. The results from electron-trigonometry are in excellent agreement with recorded data of performance.

In another application, electron-trigonometry is used to compute the *angular* magnification of a cathode ray tube with post-deflection acceleration. The outcome of this analysis is a novel type of scan-stabilizer. It uses an envelope with nonuniform spiral coating to realize a large, diverging lens. In this scan-stabilizer, beam propagation is essentially straight line. This results in a high value of deflection sensitivity (3.2 v/cm·kv) which does not change over a very wide range of screen voltages (from 2 to 20 kv).

I. Introduction

THE prediction of size and position of electron images is the basic problem of electron-optical design. Its solution hinges upon the theory of the thick electron lens which has been developed to its most general mathematical formulation many years ago [1].

Unfortunately, this theory is not of much help to the practicing engineer. It is derived from the paraxial equation which has successfully resisted solution in the great majority of cases. In order to determine the six cardinal points of the lens, one needs information about principal trajectories, in addition to a complete plot of equipotentials for the field. Considering the tedious job of step-by-step graphical integration, the engineer usually resorts to an automatic curve tracer, or winds up by preparing a program for a digital computer, while forgetting about the lens altogether.

This situation is unsatisfactory in at least one respect: Analysis by computer gives only one-shot answers for specific problems. By contrast, a good general theory can point out trends and functional relationships. Electron-trigonometry (ET) has been found to be a powerful tool for the design of electron-optical devices. This shall be exemplified in Section III.

The method of electron-trigonometry can also be used to analyze systems using magnetic as well as mixed electron lenses. This will be briefly outlined in Section IV.

II. Triangle Theorems in Electron-Optics

To apply electron-trigonometry, a given axis potential is first replaced by sections, whose voltage distribution is either linear, or parabolic. The linear sections make no contributions to lens action. They can always be replaced by equivalent drift spaces, whose potential is equal to one of the two boundary potentials of the linear section, but whose length is re-adjusted. The parabolic sections on the other hand, act as ideal, thick lenses.

The combination of one such lens section between two drift spaces is henceforth referred to as a "basic electron-optical system." For such systems, extremely simple triangle relations exist, which form the body of electron-trigonometry. Image size and position can then be followed through a more complex system by repeated application of these simple rules. No trajectory information is required.

Fig. 1 shows a basic system of electrostatic electron optics. It consists of an object space a, an image space b, and a lens section l. We assume both a and b to be *nonfocusing* spaces, *i.e.*, not contributing any radial restoring forces. Such nonfocusing spaces are either field free, or they are voltage-linear, both on axis, and also on the walls of a concentric cylinder. This condition can be realized in practice by coating a resistive spiral of *uniform* pitch on the inside of a cylindrical envelope. At the ends, plane metallic disks or meshes may be used to terminate the field, if necessary.

The focusing action in Fig. 1(a) takes place over a length l, which may fill part, or all, of the total system length. Within this volume, we assume an "ideal" lens

* Received by the IRE, January 12, 1961; revised manuscript received, July 31, 1961. This work is a by-product of an R&D contract AF 33(616)-6593, sponsored by WADC, Wright-Patterson Air Force Base, Dayton, Ohio. The paper was first presented at the Fall Meeting of the Professional Group on Electron Devices, Washington, D. C.; October 27–28, 1960.

† General Electric Co., Cathode Ray Tube Dept., Syracuse, N. Y.

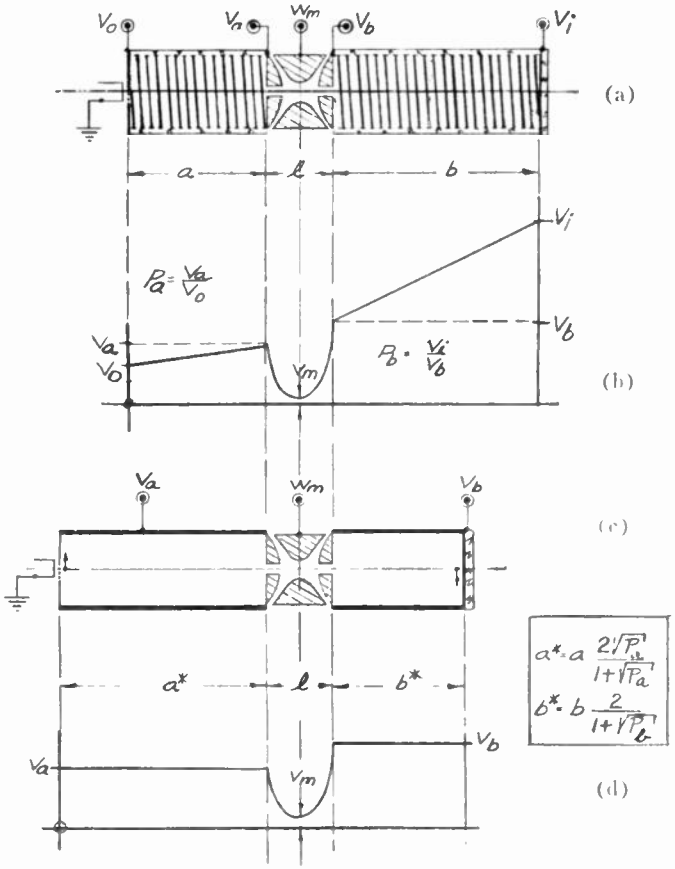

Fig. 1—Voltage-linear sections and equivalent drift spaces.

field, characterized by radial force components, that stay proportional to radius throughout, and are independent of axial position. This condition is met, if the potential distribution on axis is *parabolic*, *i.e.*, a general quadratic form in z. Rudenberg [2] has shown in 1948 that one way to realize such ideal lenses consists in using hyperbolic pole pieces similar to the arrangement shown in Fig. 1(a) and 1(c). Such structures are therefore also known as "hyperbolic lenses."

A. Linear and Constant Voltage Sections

The system of Fig. 1(a) includes two sections with linear acceleration, as indicated in Fig. 1(b) by the voltage ratios P_a and P_b for object- and image-space, respectively. This system can be replaced by an electron optical equivalent, as shown in Fig. 1(c). Here, the voltage-linear spiral sections a and b are replaced by field free drift spaces of a different length (a^* and b^*), meeting the lens section (l) at its original boundary voltages V_a and V_b. The new voltage distribution is shown in Fig. 1(d). Object and image sizes remain unchanged in the process, but the new drift-lengths are readjusted to meet (1):

$$a^* = a\,\frac{2\sqrt{P_a}}{1+\sqrt{P_a}} \qquad b^* = b\,\frac{2}{1+\sqrt{P_b}}\,. \tag{1}$$

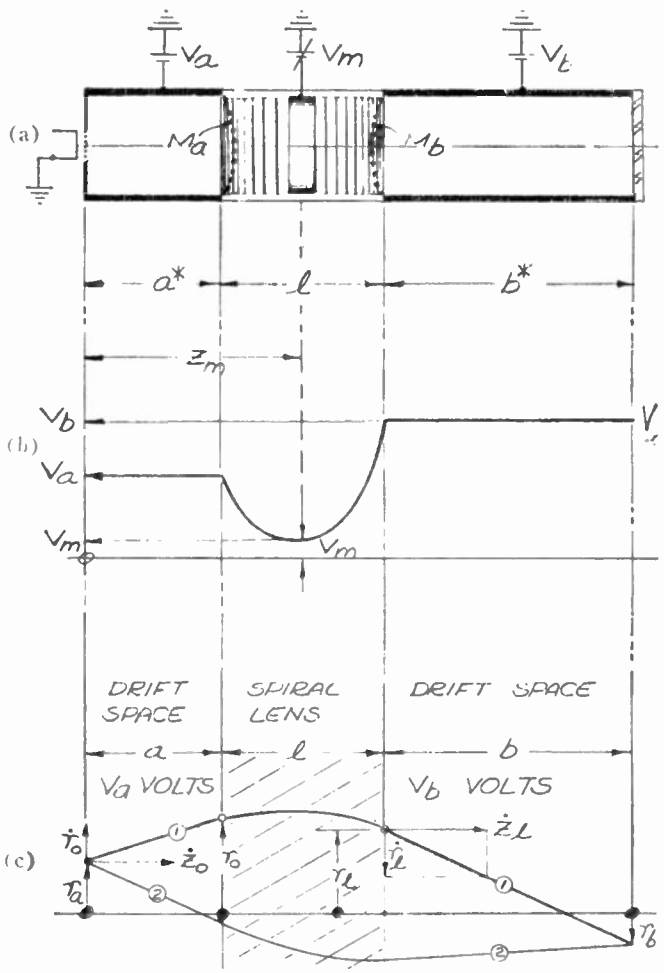

Fig. 2—Triangle theorem for positive electron lenses.

B. Hyperbolic Lens Section

The system is now transformed into that shown in Fig. 2(a) and 2(b). This arrangement is equivalent to Fig. 1(c) and 1(d), except that the hyperbolic lens is realized here in an alternative form. A lens cylinder of length l is coated on the inside by a set of *nonuniform* resistive spirals having variable, rather than constant, pitch. This "spiral lens" unit is equivalent to the embodiment used in Fig. 1, and either type may be used to provide the parabolic section of axis potential required for focusing. The lens cylinder has a much larger aperture, but it requires termination by a mesh (M_a, M_b) whenever a discontinuity of the gradient has to be realized.

Electron-optically, an ideal hyperbolic lens is fully characterized by its length l, and by its *power constant* c. The latter is the constant of proportionality between radial force per unit charge, and radial distance of axis. Hence, c is defined by

$$c = \frac{\frac{1}{e}\cdot F_r}{r}\,. \tag{2}$$

On the other hand, F_r is linked to the space potential U by the relation

$$F_r = -e\cdot\frac{\partial U}{\partial r}. \tag{3}$$

In systems with cylinder-symmetry, we have the basic relation

$$U = V - \tfrac{1}{4}r^2V'' + \cdots, \tag{4}$$

where V is the axis potential. Thus, for a parabolic section,

$$\frac{\partial U}{\partial r} = -\frac{1}{2}V''\cdot r. \tag{5}$$

Combining (2), (3) and (5) yields a general expression for the power constant of an electrostatic hyperbolic lens:

$$c = \frac{1}{2}\frac{d^2V}{dz^2}. \tag{6}$$

This may be positive or negative. In order for c to be a constant, the axis potential must be parabolic, *i.e.*, of the form

$$V = V_m + c(z - z_m)^2. \tag{7}$$

Here, V_m is the potential minimum or maximum and z_m is its axis coordinate [See Fig. 2(b)]. The distribution (7) on axis calls for a hyperbolic space potential U, which is found from (7) and (4):

$$U = V_m + c[(z - z_m)^2 - \tfrac{1}{2}r^2]. \tag{8}$$

This space potential U determines the design of the nonlinear spiral coatings and also the shape and curvature of any terminating meshes as used for instance in Fig. 2(a).

One important consequence of (8) is the fact that the potential distribution $W_{(z)}$ on the wall of a cylinder is parabolic, if this is true for its axis potential $V_{(z)}$. If D is the cylinder diameter, we have from (8),

$$W_{(z)} = V_{(z)} - \frac{c}{8}D^2. \tag{9}$$

An application for this will be described in Section III-C.

Finally, we can express the power constant c in terms of the voltages V_a and V_b at the lens boundaries z_a and z_b. Inserting this into (6) and (7) yields:

$$c = \frac{V_b - V_a}{l^2} - \frac{V_a'}{l}. \tag{10}$$

This simple relation for the power of a hyperbolic lens is best illustrated graphically. Fig. 3 shows part of some arbitrary functions of axial potential, featuring two sections A and B, which are practically straight, and an intermediate section C, which is curved. The latter is to be replaced by a parabola with continuity of slope at both ends. If this is done, the junction-

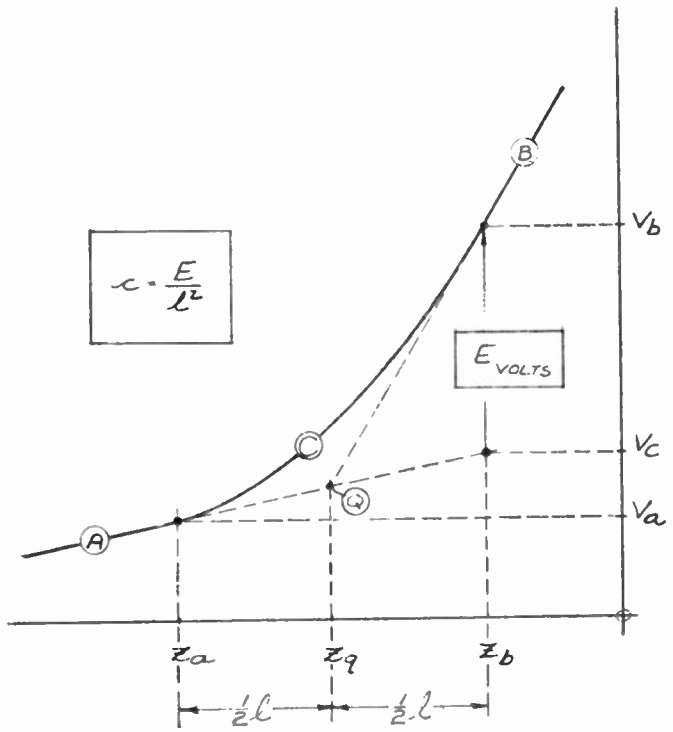

Fig. 3—Parabolic curve-fitting.

abscissas z_a and z_b will observe mirror symmetry with respect to the abscissa z_q of the intersection Q. As a result, the length l of the equivalent "Rudenberg" section is defined, if only one of the junction voltages, V_a or V_b is given. The power constant c of this parabolic lens section can then be read directly off the sketch below. We have

$$c = \frac{E}{l^2} \tag{10a}$$

where E is the voltage difference $V_b - V_c$, to be read off the graph as shown, both by magnitude and sign.

The power factor c is positive for a converging, and negative for a diverging, electron lens. Numerically, it ranges in practical devices from about 500 v/in² to about 50,000 v/in² and beyond. The smaller figure occurs in lens fields of large volume, such as the bulb spiral lens shown in Fig. 9. The high values for c are found in focusing lenses for cathode ray tubes, including the main focus lens in picture tubes. Still higher lens powers are used in the electron microscope and also in modern micro-gun designs, as used in cathode ray tubes for ultra-high resolution.

C. Triangle Theorem for a Positive System

We are now going to derive certain rules of electron-trigonometry, also called "triangle-theorems," or "delta-rules" for short. These delta-rules are valid for electron-optical systems such as Figs. 2 and 4, comprising one hyperbolic lens between two drift spaces, all of arbitrary length. For simplicity, we call such a basic system positive or negative, depending on the sign of the lens-power used.

Within the hyperbolic field, the electron trajectories are expressed by fairly simple equations (see appendixes). Thus, it is possible to describe the electron path through a basic system such as Fig. 2(c) by a set of four equations:

$$r_0 = r_a + a\frac{\dot{r}_0}{\dot{z}_0}, \tag{11}$$

$$r_l = r_0 \cos\varphi_c + \frac{\dot{r}_0}{\omega}\sin\varphi_c, \tag{12}$$

$$\dot{r}_l = \dot{r}_0 \cos\varphi_c - \omega r_0 \sin\varphi_c, \tag{13}$$

$$r_b = r_l + \dot{r}_l\frac{b}{\dot{z}_l}. \tag{14}$$

In this set, the first and last equation simply describe linear propagation in object- and image-space, respectively. Eqs. (12) and (13) connect the radial position and velocity at the lens output to their counterparts at the lens input. Specifically, the parameters ω and φ_c are the "frequency" and the transit angle, or "phase," of a hyperbolic lens. These data are found from length l and power constant c of the lens, by using (15) and (16) (see Appendix I).

$$\omega = \sqrt{\eta c}, \quad \text{where} \quad \eta = e/m \tag{15}$$

$$\varphi_c = \sqrt{2}\cdot\tanh^{-1}\frac{l\sqrt{c}}{\sqrt{V_a}+\sqrt{V_b}}. \tag{16}$$

Eqs. (11) through (14) can now be used to find the four unknowns including r_0, r_l, $\dot{r}_l$, and r_b. Specifically, the image size r_b then appears in the general form

$$r_b = M\cdot r_a + N\cdot\dot{r}_0, \tag{17}$$

where M and N are expressions which contain only axial, but no radial, velocity components [see (18) and (19)]. We have:

$$M = \cos\varphi_c - \frac{b}{\dot{z}_l}\omega\sin\varphi_c \tag{18}$$

$$N = \left(\frac{b}{\dot{z}_l}+\frac{a}{\dot{z}_0}\right)\cdot\cos\varphi_c + \left(\frac{1}{\omega}-\frac{a}{\dot{z}_0}\cdot\frac{b}{\dot{z}_l}\omega\right)\sin\varphi_c. \tag{19}$$

Inspection of (17) shows that r_b may become an "image" of r_a. In order for this to occur, it is necessary for the factor N to disappear from (17) (focusing condition). Once N is zero, the coefficient M in (17) indicates the magnification of the electron-image.

The focusing condition $N=0$ (19) assumes a surprisingly simple form if we introduce two new phase angles, one for the object- and one for the image-space. These are defined as

$$\text{object phase: } \varphi_a = \tan^{-1}\frac{a}{\sqrt{V_a}}\sqrt{\frac{c}{2}}, \tag{20a}$$

$$\text{image phase: } \varphi_b = \tan^{-1}\frac{b}{\sqrt{V_b}}\sqrt{\frac{c}{2}}. \tag{20b}$$

In terms of these three phase angles, which include the lens phase from (16), image formation in a system such as Fig. 2(a), or its equivalent Fig. 1(c), can be expressed by a simple triangle relation:

$$\boxed{\varphi_a + \varphi_b + \varphi_c = \pi}. \tag{21}$$

This permits one to find the image phase angle φ_b, and thus the image position b (20b), once object and lens phase are known, and vice versa. The image size is then also immediately known by introducing (20), (21) and (16) into expression (18) for M. For the system magnification this yields the simple relation

$$M_+ = -\frac{\cos\varphi_a}{\cos\varphi_b}. \tag{22}$$

The above developments may be summarized as follows:

Triangle theorem for a positive system: If an electron image is formed by a system including one positive lens element between two drift spaces, the sum of the three phase angles for object-, lens- and image-space amounts to 180°. If lens phase plus object phase add up to more than 90°, the image is real and inverted. If that sum is less than 90°, the image is virtual and erect.

Applications for this triangle theorem will be given below. However, one interesting consequence of it may be mentioned here. By the use of (20a) and (20b), expression (22) for the magnification of a positive system is readily transformed into the form

$$M_+ = -\sqrt{\frac{\frac{2}{c}+\frac{b^2}{V_b}}{\frac{2}{c}+\frac{a^2}{V_a}}}. \tag{22a}$$

For the lens power c, we know from (10) that it increases with decreasing thickness l of the lens. Thus, it follows from inspection of (22a) that the magnification of a positive system with one thick lens is intermediate between the "classical" value

$$M_+ = -\frac{b}{a}\sqrt{\frac{V_a}{V_b}}$$

for a very short lens, and the value $M_+ = -1$ which results from (22a) for a long lens, occupying most, if not all, of the total system length.

D. Triangle Theorem for a Negative System

A similar, but slightly different, delta-rule governs image formation in a system comprising one negative lens element between two drift spaces. A "negative system" of this kind is shown in Fig. 4(a), and its axis potential V in Fig. 4(b). As before, we introduce three

phase angles ϕ_a, ϕ_b, and ϕ_c for the two drift spaces, and for the lens volume, respectively. These are (see Appendix II for derivation)

$$\phi_a = \tanh^{-1} \frac{a}{\sqrt{V_a}} \sqrt{\frac{c_-}{2}}, \tag{23a}$$

$$\phi_b = \tanh^{-1} \frac{b}{\sqrt{V_b}} \sqrt{\frac{c_-}{2}}, \tag{23b}$$

$$\phi_c = \sqrt{2} \tan^{-1} \frac{l\sqrt{c_-}}{\sqrt{V_a} + \sqrt{V_b}}. \tag{23c}$$

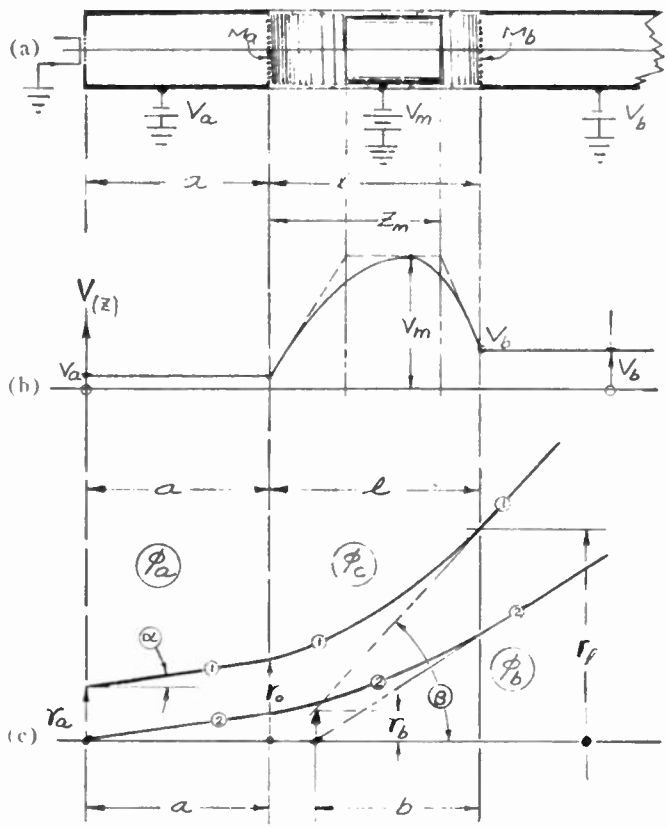

Fig. 4—Triangle theorem for negative electron lens.

Here, c_- is the absolute value of the power constant c of the negative lens: $c_- = |c|$. c_- is always positive, although c is negative in this case. A comparison with (16) and (20) for phases in a positive system shows that hyperbolic functions there have been replaced by cyclometric functions here and vice versa. In terms of these new phase angles ϕ, we find another triangle theorem to hold for a negative system:

Delta-rule for a negative system:

a) Image condition:

$$\boxed{\phi_a + \phi_b + \phi_c = 0}. \tag{24}$$

b) Magnification:

$$M_- = + \frac{\cosh \phi_a}{\cosh \phi_b}. \tag{25}$$

It can be seen from (25) that the negative electron lens is always noninverting, since M_- is positive. If the lens forms a virtual image, r_b, from a real object, r_a (see Fig. 4), this image is demagnified ($\phi_a > 0; |\phi_b| > \phi_a; M_- < 1$). By contrast, a magnified ($M_- > 1$) real image ($\phi_b > 0$) may be formed by a negative lens, if a virtual object is placed behind it. ($\phi_a < 0; \phi_b < |\phi_a|$). This situation exists for instance in electrostatic focusing by means of a bipotential lens (see Section III-A).

The two triangle-rules as introduced above are summarized for practical use in Fig. 5. For a negative electron lens, the delta theorem is stated in two versions which are supplementary. The alternate form for ϕ_a^* or ϕ_b^* is needed, if the expressions for ϕ_a or ϕ_b exceed unity, *i.e.*, the range of the function $\tanh^{-1}\phi$.

In any practical application of electron-trigonometry, a rule of signs should be observed as follows: trace a path from object, through lens, to image. Any vector (a, b, l) which points in the direction of electron flow,

Converging lens c positive; $c_+ = \|c\|$	Diverging lens c negative; $c_- = \|c\|$	
$\varphi_a = \tan^{-1} \frac{a}{\sqrt{V_a}} \sqrt{\frac{c_+}{2}}$	$\phi_a = \tanh^{-1} \frac{a}{\sqrt{V_a}} \sqrt{\frac{c_-}{2}}$	$\phi_a^* = \tanh^{-1} \frac{1}{a} \sqrt{\frac{2V_a}{c_-}}$
$\varphi_b = \tan^{-1} \frac{b}{\sqrt{V_b}} \sqrt{\frac{c_+}{2}}$	$\phi_b = \tanh^{-1} \frac{b}{\sqrt{V_b}} \sqrt{\frac{c_-}{2}}$	$\phi_b^* = \tanh^{-1} \frac{1}{b} \sqrt{\frac{2V_b}{c_-}}$
$\varphi_c = \sqrt{2} \cdot \tan^{-1} \frac{l\sqrt{c_+}}{\sqrt{V_a} + \sqrt{V_b}}$	$\phi_c = \sqrt{2} \cdot \tan^{-1} \frac{l\sqrt{c_-}}{\sqrt{V_a} + \sqrt{V_b}}$	$\phi = \sqrt{2} \cdot \tan^{-1} \frac{l\sqrt{c_-}}{\sqrt{V_a} + \sqrt{V_b}}$
$\varphi_a + \varphi_b + \varphi_c = \pi$	$\phi_a + \phi_b + \phi_c = 0$	$\phi_a^* + \phi_b^* + \phi_c = 0$
$M_+ = - \frac{\cos \varphi_a}{\cos \varphi_b}$	$M_- = + \frac{\cosh \phi_a}{\cosh \phi_b}$	$M_- = - \frac{\sinh \phi_a^*}{\sinh \phi_b^*}$

Fig. 5—Rules of electron-trigonometry.

counts positive; if opposed to the flow, negative. The same signs also apply to the respective phase angles used in the triangulations.

III. Applications of Electron-Trigonometry

To illustrate the use of electron-trigonometry, two applications of it are presented below. The first is of the nature of a test case: it is the well-known problem of the two cylinder lens [3]. This is a two-lens system, which will be analyzed by means of the delta-rules for both positive and negative lens elements.

The second application given here shows how electron-trigonometry may be used to compute angular, rather than lateral, magnification. Here, the theory points the way to a novel type of post deflection accelerator. This case is presented to show the use of the new method for the design of electron-optical devices.

A. *The Two-Cylinder, Bi-Potential Lens*

The system under consideration is shown in Fig. 6(a). Two cylinders of equal diameter, and of length l_1 and l_2, are connected to voltages V_1 and V_2, respectively. The grounded cathode K illuminates a wire mesh at the entrance to the first cylinder. We wish to find size and position of the electron image of this mesh, as a function of the voltage ratio $P = V_2 : V_1$. For two cylinders of equal diameter D and narrow spacing, as shown in Fig. 6(a), F. Gray [4] has given an accurate expression for the axis potential:

$$V = \frac{V_1 + V_2}{2} + \frac{V_2 - V_1}{2} \cdot \tanh\left(2.64\,\frac{z}{D}\right). \quad (26)$$

We are replacing this function by two parabolic segments which cover the same range of voltages (from V_1 to V_2), and which are joined at the same slope as the original function (26). This approximation is shown in Fig. 6(b). The two parabolas are

$$1)\ V = V_1 + c_+(z + \lambda)^2, \quad (27)$$

$$2)\ V = V_2 + c_-(z - \lambda)^2. \quad (28)$$

The first represents a positive lens with the power constant

$$c_+ = \frac{V_2 - V_1}{2\lambda^2}. \quad (29)$$

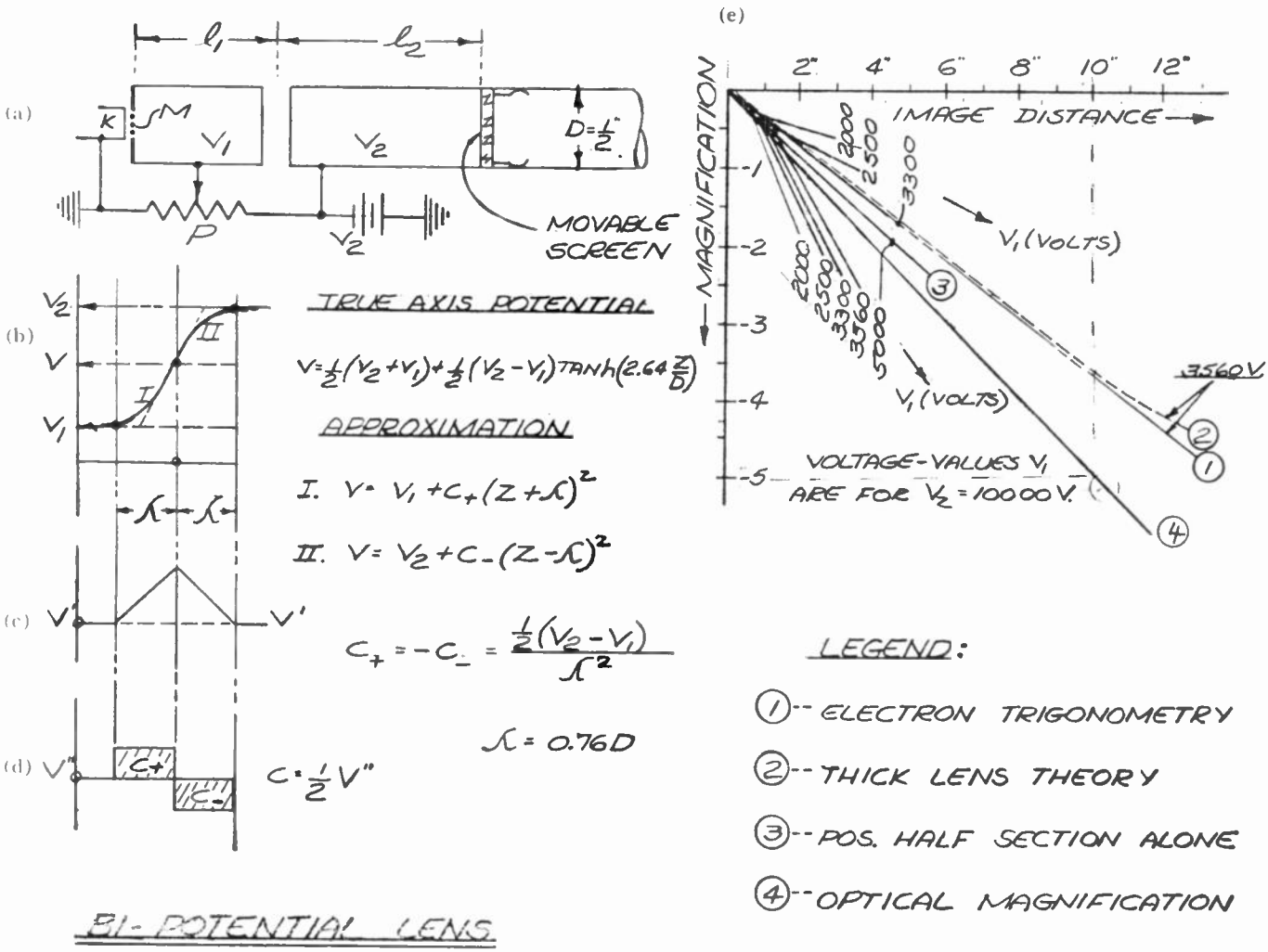

Fig. 6—Analysis of the bi-potential lens.

The second is a negative lens with the same power:

$$c_- = -c_+. \tag{30}$$

The thickness of both lenses follows from (26),

$$\lambda = 0.76D = 0.38''. \tag{31}$$

Both lens sections are shown in Fig. 6(d). We apply ET to the first lens. The first cylinder has the dimensions $l_1 = 2$ in, $D = \frac{1}{2}$ in. The object distance then becomes, with (31): $a = l_1 - \lambda = 1.62$ in. The object phase angle then follows with (29), (31), and $P = V_2 : V_1$ as:

$$\varphi_a = \tan^{-1} 2.14\sqrt{P-1}. \tag{32}$$

The lens phase follows from (16) as:

$$\varphi_c = \sqrt{2}\tanh^{-1}\frac{\sqrt{P-1}}{\sqrt{2}+\sqrt{P+1}}. \tag{33}$$

The image phase now follows from the triangle rule for a positive lens,

$$\varphi_b = \pi - \varphi_a - \varphi_c. \tag{21}$$

Hence, the image distance b of the first lens is [from (20b)]

$$b_+ = \sqrt{2}\cdot\lambda\frac{\sqrt{P+1}}{\sqrt{P-1}}\cdot\tan\varphi_b, \tag{34}$$

and the magnification of the first lens [from (22)]

$$M_+ = -\frac{\cos\varphi_a}{\cos\varphi_b}. \tag{22}$$

This has been plotted in Fig. 6(e) as curve no. 3 which presents the action of the first, positive lens section acting alone.

We now proceed to the second, diverging lens section of the two-cylinder system. This negative lens section looks at the image defined by (34) and (22) as a virtual object, and projects a real, magnified image from it. Hence, we enter b_+ from (34) into the triangulation of the second lens as a negative object distance:

$$a_2 = -b_1. \tag{35}$$

Hence, the object phase becomes:

$$\phi_a = \tanh^{-1}\frac{\sqrt{2}\cdot\lambda}{a}\sqrt{\frac{P+1}{P-1}}. \tag{36}$$

The phase angle of the negative lens follows from (23c) as:

$$\phi_c = \sqrt{2}\cdot\tan^{-1}\frac{\sqrt{P-1}}{\sqrt{2P}+\sqrt{P+1}}. \tag{37}$$

The image phase follows from the triangle theorem for negative lenses (24),

$$\phi_b = -\phi_c - \phi_a. \tag{24}$$

Finally, the image distance is found from (23b),

$$b = \frac{2\lambda}{\tanh\phi_b}\sqrt{\frac{P}{P-1}}. \tag{38}$$

The magnification of the negative section is known from (25) of the second triangle theorem,

$$M_- = -\frac{\sinh\phi_a^*}{\sinh\phi_b^*}. \tag{25}$$

The size of the final image observed on the screen is then the product of the magnifications from both lenses, as found from (22) and (25),

$$M_{\text{total}} = M_+ \cdot M_-. \tag{39}$$

This is plotted in Fig. 6(e) as curve no. 1. One can see, by comparison with curve no. 3, that the combined system requires a much lower voltage V_1 than the positive section alone to focus at a given throw. It is also interesting that the throw increases fast (from 4 in to 12 in) with only a 3 per cent change of voltage on the first cylinder (300 v out of 10,000 v on the screen). Also, the over-all magnification is somewhat smaller for the composite system than for the positive lens component alone, and both values are again smaller than the distance ratio, *i.e.*, the optical magnification by a thin lens, placed between the two cylinders.

It is noteworthy that the electronic magnification when plotted vs object distance, is essentially a straight line through the origin. This justifies the introduction of an "electron-optical factor" k,

$$k = m_{\text{electronic}} : m_{\text{optical}}. \tag{40}$$

This factor is a characteristic number for any electron-optical system. In accelerating systems of this type, k is smaller than unity, but not as small as the root-of-voltage formula, which is often used as a first approximation.

More important, however, than these details seems to be the experience that electron-trigonometry has here been applied to an electron-optical device which is definitely "non-ideal." The results are in excellent agreement with data gathered by conventional methods. Curve no. 2 in Fig. 6(e) presents the performance of this two-cylinder lens as recorded in test-book literature [3]. The agreement is within the accuracy of slide rule and of measurement.

B. Triangle Theory for Angular Magnification

In some applications of cathode ray tubes, one is interested in the stabilization of deflection in the presence of post deflection acceleration (PDA). In other applications, one wishes to magnify some small initial sweep by the action of a suitable electrostatic field after deflection. To design such systems, it is necessary to predict the amount of angular magnification which can be realized within a given system.

Fig. 7 shows the basic configuration for scan magnification. Point A is the center of a small, initial deflection α. After drifting through a field-free space a, the predeflected ray enters into a lens field of the length l. It then leaves this field under an increased angle β and traverses a second drift space, before reaching the screen. Intersection of the outgoing ray with the axis defines a point B, which is by definition an image point of A. Hence, its position can be found by electron-trigonometry, as shown before. The actual scan magnification $S = R_b/R_a$, as observed on the screen, can be read off Fig. 7 as

$$S = \frac{R_b}{R_a} = \frac{\tan \beta}{\tan \alpha}\left[1 - \frac{a + l + b}{L}\right]. \tag{41}$$

Here, the second factor indicates the influence of drift spaces surrounding the lens. Note that b is the only variable in this term. It counts negatively for a diverging lens, as shown in Fig. 7. The first factor,

$$m_\alpha = \tan \beta / \tan \alpha, \tag{42}$$

is an expression for angular magnification. A formal analysis of the electron path in Fig. 7, assuming the lens volume to be confined between plane boundaries, leads to an expression of the form

$$m_\alpha \cdot M \cdot \sqrt{P} = 1; \qquad P = V_b/V_a. \tag{43}$$

This equation provides the desired link between angular and lateral magnification. It closely resembles the fundamental theorem by Helmholtz-Lagrange, except for the fact that a ratio of sines, rather than tangents, occurs there [5]. Numerically, this difference stays within 10 per cent for sweep angles up to 50°.

The general expression for scan magnification is a combination of (41) and (43):

$$S = \frac{1}{M \cdot \sqrt{P}}\left[1 - \frac{a + l + b_{(P)}}{L}\right] \tag{44}$$

This formulation suggests that:

1) Acceleration opposes, and deceleration enhances, scan magnification.

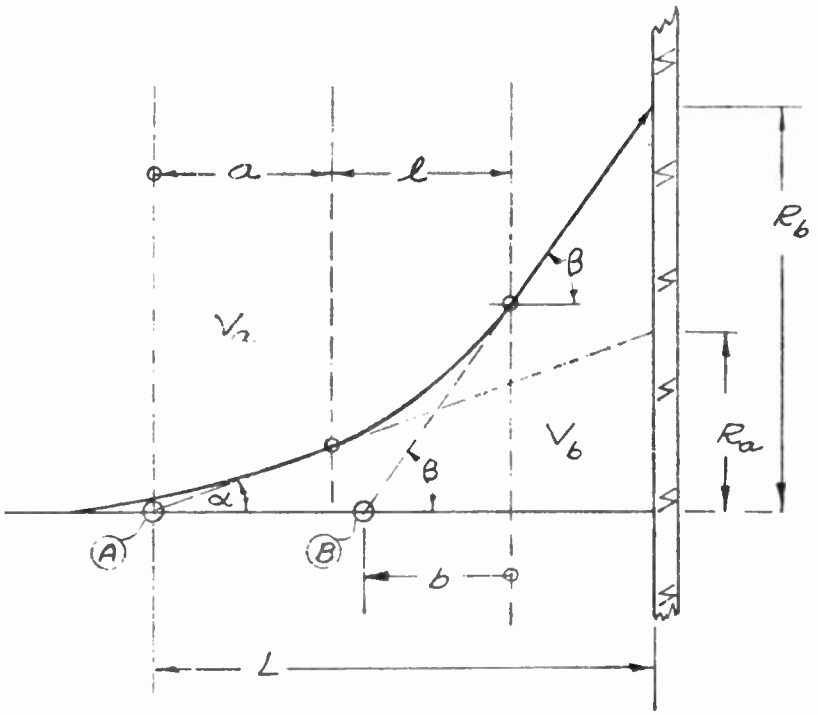

$$m_\alpha = \frac{\tan \beta}{\tan \alpha}$$

$$P = V_b : V_a$$

$$M_- = + \frac{\cosh \phi_a}{\cosh \phi_b}$$

$$M_+ = - \frac{\cos \phi_a}{\cos \phi_b}$$

SCAN MAGNIFICATION:

$$S = \frac{R_b}{R_a} = \frac{1}{M \cdot \sqrt{P}}\left[1 - \frac{a+l+b}{L}\right]$$

ANGULAR MAGNIFICATION:

$$m_\alpha \cdot M \cdot \sqrt{P} = 1$$

Fig. 7—Analysis of scan magnifiers.

2) A system using a diverging lens ($M<1$; b negative) is more promising than a system using a positive lens (b positive). By comparison, the system with a positive scan-magnifier lens requires greater length and is less efficient.

Reference is now made to Fig. 8(a). This shows one way to realize a large negative lens of the accelerating type. The lens is constructed by the deposition of a nonuniform, resistive spiral coating on the inside of a cylindrical envelope. This "spiral lens" must have a decreasing, *i.e.*, nonuniform, turn density in the direction toward the screen. The latter, in turn, is surrounded by a conductive band, which projects by $\frac{1}{4}\sqrt{2}$, or 0.35, screen diameters backward towards the gun. A drift space (a) after deflection is an essential component in this spiral-lens tube as we shall see. We compute, by electron-trigonometry, the scan magnification S in this tube using (44). Since the tube has no drift space after the lens l, we have $a+l=L$, and (44) reduces to

$$S = \frac{1}{M_- \cdot \sqrt{P}} \cdot \frac{-b}{L} \cdot \tag{45}$$

Here, M is the magnification of the negative spiral lens, given above as

$$M_- = \frac{\cosh \phi_a}{\cosh \phi_b} \cdot \tag{25}$$

We start by computing the object phase ϕ_a from (23a). Introducing the lens power,

$$c_- = \frac{V_b - V_a}{l^2}, \tag{46}$$

and the post-acceleration factor $P = V_b/V_a$, (23a) becomes

$$\phi_a = \tanh^{-1} 0.71 \cdot \frac{a}{l} \cdot \sqrt{P-1}. \tag{47}$$

Next, we formulate the lens phase ϕ_c. Its basic equation (23c) transforms with (46) into

$$\phi_c = \sqrt{2} \tan^{-1} \frac{\sqrt{P-1}}{1+\sqrt{P}} \cdot \tag{48}$$

From (47) and (48), we now get the image phase ϕ_b, by using the delta-theorem for negative lenses:

$$\phi_b = -\phi_a - \phi_c. \tag{24}$$

This phase angle is negative. It permits to find the lateral magnification M_- by going into (25) with ϕ_b, and with ϕ_a from (47). Knowing ϕ_b, we also find the image distance b. From (23b) we obtain, after some manipulation,

$$b = l \sqrt{\frac{2P}{P-1}} \cdot \tanh \phi_b. \tag{49}$$

We now have all necessary data to use (45) for the computation of scan magnification in the spiral-lens tube. This has been done in Fig. 8(c) for a wide range of post acceleration, and for various values of the funnel-to-bulb ratio a/L. It will be seen from Fig. 8(c) that in the absence of any object-drift length ($a=0$), the diverging spiral lens is completely ineffective! At a post acceleration of 10:1, the deflection loss then amounts to 50 per cent, which is no better than standard practice with a uniform spiral anode. However, as the relative funnel length a/L is increased, the spiral lens section l becomes shorter, and its power increases with $1/l^2$. The spiral thus becomes rapidly more effective in opposing deflection losses from post acceleration. The point of balance is reached for $a/L=0.56$. Beyond that, there is some slight overcompensation (about 20 per cent). At the critical funnel ratio, the theory predicts the raster size to stay constant within 3 per cent over a 10:1 range of post acceleration!

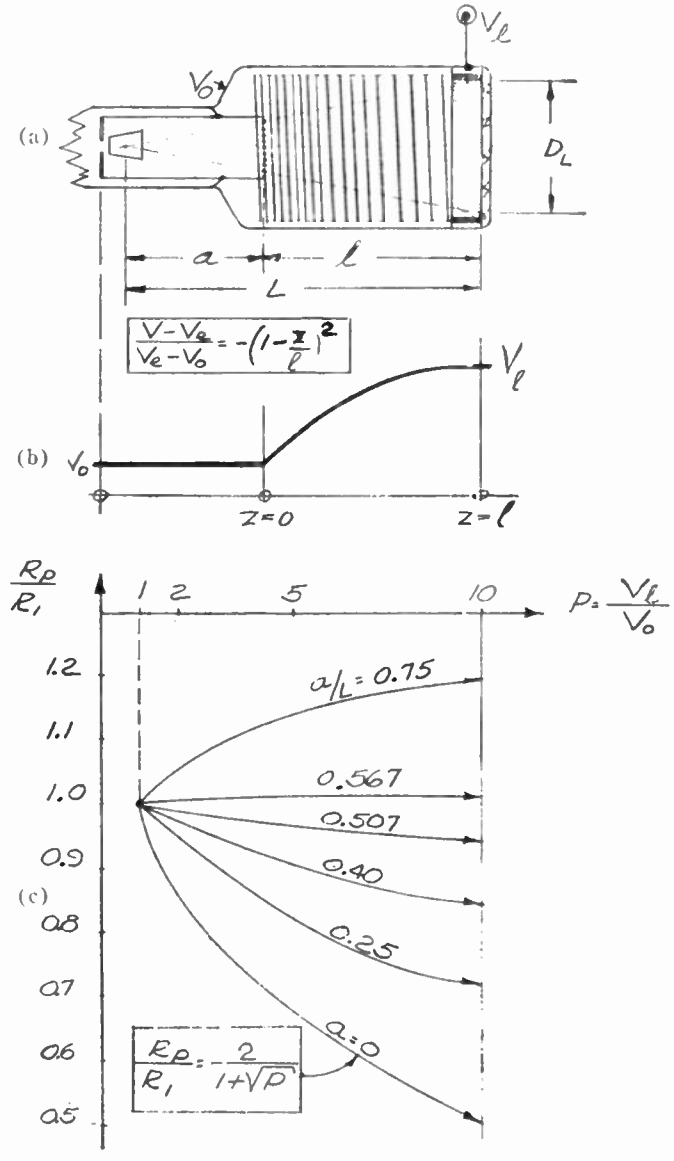

Fig. 8—Scan stabilization by a spiral lens.

C. An Experimental Test

The above predictions of electron-trigonometry were put to a test by constructing an experimental cathode ray tube, which was built in close correlation to the theoretical design. Fig. 9 shows a photograph of this tube, whose purpose it was to achieve constant deflection sensitivity over a wide range of screen voltages.

The tube consists essentially of a cylindrical bulb, coated by a resistive spiral with nonuniform pitch. The specific turn-density per inch varies in such a manner that the voltage gradient decreases linearly with progress toward the screen. The screen is metallized, and framed by a conductive band, which projects back by 0.36 screen diameters. The voltage distribution along the wall is parabolic, as shown in Fig. 8(b). This establishes within the bulb a diverging lens, which approaches the ideal field quite well, as confirmed by experience.

A second, essential feature is the fairly long unipotential drift tube between the internal deflection yoke [6] and the spiral input. This funnel is at the average deflection potential, *i.e.*, the second anode voltage. At the far end, it is covered by a wire gauze.

Fig. 10 shows a photograph of the actual performance of this spiral lens stabilizer. Four conditions are shown with screen voltages going through 1–3.5–8.5 and 21 kv, while the second anode was held constant at 1000 v. The spiral lens stabilizer (left), is shown side-by-side with a conventional monoband intensifier (right), all voltages, including deflection and acceleration, being connected in parallel on both tubes. The spiral tube was found to have a high value of deflection sensitivity —3.2 v cm. kv—and this value did not change over the very wide range of screen voltages used in the test.

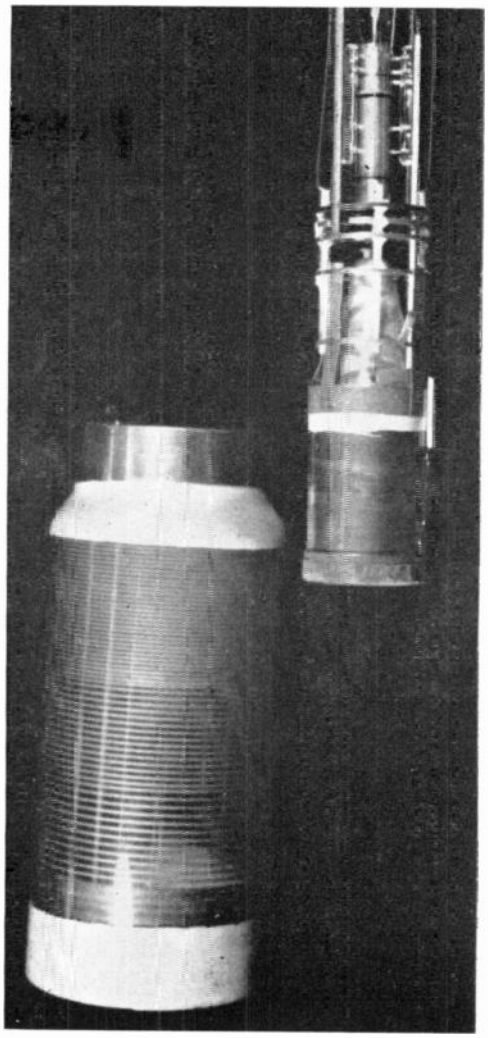

Fig. 9—Spiral-lens tube assembly.

IV. Electron-Trigonometry for Magnetic and Mixed Systems

In the preceding sections, the method of electron-trigonometry has been presented in connection with purely electrostatic electron-optics. However, the method applies equally well to electron-optical systems which employ magnetic lenses, either alone, or in combination with electrostatic lenses. To prepare a problem of this kind for electron-trigonometry, the system is again subdivided into sections, which have a linear, or a parabolic, potential distribution. The magnetic field, on the other hand, is replaced by the average value which it has across each section [7].

Using polar coordinates r and θ, the following equations hold for each such section:

$$\ddot{r} - r\dot{\theta}^2 = -\eta r\left[\tfrac{1}{2}V'' + \dot{\theta}B\right], \tag{50}$$

$$\frac{1}{r}\cdot\frac{d}{dt}(r^2\dot{\theta}) = \eta\dot{r}B \tag{51}$$

$$\ddot{z} = \eta V''. \tag{52}$$

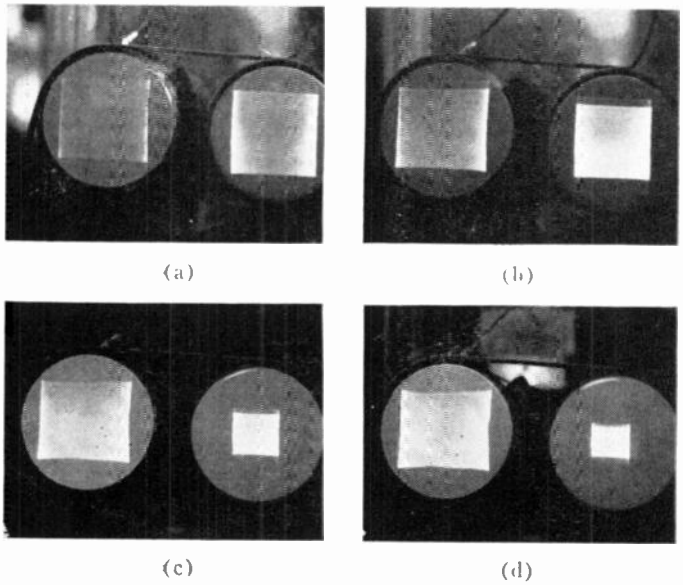

(a) (b) (c) (d)

Fig. 10—Scan stabilizer test: spiral-lens tube (left)—monoband tube (right). Second anode voltage: 1000 volts. Screens operating at: (a) 1000 v, (b) 3500 v, (c) 8500 v, (d) 21,000 v.

Undistorted image formation is one solution of these equations, since, for $B=$constant, (51) is satisfied by

$$\dot{\theta} = \tfrac{1}{2}\eta B = \text{constant}. \tag{53}$$

This implies a rotation of the entire image at the local Larmor frequency, independent of radius. It then follows from (50) that

$$\ddot{r} = -\eta r\left[\frac{1}{2}V'' + \frac{\eta B^2}{4}\right]. \tag{54}$$

Hence, an observer on a reference plane through axis, which rotates with the Larmor frequency, will find the beam subject to a composite lens field with an effective power constant of

$$c_{\text{total}} = c_m + c_e, \tag{55}$$

where

$$c_m = \tfrac{1}{4}\eta B^2 \tag{55a}$$

and

$$c_e = \tfrac{1}{2}V''. \tag{55b}$$

Here, the magnetic lens power c_m is always positive and proportional to e/m, while the electric lens power is independent of e/m, and can have either polarity. Hence, our observer on the rotating reference plane gets correct results from electron-trigonometry, if he uses (56) for the phase φ_e of the mixed lens,

$$\varphi_e = \sqrt{2}\tanh^{-1}\frac{l\sqrt{c_e+c_m}}{\sqrt{V_0}+\sqrt{V_l}}\cdot \tag{56}$$

Meanwhile, the magnetic field rotates the reference plane through an angle of

$$\psi = \dot{\theta}\cdot T = \tfrac{1}{2}\eta B\cdot T, \tag{57}$$

where T is the transit time through the lens. If the axis potential has a quadratic form

$$V = a + bz + cz^2, \tag{58}$$

then it can be shown by simple integration that the transit time T is always given by:

$$T = \int_0^l \frac{dz}{\sqrt{2\eta V}} = \sqrt{\frac{2}{\eta c_e}}\cdot\tanh^{-1}\frac{l\sqrt{c_e}}{\sqrt{V_0}+\sqrt{V_l}}\cdot \tag{59}$$

Here V_0 and V_l are the potentials at the two boundaries to the section. This leads to (60) for the image rotation per section:

$$\psi = \sqrt{2}\cdot\sqrt{\frac{c_m}{c_e}}\cdot\tanh^{-1}\frac{l\sqrt{c_e}}{\sqrt{V_0}+\sqrt{V_l}}\cdot \tag{60}$$

A comparison of (56) for the lens phase φ_e, with (60) for the angle of rotation ψ, shows that the two angles are generally *not* equal, as long as the mixed lens has an electrostatic component ($c_e\neq 0$). This becomes even more evident, if elemental angles are written down for a very thin slice of the mixed field. Eq. (56) then reduces to

$$\Delta\varphi_e = \sqrt{\frac{c_e+c_m}{2V}}\cdot\Delta z \tag{56a}$$

and (60) becomes[1]

$$\Delta\psi = \sqrt{\frac{c_m}{2V}}\cdot\Delta z. \tag{60a}$$

It is now evident, that the two angles φ_e and ψ become identical, if the lens section is purely magnetic ($c_e=0$). This includes the practically important case of magnetic focusing in the presence of a constant, or zero, axial electric field ($V=a+bz$). In systems of this kind the phase concept assumes a physical meaning: it can be directly observed as the angle of rotation of an electron image!

V. Automatic Computation

During the past two years electron-trigonometry has been applied in these laboratories to a great variety of problems in electron-optics. Quite generally the method has been found to provide reliable, and often quantitative, guidance during the early design stages. In view of this experience and in order to save time, it was decided to prepare a program of electron-trigonometry for an IBM 709 digital computer. This work was done under the direction of B. A. Findeisen of this Department, and in cooperation with the Heavy Military Equipment Department of the General Electric Company. At present we are in a position to compute the over-all electron-optical effect of as many as 250 subsections of a given axis potential. In this program, the computer automatically evaluates the power constant of each subsection and then uses this data to find the new image information by "electron-trigonometry." Besides saving time, this method offers the important advantage of eliminating the factor of human judgment, which is ever-present, if field-approximations have to be found by graphical methods.

Appendix I

Phase Angle in a Positive Lens

Within a hyperbolic lens, the power factor c is a constant, and the equations of motion are linear and harmonic. They read

$$\ddot{r} = -\eta c r, \tag{61}$$

$$\ddot{z} = 2\eta c(z - z_m), \tag{62}$$

[1] Eq. (60a) leads to the well-known expression for image rotation by a thick magnetic lens if the value for c_m from (55a) is introduced prior to integration of (60a) through the lens field.

where z_m is the position of the minimum axis potential, and $\eta = e/m$. At the start, we have

$$t = 0 \quad z = 0 \quad r = r_0 \quad \dot{z}_0 = \sqrt{2\eta V_0} \tag{63}$$

and at the end,

$$t = T \quad z = l \quad r = r_l \quad \dot{z}_e = \sqrt{2\eta V_l}. \tag{64}$$

The general solution of (61) and (62) is

$$r = r_0 \cos \omega t + \frac{\dot{r}_0}{\omega} \sin \omega t \tag{65}$$

$$z = z_m(1 - \cosh \sqrt{2}\omega t) + \frac{\dot{z}_0}{\sqrt{2}\omega} \sinh (\sqrt{2}\omega t). \tag{66}$$

Here, we introduced

$$\omega = \sqrt{\eta c} \tag{15}$$

as the frequency of the lens. Fitting this into the boundary condition (64) yields

$$l = z_m[1 - \cosh \sqrt{2}\varphi_c] + \frac{\dot{z}_0}{\sqrt{2}\cdot\omega} \sinh (\sqrt{2}\varphi_c) \tag{67}$$

and

$$\dot{z}_e = \dot{z}_0 \cosh (\sqrt{2}\varphi_c) - \sqrt{2}\omega z_m \cdot \sinh (\sqrt{2}\varphi_c). \tag{68}$$

These are two equations for the position z_m of the potential minimum, and also for the lens phase φ_c. Solving for the latter, we obtain the expression

$$\varphi_c = \omega T = \sqrt{2}\cdot\tanh^{-1} \frac{l\sqrt{c}}{\sqrt{V_0} + \sqrt{V_l}} \tag{16}$$

as used in the text.

Appendix II

Phase Angle in a Negative Lens

For a negative power constant, $c<0$ $|c| = c_-$, the lens frequency $\omega = \sqrt{\eta c}$ becomes imaginary. Introducing, instead, its absolute value

$$\Omega = \sqrt{\eta \cdot c_-} \tag{69}$$

the equations of motion now read:

$$\ddot{r} = \Omega^2 r \tag{70}$$

$$\ddot{z} = -2\Omega^2(z - z_m). \tag{71}$$

Their solutions are

$$r = r_0 \cosh (\Omega t) + \frac{\dot{r}_0}{\Omega} \sinh (\Omega t), \tag{72}$$

$$z = z_m(1 - \cos (\sqrt{2}\Omega t)) + \sqrt{\frac{V_0}{c_-}} \sin (\sqrt{2}\Omega t). \tag{73}$$

Eq. (23c) for the lens phase ϕ_c follows from fitting (73) into boundary conditions similar to (63) and (64) in Appendix I.

The expressions (23a) and (23b) for object and image phase of the negative lens follow from a system analysis, similar to the one given in the text for a system including a single, positive, electron lens.

References

[1] J. R. Pierce, "Theory and Design of Electron Beams," D. Van Nostrand Co., Inc., New York, N. Y., 2nd ed., ch. 6, pp. 72–91; 1954.

[2] R. Rudenberg, "Electron lenses of hyperbolic field structure," *J. Franklin Inst.*, pp. 311–339 and pp. 377–408; October and November, 1948.

[3] Karl R. Spangenberg, "Vacuum Tubes," McGraw-Hill Book Co., Inc., New York, N. Y.; 1st ed., 1948. See especially Fig. 13.38, p. 379.

[4] Frank Gray, "Electrostatic Electron Optics," *Bell Sys. Tech. J.*, vol. 18; January, 1939. See especially Fig. 17, p. 36.

[5] V. K. Zworykin, *et al.*, "Electron Optics and the Electron Microscope," John Wiley & Sons, Inc., New York, N. Y., sec. 10.5, p. 355; 1945.

[6] Kurt Schlesinger, "Progress in the development of post acceleration and electrostatic deflection," Proc. IRE, vol. 44, pp. 659–667; May, 1956.

[7] E. G. Ramberg, "Electron optical systems," in "Television," John Wiley & Sons, Inc., New York, N. Y., 2nd ed., ch. 4, p. 156; 1954.

New FM-AM Method of Compression, Expansion, and Multiplication*

W. R. AIKEN†, MEMBER, IRE, AND C. SÜSSKIND‡, SENIOR MEMBER, IRE

Summary—**A new method of employing the combination of two signals has been developed for magnitude compression or expansion of audio or video signals and for multiplication or other uses involving modulation with separated components (*e.g.*, instrumentation and remote control). The first signal frequency-modulates a local oscillator, whose output is limited and then amplitude-modulated by the second signal; the combined FM-AM signal is detected in such a way that the first signal is restored to its original form, but modified in amplitude by the second signal. In compression-expansion, the method controls the signal level with great speed and over a wide band without introducing noise, "bounce," or dc shift into the output; no delicate balancing or matched-tube circuits are required. In multiplication, the product of two voltages can be formed by means of a simple circuit that is extremely suitable for analog computers and similar applications.**

Introduction

THE method described below was initially developed for the purpose of achieving nearly instantaneous audio compression and expansion that would be free from the disadvantages of other methods in current use. Apart from the description contained in U. S. patents issued[1] and pending (covering, among others, all of the uses described in the present paper), the first public report[2] of the new method was largely concerned with the audio application. The present paper also describes video applications and use of the method to multiply two signals; however, the original audio application is used for the purpose of illustrating the details of the operation of the method.

Various techniques have been used to control the output of electronic amplifiers in the face of variations of the amplitude of the input signal averaged over an arbitrary interval of time. This problem is particularly familiar to engineers in the fields of audio and of radio broadcasting, and more recently, in television broadcasting. Without enumerating each of the many uses to which the present method can be put, the authors merely wish to point out that in radio transmission, for instance, a standard level of signal strength is obviously desirable from the viewpoint of optimum utilization of the transmitting facilities; automatic control of the occasional excessive modulation peaks permits a substantial increase in the signal power. In audio reproduction, the new method enables the listener to restore the full contrast present in the original signal (e.g., in vocal and instrumental music), which is generally reduced by compression introduced at the origin.

Most of the circuits that have been proposed for controlling the amplification of a signal suffer from one or more serious defects. One such defect is that the control voltage may appear in the output of the amplifier and, moreover, may be many times larger than the desired signal itself. Some attempts have been made to reduce this undesirable effect by placing a limitation on the speed of response of the control operation so that the frequency of the control voltage lies well below the frequency of the signal voltage and may be thus filtered out relatively easily. Alternately, push-pull circuits or balanced-modulator circuits have been used to cancel out the control voltage in the amplifier output. However, such remedies may restrict the control circuits to relatively low speeds of response and require expensive transformers and dynamically balanced tubes; moreover, it is usually necessary to operate amplifiers of this type at very low volume levels to maintain distortion within tolerable limits. As a result, previously proposed methods have been slow in operation, restricted in bandwidth, delicate in balance, and subject to considerable distortion.

The present method suffers from none of these difficulties. The method consists of generating a selected carrier, modulating that carrier in accordance with the desired signal, modulating the signal-modulated carrier in accordance with a control voltage that may be derived from the desired signal itself or from an independent source, and demodulating the doubly modulated carrier simultaneously with respect to both modulations in such a manner that the control voltage appears only in combination with the desired signal but is not demodulated by itself. It is found that the effects of dynamic interaction between FM and AM signals are negligible.

Expansion and Compression

Expander

To obtain expansion operation, the incoming signal is used to frequency-modulate a local oscillator (Fig. 1).[3] The resultant FM voltage is amplitude-limited if neces-

* Received by the IRE, April 10, 1961; revised manuscript received, July 24, 1961.

† Ross Radio Corp., Los Altos Hills, Calif. (Mr. Aiken is also Director of Research at Kaiser Aircraft & Electronics, Palo Alto, Calif.)

‡ University of California, Berkeley, Calif.

[1] W. R. Aiken, U. S. Patent No. 2,923,887; February 2, 1960.

[2] W. R. Aiken and C. Süsskind, "Novel compression-expansion method for audio and video use," 1959 IRE WESCON CONVENTION RECORD, pt. 7, p. 4. (Abstract only.)

[3] Phase modulation may also be used, similarly to the combination of amplitude and phase modulation described, for instance, in D. G. Fink, ed., "Television Engineering Handbook," McGraw-Hill Book Co., Inc., New York, N. Y., Sec. 13.104; 1957.

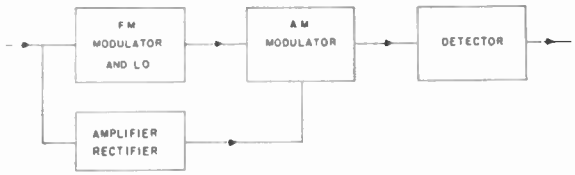

Fig. 1—Expander operation. Incoming signal frequency-modulates the local oscillator (typically a 5-Mc oscillator) and is simultaneously rectified in another circuit to provide the control signal. The FM signal is amplitude-modulated by the control signal to provide a composite signal, which is the FM signal with its amplitude *increased* by the control signal. The detector then yields the original signal with an increased relative-amplitude variation. No trace of the control signal remains.

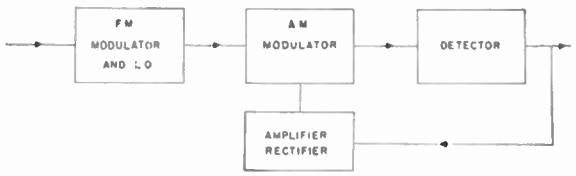

Fig. 2.—Compressor operation. Incoming signal frequency-modulates the local oscillator as in expander operation, but the control signal is now derived from the detector output and serves to decrease the amplitude of the FM signal to provide the composite signal. The detector then yields the original signal with the decreased relative amplitude variation. No trace of the control signal remains.

sary (to remove residual AM) and then amplitude-modulated by a control voltage that is also derived from the incoming signal; the control voltage is proportional to the (averaged) amplitude of the incoming signal. The output of the amplitude modulator is thus a signal that is both frequency- and amplitude-modulated; the FM content is proportional to the instantaneous value of the signal, and the AM content is proportional to the average value of the signal, as rectified in accordance with the delay bias. This bias is applied to the rectifier and serves to make its output nonlinear by shifting the diode cutoff point; the resulting increase in required signal level also changes the slope of the rectifier characteristic.

This composite signal is next detected by a Foster-Seeley or similar circuit responsive to both FM and AM, so that a demodulated signal results whose amplitude corresponds to the original signal as modified by the control signal. In other words, the output of the detector stage varies linearly with the instantaneous frequency deviation (FM) and the amplitude of the deviated carrier (AM). Since the detector cannot respond to AM in the absence of FM, only the modulating effect of the controlling signal (AM) is present in the output; the modulating signal itself does not appear. However, the restored signal now has a considerably greater dynamic range than the original signal.

Compressor

Operation as a compressor is illustrated in Fig. 2 and is substantially the same as the expansion action, except that the control signal is reversed in polarity and is derived from the output of the detector rather than from the input signal. Alternately, an independent source of control voltage may be used.

In audio applications, the method may be used in amplifiers in a relatively simple circuit for compression, limiting, or expanding. It is simpler, inherently more trouble-free, and has lower distortion and wider control range than existing circuits. Several versions of the compressor-expander for audio purposes have been demonstrated (Fig. 3), including a simplified, wholly transistorized one. Typical operating characteristics for action as expander and compressor are shown in Figs. 4 and 5 (see p. 1552), respectively. The effects of using the above mentioned delay bias are illustrated in both plots.

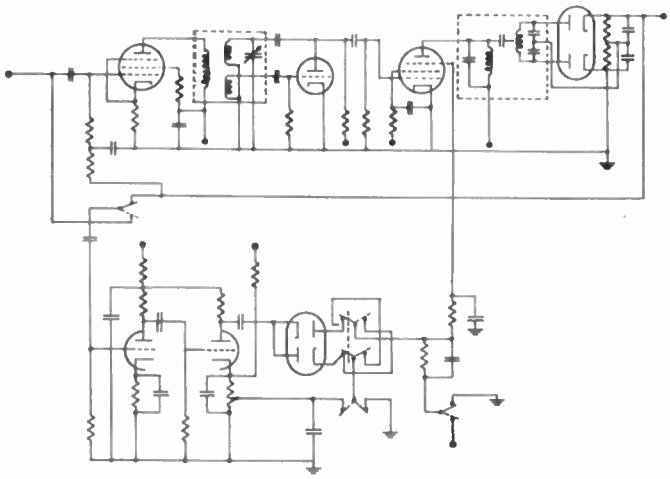

Fig. 3—Circuit diagram of early expander-compressor-limiter. Saturable reactor is used in the tuned circuit of the local oscillator (second tube) to effect frequency modulation. Later models are simplified by use of a varactor diode to replace the first (FM modulator) stage.

Video Applications

Although the method is being used to date at audio frequencies, it is inherently capable of operation at video frequencies as well. In video applications, the method can be used not only for controlling average signal levels, but for responding to individual picture elements. In this way, the shadow may be taken out of a video display or a scene may be brought out of partial shadow while another portion of the display is at high intensity. Moreover, the large dynamic range of vidicon camera tubes can be fully utilized without the danger of overloading their amplifier circuits. Such automatic control, in conjunction with voltage feedback to the vidicon tube, permits the use of high (and varying) light levels while background or average levels are maintained constant. This application can thus result in a constant-contrast display that would have numerous applications in commerical, industrial, and military telecasting.

Computer and Other Applications

The method is also applicable to a number of other uses, as in instrumentation, remote control, and indeed any uses involving modulation with separated components. It is capable of attenuating a signal by as much as 60 db without the distortion that occurs in conventional

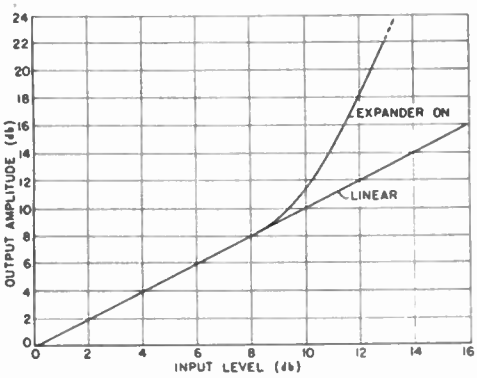

Fig. 4—Operating characteristics of expander: EXPANDER OFF yields linear characteristic, EXPANDER ON yields curved characteristic. Amount of control bias (in a back-biased diode) shifts the level at which expansion sets in (*i.e.*, the point at which the two curves diverge).

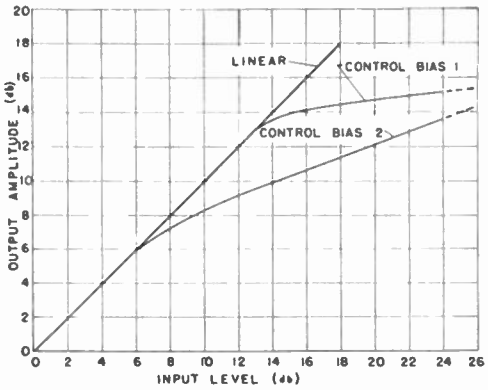

Fig. 5—Operating characteristics of compressor. Action opposite to that shown in Fig. 3 is obtained. (Two values of control bias are shown.)

circuits with nonlinear transfer characteristics. One use that holds particularly good promise of widespread practical application is as an electron *multiplier* in analog computers and similar devices. This action is demonstrated in Fig. 6.

It will be appreciated that the method described constitutes a linear electronic multiplier in which two voltages are multiplied together to obtain a product. The FM modulating voltage and the AM modulating voltage are the multiplying factors and the detector output is the product. The multiplicand may be used to frequency-modulate an RF oscillator, the multiplier may amplitude-modulate the FM signal, and the signal that is detected according to the described method represents the product.

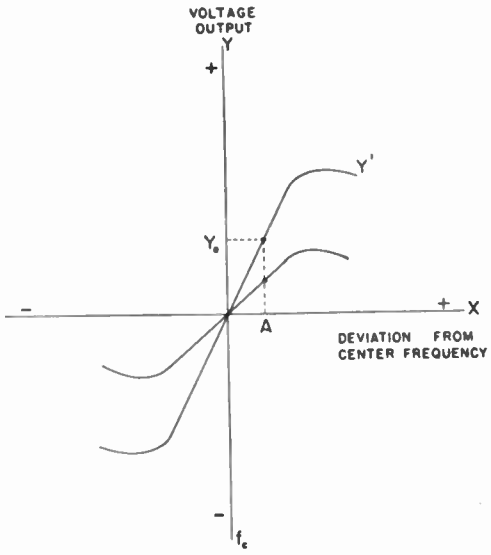

Fig. 6—Action of multiplier circuit. Multiplicand A is represented by deviation from center frequency, multiplier B, by the *slope* of the detector curve Y' (two values are shown).

The response curves of the detector are illustrated in Fig. 6. The amount of the multiplicand A, positive or negative, determines the position of the RF signal on the detector curve (positive or negative) as $+X$ or $-X$. The amount of the multiplier B determines the output-voltage amplitude, since the steepness of the detector curve depends on the amplitude of the RF signal.

If the multiplier $B=0$, the amplitude of the RF wave is zero, and the output will be along the line $X=0$. A nonzero value of the multiplier B results in an RF wave of corresponding amplitude, and the detector curve of Y' results, giving an output voltage of Y_0. In this way, the multiplicand A moves the RF signal along a detector curve whose slope is determined by the multiplier B. It should be noted that the output of the device is sensitive to both positive and negative values of the multiplicand A, and that the multiplicand and multiplier may be interchanged.

Conclusion

A new method of using the combination of two signals has been proposed and demonstrated by which compressor-expander action can be obtained without the disadvantages of existing schemes. The method is inherently capable of being used at video as well as audio frequencies, and is suitable for many other applications, notably in a multiplier circuit for computer applications

IRE Recommended Practices on Audio and Electroacoustics: Loudspeaker Measurements, 1961*

61 IRE 30.RP1

COMMITTEE PERSONNEL

Audio and Electroacoustics Committee—1959–1961

IDEN KERNEY, *Chairman*, 1959–1961
D. S. DEWIRE, *Vice Chairman*, 1959–1961
A. P. EVANS, *Vice Chairman*, 1959–1961
H. C. HARDY, *Vice Chairman*, 1959–1960

A. B. Cohen
M. Copel
D. L. Favin
E. E. Gross
R. A. Hackley
F. K. Harvey
F. S. Hird
J. Hirsch
F. L. Hopper
W. W. Lang
A. H. Lind
L. J. Malmsten
A. A. McGee
E. J. McGlinn
H. F. Olson
F. W. Roberts
R. H. Rose
V. Salmon
P. B. Williams
R. E. Yaeger

Standards Committee—1960–1961

C. H. PAGE, *Chairman*
J. G. KREER, JR., *Vice Chairman*
H. R. MIMNO, *Vice Chairman*
L. G. CUMMING, *Vice Chairman*

J. H. Armstrong
J. Avins
G. S. Axelby
M. W. Baldwin, Jr.
W. R. Bennett
J. G. Brainerd
A. G. Clavier
S. Doba, Jr.
R. D. Elbourn
G. A. Espersen
R. J. Farber
D. G. Fink
G. L. Fredendall
E. A. Gerber
A. B. Glenn
V. M. Graham
R. A. Hackbusch
R. T. Haviland
A. G. Jensen
R. W. Johnston
I. Kerney
E. R. Kretzmer
W. Mason
D. E. Maxwell
R. L. McFarlan
P. Mertz
H. I. Metz
E. Mittelmann
L. H. Montgomery, Jr.
S. M. Morrison
G. A. Morton
R. C. Moyer
J. H. Mulligan, Jr.
A. A. Oliner
M. L. Phillips
R. L. Pritchard
P. A. Redhead
C. M. Ryerson
G. A. Schupp, Jr.
R. Serrell
W. A. Shipman
H. R. Terhune
E. Weber
J. W. Wentworth
W. T. Wintringham

Measurements Coordinator

J. G. KREER, JR.

* Approved by the IRE Standards Committee, April 13, 1961. Reprints of IRE Standards 61 IRE 30.RP1 may be purchased while available from the Institute of Radio Engineers, Inc., 1 East 79 Street, New York 21, N. Y. at 0.60 per copy. A 20 per cent discount will be allowed for 100 or more copies mailed to one address.

1. Scope

These Recommended Practices define terms associated with loudspeakers and their testing, recommend various methods of testing, and indicate preferred methods of presenting information regarding their characteristics. Specific information is presented in Sections 2–7. Discussions of a more qualitative nature are given in Sections 8 and 9.

In these Practices, the tests recommended involve physical, steady-state measurements only. Work has been and is now being done on transient measurements of loudspeaker performance, but experience with these methods is still not sufficiently widespread to warrant their inclusion.

While the physical data which can be obtained as detailed in Sections 4–9, inclusive, are a helpful guide in designing and in selecting a loudspeaker for a certain purpose, they are not a complete guarantee that the subjective performance will be satisfactory. Wherever it is possible, the quality of reproduction should be checked by means of listening tests such as those described in the literature.[1]

2. Introduction

2.1 Definition

A loudspeaker is an electroacoustic transducer intended to radiate acoustic power into the air.

2.2 Types

There are two general types of loudspeakers, namely, direct-radiator and horn. The direct-radiator type of loudspeaker is arranged so that it radiates acoustic power into the air directly from one or both sides of its acoustic radiating element, or diaphragm. One side of the diaphragm may be totally isolated by means of an airtight enclosure, or, effectively, by a baffle of adequate size. In order to control the response over part of the useful frequency range, the energy radiated from the back surface of the diaphragm may be acoustically coupled to the energy radiated from the front.

The horn type of loudspeaker radiates the major portion of its acoustic power through a horn. This is a tube whose shape and cross section are chosen by design so as to increase the radiation resistance loading on the diaphragm of the loudspeaker for a substantial portion of the useful frequency range, and increase its radiated output and electroacoustic conversion-efficiency over that obtainable when it radiates directly.

Both direct-radiator and horn loudspeakers have been designed for a wide variety of applications which influence their range, directional characteristics, permissible distortion, and power handling capacity. Also, either type may be designed to operate as a single or multiunit device. One loudspeaker may be used to cover the desired frequency range. Alternatively, two or more loudspeakers, usually interconnected by means of frequency-selective electric networks, may be operated together so that each covers a portion of the desired frequency range, while the combination of loudspeakers covers the entire range.

3. Measurement Conditions

3.1 Loudspeaker Mounting

The direct-radiator loudspeaker unit should be mounted in or on the enclosure or baffle called for by the manufacturer, or it should be mounted in or on a baffle or enclosure which is completely described. The horn loudspeaker unit should be equipped with a horn specified by the manufacturer, or with a horn which is completely described.

3.2 Electrical Connections

The loudspeaker should be connected as specified by the manufacturer, with the proper networks and controls, if any, and these networks and controls should be adjusted as recommended. If not specified, the connections and adjustments used must be completely described.

If the loudspeaker is of the excited-field type, the field should be energized with the rated current.

3.3 Acoustic Environment

The acoustic environment should simulate free-field conditions to the extent that the inverse-pressure vs distance law should hold within plus or minus 1 db at all frequencies at which measurements are made.[2] Ambient noise should not affect the measurements to an extent greater than plus or minus 1 db. Departures from these conditions should be measured and described.

3.4 Test Signals

Fixed frequency, swept frequency and warbled sinusoidal signals, as well as bands of noise, may be used for loudspeaker testing as dictated by the test and the type of instrumentation being utilized. Sweep and warble rates should be sufficiently slow that response-frequency measurement results do not differ significantly from the steady-state readings. When bands of noise or warble signals are used their characteristics should be specified.

Each performance parameter of a loudspeaker must be expressed as a function of frequency if it is to be expressed completely. However, for many purposes it is desirable to condense the information to a single number which represents a weighted average over a prescribed portion of the spectrum. Such an average may be obtained by means of a signal which sweeps re-

[1] H. F. Olson, "Subjective loudspeaker testing," IRE Trans. on Audio, vol. AU-1, pp. 7–9; September–October, 1953.

[2] H. F. Olson, "Acoustical Engineering," D. Van Nostrand Co., Inc., New York, N. Y., 3rd ed., ch. 10, pp. 445–450; 1957.

peatedly through the required portion of the spectrum at a rate sufficient to give a steady reading on a suitable indicating device.[3]

The electric power input for pressure-frequency response, pressure-directional response, and impedance measurements, should be kept as low as possible consistent with the ambient noise and the sensitivity of the measuring system, in order to minimize the effects of heating and nonlinear distortion in the loudspeaker. However, when it is desired to test a loudspeaker at high levels, adequate time should be allowed for the attainment of steady-state thermal conditions. Likewise, when testing excited-field loudspeakers, steady-state thermal conditions should be attained.

3.5 Measuring System

The response of the measuring system including the microphone should be known. Nonlinear distortion should be limited to a level consistent with the type of data being obtained; however, moderate levels of system distortion are permissible for tests of maximum power capacity based upon mechanical or electrical failure. For nonlinear distortion measurements, the level of distortion products in the measuring system should have a negligible effect on the readings of distortion products produced by the loudspeaker. The reference-pressure response (fundamental) and hence, the pressure-frequency response (fundamental) by definition require measurement of the pressure at the fundamental frequency. A frequency-selective indicating or recording system may be required in order to minimize errors arising from harmonics in the output sound wave.

The microphone used for measuring the sound pressure should preferably conform to the standards given in American Standard Specification for Laboratory Standard Pressure Microphones, Z24.8-1949, or the latest revision thereof, and be calibrated by the method described therein. Other types of microphones may be used if calibrated as described in American Standard Method for the Free-Field Secondary Calibration of Microphones, Z24.11-1954, or the latest revision thereof. If the microphone employs a pressure-gradient element, it is necessary to correct for proximity effect at low frequencies.[4]

The measuring device used for single frequency measurements should provide readings which represent the rms values. For complex waves or bands of noise, the readings should be obtained by means which indicate peak and rms values for the type of complex wave used[5] or by a means with which these can be accurately correlated. When an automatic recording device is used, the rate of frequency sweep should be slow enough so that the trace does not differ significantly from the corresponding single frequency reading.

3.6 Preconditioning

Permanent changes may take place in a loudspeaker as a result of motion of the diaphragm. It is therefore desirable to subject it to a period of preconditioning by applying a signal of the type discussed in Section 9. The power of the signal should be the average value at which the loudspeaker will be used. The preconditioning should continue until changes of impedance, principal resonance and response can no longer be detected.

4. Electric Impedance Characteristics

Four electric impedances are of importance in testing loudspeakers. They concern the loudspeaker itself and the source from which it receives electric energy. It is important to determine their values in order that the loudspeaker may be tested under proper conditions with regard to such characteristics as power transfer, frequency response, and nonlinear distortion.

4.1 Electric Impedance of a Loudspeaker (Z_S)

4.1.1 Definition. The electric impedance of a loudspeaker is the complex value of the electric impedance given as a function of frequency and measured at the accessible signal terminals of the loudspeaker.

4.1.2 Method of Measurement. The loudspeaker should be mounted, connected and tested in a suitable acoustic environment as discussed in Section 3.3. The impedance should be determined from measurement of magnitudes and phase relationship of the voltage and current supplied to the loudspeaker terminals.

Note: The impedance measurement should be made at an operating level at which voltage and current waveforms are essentially sinusoidal.

4.1.3 Presentation of Data. Loudspeaker impedance data should be presented in complex form, indicating magnitude and phase angle as a function of frequency, or alternatively, resistive and reactive components as a function of frequency. Electric input conditions should be specified.

4.2 Rating-Impedance of a Loudspeaker (Z_R)

4.2.1 Definition. The rating-impedance of a loudspeaker is the value of a pure resistance which is to be substituted for the loudspeaker when the electric power supplied by the source is to be measured.

Note 1: This is sometimes referred to as nominal impedance.

Note 2: As an example, a loudspeaker having a designated rating-impedance of eight ohms is intended to be connected to the eight-ohm output tap of an amplifier.

[3] H. F. Hopkins and N. R. Stryker, "A proposed loudness-efficiency rating for loudspeakers and the determination of system power requirements for enclosures," Proc. IRE, vol. 36, pp. 315–355; March, 1948.

[4] Olson, *op. cit.*, ch. 8, p. 288 and Fig. 8.40A.

[5] L. L. Beranek, "Acoustic Measurements," John Wiley and Sons, Inc., New York, N. Y., ch. 11; 1949.

4.2.2 Evaluation. It should be noted that the rating-impedance is not the impedance of the loudspeaker at a designated reference frequency. It is, ideally, the average impedance over the frequency band transmitted by the loudspeaker, weighted by the spectrum of the signal with which the loudspeaker will be used, and by such factors as distortion and frequency response.

Note: The manufacturer usually recommends a value of rating-impedance, but when this information is lacking it may be estimated by one of the following procedures:[6]

a. For moving-coil direct-radiator loudspeakers, use the minimum value of the magnitude of the measured loudspeaker impedance in the frequency range above cone resonance, and add 10 per cent; or, measure the voice-coil dc resistance and add 20 per cent.

b. For horn loudspeakers in general, use the average of the magnitude of the measured loudspeaker impedance in the region at the center of the useful frequency band of the unit; or, as an alternative in the case of moving-coil horn loudspeakers, measure the voice-coil dc resistance and add 40 per cent.

4.3 Loudspeaker Measurement Source Impedance (Z_G)

4.3.1 Definition. The loudspeaker measurement source impedance is the value of a pure resistance to be connected in series with the loudspeaker and a constant-voltage source in order to measure the loudspeaker performance.

Note: The choice of the value of Z_G will depend upon the type of amplifier to which the loudspeaker will be connected in use.

4.4 Discussion of Impedances

The efficiency of a loudspeaker varies as a function of frequency, and depends not only upon its ability to transform electric to acoustic power, but also on its ability to accept power from a source. The source may be a power amplifier, from which maximum power consistent with prescribed distortion conditions may be obtained only with a load impedance that is not necessarily equal to the source impedance. In order to reduce the discrepancies between idealized measurements with resistive sources and actual use with an amplifier, it is necessary to specify the four impedances involved in these two processes: the three defined in this section Z_S, Z_R and Z_G, and a fourth, Z_I, the internal impedance at the output of the amplifier with which the loudspeaker is to be used.

The use of these quantities is illustrated in Fig. 1.

The relation between generator and load impedance may be expressed by the regulation of the combination,

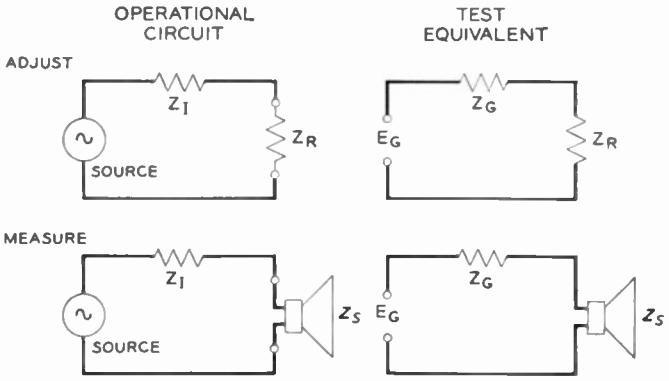

E_A is the rms value, in volts, of the open-circuit voltage of the amplifier.
E_G is the rms value, in volts, of the open-circuit voltage of the source.
Z_G is the loudspeaker measurement source impedance, in ohms.
Z_I is the internal impedance, in ohms, at the output of the amplifier with which the loudspeaker is to be used.
Z_R is the loudspeaker rating-impedance, in ohms.
Z_S is the impedance, in ohms, of the loudspeaker, measured at its terminals.

In the "ADJUST" row, the electric power P_E delivered to the loudspeaker rating-impedance, Z_R, is set by adjusting the source voltage E_G. This electric power delivered to Z_R is taken as a measure of the input power available to the loudspeaker.

Fig. 1.

where

$$\text{Regulation in db} = -20 \log_{10} \frac{\text{(terminated-circuit output voltage)}}{\text{(open-circuit output voltage)}}.$$

It is important that the regulation be stated along with other conditions of measurement.

Note: For example, a properly terminated triode amplifier has a regulation of approximately 3 db; for a matched source-load combination the corresponding regulation becomes 6 db; for a constant voltage generator, 0 db.

5. Reference Pressure Response Characteristics

5.1 Reference Pressure Response of a Loudspeaker (G_L)

5.1.1 Definition. The reference pressure response of a loudspeaker at a specified frequency, expressed in decibels, is the normalized pressure response indicating the ratio of output sound pressure level at that frequency in a free field on the principal axis referred to a distance of one meter, to the input electric power level at that frequency delivered to a resistance equal to the loudspeaker rating-impedance.

Units: The recommended reference quantities are 0.0002 microbar (dyne per cm²) for pressure and 0.001 watt for power. For convenience, the reference pressure

[6] V. Salmon, "Loudspeaker impedance," IRE Trans. on Audio, vol. AU-1, pp. 1–3; July–August, 1953. See also "Coupling the speaker to the output stage," Newsletter of the IRE-PGA, no. 3, p. 5; January, 1952.

response G_L, in db, may be expressed in the following forms:

$$G_L = h - H = 20 \log_{10} (p_L/p_0) - 10 \log_{10} (P_E/P_0)$$
$$= 20 \log_{10} p_L - 20 \log_{10} E_G + 10 \log_{10} Z_R$$
$$+ 20 \log_{10} (1 + Z_G/Z_R)$$
$$- 20 \log_{10} p_0 + 10 \log_{10} P_0$$

and, on substitution of recommended reference quantities, the expression

$$-20 \log_{10} p_0 + 10 \log_{10} P_0 = 44 \text{ db},$$

where

h is the axial free-field sound pressure level produced by the loudspeaker at a distance of 1 meter, in db referred to 0.0002 microbar (dyne per cm²).
H is the electric power level delivered to the rating-impedance, in dbm (db referred to 0.001 watt).
p_L is the axial free-field rms sound pressure at a distance of one meter, in microbars.
p_0 is the reference sound pressure, 0.0002 microbar.
P_E is the electric power, in watts, delivered to a resistance equal to the rating-impedance of the loudspeaker, where

$$P_E = \frac{E_G^2 Z_R}{(Z_G + Z_R)^2}.$$

P_0 is the reference electric power, 0.001 watt.
E_G is the rms value, in volts, of the open-circuit voltage of the source.
Z_R is the loudspeaker rating-impedance, in ohms.
Z_G is the loudspeaker measurement source impedance, in ohms.

5.1.2 Method of Measurement. The loudspeaker should be mounted, connected, and tested in a suitable acoustic environment as discussed in Section 3.

The microphone should be placed on the principal axis of the loudspeaker as specified by the manufacturer, or, if no axis is specified, on the normal to the center of the radiating area or horn mouth, and at a distance at least three times the maximum transverse dimension of the radiating area or horn mouth in order to approximate free-field conditions.

From the free-field pressure p_r, measured at a distance D(feet), the pressure p_L at one meter can be computed by the relation:

$$p_L = p_r(D/C_1),$$

or, in logarithmic form

$$p_L \text{ in db} = 20 \log_{10} p_r + 20 \log_{10} D - 20 \log_{10} C_1,$$

where

$$C_1 = 3.28 \text{ (number of feet in one meter)}.$$

5.2 Average Reference Pressure Response

When it is desired to rate a loudspeaker by means of a single value of the reference pressure response, it is preferable to take an average over a frequency band[3] rather than to cite the value obtained for any one frequency. The method used should be described.

5.3 Reference Pressure-Frequency Response

5.3.1 Definition. The reference pressure-frequency response of a loudspeaker is the reference pressure response presented as a function of frequency.

Note: The relative pressure-frequency response characteristic, commonly known as frequency response, is obtained by referring the response values at various frequencies to that at some reference frequency.

5.3.2 Presentation of Data. When presenting data on the reference pressure-frequency response of a loudspeaker, the following quantities should be specified: measured distance between the loudspeaker radiating area or horn mouth and the microphone; electric power input to the loudspeaker rating-impedance; value of this loudspeaker-rating impedance; and value of the measurement source impedance.

Note: Unless there is a special reason for using other types of graphic presentation for pressure-frequency response curves, it is recommended that the frequency scale, or abscissa, be logarithmic, and the pressure scale, or ordinate, be linear in db, and that the length of a 10 to 1 frequency interval be the length of 30 db on the ordinate scale.

6. Rating-Efficiency (η)

6.1 Definition

Rating-efficiency is the ratio, usually expressed in decibels, of the output acoustic power to the electric power delivered to a resistance equal to the loudspeaker rating-impedance, that is,

$$\eta = 10 \log_{10} (P_L/P_E),$$

where

η is the loudspeaker rating-efficiency, in db.
P_L is the total radiated acoustic power, in watts.
P_E is the electric power, in watts, delivered to a resistance equal to the rating-impedance of the loudspeaker, where

$$P_E = \frac{E_G^2 Z_R}{(Z_G + Z_R)^2}.$$

6.2 Discussion

The acoustic output of a loudspeaker can be determined under free-field conditions by combining a measurement of the pressure on the reference (usally principal) axis with the directivity index. The formula for

loudspeaker rating-efficiency η, in db, may be expressed in these terms as follows:

$$\eta = 20 \log_{10} p_L - 20 \log_{10} E_G + 10 \log_{10} Z_R + 20 \log_{10} (1 + Z_G/Z_R) - K_L - C$$

where

K_L is the loudspeaker directivity index, in db (see Section 7.1.3).

C is a constant which relates the pressure, in microbars at a distance of one meter to the acoustic power, in watts, transmitted through a sphere of 1 meter radius. For air, under standard conditions of temperature and barometric pressure, the value of this constant C is 35.2.

Note: Another method of determining loudspeaker efficiency which does not require a measurement or estimate of directivity index, utilizes a reverberant room.[7]

7. Directional Properties

In many cases, the directional characteristics of a loudspeaker can be sufficiently described by measuring one or more pressure-frequency responses along axes at chosen angles to the normal axis as specified by the manufacturer. These will indicate how well the loudspeaker response characteristics obtained on the principal axis are duplicated over an area in which listeners may be located for a given application.

In order to determine the loudspeaker rating efficiency when operating under free-field conditions, it is necessary to compute the directivity index. This requires that pressure-frequency responses be obtained at a large number of angles, or pressure-angle responses at a large number of frequencies, to provide adequate data. For many applications it is sufficiently accurate to use computed instead of measured values of the directivity index.[8] An average value, using a test signal which covers a wide band of frequencies, has been found useful in public address and sound systems engineering.[3]

7.1 Directivity Factor and Directivity Index of a Transducer

7.1.1 Directivity Factor—Definition. The directivity factor of a transducer used for sound emission is the ratio of the intensity of the radiated sound at a remote point in a free field on the principal axis, to the average intensity of the sound transmitted through a sphere passing through the remote point and concentric with the transducer. The frequency must be stated.

Note: The point of observation must be sufficiently remote from the transducer for spherical divergence to exist. See Fig. 2.

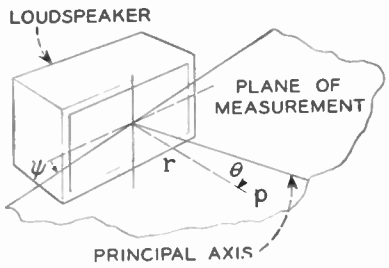

Fig. 2.

7.1.2 Directivity Index—Definition. The directivity index of a transducer is an expression of the directivity factor, in decibels, *viz.*, ten times the logarithm to the base ten of the directivity factor.

7.1.3 Directivity Index—Mathematical Expression. The directivity index may be expressed in the following form:

$$K_L = -10 \log_{10} \frac{1}{4\pi} \int_0^{2\pi} \int_0^{\pi} (p/p_r)^2 \sin \theta d\theta d\psi,$$

where

K_L is the loudspeaker directivity index, in db.

p_r is the axial free-field sound pressure, in microbars, at distance r.

p is the free-field sound pressure, in microbars at the point (r, θ, ψ).

θ and ψ are the angular polar coordinates of the system, and the principal loudspeaker axis is at $\theta = 0$.

7.1.4 Directivity Index—Method of Measurement. The loudspeaker should be mounted, connected, and tested in a suitable acoustic environment as discussed in Section 3.

The reference axis for the position of the microphone should be the principal axis of the loudspeaker as specified by the manufacturer, or, if no principal axis is specified, the normal from the center of the radiating area or horn mouth. The microphone should be placed at a distance at least three times the maximum transverse dimension of the radiating area or horn mouth. The angular steps should be as small as needed to delineate accurately the directional pattern in the plane chosen. If the loudspeaker has no axis of symmetry, the measurements should be repeated in other planes until the field is mapped.

The directivity index may then be calculated by numerical integration of the expression given under the definition above.[9]

[7] H. C. Hardy, H. H. Hall, and L. G. Ramer, "Direct measurement of the efficiency of loudspeakers by use of a reverberation room," IRE Trans. on Audio, No. AU-10, pp. 14–24; November-December, 1952.

[8] C. T. Molloy, "Calculation of the directivity index for various types of radiators," *J. Acoust. Soc. Am.*, vol. 20, pp. 387–405; July, 1948.

[9] "Calibration of Electroacoustic Transducers," ASA Z24.24; 1957. Contains information helpful in the calculation of directivity index.

8. Nonlinear Distortion

8.1 Nonlinear Distortion in a Loudspeaker

8.1.1 Definition. Nonlinear distortion in a loudspeaker is an undesired change in waveform due to deviation from a linear relationship between acoustic output and electric input.

8.1.2 Discussion. The effect of this distortion on quality constitutes one of the factors which limit the useful magnitude of the output of a loudspeaker. Some of the more important causes of this type of distortion are: (1) nonlinear force-displacement relationships in the mechanical vibrating system of the loudspeaker, (2) nonuniform flux linkage throughout the displacement range in moving-coil loudspeakers, and (3) nonlinearity in the air itself, especially in horn loudspeakers. The first two causes produce significant distortion at low frequencies for which the displacement is greatest; the third cause is significant at high frequencies.

In consequence of nonlinearity, components having frequencies other than those appearing in the electric input signal will be found in the acoustic output. For a single frequency input, these nonlinear distortion products will be harmonics and subharmonics of the original input. In the case of a complex wave input there will be, in addition, intermodulation products, *i.e.*, sum and difference frequencies of the original components and of various multiples of these components.

Nonlinear distortion is commonly determined by a measurement of the distortion products, using a microphone to convert the acoustic output of the loudspeaker to a corresponding electric signal and appropriate networks to identify and measure its various components. Distortion products fall in various parts of the spectrum, having frequencies either above or below the fundamental signal or signals by a small or large frequency interval, and may be harmonically or nonharmonically related to the original signals that produce them. Each of these products may have a different subjective importance. Furthermore, loudspeaker distortion will vary markedly with the signal frequency or frequencies even with constant input power. For these reasons, the subjective evaluation of distortion through listening tests may be more useful than measured data; and for the same reasons, no single method of measurement of distortion is standardized herein.

8.1.3 Methods of Measurement. The loudspeaker should be mounted, connected and tested in a suitable acoustic environment as discussed in Section 3.

The microphone should be placed as specified in Section 5.1.2.

Each component of the output signal may be measured individually by means of a wave analyzer which provides a narrow pass band movable over the spectrum. The pressure amplitude of each component, expressed in per cent of the amplitude of the fundamental, may be plotted vertically above a frequency scale.

Harmonics of a single fundamental may be measured by the use of a high-pass filter which effectively suppresses the fundamental and passes the harmonics without attenuation. The result, as indicated by a square-law meter (see Section 3.5), will be the root-sum-square of all harmonics present. Subharmonics will not be included.

Subharmonics may be measured with the use of a low-pass filter which suppresses the fundamental and transmits all lower frequencies without attenuation. When measured with a square-law meter the result is the rms value of all subharmonics.

Two input signals of equal amplitude are recommended for measurement of intermodulation distortion.

A filter may be considered to "suppress effectively" a fundamental if it attenuates the fundamental to an amplitude at least 10 db below that of the distortion product closest to it in frequency.

In selecting fundamental frequencies for a measurement, it should be recognized that (a) the greatest measured distortion occurs most often at the lowest frequencies; (b) distortion due to nonlinearity of the air occurs to a significant degree only in loudspeakers coupled to horns and is greatest at the higher frequencies; (c) harmonics and sum-products of plural test frequencies may not be radiated if the fundamental frequency or frequencies approach the upper limit of the effective radiating frequency range of the system, and nonlinearity may therefore be important principally in the production of difference-products; (d) difference-products may fall below the cutoff of a loudspeaker or horn and thus escape measurement; (e) harmonics and sum-and-difference-products falling in the middle portion of the frequency range of the loudspeaker, or of the ear, may be much more important subjectively than those at the extremities of the range; (f) subharmonics may be more important subjectively than harmonics; (g) nonharmonically related distortion products may be more important subjectively than harmonically related distortion products.

8.1.4 Presentation of Data. Loudspeaker distortion must be expressed as a function of frequency if it is to be expressed completely. The electric input connections to the loudspeaker and the type of equipment used for measurement must be specified.

9. Rated Power (Handling) Capacity

9.1 Power Capacity Rating of a Loudspeaker

Because of the many factors which influence the power capacity rating of a loudspeaker, no general agreement has been reached on what physical measurements should be made nor on a method of weighting the numerical value so obtained to arrive at a single rated power capacity. There is, however, general agreement on the object of such a rating.

The objective is to obtain a power capacity rating which indicates to the user that the loudspeaker will

operate satisfactorily with an amplifier having the same power rating. Some of the more important factors to consider in the rating and in deciding whether operation is "satisfactory" are:

1) operating life,
2) freedom from spurious noises (buzzes, rattles, etc.),
3) acceptable nonlinear distortion for the intended application.

The operating life may be limited by electrical failure or mechanical failure arising from mechanical or thermal causes. The acceptable noise and nonlinear distortion depend on the application. For example, more noise and distortion might be tolerated in high-level, narrow-frequency-band, public-address speech systems than in broad-band, music systems. The standardization of power capacity ratings is further complicated by the fact that the important rating factors vary greatly with frequency and the frequency dependence differs in various designs intended for the same application. At present, subjective tests are an essential part of loudspeaker rating procedures. In making physical tests for rating procedures, the following minimum requirements should be considered.

9.1.1 Testing Arrangements. The loudspeaker should be mounted and connected to the test equipment as discussed in Sections 2.1 and 3.2. The acoustic environment should simulate approximately that in which the loudspeaker will be used. The test enclosure should be of sufficient size and should employ sufficient damping that no abnormal resonances occur which might lead to abnormal mechanical fatigue in the loudspeaker.

9.1.2 Type of Test Signal. The test signal should simulate the energy distribution, both in frequency and time, of the intended signal source material. This is important in order to excite all modes of vibration that may give rise to physical fatigue or noise and to insure normal and not excessive heating. This is particularly important in moving-coil loudspeakers where the rating may be limited by the temperature of the voice coil.

The rated power capacity of the loudspeaker is normally based on the type of signal obtained from a linear system. Short-time-peak to long-time-average power ratios may be in the order of 20 db in linear speech and music systems. If the system designer intends to reproduce a modified signal, for example, a speech signal altered by substantial compression and limiting or clipping in which both the frequency and time distribution of the energy are modified, a special rating will, in general, be required.

Because of the difficulty of producing a satisfactory artificial test signal, speech and music are frequently used. This is preferably selected recorded material.

Other test signals, such as pulsed sine wave, band of noise, warbled or swept frequency, have been used. The swept frequency signal is often one in which the frequency is varied linearly with time over a specified range.

Note: For accelerated life tests the signal is frequently supplied to the loudspeaker through a limiter so operated as to give approximately a 1/8 second peak to 15 second average power ratio of 6 db. This alters the energy distribution and substantially increases the heating effects. The rated loudspeaker capacity is said to be equal to the rated amplifier output power if no failure or significant performance degradation occurs in 100 hours. What is obtained relates to a system rating since the overload characteristic of the amplifier is also involved.

9.1.3 Duration of Test. The test should be continued for a sufficient length of time to permit (a) maximum steady-state temperatures to be developed at all points in the loudspeaker structure under the specified conditions of ambient air temperature and ventilation, and (b) fatigue failures of materials to develop (in order of 10^7 stress alternations).

Coincidence Techniques for Radar Receivers Employing a Double-Threshold Method of Detection*

K. ENDRESEN† AND R. HEDEMARK†, ASSOCIATE MEMBER, IRE

Summary—**The double-threshold method of detection calls for m or more detections in n consecutive trials to decide that a target is present. With the video coincidence techniques described, the requirement is m or more consecutive pairs, or triples, in n consecutive trials. The latter methods may increase the resistance to random interference, but a certain price has to be paid in normal radar-detection range. Important questions are, 1) If the interference has a probability p of exceeding the first threshold, what is the probability that a false target will be formed using these different techniques? 2) What is the required signal-to-noise ratio for a given probability of detection when the rate of false alarm is held constant for all three techniques? The paper develops mathematical formulas to answer such questions, and also presents graphs for the cases $n=10$, 20 and 30 hits per target. Examples are worked out for $n=10$.**

Introduction

THE performance of a radar set may be degraded by unintentional interference pulses from, *e.g.*, adjacent radar sets, or by intentional interference from a jamming source. The type of interference which will be considered in the following discussion is the one where random pulses appear at the detector output. To reduce the effect of such interference, advantage may be taken of the fact that pulses, due to a real-target return, appear at a constant position during several sweep periods, whereas pulses which are not locked to the radar-pulse repetition rate may occur at random. Therefore, as is well known, the effective interference may be reduced by correlating two or more sweep periods. What is not generally known is the quantitative advantage to be expected, and how such schemes will affect the normal radar performance.

The authors have tried to establish the necessary formulas for a radar set employing certain digital-detection techniques. It is assumed that the coverage area is quantized in azimuth and range, such that each quantum, or unit element, is identical in size and shape to one normal radar echo.

Basic Concepts

Single-Pulse Detection Probability

When a target is illuminated by a pulsed-radar set, the receiver will accept a number, say n, of returns during one scan period. Each pulse is more or less contaminated by noise, and the pulse envelope will therefore fluctuate. As an example, Fig. 1 shows the probability that the signal-plus-noise amplitude exceeds a given relative threshold R_t for various signal-to-noise ratios.[1] It is here assumed that the target echo itself is steady.

The target echo will in general also fluctuate. For a monofrequency radar system, the echo from a jet aircraft may, *e.g.*, be steady during one scan, but fluctuate from scan to scan. With a frequency-jumping radar set, an aircraft echo may also fluctuate considerably from sweep to sweep. Fig. 2 shows the probability of a single noise-contaminated radar return exceeding a given threshold R_t for the extreme case when the signal itself is also noiselike. Figs. 1 and 2 apply for a single pulse. In radar detection, however, an ensemble of n pulses is considered.

In PPI systems where an operator judges whether targets are present or not, the detection process is somewhat obscure, as the role of the operator as a detection element is not precisely understood. In mathematical analyses it is assumed generally that for every unit element each noise or signal-plus-noise sample is individually detected and all n detected samples added.[2,3] A target is judged to be present if the sum exceeds a certain threshold.

To account for the operator, an *operator degradation factor* is introduced, defined as the ratio between the experimental and theoretical signal-to-noise ratios required for detection. For example, this factor may be from two to ten times (3 to 10 db).[3]

Double-Threshold Method of Detection

For automatic data extraction, digital methods are more convenient, and the detection criteria can be more exactly defined. A usual model is shown in Fig. 3(a). The individual pulse is compared with a fixed threshold R_t (*first threshold*), and is classified as a one or a zero depending upon whether or not it exceeds the threshold. For each group of n pulses the number of ones are counted, and if the sum equals or exceeds a predetermined value m (*second threshold*), a target is judged to be present.

* Received by the IRE, May 5, 1961; revised manuscript received, June 2, 1961.

† Norwegian Defence Res. Establishment, Lillestrøm, Norway.

[1] S. O. Rice, "Mathematical analysis of random noise," in "Selected Papers on Noise and Stochastic Processes," Dover Publications, Inc., New York, N. Y., pp. 238–241; 1954.

[2] E. L. Kaplan, "Signal-detection studies, with applications," *Bell Sys. Tech. J.*, vol. 34, pp. 403–437; March, 1955.

[3] W. M. Hall, "Prediction of pulse radar performance," PROC. IRE, vol. 44, pp. 224–231; February, 1956.

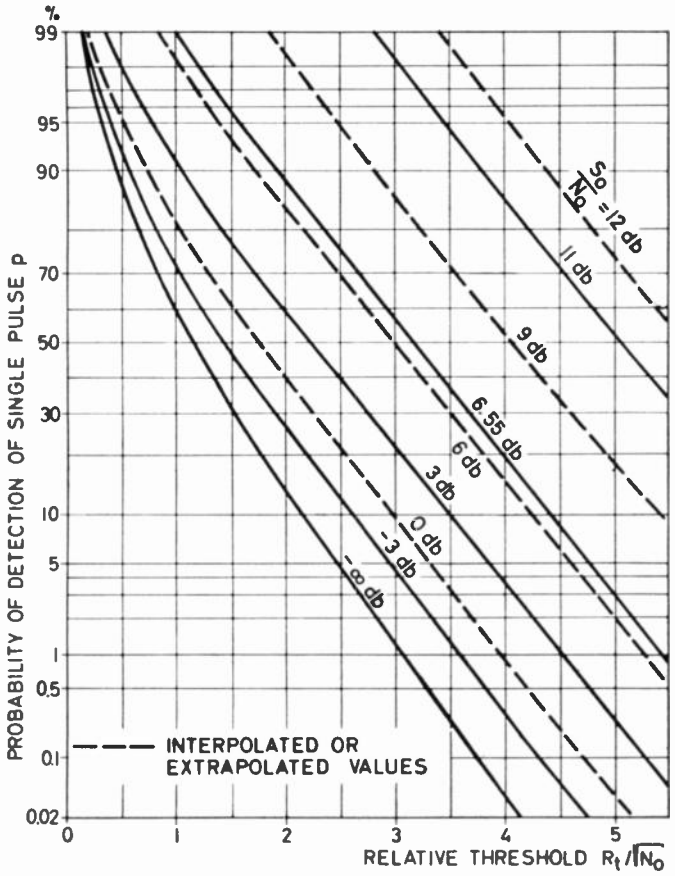

Fig. 1—Probability of detection of single pulse. No fading. S_0 = signal power. N_0 = mean noise power.

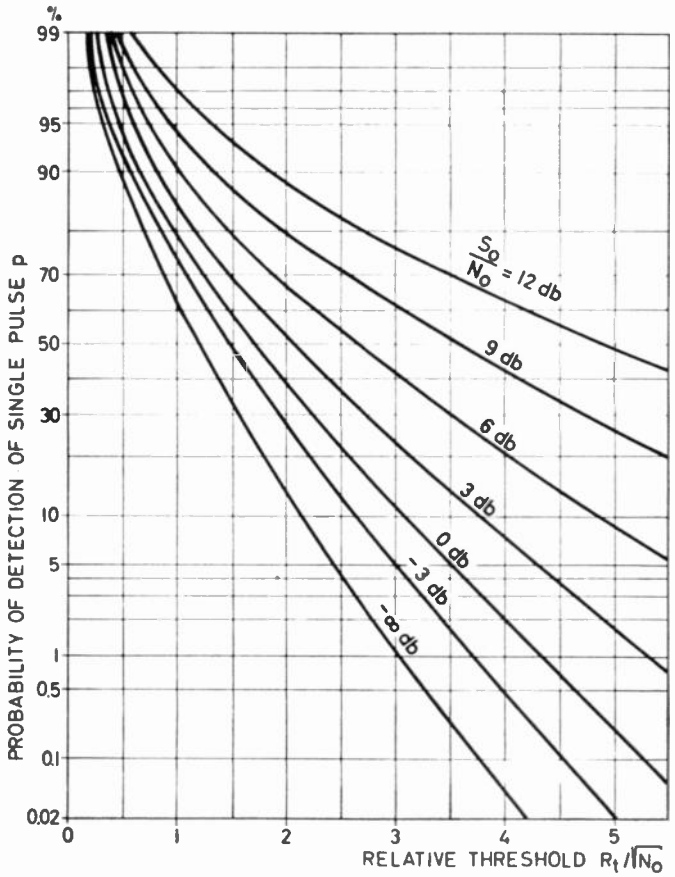

Fig. 2—Probability of detection of single pulse. Noise-like signal. S_0 = mean signal power. N_0 = mean noise power.

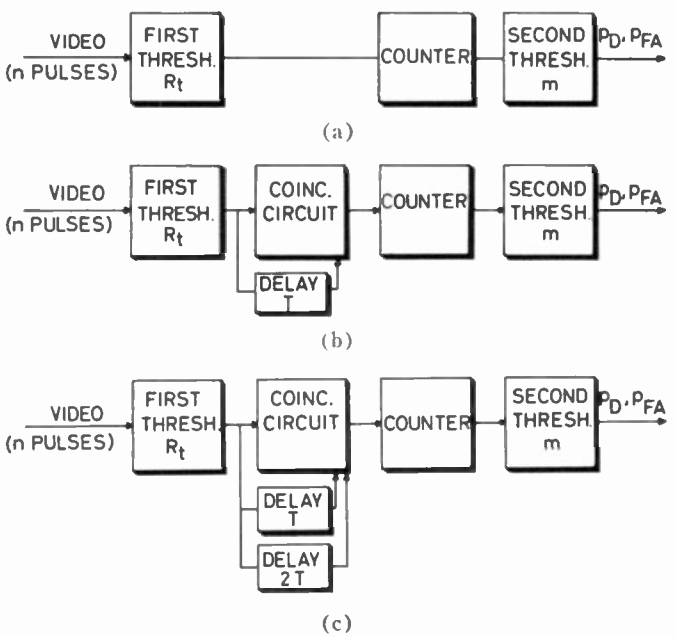

Fig. 3—Principle of coincidence circuits. (a) No coincidence. (b) Double coincidence. (c) Triple coincidence.

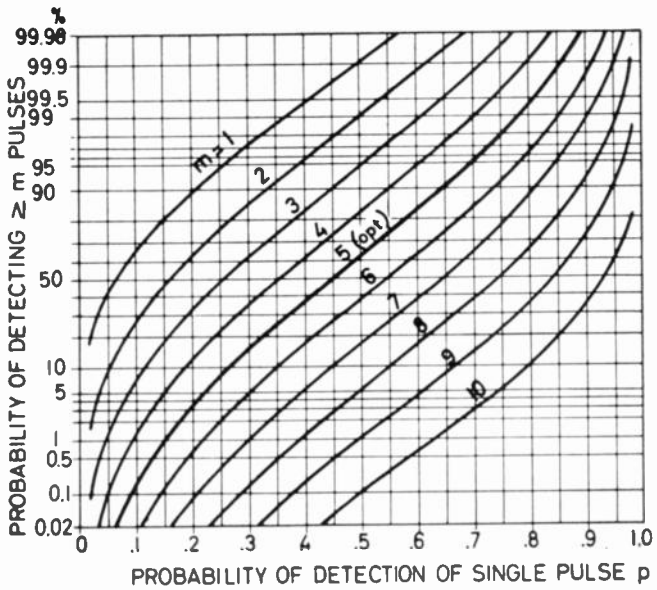

Fig. 4—Probability of detection in a system not employing coincidence techniques. $n = 10$.

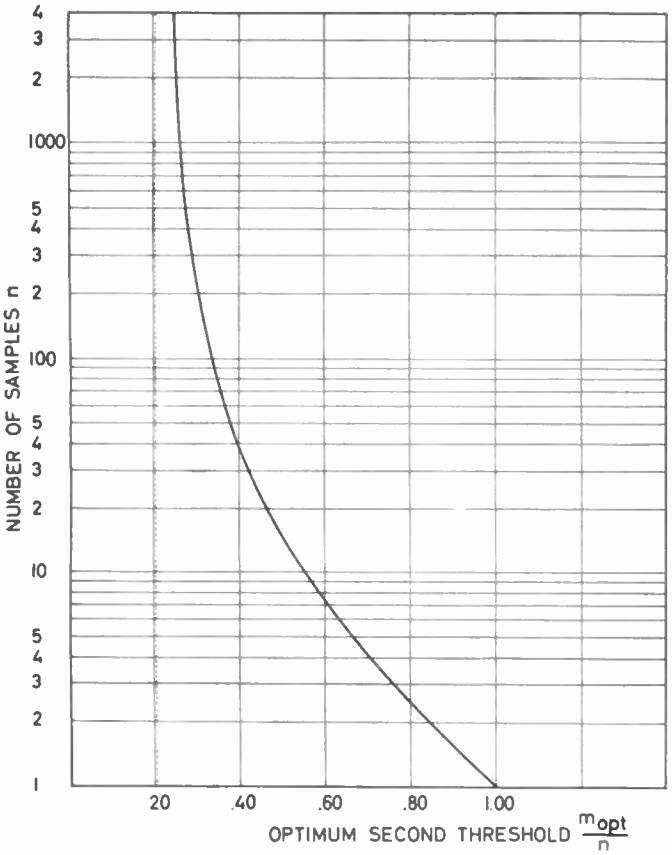

Fig. 5—Relation between the optimum second threshold and the number of samples.

Fig. 4 illustrates for the case $n = 10$ the dependence of detection probability upon the value of m and the single-pulse detection probability p. The latter value for a given signal-to-noise ratio may be obtained from Fig. 1 or Fig. 2.

Swerling[4] has shown that when m is suitably chosen, the double-threshold method requires about 1 db better signal-to-noise ratio than the post-detector integration method. An automatic system will be therefore in reality some 2–10 db better than a manual PPI system.

Fig. 5 gives (after Swerling) the approximate optimum value of the second-threshold m as a function of n.

False Alarm Rate

Whatever system is used, there is a possibility that random noise may be falsely judged as being due to a real target return. On a normal PPI oscilloscope the number of unit elements that can accommodate a target echo is of the order of 10^4–10^6. Consequently, if one requires that the mean number of false alarms occurring during one complete scan shall not exceed say one, the probability of false alarm within a given unit element should be less than, *e.g.*, 10^{-5}. This determines the thresholds to be used. In the double-threshold model, the optimum value of m is not very much influenced by the false alarm rate. The first threshold is more critical.

[4] P. Swerling, "The 'Double Threshold' Method of Detection," Rand Corp. Res. Memo. RM-1008; December, 1952.

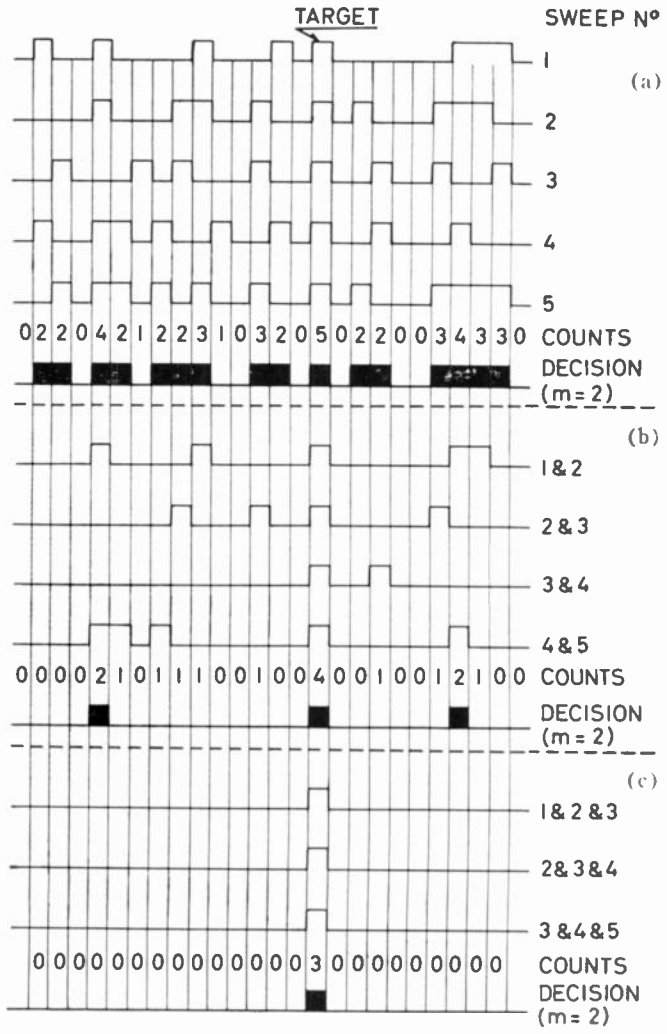

Fig. 6—Waveforms, example. (a) No coincidence (b) Double coincidence (c) Triple coincidence.

Video Coincidence Techniques

Description of Video Coincidence Circuits in a Double-Threshold System

To illustrate the principle of coincidence techniques in a double-threshold system, reference is made to Figs. 3 and 6.

In Fig. 3(a) (no coincidence) the video signal is first quantized as outlined above, and then passed to a number of counters (only one shown). Each counter only accepts pulses arriving within a certain range and azimuth interval. The range interval is equal to the duration of one normal radar pulse, and the azimuth interval equals the equivalent lobe width of the antenna. How this gating is performed will not concern the present discussion.

In Fig. 6(a) it is assumed that the number of sweeps per antenna lobe width is 5. For the purpose of illustration m is put equal to 2. One target is present; all other pulses are due to noise. The number of counts for each range interval and the corresponding decisions are indicated.

In Fig. 3(b) each sweep is coincided with the previous one. The corresponding waveforms are indicated in Fig. 6(b). The counts and decisions are indicated, assuming $m=2$ as before. In Figs. 3(c) and 6(c) each sweep is coincided with the previous two.

In the examples cited in Fig. 6, it appears that the number of false decisions is reduced as the number of coincidence inputs is increased. This is true if the interference is due to, *e.g.*, strong random-pulse jamming.

If the interference is due to noise, Fig. 6 is not representative. On the contrary, the first threshold would be set such that the number of false decisions was equal in all three cases, corresponding to the permissible false alarm rate. What would in fact vary in Fig. 6 is the detection probability for the real target.

Probabilities of Detection and False Alarm

The probabilities of detection and false alarm are derived in Appendixes I–III for the cases of one, two, and three coincidence inputs.

In the equations, the following symbols are used:

p_D = Probability of detection,
p = Probability that the received signal-plus-noise envelope exceeds the first threshold (*e.g.*, Figs. 1 and 2),
p_0 = Probability that the noise envelope exceeds the first threshold ($S_0/N_0 = -\infty$ db in Figs. 1 and 2),
p_{FA} = Probability of false alarm,
n = Number of pulses per target,
m = Second threshold. Approximate optimum values may be found from Fig. 5 (corresponding to n, $n-1$ and $n-2$ in the three cases).

No general conclusion may be drawn directly from the equations as they stand, they being solved better numerically for each case of interest. The NDRE electronic-computer FREDERIC has been programmed to give numerical values of p_D for any given n, m and p, employing the exact formulas (2), (5), and (7) presented in Appendixes I–III. Some results are given in Figs. 4 and 7–11. The optimum values of m are found from Fig. 5.

To indicate how the curves may be used, a few examples are given for the case $n=10$.

Example 1. Random Pulse Interference ($n=10$)

When the interference is due to nonsynchronized strong pulsed or frequency-swept interference, the time interval during which each sweep is perturbed is little dependent upon the value of the first threshold. Figs. 4, 7, and 8 directly give the relative time that the radar set is disturbed. Comparative curves for the optimum-integer value of m are given in Fig. 9 as functions of the mean duty cycle p_i of the interference. It will, for instance, be seen that for a moderately intense interference with $p_i=0.2$, without coincidence the radar receiver is disturbed for 3.5 per cent of the time, whereas with double and triple coincidence the figure is lowered to 0.05 per cent and 0.005 per cent, respectively. With a highly intense interference of $p_i=0.5$, which in fact would imply that an ordinary PPI is completely dis-

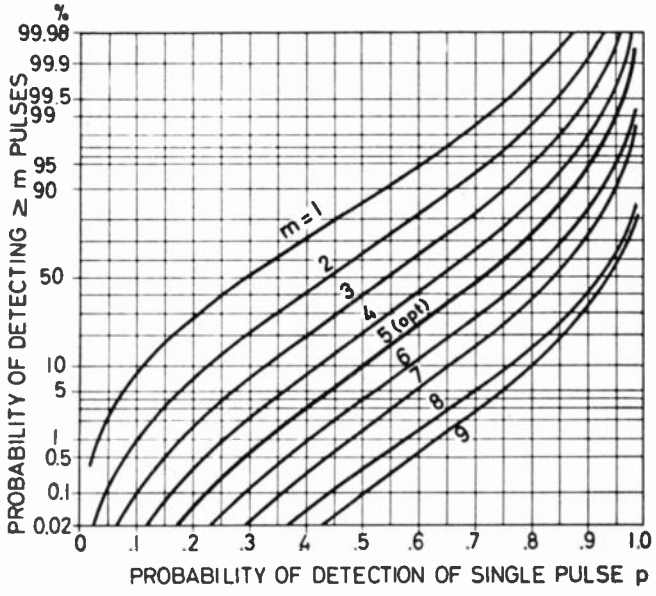

Fig. 7—Probability of detection in a system employing double coincidence techniques. $n=10$.

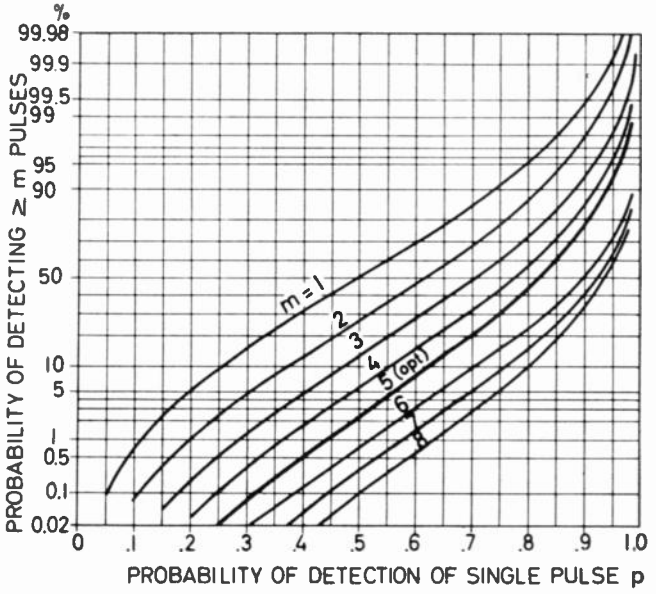

Fig. 8—Probability of detection in a system employing triple coincidence techniques. $n=10$.

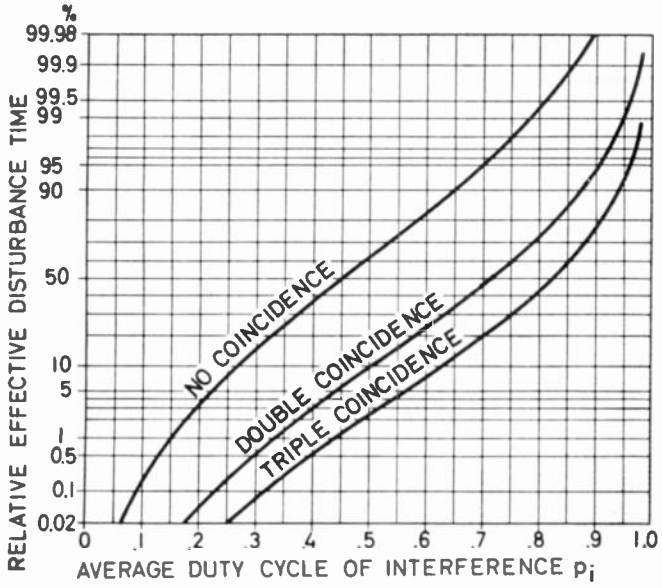

Fig. 9—Effective disturbance time. $n=10$. $m_{opt}=5$ in all three cases.

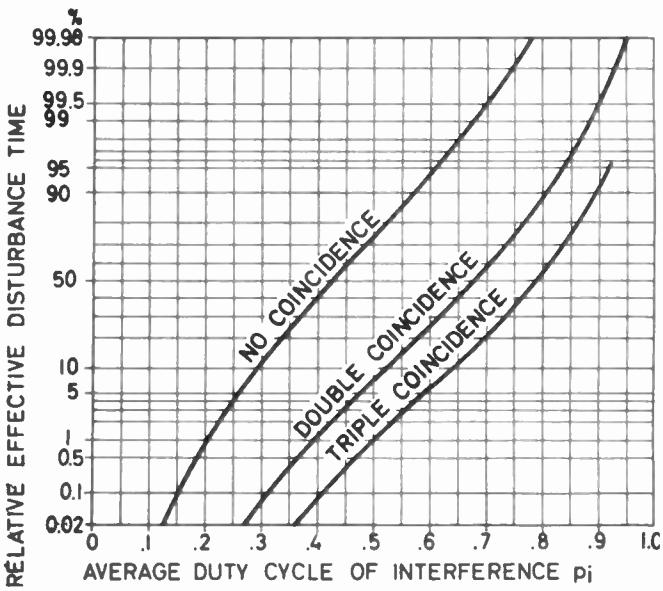

Fig. 10—Effective disturbance time. $n=20$. $m_{opt}=9$ in all three cases.

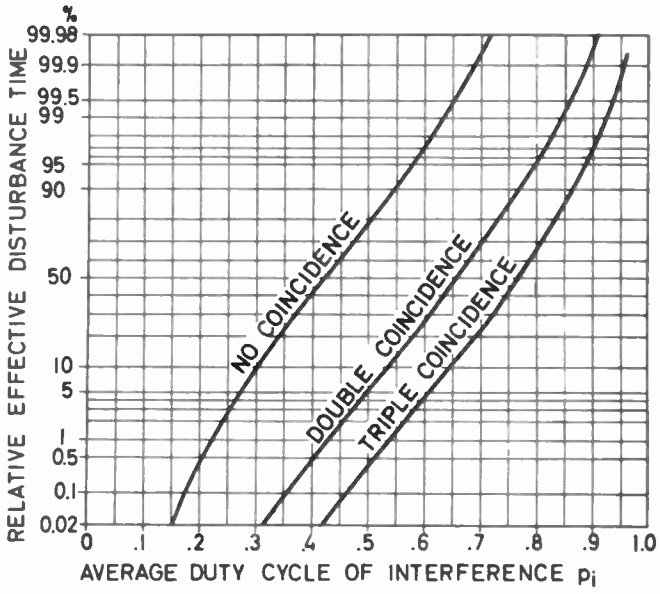

Fig. 11—Effective disturbance time. $n=30$. $m_{opt}=13$ in all three cases.

turbed, the figures are 62 per cent, 10 per cent, and 2.4 per cent, respectively.

Example 2. Noise Conditions ($n=10$)

Fig. 9 shows the advantage to be expected under the jamming types which the circuits are designed to combat. Next one might ask, what is the disadvantage, if any, under random (Gaussian) noise conditions? As an example, we may require that the false-alarm rate should equal 10^{-5}, and we seek the signal-to-noise ratios required to give a detection probability of 50 per cent or 90 per cent. Worked-out examples are given in Table I where the figures and equations used also are indicated.

It appears from Table I that for a steady signal, the required signal-to-noise ratio is increased by about 0.6 db when double diversity is used, and by 1.2 db for triple diversity, for both values of p_D indicated. For noise-like signal and $p_D=90$ per cent, double and triple coincidence require 3.2 db and 6.6 db better signal-to-noise ratio, respectively, than when no coincidence is used. For $p_D=50$ per cent, the corresponding figures are 2.3 db and 4.2 db.

An increase in required signal-to-noise ratio implies that the radar range is reduced as indicated in Table II, which assumes that the radar system obeys an inverse fourth-power law.

TABLE I

DETERMINATION OF REQUIRED SIGNAL-TO-NOISE RATIO
$n = 10(m = 5) \cdot p_{FA} = 10^{-5}$

No. of coincidence inputs		One		Two		Three	
Probability p_D of detection		90 per cent	50 per cent	90 per cent	50 per cent	90%	50%
Probability p_0 that a noise sample exceeds R_t		0.033 [Eq. (3)]		0.112 [Eq. (6)]		0.16 [Eq. (8)]	
Relative threshold $R_t/\sqrt{N_0}$		2.61 (Fig. 1 or 2 ($-\infty$ db))		2.12 (Fig. 1 or 2 ($-\infty$ db))		1.92 (Fig. 1 or 2 ($-\infty$))	
Probability p that signal-plus-noise sample exceeds R_t		0.65	0.45 (Fig. 4)	0.864	0.71 (Fig. 7)	0.94	0.82 (Fig. 8)
Required signal-to-noise ratio S_0/N_0 db	Steady signal	6	4 (Fig. 1)	6.6	4.6 (Fig. 1)	7.2	5.2 (Fig. 1)
	Noise-like signal	8.4	5 (Fig. 2)	11.6	7.3 (Fig. 2)	15	9.2 (Fig. 2)

TABLE II

RELATION BETWEEN REQUIRED INCREASE IN SIGNAL-TO-NOISE RATIO AND RANGE

Reduction in range, per cent	6	12	16	21	25	29	35
Increase in signal-to-noise ratio, db	1	2	3	4	5	6	7

CONCLUSION

When coincidence techniques are used in a double-threshold detection system, a great advantage is obtained when the interference consists of pulses of low effective duty cycle. The advantage is considerable even for high duty cycles which would in effect completely block a noncoincidence system. The advantage is greater the higher the number of coincidence inputs. Against suitably synchronized interference the advantage is lost.

When the interfering signal is random noise, coincidence techniques reduce the range. The reduction is greater the larger the number of coincidence inputs. Due to the form of the radar equation, this disadvantage may be unimportant as compared with the advantage obtained under random-pulse interference conditions.

APPENDIX I

SYSTEM WITHOUT COINCIDENCE

Consider Fig. 3(a). The probability that a video pulse exceeds the first threshold is denoted by p, and the number of samples is n. The probability of detection, *i.e.*, of receiving at least m pulses from the counter output, is found by adding terms of the binomial distribution,

$$p_D = \sum_{x=m}^{n} \binom{n}{x} p^x (1-p)^{n-x}. \tag{1}$$

This may also be expressed as

$$p_D = \binom{n}{m} p^m + (-1)^m \sum_{x=m+1}^{n} (-p)^x \binom{n}{x}\binom{x-1}{m-1} \tag{2}$$

If p_D is *very small*, as may be the case when only noise is present, the first term in (2) predominates, and the remaining terms have alternating signs. The probability of false alarm therefore is given by

$$p_{FA} \approx \binom{n}{m} p_0^m , \tag{3}$$

where p_0 is the probability that a noise pulse exceeds the first threshold.

APPENDIX II

COINCIDENCE SYSTEM WITH TWO INPUTS

Consider Fig. 3(b). The n samples are delayed by one sweep period and correlated with the undelayed signal, as shown in the example below, where digit 1 corresponds to a pulse out from the first threshold device

Input	1 0 1 1 1 0 1 1 0 0
Delayed input	1 0 1 1 1 0 1 1 0 0
Output	0 0 1 1 0 0 1 0 0

The coincidence circuit will give an output only if the delayed and undelayed sample are simultaneously 1. This requires the input signal to contain at least two 1's

in close configuration. More generally, $r+1$ 1's in close configuration will give out r 1's.

The probability of getting k 1's in a predetermined order in the input signal is

$$q(k) = p^k(1-p)^{n-k}. \tag{4}$$

The number of permutations containing k input 1's and x output 1's is denoted $P(k, x)$, and the probability of detection is given by

$$p_D = \sum_{x=m}^{n-1} \sum_{k=x+1}^{k_{\max}} p^k(1-p)^{n-k}P(k,x) + \Delta(x)\cdot(1-p)^n. \tag{5a}$$

In (5a), $\Delta(x)=1$ for $x=0$ and is zero otherwise. By a rather cumbersome counting of permutations, one finally arrives at[5]

$$P(k, x) = \binom{n+1-k}{k-x} \cdot\left[1 + \sum_{r=1}^{x}\binom{k-x-2+r}{r}\right], \tag{5b}$$

and

$$k_{\max} = \tfrac{1}{2}\left[n + x + \tfrac{1}{2}(1-(-1)^{n+x})\right]. \tag{5c}$$

When the probability $p=p_0$ that a noise pulse exceeds the first threshold is *very low*, (5) simplifies to

$$p_{FA} \approx p_0^{m+1}(n-m). \tag{6}$$

Appendix III

Coincidence System with Three Inputs

For the case illustrated in Fig. 3(c), the output will contain a 1 only if there are three 1's in close configuration in the input signal, *e.g.*,

Input	0 1 1 0 1 0 1 1 1 0 0
Delayed T	0 1 1 0 1 0 1 1 1 0 0
Delayed $2T$	0 1 1 0 1 0 1 1 1 0 0
Output	0 0 0 0 0 0 1 0 0

[5] K. Endresen and R. Hedemark, "Video Sweep to Sweep Coincidence Techniques for Radar Receivers Employing a Double-Threshold Mode of Detection," Norwegian Defence Res. Establishment, Internal Rept. No. T-209; November, 1960.

The derivation proceeds along the same pattern as in Appendix II. One first determines the number of favorable permutations $P(k, x)$ containing k input and x output 1's. Next is calculated the maximum value of k. Omitting the details, one finds after a laborious procedure[5]

$$p_D = \sum_{x=m}^{n-2} \sum_{k=x+2}^{k_{\max}} p^k(1-p)^{n-k}P(k,x) + \Delta(x)R(p,n) \tag{7a}$$

where

$$P(k, x) = \sum_{r=0}^{g(n,k,x)} \binom{(n+1-k)}{(0,5(k-x+N)+r} \cdot\binom{0,5(k-x+N)+r}{N+2r}, \cdot\left[1 + \sum_{s=1}^{x}\binom{0,5(k-x-N)-2-r+s}{s}\right], \tag{7b}$$

$$N = \tfrac{1}{2}\left[1-(-1)^{k-x}\right], \tag{7c}$$

$$\left.\begin{aligned} g(n,k,x) &= \tfrac{1}{2}(k-x-2-N) \quad \text{for } n \geq 2k-x-2 \\ g(n,k,x) &= \tfrac{1}{2}(2n-3k+x+2-N) \quad \text{for } n < 2k-x-2 \end{aligned}\right\}, \tag{7d}$$

$$k_{\max} = \tfrac{1}{3}\left\{x + 2\left[n+1-\alpha(n,x)\right\}\right. + g(\alpha), \tag{7e}$$

$$\alpha(n, x) = 0, 1 \text{ or } 2, \text{ chosen to make } k_{\max} \text{ an integer}, \tag{7f}$$

$$g(\alpha) = \begin{cases} 1 & \text{for } \alpha(n,x) = 2 \\ 0 & \text{for } \alpha(n,x) \neq 2 \end{cases}, \tag{7g}$$

$$\Delta(x) = \begin{cases} 1 & \text{for } x = 0 \\ 0 & \text{for } x \neq 0, \end{cases} \tag{7h}$$

$$R(p, n) = \sum_{k=0}^{u}\binom{n+1-k}{k} p^k(1-p)^{n-k}, \tag{7i}$$

$$u = \tfrac{1}{4}\left[2n+1-(-1)^n\right]. \tag{7j}$$

This exact equation, which is well suited for digital computation, should be used for all values of p_D greater than of the order $10^{-3}-10^{-4}$. For very small values of p_D, (7) simplifies into

$$p_{FA} \approx p_0^{m+2}(n-m-1). \tag{8}$$

Correspondence

Antenna and Receiving-System Noise-Temperature Calculation*

A Naval Research Laboratory report[1] recently completed by the writer contains results, which are here summarized, that may be of interest.

In Part I a calculated curve representing the noise temperature of a typical directive antenna in the frequency range 100 to 10,000 Mc is presented (Fig. 1) together with the method and details of the calculation. Since antenna noise temperature (averaged over all galactic directions) is virtually independent of antenna gain and beamwidth, the curve may be used as an approximation for any typical directive antenna. The assumed environmental conditions are: 1) average cosmic noise; 2) solar noise temperature ten times the quiet level, with the sun in a unity-gain minor lobe of the antenna pattern; 3) a cool-weather temperate-zone atmosphere; and 4) a fixed ground-noise contribution of 36°K, as would result with a ground at blackbody temperature 290°K viewed over a π-steradian solid angle by minor lobes averaging 0.5 gain (3 db below isotropic level). The values given by this curve may readily be modified for other conditions.

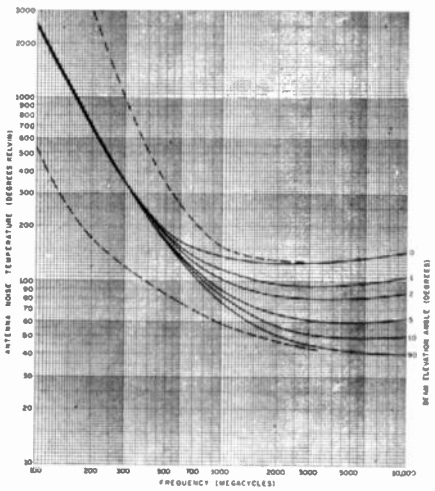

Fig. 1—Antenna noise temperature for typical conditions. Dashed curves are for maximum and minimum cosmic and atmospheric noise.

Part II presents a methodology for utilizing this antenna noise temperature in calculation of a system noise temperature, from which the total system noise power output and signal-to-noise power ratio may easily be computed. Basic concepts and definitions are first reviewed and then applied to development of formulas for noise temperatures of components of a cascade system and of the over-all system. The need for definition of both spot (frequency-dependent) noise temperature and average temperature over a pass band is pointed out, together with the need for definition of a transducer input noise temperature that reflects only the intrinsic noise.

The IRE-defined input noise temperature[2] of a two-port transducer, T_e, is interpreted to include, in the case of a multiple-input-response transducer, the effect of noise power contributed by a standard-temperature input termination via the spurious responses. For cascade-system noise-temperature calculation, a more suitable definition (in the case of a multiple-response heterodyne transducer) is obtained by postulating a zero-temperature (noise-free) input termination. The resultant transducer *output* noise temperature, divided by the conversion gain for a particular response, gives an input noise temperature referred to that response. The response thus chosen is usually designated the principal response, and this temperature is therefore called the principal-response input noise temperature, T_p. It is equivalent to T_e with the noise contribution of the standard-temperature input termination via the spurious responses deleted. Its relation to the transducer noise factor F is

$$T_p = (F - \beta)T_0, \tag{1}$$

where $T_0 = 290°K$ and β is defined by the relation

$$\beta = \frac{\int_0^\infty G(f)df}{\int_p G(f)df}. \tag{2}$$

$G(f)$ is the available transducer conversion power gain as a function of input frequency, and the integral of the denominator is taken over the principal-response band only. Since by definition,

$$T_e = (F - 1)T_0, \tag{3}$$

it follows that

$$T_p = T_e - (\beta - 1)T_0. \tag{4}$$

In a cascade system the noise-temperature contribution of a broad-band component that precedes a multiple-response transducer is shown to be expressible, subject to some mild conditions, as the sum of the spot-temperature values in the various response channels weighted by the relative gains of the channels. Utilizing this result, a formula for the noise temperature of a basic system consisting of antenna, transmission line, and a multiple-response receiver having s responses is obtained:

$$T_N = T_p + \sum_{i=1}^{s} \left[G(f_i)/G(f_p)\right] \cdot \left[T_a(f_i)/L_r(f_i) + T_r(f_i)\right]. \tag{5}$$

The frequencies f_i are the nominal frequencies of the response bands, and f_p is the principal-response frequency. L_r is the available-loss factor of the transmission-line system, including antenna dissipative losses, and T_r is the effective transmission-line output noise temperature, given by

$$T_r = T_t(1 - 1/L_r), \tag{6}$$

where T_t is the thermodynamic (Kelvin) temperature of the transmission-line lossy material. For the case of a single-response transducer ($\beta = 1$), (5) reduces to

$$T_N = T_a/L_r + T_r + T_e, \tag{7}$$

where the quantities on the right-hand side are evaluated at the nominal response frequency. (This equation, together with Fig. 1, appeared in a recent paper on radar range calculation.)[3]

This system noise temperature is referred to the receiver input terminals. If the effective signal power at this point is P_r, the receiver output signal-to-noise power ratio is

$$S/N = P_r/(kT_N B_N), \tag{8}$$

where k is Boltzmann's constant and B_N is the over-all system noise bandwidth. By suitable definition of P_r this result is applicable to simultaneous reception of signal in more than one response of a multiple-response system, as sometimes occurs in radiometry and possibly in other applications.

The system noise temperature may also be referred to the system input terminals. It is pointed out that this reference point is the only one for which a system noise temperature can be used to compare the low-noise merit of different systems, and then only if standard environmental conditions (*e.g.*, those of Fig. 1) are postulated, and if the system "input terminals" are defined to precede *all* dissipative losses, including any in what would ordinarily be considered the antenna (*i.e.*, such losses must be included in evaluation of the transmission-line loss factor, L_r). The expressions for the system noise temperature referred to the system input, corresponding to (5) and (7), are

$$T_{NI} = L_r(f_p)T_p + \sum_{i=1}^{s} \left[G(f_i)/G(f_p)\right] \cdot \left[T_a(f_i) + L_r(f_i)T_r(f_i)\right] \tag{9}$$

and

$$T_{NI} = T_a + L_r(T_r + T_e). \tag{10}$$

At the National Symposium of the IRE PGMTT in May, 1961, while the NRL report was in preparation, a five-member panel presented results of a study[4] of the

* Received by the IRE, July 7, 1961.

[1] L. V. Blake, "Antenna and Receiving-System Noise-Temperature Calculation," Naval Res. Lab., Washington, D. C., NRL Rept. No. 5668; 1961.

[2] IRE Standard 59 IRE 20.S1, "Methods of measuring noise in linear twoports, 1959" (Proc. IRE, vol. 48, pp. 60–68; January, 1960. See p. 68.)

[3] L. V. Blake, "Recent advancements in basic radar range calculation technique," IRE Trans. on Military Electronics, vol. MIL-5, pp. 154–164; April, 1961.

[4] H. A. Haus, *et al.*, "Elementary considerations of noise performance," *The Digest of Technical Papers*, 1961 PGMTT Natl. Symp., pp. 53–57.

noise-temperature method of analyzing system noise performance. They propose characterizing a multiple-response transducer by a "broad-band effective input noise temperature," T_b, which is related to T_p by the formula

$$T_p = \beta T_b. \tag{11}$$

Therefore, system noise temperature is expressible in terms of either of these quantities through this relation. Another difference in the approach of the PGMTT panel is their use of signal bandwidth, rather than system noise bandwidth, in definition of system noise temperature. Through consideration of both approaches it is hoped that more comprehensive IRE standards on transducer and system noise temperature may eventuate.

L. V. Blake
Radar Div.
Naval Research Lab.
Washington, D. C.

Nonsymmetrical Properties of Nonlinear Elements in Low- and High-Impedance Circuits*

The interest to date in parametric devices has primarily been concerned with the power conversion arising from the first-order nonlinear term in a reactance expansion. For this case it makes no difference whether a particular nonlinear element is used in series or parallel resonant circuits since the power conversion is independent of the circuit configuration. However, when the higher-order nonlinear terms are to be used for power conversion or when the perturbations on first-order power conversion due to the higher-order nonlinearities are to be considered, the circuit configuration which terminates the nonlinear device has an important influence on the operating characteristics.

To illustrate this point consider the two common methods of reactively terminating a nonlinear capacitor in order to avoid power conversion into unwanted harmonic frequencies and mixing products. The capacitor may look into a low impedance at these frequencies so that a large number of harmonic currents flow without significant voltage components, or the termination may be a high-impedance one so that a large number of harmonic voltages exist without significant currents. These two cases are illustrated by the amplifier circuits of Fig. 1, in which the voltage across the capacitor in Fig. 1(a) and the current through the capacitor in Fig. 1(b) consist essentially of the sum of only three components.

To analyze these circuits two expansions of the nonlinearity of the capacitance are useful. For a semiconductor capacitor the usual approximation for the capacitance is

* Received by the IRE, July 13, 1961.

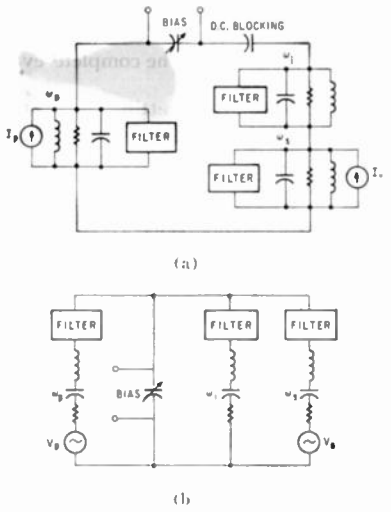

Fig. 1—Parametric amplifier circuits. (a) Low-impedance termination. (b) High-impedance termination.

$$C(v) = \frac{dq}{dv} = \frac{C_0}{\left[1 - \frac{V_B + v}{\phi}\right]^n} = \left[\frac{C_0\phi^n}{(\phi - V_B)^n}\right] \cdot \frac{1}{\left[1 - \frac{v}{\phi - V_B}\right]^n} = \frac{C_B}{\left[1 - \frac{v}{\phi - V_B}\right]^n}, \tag{1}$$

where C_B is the average capacitance at the (generally negative) bias voltage V_B, and v and q are the ac variations about the bias point. The charge variation on the capacitor may be expanded as a Taylor series in the voltage as

$$q(t) = C_B v(t) + \mathcal{C}_a v^2(t) + \mathcal{C}_b v^3(t) + \cdots = C_B v(t) + \frac{nC_B v^2(t)}{2!(\phi - V_B)} + \frac{n(n+1)C_B v^3(t)}{3!(\phi - V_B)^2} + \frac{n(n+1)(n+2)C_B v^4(t)}{4!(\phi - V_B)^3} + \cdots \tag{2}$$

and the voltage in terms of the charge as,

$$v(t) = S_B q(t) - S_a q^2(t) - S_b q^3(t) - \cdots = \frac{1}{C_B} q(t) - \frac{nq^2(t)}{2!(\phi - V_B)C_B^2} - \frac{(1-2n)nq^3(t)}{3!(\phi - V_B)^2 C_B^3} - \frac{(2-3n)(1-2n)nq^4(t)}{4!(\phi - V_B)^3 C_B^4} - \cdots \tag{3}$$

Although either of these expansions may be used in the analysis of these circuits, the use of the improper expansion is mathematically cumbersome and does not lead to a good physical understanding of the characteristics of the circuit. Thus, the expansion should be made in terms of the variable consisting of the sum of the fewest components, with (2) being used for the circuit of Fig. 1(a), and (3) for Fig. 1(b).

In the three frequency systems illustrated, the even terms in the equations cause power conversion. In this respect the two circuits are equivalent, if higher-order perturbations are neglected, as may be seen by computing the figure of merit, often used, of relative change in the average capacitance or elastance due to the pumping.

$$\frac{\Delta C_B}{C_B} = \frac{\mathcal{C}_a |v(t)|}{C_B} = \frac{n|v(t)|}{2!(\phi - V_B)} \tag{4}$$

$$\frac{\Delta S_B}{S_B} = \frac{S_a |q(t)|}{S_B} = \frac{n|q(t)|}{2!(\phi - V_B)C_B} = \frac{n|v(t)|}{2!(\phi - V_B)}. \tag{5}$$

The other terms in the expansions do not have this symmetry. The third term leads to a susceptance in each resonant circuit of Fig. 1(a) with the value

$$jB_i = j\mathcal{C}_b(|V_i|^2 + 2|V_k|^2 + 2|V_l|^2), \tag{6}$$

and likewise a reactance in the circuit of Fig. 1(b) of

$$jX_i = j\frac{3}{4}\frac{S_b}{\omega_i^2}\cdot\left(\frac{|I_i|^2}{\omega_i^2} + 2\frac{|I_k|^2}{\omega_k^2} + 2\frac{|I_l|^2}{\omega_l^2}\right), \tag{7}$$

where the V's and I's are the peak values of the voltages across and the currents through the varactor. These terms cause a signal-dependent and mutually-coupled susceptance or reactance which produces nonsymmetrical resonance curves and accounts for the jump phenomenon observable in nonlinear resonant systems. The significance of these expressions is that the reactance perturbation may be eliminated by using an abrupt-junction varactor ($n = \frac{1}{2}$) while the same cannot be done for the susceptances with presently available semiconductor capacitors. When the third term in the voltage expansion is eliminated by using an abrupt-junction varactor, all higher-order terms which cause reactive and power conversion perturbations also vanish. This result predicts that an abrupt-junction varactor used in a high-impedance circuit will give low phase distortion under high signal conditions, and that this is a good method of building large signal amplifiers and phase-distortionless limiters. This has been supported experimentally by measurements of phase distortion in parametric limiters using abrupt and graded-junction varactors at 30 Mc.[1]

In situations where higher-order terms in the expansions are to be used for power conversion, such as in parametric amplifiers using LF pumping, in third and higher harmonic generators, and in one-third and lower subharmonic generators, the series-resonant configuration should not be used with an abrupt-junction varactor.

A plot of the rate at which the first three nonlinear terms in the voltage expansion change with the junction exponent is shown in Fig. 2. It can be seen that the S_b term goes through 0 at $n = \frac{1}{2}$ with a rather steep slope so that to achieve good cancellation of this term careful selection of the varactor will be necessary, and biasing of the device should

[1] Private communication with W. T. Jones of Sylvania Waltham Labs., Waltham, Mass.

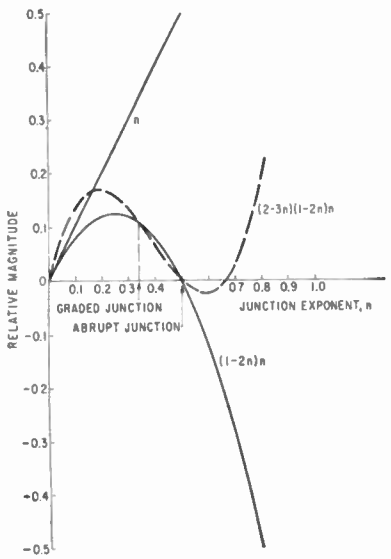

Fig. 2—Relative magnitude of terms in the voltage expansion.

be done so that (1) is valid over the expected range of voltage variation with constant n. It is also clear that $n=\frac{2}{3}$ is a good exponent value to use in systems depending upon the third term in the expansion for power conversion since this will eliminate all higher-order perturbations. However, the reactance perturbation corresponding to (7) will still be present in this case.

Further developments in semiconductor technology may make it possible to control the individual nonlinear terms in the charge and voltage expansions and therefore to make possible tailor-made nonlinear elements for given applications. Until then, however, we must be content to use the available nonlinear characteristics as judiciously as we can.

A. L. Helgesson
Applied Research Lab.
Sylvania Electronic Systems
Waltham, Mass.

Improved Tungsten Evaporation Filament for Gold-Silver Alloy*

In the fabrication of Mesa transistors, base stripes are formed by evaporating a gold-silver alloy in a vacuum of less than 5×10^{-5} mm of Hg. The stripe thickness, 2000 Å, is very critical and plays a major role in the electrical characteristics of the finished units. In order to control such thickness to a high degree of accuracy, it is essential that the required amount of alloy be evaporated *completely*.

The evaporation takes place at the bottom of a tungsten conical basket filament, whose temperature is electrically controlled. A phenomenon, frequently arising in this process, is that the molten alloy does not adhere to the tungsten filament and drops off, thus making the complete evaporation impossible.

A solution to this wetting problem has been found by precoating the W filament with platinum. One inch of platinum wire, 0.020 inch in diameter, was coiled around the bottom of the conical basket and melted thereon. The resulting coating proved ideal as a medium to which the molten alloy adheres perfectly.

In order to ascertain that no significant amount of platinum was being evaporated in the process, a coated tungsten filament was weighed before and after 10 evaporation runs. Its weight change was compared with that of an uncoated control filament used for an equal number of runs. No appreciable difference in weight change was found between the two filaments.

To determine that no deleterious but undetected amount of platinum was being deposited on the stripes and affecting the electrical properties, 1000 devices processed with the new technique and 1000 control devices were compared. No significant difference was found between the two groups.

Platinum-coated tungsten filaments, which last as long as the uncoated filaments, have completely eliminated the lack of adhesion problem, thus offering considerable savings in time, labor and expensive materials.

These results extend the findings of L. Holland,[1] who remarks that Ag can be kept in W basket by binding fine platinum wire on the outside.

The author is grateful to Dr. R. J. Gnaedinger, Jr. for valuable comments.

Frank G. Pany
Semiconductor Products Div.
Motorola, Inc.
Phoenix, Ariz.

* Received by the IRE, August 1, 1961.

[1] L. Holland, "Vacuum Deposition of Thin Films," Chapman and Hall, Ltd., London, Eng., p. 112; 1958.

Some Operating Characteristics of Flash-Pumped Ruby Lasers*

In the course of a series of experiments with ruby optical masers, several observations have been made which may be useful in the planning and interpretation of future experiments.

Five lasers of various characteristics were used. All of them were made according to conventional designs.[1] Evaporated silver coatings were applied so that one end had an estimated transmission of about 1 per cent and the other end was opaque. Pumping was performed by a GE Type 524 helical quartz, Xenon-filled photoflash lamp. All experiments were done at room temperature. The pumping energy was supplied by an appropriate electronic circuit and a condenser bank capable of reaching the maximum ratings of the flash lamp (4000 volts and 4000 joules).

It was found that the pumping energy required to start laser oscillation depends upon the dimensions of the laser and upon the condition of its surfaces. Table I gives some threshold voltage values interpolated from the measurements. Fig. 1 shows curves of measured threshold voltages V for the various lasers. Two curves each for lasers Nos. 1, 4, and 5 show the effect of resilvering.

The thresholds could be determined easily and repeatably to within ±5 volts. Placement of the ruby within the flash tube could be varied by $\frac{1}{4}$ in without changing the threshold voltage more than 50 volts.

One unexpected result was that the pumping energy alone did not characterize adequately the laser threshold, contrary to the assumption used in previous publications.[1,2] Fig. 1 shows that the threshold pumping energy W and charge Q vary in a linear manner with variations of the supply capacitance C, for a given laser and flash tube. It appears that the highest efficiency is obtained with high voltages and an appropriately small condenser.

To explore the nature of the "capacitance effect" and to explain the straight lines plotted in Fig. 1, preliminary measurements of the light emitted by the flash tube and by a laser were made. For each measurement, a Type 931A photomultiplier was used, driving an oscilloscope through a coaxial cable properly terminated so as to preserve the HF structure of the light pulses.

To sample the flash-tube light, a diffuser of ground sapphire rod was mounted at the center of the flash-tube helix. The light was filtered through blue-green copper chelate solution, which transmits from about 4200 to 6200 Å, in an attempt to eliminate light at wavelengths not directly useful for pumping, and was attenuated by several layers of paper. The laser beam was also attenuated with paper. Both attenuators were adjusted until the largest signals obtained were within the almost-linear range of the photomultipliers.

The pumping light pulses were found to have a smooth exponential rise lasting about 0.2 msec, one or two sharp peaks, and a smooth exponential fall which was 90 per cent completed in 1.7 msec for 558 mfd and 0.8 msec for 258 mfd. The laser beam began after a delay depending upon the voltage applied. The envelope of its oscillogram was about the same shape, and ceased at about the same time, as the pumping light pulse. The envelope has a superimposed band of "noise" pulses presumably arising from statistical fluctuations of the gain of the laser oscillator, resembling those reported elsewhere. The frequencies present exceeded 100 kc and appeared to increase with the voltage.

Table II shows that the pumping light pulse has a duration t nearly proportional to the capacitance C used, and an amplitude h governed chiefly by the applied voltage V.

* Received by the IRE, June 26, 1961; revised manuscript received, July 31, 1961.

[1] R. J. Collins, *et al.*, "Coherence narrowing directionality and relaxation oscillation in the light emission from ruby," *Phys. Rev. Lett.*, vol. 5, no. 7, pp. 303–305; October, 1960.

[2] M. Ciftan, *et al.*, "A ruby laser with an elliptic configuration," Proc. IRE, pt. 1, vol. 49, pp. 960–961; May, 1961.

TABLE I
CHARACTERISTICS OF SEVERAL RUBY LASERS

No.	Diam. (in)	Length (in)	C-Axis orientation	Threshold with 300 mfd		
				Potential (volts)	Charge (coulombs)	Energy (joules)
1	0.500	1.37	0°	3500	1.05	1840
2	0.250	1.50	0°	3000	0.90	1350
3	0.250	1.50	0°	2900	0.87	1260
4	0.100	0.75	0°	2610	0.78	1020
5	0.100	0.75	90°	2550	0.76	970

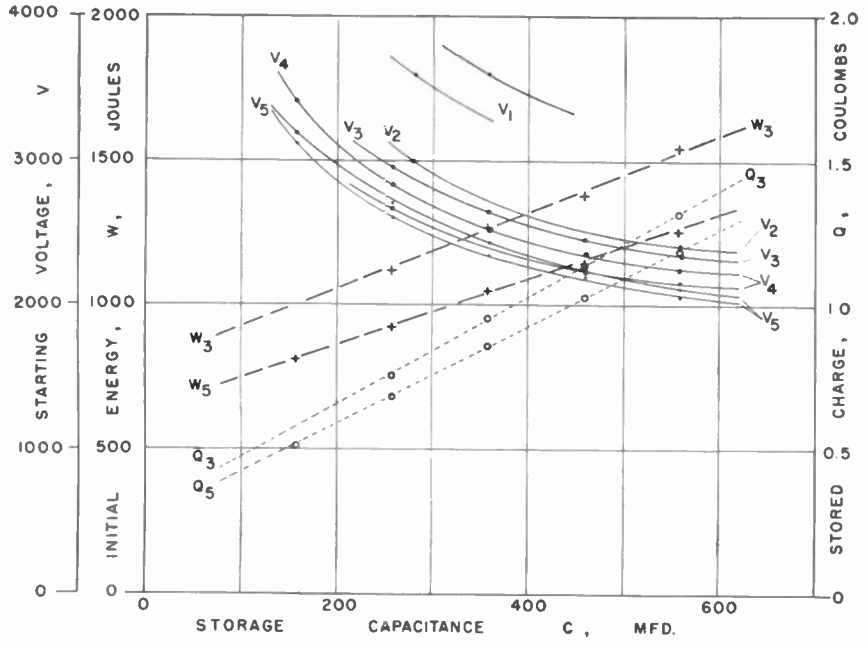

Fig. 1— Threshold conditions for five different lasers. (Two different silverings used on some.)

TABLE II
LIGHT PULSE CHARACTERISTICS

Capacitance mfd	Xenon Lamp, (Blue-Green)				No. 5 Laser (Red)		
	Initial voltage	Peak amplitude volts	Peak time, msec	Duration msec	Peak amplitude volts	Start time, msec	Duration msec
558	4000	0.15	0.2 0.3	3.5	0.16	0.1	1.7
	3500	—	—	—	—	—	—
	3000	0.07	0.2 0.4	3.5	0.04	0.3	1.0
	2500	—	—	—	0.0075	0.6	0.7
	2000	0.015	0.2 0.6	3.5	0.000	—	—
258	4000	0.14	0.2 0.25	1.5	0.10	0.1	0.7
	3500	—	—	—	0.06	0.25	0.65
	3000	0.07	0.2 0.3	1.5	0.01	0.4	0.4
	2500	—	—	—	—	—	—
	2000	0.017	0.2	2.0	0.000	—	—

approximately as $h = KI^n$. This fact, together with the capacitance effect, gives the formula $h = (AI/t + B)^n$, implying that the minimum light intensity required to start laser action is an inverse function of the time over which it is applied, plus a constant.

A simple test with selected polaroids which were effective in the red part of the spectrum showed that the stimulated optical emission from laser No. 5 was plane polarized. The electric vector of the emerging laser beam was at right angles to the optic axis of the crystal, in agreement with a result recently reported by others.[3] Wide variations of pumping energy did not change the effect. The much weaker fluorescent output, however, did not seem to be plane polarized. As expected, no trace of plane polarization could be found in the beams from laser No. 3 and laser No. 4, which are optically symmetrical about their cylindrical axes. Attempts to find circularly polarized light failed also.

The author wishes to thank the following for their valuable suggestions, help, and encouragement during this work: Dr. R. J. Collins, Dr. G. Pish, G. Damewood, and W. Bradshaw.

JOHN C. COOK
Southwest Research Institute
San Antonio, Tex.

[3] I. D. Abella and H. Z. Cummins, "Thermal tuning of ruby optical maser," *J. Appl. Phys.*, vol. 32, pp. 1177–1178; June, 1961.

Repetitive Hair-Trigger Mode of Optical Maser Operation*

The ruby optical maser has a characteristic relaxation time between the E excited state and the ground state of the order of several milliseconds,[1] by means of spontaneous emission. This emission time is of course greatly reduced when the population inversion is sufficient to give rise to stimulated emission, *i.e.*, optical maser action.[2,3] For three-level devices such as ruby a very sizeable portion of the pumping energy is required just to transport half of the ground state population to the excited state and so bring the optical maser to the point of oscillation. The additional amount to provide stimulated emission is relatively small.

One may then conjecture that it would be useful to provide enough excitation to bring an optical maser to the almost oscillating condition, and, since there is then no stimulated emission and the relaxation time is relatively long, one can provide a relatively small amount of energy at a later time (provided this time is small compared to the relaxation time) and thus accurately control the time of the output with little or no jitter and achieve a kind of *hair-trigger* type of operation.

In the past control of the pumping pulse has been inadequate to obtain even repeatable performance let alone this hair-trigger operation. We have demonstrated an alternative method of obtaining a short pulse of coherent light. The idea was to use the indication of optical maser output as a kind of preparation state and then, by the application of a much less energetic sharp pulse some time later (short compared to the relaxation time), to stimulate a short emission. Since the optical maser crystal is just a shade below the threshold of oscillation, this relatively low-energy excitation pulse was found sufficient to bring about an immediate emission pulse.

A crude experiment was performed in which a ruby, encircled by a small spiral flash tube, is in turn placed within a second larger spiral flash tube so that the ruby and flash tubes are all coaxial. (See Fig. 1.) A pulse of light, fairly rectangular in shape, is caused to be emitted from the outer flash tube. This pulse has just sufficient duration for the ruby to begin emitting in optical maser action. Then the pulse is switched off, and the optical maser action ceases. Approximately 100 μsec later a very short fairly low-energy pulse is applied to the inner flash tube, and the ruby is seen to emit 1 or 2 μsec later. The emitted optical maser pulse is found to be much more vigorous than the pulse normally emitted, such as in the preparation state.

Fig. 2 shows the trace of such an experiment. Because of the unfavorable geometry of the outer flash tube, the *preparation-state*

* Received by the IRE, July 14, 1961; revised manuscript received, July 26, 1961.

[1] S. Sugano and Y. Tanabe, "Absorption spectra of Cr^{3+} in Al_2O_3," *J. Phys. Soc. (Japan)*, vol. 13, pp. 880–899; August, 1958.

[2] T. H. Maiman, "Optical maser action in Ruby," *Brit. Commun. and Electronics*, vol. 7, pp. 674–675; September, 1960. Also *Nature*, vol. 187, pp. 493–494; August, 1960.

[3] R. J. Collins, *et al.*, "Coherence, narrowing directionality and relaxation oscillations in the light emission from Ruby," *Phys. Rev. Lett.*, vol. 5, pp. 303–305; October, 1960.

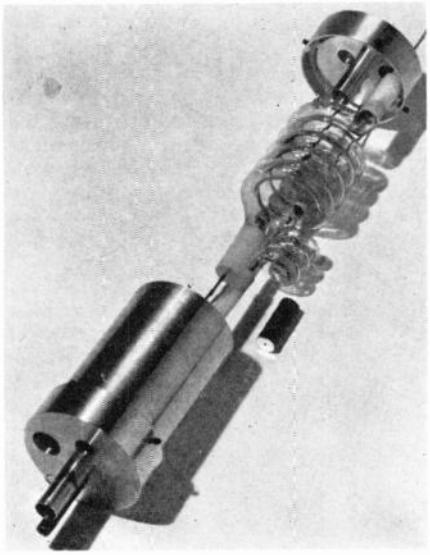

Fig. 1—Exploded view of coaxial flash tube and ruby used in hair-trigger LASER experiment.

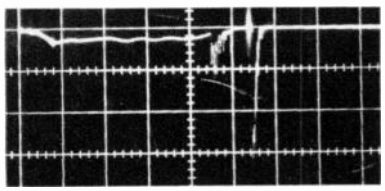

Fig. 2—Trace of LASER emission during hair-trigger experiment. Scale is 100 μsec per major division.

pulse was of 400 μsec duration and required approximately 1200 watt-seconds before emission occurred. The pulse from the inner flash tube was only 60 watt-seconds and yielded, as seen, an optical maser emission in the hair-trigger mode several times as large as obtained in the preparation state.

For applications such as the COLIDAR (*CO*herent *LI*ght *D*etecting *A*nd *R*anging) pulsed ranging system,[4] it would be highly desirable to have periodic, controllable low-jitter pulses.

We propose to accomplish this by use of the radiation of optical maser output as a preparation for what we shall call the *repetitive hair-trigger mode* of operation. That is, the optical maser would be excited to where it emits. The excitation would then be turned off, and short bursts of excitation applied with a periodicity short compared to the relaxation time. This would cause a periodic optical maser output in predictable fashion.

We make the simplified assumption that after the preparation phase the population dips slightly below the threshold and then decays exponentially. The energy required to excite a pulse in the repetitive hair-trigger mode is then the amount required to bring the system back up to threshold.

Let E_p = threshold energy for preparation phase, r = pulse repetition rate, E = threshold energy per pulse in the repetitive hair-trigger mode, p = the required power for the repetitive hair-trigger mode, ΔE_p = the immediate energy drop below threshold following an emission, and τ = characteristic decay time. Then roughly,

$$E \cong E_p(1 - \exp(-)1/r\tau) + \Delta E_p. \quad (1)$$

For $r \gg 1/\tau$ we obtain

$$E \cong E_p(1/r\tau) + \Delta E_p \quad (2)$$

and

$$p = rE \cong E_p/\tau + \Delta E_p. \quad (3)$$

Although precise values of the parameters in the above equations await experimental determination, it is evident that the much higher relative efficiency of this mode should make it possible to increase not only the duty cycle, but the peak output as well. It is obvious that the jitter between optical maser output and pump input should be greatly reduced.

M. L. Stitch
E. J. Woodbury
J. H. Morse
Hughes Aircraft Co.
Culver City, Calif.

[4] M. L. Stitch, E. J. Woodbury, and J. H. Morse, "Optical ranging system uses laser transmitter," *Electronics*, vol. 34, pp. 51–53; April 21, 1961.
M. L. Stitch, F. J. Meyers, J. H. Morse, and E. J. Woodbury, "Breadboard COLIDAR (coherent light detecting and ranging) system (uncl.)," *Proc. 5th Natl. Convention on Military Electronics*, pp. 279–284; June, 1961.
D. A. Buddenhagen, B. A. Lengyel, F. J. McClung, Jr., and G. F. Smith, "An experimental laser radar," 1961 IRE International Convention Record, pt. 5, pp. 285–290.

WWV and WWVH Standard Frequency and Time Transmissions*

The frequencies of the National Bureau of Standards radio stations WWV and WWVH are kept in agreement with respect to each other and have been maintained as constant as possible with respect to an improved United States Frequency Standard (USFS) since December 1, 1957.

The nominal broadcast frequencies should for the purpose of highly accurate scientific measurements, or of establishing high uniformity among frequencies, or for removing unavoidable variations in the broadcast frequencies, be corrected to the value of the USFS, as indicated in the table below. The corrections reported have been arrived at by means of improved measurement methods based on LF and VLF transmissions.

The characteristics of the USFS and its relation to time scales such as ET and UT2 have been described in a previous issue,[1] to which the reader is referred for a complete discussion.

The WWV and WWVH time signals are also kept in agreement with each other. Also they are locked to the nominal frequency of the transmissions and consequently may depart continuously from UT2. Corrections are determined and published by the U. S. Naval Observatory. The broadcast signals are maintained in close agreement with UT2 by properly offsetting the broadcast frequency from the USFS at the beginning of each year when necessary. This new system was commenced on January 1, 1960. A retardation time adjustment of 20 msec was made on December 16, 1959; another retardation adjustment of 5 msec was made at 0 UT on January 1, 1961.

WWV Frequency
With Respect to U. S. Frequency Standard

1961 July	Parts in 10^{10}†
1	−149.0
2	−149.2
3	−149.1
4	−149.0
5	−148.9
6	−149.5
7	−149.6
8	−149.8
9	−150.0
10	−149.9
11‡	−149.8
12	−150.7
13	−150.4
14	−150.1
15	−149.8
16	−149.4
17	−149.5
18	−149.5
19	−149.7
20	−149.9
21	−150.0
22	−150.2
23	−150.4
24	−150.5
25	−150.9
26	−151.1
27	−151.2
28	−151.2
29	−151.3
30	−151.1
31	−150.9

† A minus sign indicates that the broadcast frequency was low. The uncertainty associated with these values is $\pm 5 \times 10^{-11}$.
‡ WWV adjusted -1×10^{-10} on July 11.

National Bureau of Standards
Boulder, Colo.

* Received by the IRE, August 24, 1961.
[1] Refer to "National standards of time and frequency in the United States," Proc. IRE (Correspondence), vol. 48, pp. 105–106; January, 1960.

Correction to "Stable Low-Noise Tunnel-Diode Frequency Converter"*

In the second paragraph of the above,[1] the statement is made that any noise sources in the nonlinear resistance are completely mismatched in the case $g_c = g_0$, and $g_0/g_c \to 0$. This statement must be qualified: the noise sources will be completely mismatched (and the noise figure approach unity) only if in addition $Y_0/Y_1 \to 1$, where Y_0 and $2Y_1$ are, respectively, the average and the fundamental coefficients of the Fourier expansion of the equivalent modulated mean-square noise current in the nonlinear resistor.[2]

F. Sterzer
A. Presser
Electron Tube Div.
RCA
Princeton, N. J.

* Received by the IRE, August 1, 1961.
[1] F. Sterzer and A. Presser, Proc. IRE (Correspondence), vol. 49, p. 1318; August, 1961.
[2] See, for example, M. J. O. Strutt, "Noise-figure reduction in mixer stages," Proc. IRE, vol. 34, pp. 942–950; December, 1956.

Lossy Coupling in Parametric Amplifier*

Heffner and Wade's method of analysis,[1] originally applied to a two-resonant circuit parametric amplifier with lossless coupling branch, may be extended successfully in the case of an amplifier with lossy coupling branch. Adopting their assumptions that 1) the network is linear, 2) voltages of frequencies other than resonant frequency may be neglected in respect to the resonant-frequency voltage across each circuit, and 3) the diode-cartridge capacitance may be included in parallel into both the resonant circuits (since it influences only resonant frequencies of the circuits), one comes to the equivalent circuit of the amplifier shown in Fig. 1. For simplicity, the pump and bias circuits are not indicated in the figure and the load resistance has been included in the loss-resistance of the first (amplifying action) or second (mixing action) resonant circuit. Furthermore, the cosinusoidal form of all the time-varying quantities is assumed in the following according to the general relation

$$a = a(\omega_a t) = \overline{A}\cos(\omega_a t + \phi_a) = \tfrac{1}{2}(Ae^{j\omega_a t} + A^* e^{-j\omega_a t}). \quad (1)$$

Thus, for the case $\omega_3 = \omega_1 + \omega_2$, one may calculate the current i_c in the coupling lossy branch according to

$$r_s i_c + \frac{1}{C_0 + c(\omega_3 t)}\int i_c dt = u_1(\omega_1 t) - u_2(\omega_2 t). \quad (2)$$

As the equation is linear, it may be split into two separate equations with exciting functions $u_1(\omega_1 t)$ and $-u_2(\omega_2 t)$, respectively, leading to two solutions i_{c1} and i_{c2}, each of which has components at angular frequencies ω_1 and ω_2. Using the perturbational method for solving (2) and taking advantage of earlier assumed linearity of the network which in the case of parametric diode means $C_0 \gg \overline{C}$, one may confine himself to consider only the first two approximation terms in the series solution.[2] Then, according to the general notation of (1), the complex amplitudes of the current i_c can be found as

$$I_{c1}' = \frac{U_1}{Z_c(\omega_1)};\quad I_{c1}'' = \frac{CU_1^*}{2j\omega_1 C_0^2 Z_c^*(\omega_1) Z_c(\omega_2)}$$
$$I_{c2}'' = \frac{-U_2}{Z_c(\omega_2)};\quad I_{c2}' = \frac{-CU_2^*}{2j\omega_2 C_0^2 Z_c(\omega_1) Z_c^*(\omega_2)}, \quad (3)$$

where primes and double primes denote that complex amplitudes correspond to angular frequencies ω_1 and ω_2, respectively, and

$$Z_c(\omega) = r_s(\omega) + \frac{1}{j\omega C_0} \quad (4)$$

is the time-average impedance of the coupling branch of Fig. 1 at the given angular frequency ω.

* Received by the IRE, May 29, 1961; revised manuscript received, June 5, 1961.

[1] G. Wade and H. Heffner, "Gain, bandwidth and noise characteristics of a variable parameter amplifier," *J. Appl. Phys.*, vol. 29, pp. 1321–1331; September, 1958.

[2] K. Grabowski, Thesis, Dept. of Telecommunication, Gdansk Inst. Tech., Poland; 1960 (in Polish). Also, "An application of the perturbational method to the analysis of a parametric amplifier and mixer," *Bull. Acad. Polon. Sci.*, Sér. sci. techn., vol. 7, pp. 515–524; September, 1960 (in English).

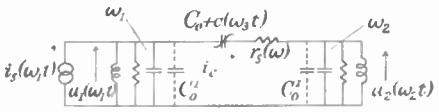

Fig. 1.

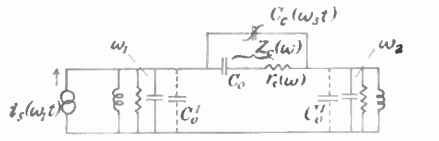

Fig. 2.

It is possible to show[2] that (3) leads to the equivalent circuit of the parametric amplifier shown in Fig. 2, where the amplitude of the equivalent variable capacitance $\overline{C}_c$ is related to the amplitude of the actual variable capacitance $\overline{C}$ according to the relation

$$\overline{C}_c = \overline{C}\{[1+\tan^2\delta(\omega_1)][1+\tan^2\delta(\omega_2)]\}^{-1/2}, \quad (5)$$

where

$$\tan\delta(\omega) = \omega C_0 r_s(\omega). \quad (6)$$

Now, the constant in time branch $Z_c(\omega)$ [from (4)] may be inserted in parallel in both the circuits, and finally, there remains a circuit which is identical to that of Heffner and Wade. Therefore, one may use all their formulas, replacing in them actual capacitance-amplitude $\overline{C}$ by $\overline{C}_c$ and adding to the admittances of both circuits the admittance $1/Z_c(\omega)$.

As a simple illustration of this procedure, let us examine the condition for the setting up of oscillations in the amplifier. For the lossless coupling, the condition[1] was

$$\overline{C}^2 \geq \frac{4G_1(\omega_1)G_2(\omega_2)}{\omega_1\omega_2}. \quad (7)$$

Now, for coupling with losses, by (5) and (7), there results

$$\overline{C}^2 \geq \frac{4G_{1c}(\omega_1)G_{2c}(\omega_2)}{\omega_1\omega_2}[1+\tan^2\delta(\omega_1)]\cdot[1+\tan^2\delta(\omega_2)], \quad (8)$$

where the subscript c at resonant conductances indicates that they include losses of the coupling branch.

In the case of ideal circuits, *i.e.*, those in which the only losses in the network are those of the series resistance of the diode, the condition (8) becomes

$$C^2 \geq 4C_0^2 \tan\delta(\omega_1)\tan\delta(\omega_2). \quad (9)$$

Introducing the capacitance modulation factor $m_c = \overline{C}/C_0$, the last formula may be rewritten in a more pronounced manner as

$$[\tan(\omega_1)\tan(\omega_2)]^{1/2} \leq \frac{m_c}{2}. \quad (10)$$

In the microwave range, the parameter $r_s(\omega)$ usually does not depend on frequency; therefore, the condition for the setting up of oscillations in the amplifier finally becomes

$$r_s C_0 \omega_{av} \leq \frac{m_c}{2}, \quad (11)$$

where ω_{av} is the geometric mean value of resonant angular frequencies of the amplifier.

Since, here, both resonant circuits have been eliminated by assuming them lossless, (10) or (11) might be useful as a definition of cutoff frequencies of a given parametric diode with an available capacitance-modulation factor m_c, average bias capacitance C_0 and series resistance r_s.

Krzysztof Grabowski
Telecommunication Dept.
Gdansk Inst. Tech.
Gdansk, Poland

Discussion of Calculation of False Alarm Rate*

In their interesting article, Thaler and Meltzer[1] give an expression for false alarm rate, which is

$$F = M\frac{Q(T)}{Q(0)}, \quad (1)$$

where F is the false alarm rate, M is the expected number of positive crossings of the the mean, $Q(T)$ is the probability density of the noise amplitude at threshold setting T (where T is in units of standard deviations measured from the mean), and $Q(0)$ is the probability density of the noise amplitude at the mean. They state that this expression holds whenever the threshold is set sufficiently far above the mean level of the noise.

Expression (1) does not actually hold in general. A more correct expression is

$$F = M\frac{\int_T^\infty Q(x)dx}{\int_0^\infty Q(x)dx}, \quad (2)$$

where $Q(x)$ is the probability density of the noise amplitude, and x is the amplitude in units of standard deviations measured from the mean.

In one of the cases analyzed in the paper, that of the square-law detector, (1) and (2) do agree. The agreement occurs in this case, however, only because the post-detector probability density function happens to be a simple negative exponential, the chi-squared function with two degrees of freedom.

W. M. Rogers, Jr.
Radiation Inc.
Melbourne, Fla.

* Received by the IRE, February 28, 1961.

[1] S. Thaler and S. Meltzer, "The amplitude distribution and false alarm rate of noise after post-detection filtering," PROC. IRE, vol. 49, pp. 479–485; February, 1961.

Author's Comment[2]

The expression for false alarm rate given in our paper is an experimental result of the simulation study described. In each instance studied, the false alarm rate (defined as the number of threshold crossings per second) after post-detection filtering was found to be proportional to the amplitude

[2] Received by the IRE, March 20, 1961.

probability density, rather than to the integral of the density as suggested by Rogers. The former conclusion is the one expected since it agrees with a theoretical result (applicable to noise with a Gaussian amplitude distribution) given by Rice.[3] The integral of the probability density equals the product of the average duration of each threshold crossing and the frequency of such crossings. Since both change in the same way with threshold level, the integral changes faster than the frequency of the crossings.

When the threshold is too close to the mean level of the noise, some of the threshold crossings become so close together that it may not be appropriate to count each crossing as a separate false alarm. This effect was negligible at useful false alarm rates. The elimination of some threshold crossings at very high false alarm rates would have caused the false alarm rate to change more slowly with threshold than the frequency of threshold crossings.

S. THALER
RCA
Van Nuys, Calif.
S. MELTZER
Hughes Aircraft Co.
Culver City, Calif.

[3] S. O. Rice, "Mathematical analysis of random noise," *Bell Sys. Tech. J.*, vol. 23, pp. 282–332, July, 1944; vol. 24, pp. 46–156, January, 1945.

Microwave Radiation Hazards*

Mumford's paper[1] offers a much needed summary of the biological hazards of RF radiation, plus data on prediction, measurement and instrumentation. Going one step further, we have also observed that in addition to the biological hazards of direct exposure to microwave radiation, there can be hazardous secondary effects to technicians working in field intensities that might be considered acceptable from a biological standpoint.

Objects made of conducting materials that are located in field intensities of only one or two milliwatts per square centimeter can easily serve to couple sufficient RF energy to be hazardous. For example, observations have been made where a man carrying a wrench in each hand formed a dipole, coupling sufficient energy to produce a warming sensation in the body. It was also observed that an electrical shock can be produced when two wrenches or two rods are brought together, and then separated drawing a small arc. In the particular incident, the radiation sources was a pulse radar which produced a fairly substantial peak power. The voltage causing the shock was undoubtedly the envelope of the RF resulting from arc rectification. The electrical shock received from field intensities of only one or two milliwatts per square centimeter was sufficient to discourage venturing into a higher field intensity to repeat the experiment.

While it appears improbable that an electrical shock hazard exists from the standpoint of an electrocution, this condition should be given recognition. Obviously a man working in such a precarious position as on a steel tower might have sufficient reaction to such a shock as to cause him to fall. On the basis of these experiences it would appear advisable to show due respect for field intensities even as low as one-tenth milliwatt per square centimeter.

THOMAS G. CUSTIN
Missile Detection Sys. Sect.
General Electric Co.
Syracuse, N. Y.

* Received by the IRE, March 2, 1961.

[1] W. W. Mumford, "Some technical aspects of microwave radiation hazards," PROC. IRE, vol. 49, pp. 427–447; February, 1961.

Power Limiting in the 4-kMc to 7-kMc Frequency Range Using Lithium Ferrite*

Extensive investigations into the use of yttrium iron garnet (YIG) for microwave power limiters have been reported in the literature.[1–4] The threshold for limiting occurs at particularly low power levels if the microwave frequency and biasing dc magnetic field are chosen for *coincidence* of the uniform precession and subsidiary ferromagnetic resonances. The coincidence region of a sphere is the frequency octave defined by $4\pi M/3 \leq \omega/\gamma \leq 8\pi M/3$, where M is the saturation magnetization and γ is the gyromagnetic ratio. For a YIG sphere with $4\pi M = 1750$ gauss, the coincidence region extends from 1600 Mc to 3200 Mc. Nonmagnetic ions such as Ga and Al can be substituted into YIG to lower the magnetization[5] and to shift the coincidence region to lower frequencies. *Coincidence* limiters have been made to operate in the 1000-Mc region with Ga-YIG.

The purpose of this note is to report experimental evidence indicating the practicability of extending the useful range of coincidence limiters to about 7000 Mc. The coincidence octave for a sphere of lithium ferrite[6] which has a $4\pi M$ of 3900 Gauss at room temperature, extends from 3640 Mc to 7280 Mc covering a frequency range of particular importance in microwave communications. The limiter structure consists of two rectangular cross-section, half-wavelength strip transmission-line cavities, and its operation is essentially the same as those previously employed.[3] It will suffice here to present the limiter characteristics.

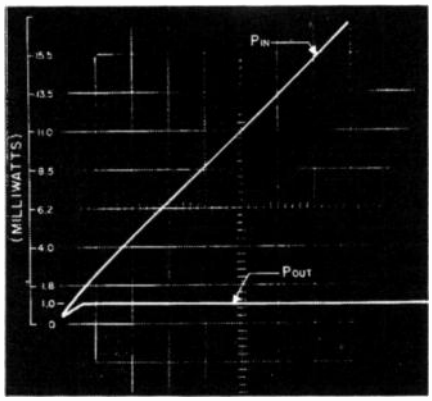

Fig. 1—Characteristic of the lithium ferrite limiter at 5200 Mc. The upper curve shows the input power and the lower curve shows the limited output power. At 1 w of input power the output remained less than 1.5 mw.

Limiting was observed at 5200 Mc at an output power level of 1 mw with an essentially flat characteristic which rose only to 1.5 mw at about 1 w of input power. Fig. 1 is a picture of an oscilloscope presentation of the output power vs input power showing the sharp break at the limiting threshold. The limiting power level can be raised to other predetermined values by simple modifications of the microwave structure. The single crystal sphere used in this limiter had $\Delta H = 8$ oersteds and $\Delta H_k = 3.6$ oersteds for spin waves of 5000 Mc measured along the [111] (easy) axis[7] of magnetization.

In view of the present extensive use of the 4000-Mc to 7000-Mc frequency range, the results presented here indicate that the *coincidence* limiter using lithium ferrite may find important applications in microwave systems.

F. C. ROSSOL
Bell Telephone Labs., Inc.
Murray Hill, N. J.

* Received by the IRE, August 1, 1961.

[1] R. W. DeGrasse, "Low-loss gyromagnetic coupling through single crystal garnets," *J. Appl. Phys.*, vol. 30, pp. 155–156S; April, 1959.

[2] C. N. Patel, "Investigations of Magnetically Tunable Narrow Bandpass Nonreciprocal Filters Using Ferrimagnetic Resonators," Stanford Electronics Labs., Stanford, Calif., Tech. Rept. no. 411-1; April, 1961.

[3] F. J. Sansalone and E. G. Spencer, "Low-temperature microwave power limiter," IRE TRANS. ON MICROWAVE THEORY AND TECHNIQUES, vol. MTT-9, pp. 272–273; May, 1961.

[4] P. S. Carter, "Magnetically tunable microwave filters using single-crystal yttrium iron garnet resonators," IRE TRANS. ON MICROWAVE THEORY AND TECHNIQUES, vol. MTT-9, pp. 252–260; May, 1961.

[5] E. G. Spencer and R. C. LeCraw, "Linewidth narrowing in gallium substituted yttrium iron garnet," *Bull. Am. Phys. Soc.*, pt. 1, ser. 2, vol. 5, p. 58; January 1960.

[6] The lithium ferrite samples used in this work were grown by J. W. Nielsen at Bell Telephone Labs., and with considerable improvement later at Airtron, Inc.

[7] R. T. Denton and E. G. Spencer, "Ferromagnetic resonance losses in lithium ferrite as a function of temperature," *J. Appl. Phys.* (to be published). See also the earlier paper by: A. D. Schnitzler, V. J. Folen, and G. T. Rado, "Ionic ordering effects in the ferromagnetic resonance of lithium ferrite monocrystals," *J. Appl. Phys.*, vol. 31, pp. 348–349S; May, 1960.

Phase Inverters Utilizing Controlled Superconductors*

In a recent article[1] it was pointed out that controlled superconductors may be employed in several classes of linear amplifiers. One amplifier configuration discussed

* Received by the IRE, May 26, 1961.

[1] P. M. Chirlian and V. A. Marsocci, "The Controlled superconductor as a linear amplifier," IRE TRANS. ON COMPONENT PARTS, vol. CP-8, pp. 84–88; June, 1961.

was a push-pull circuit such as the one shown in Fig. 1. Such push-pull circuits may be operated class B to improve their operating efficiency. It is the purpose of this note to show that the phase-inverting driver transformer is not necessary since the phase inversion may be implemented directly by the use of controlled superconductors. Therefore, the space-saving aspects of the thin-film geometry can be maintained. Two examples of phase-inverting circuitry are shown in Fig. 2(a) and (b). It is of particular interest to note that in the circuit of Fig. 2(a) the phase inversion is obtained by the interesting property of the controlled superconductor which is that the phase of the output signal may be shifted 180° by reversing the polarity of one of the bias batteries.

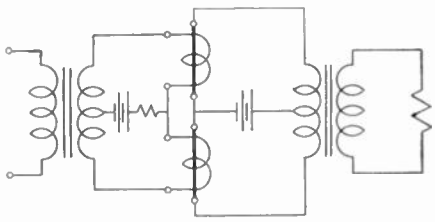

Fig. 1—A controlled-superconductor push-pull amplifier. Note that the symbolism used here applies to all types of controlled superconductors and not just to wire cryotrons.

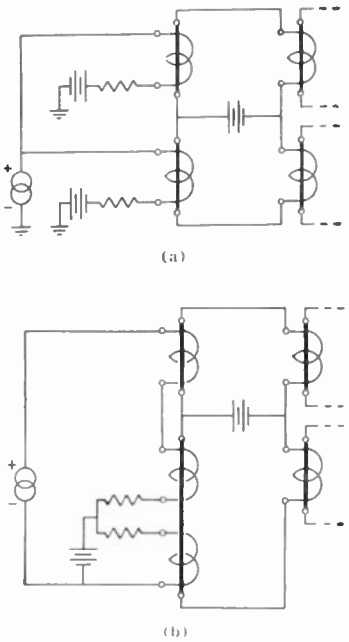

Fig. 2—Phase inverters employing controlled superconductors.

This property is further discussed in the above-mentioned article. The second phase-inverter circuit only requires one input-bias battery; however, it has the disadvantage that it requires an additional control element.

P. M. Chirlian
V. A. Marsocci
Dept. of Elec. Engrg.
Stevens Institute of Technology
Hoboken, N. J.

A Ferrimagnetic Limiter-Isolator*

It has been generally known for some time that a ferrimagnetic power limiter can be built.[1,2] When the RF power level in a ferrimagnetic material exceeds a certain threshold value, and given a particular set of physical circumstances, a subsidiary absorption peak will appear at a value of dc field somewhat below that required for resonance. This nonlinear characteristic[3] of ferrites and garnets can be utilized to build a limiter-isolator.

The threshold power level for the onset of nonlinear absorption is very important in determining the usefulness of a microwave power limiter. In practice this critical level is determined not only by the intrinsic properties of the material and the frequency of operation, but also by the size and shape of the material and the structural configuration in which the material is used. In rectangular waveguide this threshold power level has been studied using a vertical slab of nickel-zinc ferrite in the configuration shown in Fig. 1.

The critical level for nonlinear absorption can be attained at a lower incident power level for a small slab of ferrimagnetic material if it is placed in the region of circular polarization as shown from the data in Fig. 1. Care must be taken to insure that the slab does not appreciably effect the normal microwave fields in the waveguide. This region of circular polarization of the microwave magnetic field is also noted as the region utilized in designing ferrimagnetic isolators. With the material located in this region, the "spin waves" (the mechanism for nonlinear absorption) receive little or no excitation from the forward wave in the waveguide; however, the reverse wave heavily excites the spin waves and hence absorption is found to be nonreciprocal.

Data taken at X band with the material in dielectrically loaded double ridge waveguide are shown in Fig. 2. The material in this case was yttrium-aluminum-iron garnet. The limiting action is noted as the difference between absorption at low power and at 10 kw for the reverse wave. The nonreciprocal action of the structure is seen by comparing the forward wave with the reverse wave data at high power. Similar data are shown in Fig. 3 where yttrium-iron garnet slabs are located near the region of circular polarization in double ridge C-band waveguide. The threshold in this structure is seen to be approximately 100 watts. The small absorption peak in the forward wave at the field for main resonance results from locating the material slightly out of the region of circular polarization. Lower thresholds have been obtained; however, it has been found more difficult to obtain good circular polarization when using these low threshold configurations.

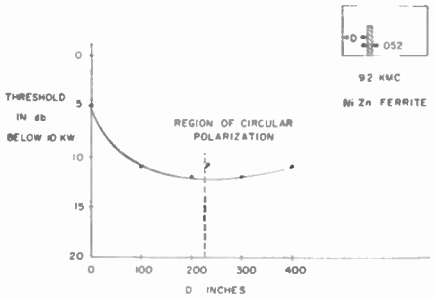

Fig. 1—Threshold power level (db below 10 kw) for a nickel-zinc ferrite as a function of position in rectangular X-band waveguide.

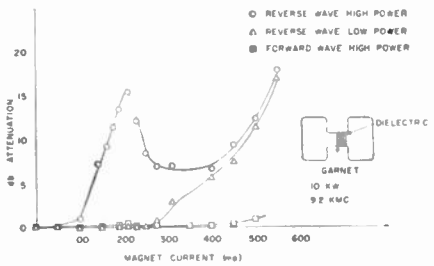

Fig. 2—Subsidiary resonance region showing the high and low power response of an yttrium-aluminum-iron garnet in dielectrically loaded double ridge X-band waveguide.

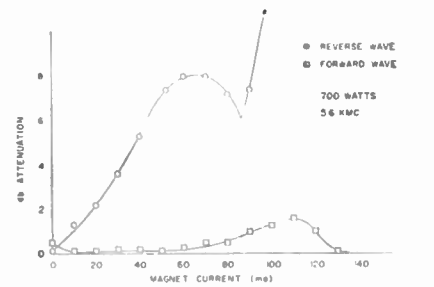

Fig. 3—Subsidiary resonance region using yttrium-iron garnet slabs near the region of circular polarization in double ridge C-band waveguide.

If the ferrimagnetic material is sufficiently long, the attenuation above the threshold will increase with increasing power, resulting in a constant back load on the microwave source. Thus, high power isolators can be constructed utilizing the subsidiary resonance. A device operating in this fashion can also be used as a power limiter, as illustrated in Fig. 2 by the low insertion loss of the low power reverse wave. Possibly the most unique application of the device would be the use of it in the antenna arm of the duplexer of a radar system. It would pass the high power transmitted pulse virtually unattenuated, but would attenuate any high power reflections from the antenna, or high power interfering signals from other sources and would pass any low power received signals virtually unattenuated. It would thus be an isolator, a limiter, and a high power interference suppressor. All of these functions are performed passively and simultaneously.

J. Brown
G. R. Harrison
Applied Physics Section
Sperry Microwave Electronics Co.
Clearwater, Fla.

* Received by the IRE, June 26, 1961.

[1] G. S. Uebele, "Characteristics of ferrite microwave limiters," IRE Trans. on Microwave Theory and Techniques, vol. MTT-7, pp. 18–23; January, 1959.
[2] R. L. Martin, "High-power effects in ferrite slabs at X-band," *J. Appl. Phys.*, vol. 30, pp. 1595–1605; April, 1959.
[3] H. Suhl, "The theory of ferromagnetic resonance at high signal powers," *J. Phys. and Chem. of Solids*, vol. 1, pp. 209–227; April, 1957.

On the Impedance of Long Wire Suspended Over the Ground*

Much has been written over the years on the subject of the impedance of wires lying on the ground or suspended above it.[1] The possibility that a long horizontal wire will be a feasible radiator of VLF radio waves has reopened interest in the problem. It is the purpose of this note to outline a rather simple solution for the impedance of an infinitely long wire located at a height h over a homogeneous flat ground.

Choosing a rectangular coordinate system (x, y, z), the ground is defined by the space $z<0$. The wire is located at $z=h$ and is parallel to the x axis. Now for VLFs (*i.e.*, less than 30 kc), and since the height h is to be much less than the wavelength, it is permissible to neglect displacement currents both in the air and in the ground. For a uniform current I in the wire of radius a, the electric field has only an x component and is given formally by[2,3]

$$E_x = \frac{i\mu\omega}{2\pi} I\left[\log\left\{\frac{x^2+(h+z)^2}{x^2+(h-z)^2}\right\}^{1/2} + 2\int_0^\infty \frac{e^{\lambda(h+z)}}{\lambda+(\lambda^2+\gamma^2)^{1/2}}\cos(\lambda x)d\lambda\right],$$

where $\gamma^2 = i\sigma\mu\omega$ and μ is the magnetic permeability (assumed constant everywhere) and σ is the conductivity of the ground. It follows from the basic definition that the self impedance Z per unit length is given by

$$Z = \lim_{\substack{z\to h\\ x\to a}}\left[\frac{E_x}{I}\right].$$

Therefore

$$Z = \frac{i\mu\omega}{2\pi}\left[\frac{1}{2}\log\left(1+\frac{4h^2}{a^2}\right)+P\right],$$

where

$$P = 2\int_0^\infty \frac{e^{2\lambda h}}{\lambda+(\lambda^2+\gamma^2)^{1/2}}\cos\lambda a\, d\lambda.$$

This can be rewritten as

$$P = P_+ + P_-,$$

where

$$P_\pm = \int_0^\infty \frac{e^{-\lambda(2h\pm ia)}}{\lambda+(\lambda^2+\gamma^2)^{1/2}}d\lambda.$$

Introducing the variable $g=\lambda/\gamma$ and the parameter $\alpha=\gamma(2h\pm ia)$, the above is written as

$$P_\pm = \int_0^{\infty e^{-i\pi/4}} \frac{e^{-\alpha g}}{g+(1+g^2)^{1/2}}dg.$$

The integration contour now extends from the origin along a straight line in the fourth quadrant which makes an angle of 45° with the real axis. Noting that $\alpha \cong |\alpha| e^{-i\pi/4}$ and that the poles of the integral are of the imaginary axis, it is seen that the integration contour can be deformed to the real axis. Then, multiplying numerator and denominator by $(1+g^2)^{1/2}-g$, it readily follows that

$$P_\pm = \int_0^\infty [(1+g^2)^{1/2}-g]e^{-\alpha g}\,dg = T(\alpha) - \frac{1}{\alpha^2},$$

where

$$T(\alpha) = \int_0^\infty (1+g^2)^{1/2}e^{-\alpha g}\,dg.$$

The definite integral $T(\alpha)$ can be expressed in terms of known functions as follows:

$$T(\alpha) = \frac{\pi}{2\alpha}\left[H_1(\alpha) - Y_1(\alpha)\right],$$

where $H_1(\alpha)$ is the Struve's function[4] of order one, and $Y_1(\alpha)$ is the Bessel function of the second type of order one. The final solution is thus,

$$P = T[\gamma(2h+ia)] - \frac{1}{\gamma^2(2h+ia)^2} + T[\gamma(2h-ia)] - \frac{1}{\gamma^2(2h-ia)^2}.$$

For purposes of computation it is necessary to employ the series formula,

$$H_1(\alpha) = \frac{2}{\pi}\left[\frac{\alpha^2}{1^2\cdot 3} - \frac{\alpha^4}{1^2\cdot 3^2\cdot 5} + \frac{\alpha^6}{1^2\cdot 3^2\cdot 5^2\cdot 7} - \cdots\right],$$

and tables for $Y_1(\alpha)$ which are available for complex values of α.[5] For small values of α corresponding to low heights, the following formula may be useful:

$$T(\alpha) - \frac{1}{\alpha^2} = -\frac{\Gamma+\log(\alpha/2)}{2} + \frac{1}{4} + \frac{\alpha}{3} + \text{terms in } \alpha^2, \alpha^3, \text{ etc.}$$

Γ is Euler's constant and is equal to 0.5773.

Of particular interest is the real part of the impedance, or resistance ΔR, per unit length. For the usual case $h \gg \alpha$ and thus

$$\Delta R \cong \frac{\mu\omega}{8}\left[1 - \mathrm{Re}\left(i\frac{16}{3}(\gamma h) + \text{terms in } (\gamma h)^2, (\gamma h)^3, \text{ etc.}\right)\right] \cong \frac{\mu\omega}{8}\left[1 - \frac{8\sqrt{2}}{3}\sqrt{\sigma\mu\omega}\,h + \cdots\right].$$

Or if $\sqrt{\sigma\mu\omega}\cdot h \ll 1$,

$$\Delta R \cong \frac{\mu\omega}{8},$$

which is conveniently written

$\Delta R = \pi^2/10\, f_{kc}$ ohms per km when f_{kc} is the frequency in kc/sec.

JAMES R. WAIT
National Bureau of Standards
Boulder, Colo.

* Received by the IRE, May 22, 1961.

[1] E. D. Sunde, "Earth Conduction Effects in Transmission Systems," D. Van Nostrand Co., Inc., New York, N. Y.; 1949. (A good survey of the early work is given here.)

[2] J. R. Wait, "Fields of a line source of current over a stratified conductor," *Appl. Sci. Res.*, sec. B, vol. 3, pp. 279–292; 1953.

[3] J. R. Carson, "Wave propagation in overhead wires with ground return," *Bell Sys. Tech. J.*, vol. 5, pp. 539–554; October, 1926.

[4] G. N. Watson, "Theory of Bessel functions," Cambridge University Press, Cambridge, Eng. 2nd ed.; 1944. (Struve's function is defined on page 328.)

[5] Natl. Bur. of Standards, "Tables of Bessel Functions $Y_0(z)$ and $Y_1(z)$ for Complex Argument," Columbia University Press, New York, N. Y.; 1950.

Masers, Lasers, and the Ether Drift?*

It is the purpose of this letter to suggest that the ether drift experiment of Cedarholm, Bland, Havens, and Townes[1] (hereafter referred to as CBHT), performed with two opposed ammonia masers, has given a null result because it is not affected by an ether drift, contrary to the expectations of its authors. From a consideration of the error in this experiment a new ether drift test employing an optical laser is proposed.

Two of the authors[2] have apologized for performing the experiment, since it seemed obvious to every right-thinking physicist that the null result was inevitable. On the other hand, the experiment, if true, could have considerable impact, since it has moved the upper limit for an ether drift from the previous value of 1.5 km/sec established by Joos, down to 0.015 km/sec.[3] Since this is less than the motion of a terrestrial laboratory due to the earth's rotation (about 0.3 km/sec in temperate latitudes), it would seem fruitless to look any more for ether drift effects. However, because of the importance of determining just this point, namely, whether or not the velocity of light is constant with respect to the earth's gravitational field, it was felt desirable to examine closely the basis for the null result of the CBHT experiment.

The theory is best given in the authors' words,[1] discussing "the change in frequency of a beam-type maser due to ether drift, assuming the molecules in the beam to have a velocity u with respect to the cavity through which they pass, and the cavity to have a velocity v with respect to the ether. The shift may be simply discussed by assuming that if v is zero, radiation is emitted perpendicularly to the molecular velocity so that there is no Doppler shift. If the cavity and beam are then transported at velocity v through the ether in a direction parallel to u, radiation must be emitted by the molecules slightly forward at an angle $\phi=\pi/2-v/c$ with respect to u. The fractional change in frequency due to the Doppler effect is then $E=u/c\cos\phi$ or uv/c^2 due to motion through the ether, assuming that the proper molecular frequencies are unchanged by such motion." It is further assumed that this Doppler-shifted radiation is received by the cavity walls, and hence becomes the operating frequency of the maser. Since the shift depends on the magnitude and orientation of the ether drift v with respect to u, two masers with beams going in opposite directions should show a change in beat frequency when their orientation is changed with respect to the earth, or a diurnal effect due to the earth's rotation if they are kept in a fixed position.

This theory was first propounded by Moeller[4] in a far from lucid fashion. The flaw in the theory arises from the fact that

* Received by the IRE, August 4, 1961.

[1] J. P. Cedarholm, et al., "New experimental test of special relativity," *Phys. Rev. Lett.*, vol. 1, p. 342; November, 1958.

[2] J. P. Cedarholm and C. H. Townes, "A new experimental test of special relativity," *Nature*, vol. 184, p. 1350; October 31, 1959.

[3] C. H. Townes, "Quantum Electronics," Columbia University Press, New York, N. Y., p. 581; 1960.

[4] C. Moeller, "On the possibility of terrestrial tests of the general theory of relativity," *Il Nuovo Cimento*, (Suppl.), vol. 6, ser. 10, no. 1, p. 381; 1957.

both Moeller and CBHT believe that the wavefronts from the molecule are slightly tilted with respect to the molecule's velocity by the ether drift. A close examination of Moeller[5] discloses no mechanism for producing a tilt, and leads to the conclusion that the wavefronts of radiation emitted at right angles to the molecule's velocity arrive at the cavity wall still parallel to the molecule's velocity and with no Doppler shift, regardless of ether drift.

Following a suggestion of Brillouin,[6] we may represent the radiation from a molecule by the idealized diagram of Fig. 1. Here the upper plane B, illuminated by plane-parallel radiation, is traveling with the beam velocity u relative to the stationary plane C, which will represent the cavity walls. The aperture in plane B allows radiation to reach C, and will represent a molecule which is emitting radiation at right angles to the beam velocity. The path of the radiation from the molecule to the cavity walls is then as shown. We see that, although to the cavity walls the radiation appears to be coming in a line inclined to the perpendicular by the angle $\theta=u/c$, the wavefronts themselves arrive unchanged in direction, having traveled the intervening space with velocity c. They arrive at C at the same rate with which they left B, and there is no Doppler shift in this case. If now we add an ether drift v to the left, as shown, the only effect of this will be to increase the angle of deflection of the beam to the value $\theta'=(u+v)/c$ while leaving the wavefronts still parallel to the beam and the cavity walls. Once again, these wavefronts still arrive at the cavity wall with velocity c, and no Doppler shift is produced.

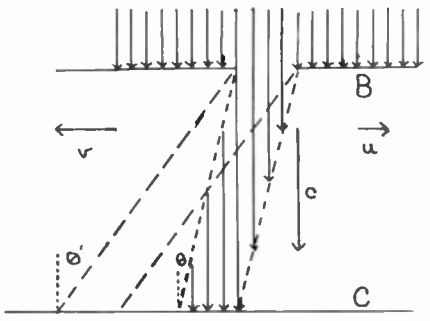

Fig. 1.

This is really just an elaborate way of explaining why, in prerelativity physics, no Doppler effect is found at a receiver when its distance from a transmitter remains constant, regardless of any ether drift. Since the transmitter is the ammonia molecule, and its distance from the cavity wall, the receiver, remains constant, no Doppler effect can be produced.

We see then that the null result of the ammonia maser experiment is a sort of built-in effect, inasmuch as the result will always be zero, regardless of any ether drift.

[5] C. Moeller, "The Theory of Relativity," Oxford University Press, New York, N. Y., ch. 1, pp. 1–15, 1957.

[6] L. Brillouin, "Wave Propagation and Group Velocity," Academic Press, Inc., New York, N. Y., p. 14; 1960.

From a consideration of Fig. 1, which was used by Brillouin to illustrate stellar aberration, one is led to inquire, "Why not perform a terrestrial aberration experiment to measure small ether drifts?" For a drift of 0.3 km/sec, which might be due to the earth's rotation, the aberration angle will be $0.3/3\times10^5$ or 10^{-6} radians. Since recent experiments by Jones[7] have measured the deflection of a light beam down to 2×10^{-12} radians, the aberration experiment should be easy. Alas, this is not the case, and for a curious reason. It has been pointed out to the author that, using conventional point light sources and collimators, a terrestrial aberration experiment for measuring ether drift is impossible. This is because the source and collimating lens are also immersed in the drift, if it exists, and a deflection of the beam beyond the lens will not be found, since the ether drift will cause inclined wavefronts to enter the collimator; the angle of inclination being just sufficient to compensate for the ether drift deflection beyond the lens.

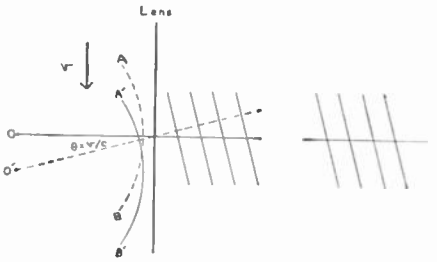

Fig. 2.

This can be seen from Fig. 2, which shows what happens in a collimator when a transverse ether drift exists. In the absence of an ether drift, the lens sees the spherical wavefront AB emitted from O, and turns this into a plane wavefront normal to the axis. In the presence of transverse drift, the lens sees the wavefront $A'B'$, which is displaced from AB in the direction of v. This wavefront appears to the lens to come from O', a point off the axis. From the geometry, a central ray through O' makes an angle $\theta=v/c$ with the axis, and the lens turns the displaced wavefront into an almost plane wavefront inclined to the axis by the same angle. The pencil enclosing these inclined waves continues to travel parallel to the axis, since the ether drift balances the tendency of the waves to depart from the direction of the axis. A few moments of thought will convince the reader that reflection from mirrors, taking account of the relative change in ether drift, will not in any case allow the reflected pencil of inclined wavefronts to depart from the path pursued by a similar pencil of normal wavefronts in the absence of ether drift.

This compensation is so good that one almost suspects that it is another law of nature that we cannot detect an ether drift by an aberration experiment. However, many of the effects observed in crystal optics are due to a similar anisotropy, and are observable only because a pencil of plane wavefronts normal to the pencil can be introduced into the crystal.

We may then look for a source of such wavefronts, not affected by ether drift, and a likely candidate seems to be the optical laser. This device is constrained to emit the largest part of its radiation with wavefronts parallel to the end plates, since this is the steady-state mode preferred by the laser. In the presence of a transverse ether drift, it is probably possible to set up a mode of inclined wavefronts similar to the emergent beam of Fig. 2, in which the waves are reflected from the end plates in such a manner that the back and forth propagation of energy is in the direction of the laser axis. In the case of the mode comprising waves parallel to the end plates, a transverse ether drift would cause the wavetrain to drift away from the axis. On the other hand, the active nature of the laser process may compensate this loss.

In any event, theory does not now tell us which mode the laser prefers, and it will be of interest to try one as a source in an aberration experiment. Following Jones' technique, it should be possible to form a coarse grating on the emitting plate, and let its image, without further collimation, fall on a similar obscuring grating with a radiation detector behind it. For a separation of one meter, the image of the first grating should be displaced $\pm10^{-1}$cm for a v/c of 10^{-6}.

While the maser, in the form of the CBHT experiment, seems to have failed us, the laser may save the day. The laser experiment is now under way.

C. W. Carnahan
120 Fawn Lane
Menlo Park, Calif.

[7] R. V. Jones, "The velocity of light in a transverse magnetic field," *Proc. Roy. Soc.*, vol. 260, p. 47; February, 1961.

Matrix Analysis of Networks Having Infinite-Gain Operational Amplifiers*

It is the object of this note to describe and prove a method of analyzing linear-lumped time-invariant networks that contain an operational amplifier having infinite gain. The generalization for the case of several operational amplifiers in a network is immediate and need not be described.

An operational amplifier of gain A operating between nodes i and j introduces a constraint into the network by forcing the voltage e_j of node j (with respect to the reference node) to follow that of node e_i so as to maintain the relation

$$e_j = Ae_i \qquad (1)$$

without, however, loading node i. The method of analyzing constrained networks

* Received by the IRE, May 5, 1961.

is applicable to this case.[1] It prescribes in this instance the following way of constructing the required admittance matrix Y from the admittance matrix Y of the network without the constraint: in Y add column j multiplied by A to column i and subsequently delete row and column j. The result is Y. This procedure eliminates the constrained node j from the network equations.

The method is not immediately applicable to the case $A \to \infty$ because of the apparent singularity introduced by the transition to infinity. In this case of infinite gain we shall eliminate the source currents operating into node j, as before, but shall retain e_j

$$Y = \begin{array}{c} \\ 1 \\ 2 \\ 3 \\ 4 \end{array} \begin{array}{c} \begin{array}{cccc} 1 & 2 & 3 & 4 \end{array} \\ \begin{bmatrix} G_1 & -G_1 & 0 & 0 \\ -G_1 & G_1+G_2+G_3+sC_1 & -G_2 & -G_3 \\ 0 & -G_2 & G_2+sC_2 & -sC_2 \\ 0 & -G_3 & -sC_2 & G_3+sC_2 \end{bmatrix} \end{array},$$

and eliminate e_i, the voltage of the driving node. The following simple rule obtains: to obtain Y, delete in Y the row corresponding T to the driven node and the column corresponding to the driving node.

Turning now to the proof of this rule, we could start from the rule that applies to finite constraints. An independent proof will be found simpler and more instructive.

Eq. (1) becomes, for $A = \pm \infty$,

$$e_i = 0, \tag{2}$$

making node i a "virtual ground." The operational amplifier injects into node j a current $i_{(a)j}$, of such intensity as to enforce (2). Shifting i and j for convenience into leading positions in the matrix representation, we have now (2) and

$$Y \begin{bmatrix} e_i \\ e_j \\ \vdots \end{bmatrix} = \begin{bmatrix} i_{(a)i} \\ i_{(a)j} \\ \vdots \end{bmatrix} + i_{(a)j} = i_{(a)}, \tag{3}$$

where the right-hand side is the source-current vector. Making use of (2) in (3) we see that column i in Y and the entry e_i can be omitted on the left-hand side. We intend to eliminate the unknown $i_{(a)i}$ as well. This is achieved by deleting the jth equation of (3), *i.e.*, by deletion of row j in Y and entry j in $i_{(a)}$. The result is

$$Y \begin{bmatrix} e_j \\ \vdots \end{bmatrix} = \begin{bmatrix} i_{(a)i} \\ \vdots \end{bmatrix}. \tag{4}$$

Y is used, as always, for the calculation of system functions. For example, provided p is not driven and q is not driving,

$$H_{pq} = e_q/e_p = (Y^{-1})_{qp} i_{(a)p}/(Y^{-1})_{pp} i_{(a)p} = Y^{pq}/Y^{pp}, \tag{5}$$

where superscripts denote cofactors.

[1] A. Nathan, "Matrix analysis of constrained networks," IEE Monograph No. 399E; September, 1960. Republished in Pt. C of *Proc. IEE*, vol. 108, pp. 98–106; March, 1961.

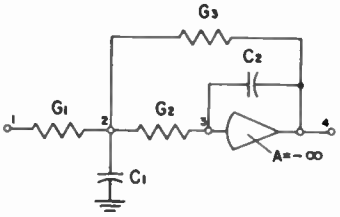

Fig. 1.

In general, Y can be written down without first writing Y. As an example consider the "double integrator" of Fig. 1. We have

and therefore,

$$Y = \begin{array}{c} \\ 1 \\ 2 \\ 3 \end{array} \begin{array}{c} \begin{array}{ccc} 1 & 2 & 4 \end{array} \\ \begin{bmatrix} G_1 & -G_1 & 0 \\ -G_1 & G_1+G_2+G_3+sC_1 & -G_3 \\ 0 & -G_2 & -sC_2 \end{bmatrix} \end{array},$$

and the transmittance from 1 to 4,

$$H_{14} = Y^{14}/Y^{11} = \frac{G_1G_2}{\begin{vmatrix} G_1+G_2+G_3+sC_1 & -G_3 \\ -G_2 & -sC_2 \end{vmatrix}} = \frac{-1}{T_1T_2s^2+T_2s(1+R_1/R_2+R_1/R_3)+R_1/R_3},$$

where $T_\alpha = R_\alpha C_\alpha$ and $R_\alpha = 1/G_\alpha$.

Amos Nathan
Faculty of Elec. Engrg.
Israel Institute of Technology
Haifa, Israel

A Self-Balancing Current Meter and Recorder*

An undesirable voltage drop is usually introduced across the terminals for current measurement by conventional[1] devices. This may be caused by current flow through a meter resistance or intentionally generated across a standard resistance when and where it is desired to convert the measurement to one of voltage. This extraneous potential often causes difficulties in the measurement of current-voltage relations in the fractional volt range.

With negative feedback techniques it is possible to measure currents without introducing a voltage drop across the measurement terminals. A conventional operational amplifier may be used as a fast instrument giving an output proportional to input current while keeping the potential difference across the input terminals very close to zero by feedback.[2–5] For steady or slowly changing currents, a servo self-balancing and recording potentiometer may be converted, by minor circuit changes described in this note, into a zero input impedance current recorder.

A servo system which gives an output motion proportional to the input current, while holding the potential across its input terminals at a minimum, is shown schematically in the upper part of Fig. 1. A network composed of a standard resistor R_1 in series with a fraction of a much lower resistance slidewire R_2 is connected across the input terminals. An amplifier senses the dc potential difference between the input terminals and applies torque to the motor when this voltage differs from zero. The wiper of the R_2 slidewire will then move so that the voltage across its upper portion will balance (be equal and of opposite polarity to) the potential developed across R_1 by an input current, I_1. If I_2 is much greater than I_1, the motor and wiper movement will be proportional to I_1. R_1 determines the current range for a nominal full scale potential across R_2; R_3 provides the usual calibration adjustment.

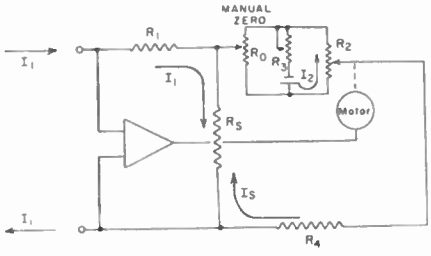

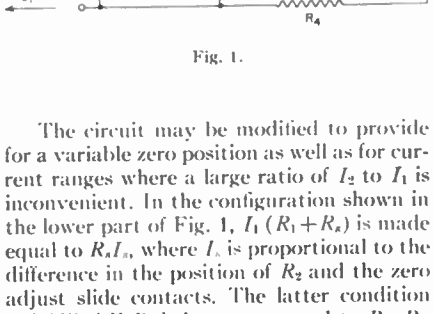

Fig. 1.

The circuit may be modified to provide for a variable zero position as well as for current ranges where a large ratio of I_2 to I_1 is inconvenient. In the configuration shown in the lower part of Fig. 1, $I_1(R_1+R_x)$ is made equal to R_xI_x, where I_x is proportional to the difference in the position of R_2 and the zero adjust slide contacts. The latter condition is fulfilled if R_4 is large compared to R_2, R_x.

* Received by the IRE, June 27, 1961.

[1] The work described here was completed before the recently introduced commercial devices which "clip on" rather than being inserted into the circuit.

[2] I. Pelchowitch and J. J. Zaalberg van Zelst, "A wide-band electrometer amplifier," *Rev. Sci. Instr.*, vol. 23, pp. 73–75; February, 1952.

[3] J. Praglin, "A new high stability micromicroammeter," IRE Trans. on Instrumentation, vol. I-6, pp. 144–147; June, 1957.

[4] J. W. Moore, "Electronic control of some active bioelectric membranes," Proc. IRE, vol. 47, pp. 1869–1880; November, 1959.

[5] J. Praglin and W. A. Nichols, "High-speed electrometers for rocket and satellite experiments," Proc. IRE, vol. 48, pp. 771–779; April, 1960.

and R_0. Several commercially available self-balancing potentiometers may be converted to this "currentometer" circuit with only a few wiring changes. For preliminary tests, a simple inexpensive commercial potentiometer (Varian Assoc., Model G10, 10 mv full scale) was chosen for modification and testing. Table I gives the resistance values for full scale currents ranging from 10 μa to 0.01 μa (supplied from a source resistance of 10^6 ohms).

TABLE I

Full Scale Current	R_1	$R_4 = 49$ kΩ
10 μa	27 Ω	$R_0 = 1$ kΩ
1.0	9 kΩ	$R_0 = 5$ kΩ
0.1	100 kΩ	$R_2 = 5$ kΩ
0.01	1.0 megΩ	$R_3 = 1.5$ kΩ

The value of I_x varied from zero to 10 μa for full scale movement. The damping adjustment circuit normally used in the potentiometric configuration of this recorder was not required but the 1 mfd capacitor normally across R_1 was retained. The potential drop across the current measurement terminals, or "error voltage" was monitored and found to have an offset of about 200 μv and a dead-space of ± 25 to 50 μv. This dead-space amounted to about $\pm 3 \times 10^{-10}$ a and was small enough to give excellent tracking and reproducibility on all except the most sensitive current range (0.01 μa full scale).

It is also possible to change the current range by setting $R_1 = 0$ and varying R_4. In this case, I_x is made the equal and opposite of I_1. With this circuit arrangement, the response of the modified Varian G-10 became rather sluggish in the 0.1 μa full scale range. This may have occurred because the source impedance of the balancing current ($R_4 = 5$ megohms) was large with respect to the input impedance of this amplifier (about 0.5 megohm). This might still be a usetul circuit arrangement for use with amplifiers of higher gain and input impedance.

JOHN W. MOORE
Dept. of Physiology
Duke Univ. Medical Center
Durham, N. C.
Formerly Lab. of Biophysics
Natl. Institutes of Health
Bethesda, Md.

Reciprocal Relations in an *N*-Slab Dielectric*

Transmission and reflection properties of radomes and plasma sheaths about missiles are typical of many current problems involving the propagation of radio energy through a dielectric. In such problems it is often convenient to represent the actual dielectric by a number of parallel contiguous slabs whose electrical properties are homogeneous and isotropic in each slab.

During a study in this area it became important to determine whether or not such a dielectric model exhibits reciprocal properties for its transmission and reflection coefficients. This note presents a proof that the transmission coefficients are identical for both directions of transmission but that the reflection coefficients are not.

The method and notation used follows that of Stratton.[1] He derives expressions for the transmission and reflection properties of a single slab separating two semi-infinite media having different electrical constants.

Consider a plane electromagnetic wave normally incident upon a dielectric made of n homogeneous parallel slabs, the ith slab having thickness d_i and propagation constant k_i (Fig. 1). The quantities E_I, E_R, and

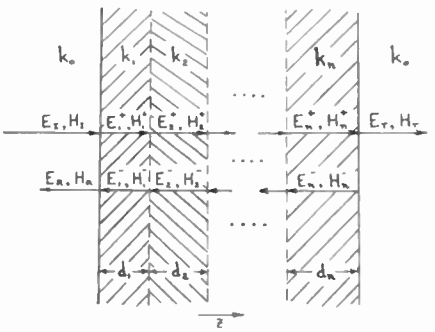

Fig. 1—Dielectric model.

E_T designate the electric intensities of the incident, reflected, and transmitted waves at their respective interfaces. The corresponding magnetic intensities are

$$H_I = \frac{k_0}{\omega\mu_0} E_I; \quad H_R = \frac{k_0}{\omega\mu_0} E_R; \quad H_T = \frac{k_0}{\omega\mu_0} E_T.$$

The total E- and H-waves in the ith slab are the sums of the forward- and backward-traveling components in this slab and are

$$\left.\begin{aligned} E_i &= E_i^+ e^{jk_i z} + E_i^- e^{-jk_i z} \\ H_i &= \frac{k_i}{\omega\mu_i}\left(E_i^+ e^{jk_i z} - E_i^- e^{-jk_i z}\right) \end{aligned}\right\} \quad 0 \le z < d_i.$$

The expressions for the continuity of the E- and H-vectors across the ith interface (counting from left to right) are

$$\begin{aligned} &e^{jk_{i-1}d_{i-1}} E_{i-1}^+ + e^{-jk_{i-1}d_{i-1}} E_{i-1}^- \\ &\quad - E_i^+ - E_i^- = 0 \\ &k_{i-1} e^{jk_{i-1}d_{i-1}} E_{i-1}^+ - k_{i-1} e^{-jk_{i-1}d_{i-1}} E_{i-1}^- \\ &\quad - k_i E_i^+ + k_i E_i^- = 0 \quad i = 1, 2 \cdots n+1 \end{aligned}$$

since $\mu_0 = \mu_1 = \mu_2 = \cdots = \mu_n$. In the last pair the terms E_T, $k_0 E_T$ replace the zeros in the right members. The quantity d_0 is taken as zero. The determinant of this set of $2n+2$ linear equations is designated D. The determinants obtained by replacing the first and second columns of D by the column matrix $(0, 0, 0, \cdots 1, k_0)_{c+1}$ are designated N_T and N_R, respectively. The transmission and reflection coefficients T and R are defined by

$$T = \frac{E_T}{E_I}, \qquad R = \frac{E_R}{E_I},$$

so that

$$T = \frac{D}{N_T}, \qquad R = \frac{N_R}{N_T}.$$

Assume now that the wave propagates from right to left. All the E- and H-vectors, transmission and reflection coefficients, and determinants for this case are designated by primes on corresponding quantities for the opposite direction.[2] At the ith interface

$$\begin{aligned} &e^{jk_i d_i} E_i^{+\prime} + e^{-jk_i d_i} E_i^{-\prime} - E_{i-1}^{+\prime} \\ &\quad - E_{i-1}^{-\prime} = 0 \\ &k_i e^{jk_i d_i} E_i^{+\prime} - k_i e^{-jk_i d_i} E_i^{-\prime} - k_{i-1} E_{i-1}^{+\prime} \\ &\quad + k_{i-1} E_{i-1}^{-\prime} = 0 \end{aligned}$$

where i runs from $n+1$ to 1. The first and last pairs ($i = n+1$, $i = 1$) are

$$E_I' + E_R' - E_n^{+\prime} - E_n^{-\prime} = 0$$

$$k_0 E_I' - k_0 E_R' - k_n E_n^{+\prime} + k_n E_n^{-\prime} = 0$$

and

$$e^{jk_1 d_1} E_1^{+\prime} + e^{-jk_1 d_1} E_1^{-\prime} = E_T'$$

$$k_1 e^{jk_1 d_1} E_1^{+\prime} - k_1 e^{-jk_1 d_1} E_1^{-\prime} = k_0 E_T'.$$

The determinants, D, D' are equal to $(-2)^{n+1} k_0 k_1 k_2 \cdots k_{n-1} k_n$.

We now demonstrate that $N_T = N_T'$ and that $N_R \neq N_R$. Apply the following transformations to N_T. Multiply the third, fourth, $\cdots$ $(2n+1)$th, $(2n+2)$th columns by $e^{-jk_1 d_1}$, $e^{jk_1 d_1}$, $\cdots$, $e^{-jk_n t_n}$, $e^{jk_n d_n}$, respectively. Interchange the first and second columns, third and $(2n+2)$th columns, fourth and $(2n+1)$th columns, etc. for a total of $(n+1)$ interchanges. Next, apply a row interchange as follows. If n is even, there will be n interchanges: first and $(2n+1)$ rows, second and $(2n+2)$th rows, third and $(2n-1)$th rows, fourth and $2n$th rows, etc. with the $(n+1)$th and $(n+2)$th rows fixed. If n is odd there will be $n+1$ interchanges of rows, the same as before, now with the $(n+1)$th and $(n+2)$th row being interchanged. Multiply all odd rows by (-1). After multiplying both the first and second columns by (-1) we obtain a determinant whose elements are identical to N_T'. Since there is always an even number of sign interchanges, we have $N_T = N_T'$ so that $T = T'$.

If these same transformations (with the exception of the last one) are applied to N_R, we obtain a determinant which differs from N_R' only in the sign of a_{11}, $a_{2n+1,2}$ elements which are now (-1). Thus, N_R' cannot equal N_R and so $R \neq R'$. This difference in the reflection coefficient is compensated by the change in the absorption of the dielectric slabs.

R. HOLLIS
The Martin Co.
Baltimore, Md.

* Received by the IRE, July 10, 1961.

[1] J. A. Stratton, "Electromagnetic Theory," McGraw-Hill Book Co., Inc., New York, N. Y., pp. 511–516; 1941.

[2] The wave is now incident upon the $(n+1)$th interface.

Construction of Probability Densities from Their Moments*

Most engineering problems involving stochastic variables lead to Gaussian distributions or distributions derived by functional mappings of Gaussian distributions. It is easy to show how dreadful it would be if such were not the case. The *a priori* simple problem of the construction of a probability density from the knowledge of its moments is a case in point. This is not a trivial problem because the results of a number of measurements can only lead to two interpretations: 1) an estimate for the probability of occurrence of a given value provided this value did occur and 2) an estimate of the moments. The second interpretation is less restrictive and is less subject to variations when a new set of measurements becomes available. The accuracy of the estimates of the moments, however, is poorer the higher the degree of the moment, so that in practice only a finite number of moments can be estimated.

With this in mind, let us try to find the probability density $p(r)$ when the moments m_i are given from m_1 to m_n.

It is well known that the knowledge of a number of moments of a probability density does not lead, in general, to more accurate prescriptions for the construction of this density than the Dieudonné-Markov inequalities. In general, one cannot form a sequence of approximations,

$$p_n(r) = f_n(m_1, m_2 \cdots m_n, r), \tag{1}$$

converging toward the density $p(r)$ when n increases indefinitely. Nor can one, in general, form a convergent series of the form

$$p(r) = \sum_{n=1}^{\infty} p_n(r). \tag{2}$$

Any probability density, however, has a Fourier transform,

$$\bar{p}(f) = \int_{-\infty}^{+\infty} p(r) \exp(-2\pi i f r) dr. \tag{3}$$

The exponential can be expanded in power series of the argument. Integrating, one obtains

$$\bar{p}(f) = \sum_n (-2\pi i)^n \frac{f^n m_n}{n!}. \tag{4}$$

The series (4) is convergent provided the moments do not increase too rapidly with n.

The convergence will depend on the behavior of $p(r)$ for large magnitudes of r. Even as rapidly decreasing a function as the Gaussian distribution does not yield a convergent series. On the contrary, suppose that $p(r)$ has a compact domain such that $p(r)$ is certainly zero for

$$|r| > R. \tag{5}$$

One can write

$$r = R\theta \tag{6}$$

$$p(r) = p(\theta) \tag{7}$$

$$m_n = R^{n+1}\mu_n \tag{8}$$

$$\mu_n = \int_{-1}^{+1} p(\theta)\theta^n d\theta. \tag{9}$$

* Received by the IRE, July 12, 1961.

Using vertical bars for absolute value, one obtains

$$|\mu_n| \leq \int_{-1}^{+1} p(\theta)|\theta|^n d\theta. \tag{10}$$

The upper bound [right-hand side of (10)] for the absolute value of μ_n tends toward zero when n increases indefinitely. The corresponding series (4) is convergent.

Even when the series (4) is convergent, its inverse Fourier transform P is paradoxical;

$$P(r) = \sum_n \frac{(-1)^n}{n!} \delta_0^N(r) m_n \tag{11}$$

where δ_0^N is the nth derivative of the Dirac delta function placed at the origin. The function $P(r)$ has the same moments as $p(r)$ but is not equal to $p(r)$. This is possible because $P(r)$ is not a probability density and is not positive definite.

In order to transform $P(r)$ into a probability density, one can use the Taylor expansion of the Dirac delta function placed at a distance r_i from the origin;

$$\delta_{r_i}(r) = \sum_n \frac{(-1)^n}{n!} r_i^n \delta_0^N(r). \tag{12}$$

The Taylor expansion is sufficiently correct in distribution theory,[1] because one can write

$$\delta_{r_i}(\phi) = \phi(r_i) = \sum_n \frac{r_i^n}{n!} \phi^N(0). \tag{13}$$

The functions ϕ are the usual functions of the class D. The Taylor series of a ϕ function is well defined nearly everywhere. The series is, however, not defined on the boundary of the compact domain of the function. Thus, (13) is correct for almost all ϕ functions, but not for all and this is why the word sufficiently is added. We now write

$$P(r) = \sum_i a_i \delta_{r_i}(r), \tag{14}$$

where the a_i are either positive constants or zero. Using the Taylor expansion (12)

$$P(r) = \sum_n \frac{(-1)^n}{n!} \left(\sum_i a_i r_i^n \right) \delta_0^N(r). \tag{15}$$

Equating (11) and (15),

$$\sum_i a_i r_i^n = m_n. \tag{16}$$

The function $P(r)$ (14) has the same moments as $p(r)$ provided the set of conditions (16) is satisfied. If one adds to this set of conditions that all a_i must be positive, the function $P(r)$ becomes a possible probability density. Because two probability densities which have the same moments are the same, one must have

$$a_i = \epsilon p(r_i). \tag{17}$$

The parameter ϵ is an infinitely small quantity such that $\epsilon\delta$ is the Kronecker delta. The introduction of ϵ in distribution theory permits one to define unambiguously the product of distributions and thus to generalize this essentially linear theory. In practice one does not know the higher moments with any accuracy so that one is forced to construct $p(r)$ from a finite number of moments. The set of conditions (16) is a linear inhomogeneous set in a_i. The characteristic determinant is a Van der Monde determinant. It can only be zero if two r_i are chosen equal. Thus, the set of conditions (16), restricted to a finite number of a_i equal to the finite number of available moments, has always a well-defined solution for any chosen set of r_i. The restriction that the a_i must all be positive, restricts the possible choice of r_i. Because of the essential additivity of moments, sums of properly weighted solutions are also solutions. Thus assuming all solutions obtained to be equally probable, one finds for each value of r a probability density $p_r^*(p)$ for the value of the probability density $p(r)$.

P. A. Clavier
Aeronutronic Div.
Ford Motor Co.
Newport Beach, Calif.

[1] L. Schwartz, "Theorie des Distributions," Hermann and Co., Paris, France, vols. 1 and 2; 1950.

A Simple Passive-Element Electrical Analog to a Gyro*

The writer has found a very simple electrical analog to a free gyroscope which, to his knowledge, has not been previously reported in the literature.

Consider a gyroscope system with principal axes in the directions x, y, and z. Let the angular momentum of the gyro wheel be z directed and of magnitude Ω, the principal moments of inertia be I_x and I_y (including gimbals), the angular velocities be ω_x and ω_y, and external torques be T_x and T_y. The linearized equations of motion are:

$$I_x\dot{\omega}_x + \Omega\omega_y = T_x$$

$$I_y\dot{\omega}_y - \Omega\omega_x = T_y.$$

In matrix form:

$$\begin{vmatrix} \frac{I_x}{\Omega} s & 1 \\ -1 & \frac{I_y}{\Omega} s \end{vmatrix} \begin{vmatrix} \omega_x \\ \omega_y \end{vmatrix} = \begin{vmatrix} \frac{T_x}{\Omega} \\ \frac{T_y}{\Omega} \end{vmatrix}.$$

The above form clearly shows[1] why a passive element electrical analog in which both gyro equations are the analogs of loop or node equations cannot be found. The off-diagonal terms of the matrix would represent mutual impedances or mutual admittances, and hence would have to be identical. The matrix can be reordered, bringing the terms 1, -1, onto the diagonal, but a passive-element analog still cannot be found, since the -1 represents a negative self-impedance or admittance, not realizable with passive elements.

* Received by the IRE, July 17, 1961.

[1] J. A. Aseltine, "Transform Methods in Linear Systems Analysis," McGraw-Hill Book Co., Inc. New York, N. Y., pp. 75–82; 1958.

Consider the circuit shown in Fig. 1. The node equation is

$$i + C\frac{dV}{dt} = i_s.$$

The loop equation for the L-C loop is

$$L\frac{di}{dt} - V = V_s.$$

In matrix form

$$\begin{vmatrix} CS & 1 \\ -1 & LS \end{vmatrix} \begin{vmatrix} V \\ i \end{vmatrix} = \begin{vmatrix} i_s \\ V_s \end{vmatrix}.$$

Comparison shows that the following analogue is valid,

$$C = \frac{I_x}{\Omega} \qquad L = \frac{T_y}{\Omega}$$
$$V = \omega_x \qquad i = \omega_y$$
$$i_s = \frac{T_x}{\Omega} \qquad V_s = \frac{T_y}{\Omega}.$$

For gyro systems of ordinary dimensions, realizable values of L and C would result.

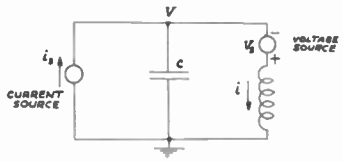

Fig. 1.

A floated gyro, floated around the x axis with viscous constant D, can be represented by addition of a resistor, $R = \Omega/D$, in parallel with C.

A rate gyro, restrained around the x axis with a spring of constant K, can be represented by adding an inductor, $L = \Omega/K$, in parallel with C.

ROBERT W. REDLICH
Elec. Engrg. Dept.
Clarkson College of Technology
Potsdam, N. Y.

Measurement of Tunnel-Diode Conductance Parameters*

An accurate knowledge of the instantaneous incremental conductance (g_d) of a tunnel diode that is operating as a mixer (down converter) is necessary in order to correlate the theoretical and experimental data of such a diode's performance. This note briefly describes a method of determining g_d that has proven useful in work on tunnel-diode mixers at Philco's Western Development Laboratories.

This method assumes that the local oscillator voltage v_1 is sinusoidal and that

* Received by the IRE, July 5, 1961. Performed under Contract AF 04(647)-532, AFBMD, Los Angeles, Calif.

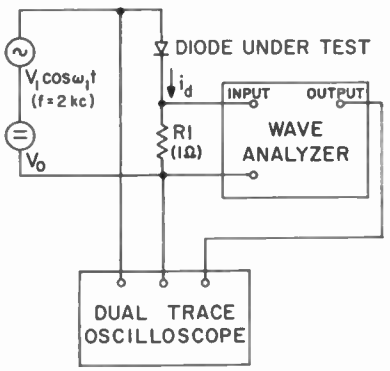

Fig. 1—Principle of test setup.

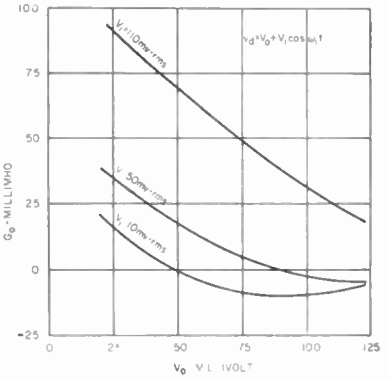

Fig. 2—G_0 vs diode bias.

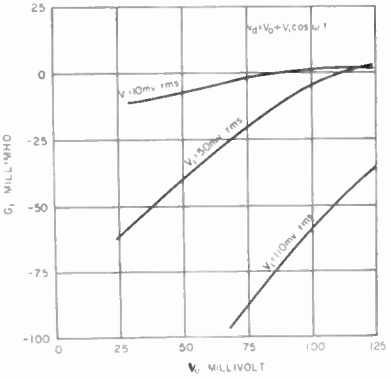

Fig. 3—G_1 vs diode bias.

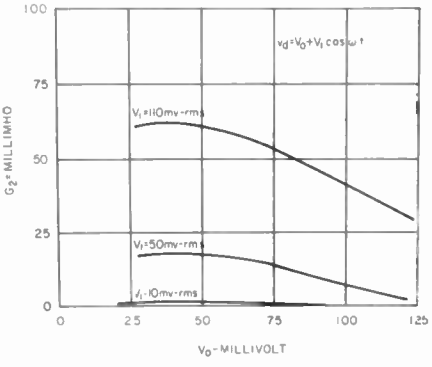

Fig. 4—G_2 vs diode bias.

g_d is a function of v_1 for a given direct voltage bias, V_0. We may therefore write

$$v_1 = V_1 \cos\omega_1 t$$

and

$$g_d = G_0 + G_1 \cos\omega_1 t + \cdots + G_n \cos n\omega_1 t,$$

where the coefficients $G_0, G_1, \cdots, G_n$ depend on only V_0 and V_1 for a given tunnel diode. The determination of g_d is based on the relationship between g_d and the current, i_d, through the diode. This relationship is given by

$$G_0 = \frac{1}{V_1}\left[I_1 + 3I_3 + 5I_5 + \cdots + \begin{cases} nI_n & (n \text{ odd}) \\ (n+1)I_{n+1} & (n \text{ even}) \end{cases}\right],$$

$$G_1 = \frac{2}{V_1}\left[2I_2 + 4I_4 + 6I_6 + \cdots + \begin{cases} (n+1)I_{n+1} & (n \text{ odd}) \\ nI_n & (n \text{ even}) \end{cases}\right],$$

$$G_2 = \frac{2}{V_1}\left[3I_3 + 5I_5 + 7I_7 + \cdots + \begin{cases} nI_n & (n \text{ odd}) \\ (n+1)I_{n+1} & (n \text{ even}) \end{cases}\right],$$

$$\vdots$$

$$G_n = \frac{2}{V_1}(n+1)I_{n+1},$$

where $I_1, I_2, \cdots, I_{n+1}$ are the coefficients of the Fourier series representation of i_d, *i.e.*,

$$i_d = I_0 + I_1 \cos\omega_1 t + \cdots + I_{n+1} \cos(n+1)\omega_1 t.$$

Thus g_d may be determined by a measurement of V_1 and of the coefficients I_q, where $q = 1, 2, \cdots, n+1$.

The test setup used for the measurement of I_q is shown, in principle, in Fig. 1. The dual-trace oscilloscope is used to determine the sign of I_q, while the magnitude of I_q is determined by dividing R_1 into the voltage reading on the wave analyzer. The value of R_1 is chosen so small that the voltage drop across it has a negligible effect on the accuracy of the measurements. Some of the results obtained with this setup for a GE type ZJ56 diode are shown in Figs. 2–4.

Some values of G_0 and G_1 that were measured in this manner at audio frequencies have been found to be applicable at UHF frequencies. Thus, good agreement was found between the measured and calculated conversion gain and noise figure for a tunnel diode operating at 420 Mc. Further, this agreement was obtained not only at a single point but over a range of bias and local oscillator signal levels.[1]

BENT CHRISTENSEN
Space Sciences Dept.
Philco Western Dev. Labs.
Palo Alto, Calif.

[1] For more details, see "Semiannual Report of Advanced Equipment Studies," Philco Corp., Palo Alto, Calif., WDL-TR-1481, Section I: February 15, 1961.

Experiments with Nonreciprocal Parametric Devices*

It has been pointed out by Kamal[1] that parametric diodes may be used to realize nonreciprocal networks. Recently, Baldwin[2] proposed a unilateral amplifier employing two parametric diodes pumped in quadrature.

For some time now we have been experimenting along similar lines with various nonreciprocal parametric devices. The following is a report on the results of this work.

The first of these experimental devices (Fig. 1) is a 200-Mc unilateral amplifier of the sort described by Baldwin. The two signal circuits consist of strip line resonators A and A' coupled by a quarter wavelength section of a 50-ohm cable. The common idler circuit also consists of a strip transmission line BB' capacitively loaded at both ends by parametric diodes C and C' which are also part of the signal circuits. Signal and idler circuits are separated by sections of coaxial line D and D' acting as short circuits for idler and pump frequencies and as additional capacitive loads at the signal frequency.

Pump power at 850 Mc is supplied to the diodes through small capacitors E and E' which are tuned out by coaxial stubs F and F'. A 3-db directional coupler provides the necessary 90° phase shift in the pump input circuits. At the pump frequency these circuits are separated by means of a tunable stub G in the center of the idler circuit; dc bias is also supplied at this point.

The idler circuit may be tuned from 600 Mc to 700 Mc by varying the bias voltage.

We used a matched pair of Microwave Associates' diodes No. MA-4202X. Although we were able to achieve satisfactory nonreciprocal amplification, it was observed that for a given amount of pump power, maximum gain occurred at the edge rather than in the center of the signal band.

Shifting the response back to the center of the band by detuning the idler circuit, more pump power was required for the same gain. Detailed analysis reveals the existence of a particular combination of nonzero idler and signal circuit reactances which requires less pump power than the case in which all reactances are tuned out. In this detuned condition, however, the device is no longer matched and the gain in the backward direction is larger than unity. Consequently, we might expect the noise figure to be worse than in the ideal condition.

In our case we measured a 4-db noise figure; the predicted noise figure was of the order of 1–2 db.

In agreement with the theory, we found the device to have a constant gain-bandwidth product.

The second device with which we have experimented is shown in Fig. 2. This is a 100-kc circulator. The double-tuned circuit formed by L_1 and L'_1, together with the parametric diodes D and D' is tuned to 2.5

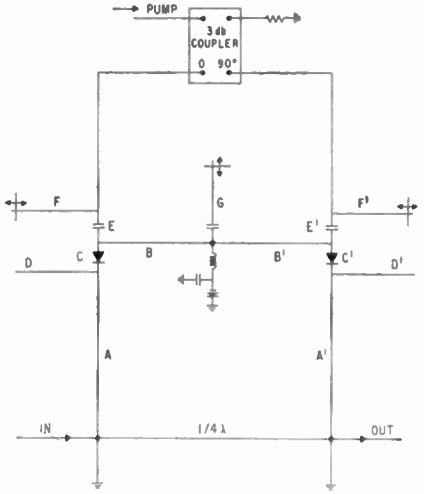

Fig. 1—Circuit diagram of 200-Mc unilateral amplifier.

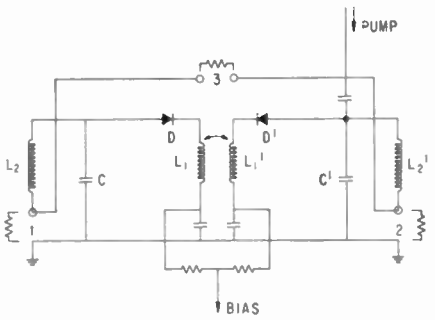

Fig. 2—Circuit diagram of 100-kc circulator.

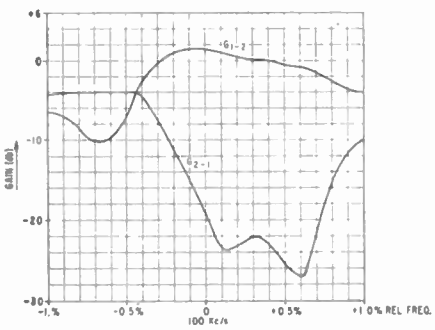

Fig. 3—Gain and isolation characteristics of 100-kc circulator.

Mc and has a bandwidth of approximately 200 kc. This circuit is excited by the pump at 2.5 Mc and will support both upper and lower sidebands.

It is separated from the signal circuits by means of bypass capacitors C and C' which are tuned out by 100 kc by L_2 and L'_2.

The three ports of the circulator are indicated by 1, 2 and 3. By properly matching port 3 we were able to achieve isolation greater than 20 db over a 0.7 per cent band, while forward insertion gain varied from +1 db to −1 db (see Fig. 3).

It is a pleasure to acknowledge Dr. R. Adler's support and valuable suggestions.

A. Korpel
P. Desmares
Research Dept.
Zenith Radio Corp.
Chicago, Ill.

* Received by the IRE, August 7, 1961.

[1] A. K. Kamal, "A parametric device as a nonreciprocal element," Proc. IRE, vol. 48, pp. 1424–1430; August, 1960.

[2] L. D. Baldwin, "Nonreciprocal parametric amplifier circuits," Proc. IRE, vol. 49, p. 1075; June, 1961.

New Form of Plasma Dispersion Formula Usable for Analog Computing*

For electric analog computation of Sellmeier's dispersion formula[1] of a Lorentz plasma in the absence of collisions and of a magnetic field,

$$\mu^2 = 1 - X = 1 - \frac{f_N^2}{f^2} \tag{1}$$

(f = wave frequency and f_N = plasma frequency) can very easily be represented with sin- and cos-generators. This is not so when the magnetic field influence is introduced. Indeed, the Appleton[2]-Lassen[3] formula looks rather discouraging when

$$\mu^2 = 1 - X \Big/ \left\{1 - iZ - \frac{\frac{1}{2}Y_T^2}{1 - X - iZ} \pm \left[\frac{\frac{1}{4}Y_T^4}{(1 - X - iZ)^2} + Y_L^2\right]^{1/2}\right\} \tag{2}$$

($Y_T = f_H/f \cos\theta$, $Y_L = f_H/f \sin\theta$, $Z = \nu/2\pi f$, f_H gyrofrequency in the magnetic field B, ν effective collision number of electrons, θ angle between wave normal and magnetic field B). Now, as (1) is the asymptotic form of (2) for $f \gg f_H$, $Z \ll 1$, it is useful to write (2) in the form of (1) with an appropriate correction term M, *viz.*,

$$\mu^2 = 1 - X/(1 - iZ - M) \tag{3}$$

where

$$M = \frac{\frac{1}{2}Y_T^2}{(1 - X - iZ)} \mp \left[\frac{\frac{1}{4}Y_T^4}{(1 - X - iZ)^2} + Y_L^2\right]^{1/2} \tag{4}$$

When the square root is eliminated, the terms with Y_T^4 cancel out and we have for M the simple equation

$$M^2 - M\frac{Y_T^2}{(1 - X - iZ)} - Y_L^2 = 0 \tag{5a}$$

or

$$M^2 \cdot (1 - X - iZ) - M \cdot Y_T^2 - (1 - X - iZ)Y_L^2 = 0. \tag{5b}$$

The two roots $M+$ and $M-$ correspond to the two principal polarizations, $M+$ to the electronic[4] *extraordinary* one and $M-$ to the ionic[4] *ordinary* one. In the case $Z = 0$ (no collisions), it is easily seen that in the X range admitted for propagation ($0 \leq X < 1$) we have

$$M_+ > |Y_L| \quad \text{and} \quad |Y_L| < M_- < 0. \tag{6}$$

* Received by the IRE, July 5, 1961. This work was supported by a research grant from Bundes Wirtschafts Ministerium, no. A 190, 1959.

[1] W. Sellmeier, see P. Drude, "Lehrbuch der Optik," 1900.

[2] E. V. Appleton, "The influence of the earth's magnetic field in wireless transmission," *Proc. Union Radio Sci. Internatl.*, 1 (1928), 2 (lecture presented October 13, 1927, Washington, D. C.).

[3] H. Lassen, "Über den Einfluss des erdmagnetischen Feldes auf die Fortpflanzung der elektrischen Wellen der drahtlosen Telegraphie in der Atmosphäre," *Elek. Nach.-Tech.*, vol. 4, pp. 324–334; August, 1927.

[4] R. W. Larenz, "Beitrag zur Magneto-Hydrodynamik kompressibler Medien," lecture presented at Bad Salzuflen, Germany; April, 1952 (unpublished).

For analog computing, we suppose $Z=0$. It is not interesting to use the analytical solution of (5). However, it is easier to represent (5b) directly in the form

$$MY_T^2 = (1 - X)M^2 - Y_L^2. \qquad (7)$$

It is seen from (6) that in (4) the expression in brackets should get the positive sign for M_+ and the negative for M_-. So as $(1-X)>0$, the distinction between the principal components can simply be made by means of a diode giving one or the other sign in (7).

M could be computed from X, Y_T, Y_L; but with our analog circuit representing (7), we actually use f^2, $(1-X)/f_T^2$, f_L^2 (Fig. 1,

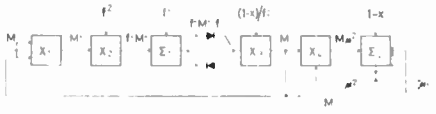

Fig. 1.

left side). The square of the refraction index μ^2 is finally calculated from (3) in the form

$$\mu^2 = 1 - X - M(1 - \mu^2) \qquad (8)$$

with the circuit of Fig. 1, right side, with the inputs: M, $(1-X)$. The total arrangement used only four multipliers and two operational amplifiers. The diode switch enables the distinction between both magneto-ionic components.

H. Porsche
K. Rawer
Ionosphären Institut
(im FTZ der Deutschen Bundespost)
Breisach/Rhein
Germany

The Expanded Reactance Series Resonator—"ERSER"*

Synopsis

ERSER is a circuit element wherein the bandwidth between the infinities of a series resonant circuit constructed from transmission line elements can be exchanged for increased steepness of the reactance slope through resonance. It finds application in B.P. filters made of T.L. elements where a compact unit of high reactance slope with change of frequency is required to be made with practical values of the characteristic impedance. In freedom from spurious responses and low insertion loss, it is superior to the alternative method of using a S.C. T.L., an integral number of $\lambda/2$ long at the resonant wavelength λ_0.

Referring to Fig. 1, ERSER consists of a S.C. transmission line of low-characteristic impedance Z_{O_1}, especially made to have high Q, terminating a T.L. of C.I. Z_O, each line being effectively $\lambda_0/4$ long. Air is used as the dielectric. Trimming adjustment can be provided by a thread T at the low-current center of the unit. The input impedance of ERSER at $100K$ per cent above the series resonant frequency, writing $\rho \equiv Z_O/Z_{O_1}$, is

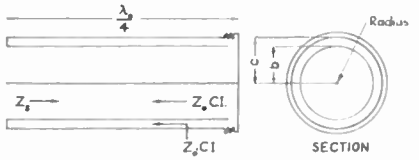

Fig. 1.—Longitudinal and cross sections of ERSER transmission line unit

$$\rho = \frac{Z_O}{Z_{O_1}}.$$

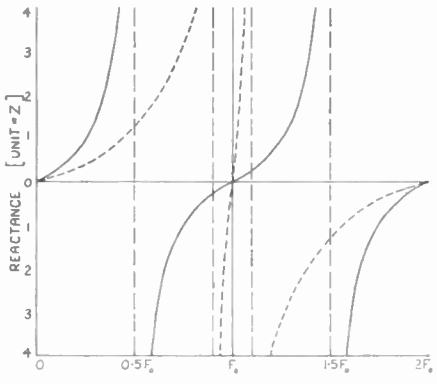

(a)

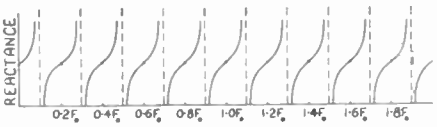

(b)

Fig. 2.—(a) Reactance curves of ERSER for $\rho=9$.
Compare with 0.5 λ S.C. T.L. ($\rho=1$).
Asymptotes are shown.
Note bandwidth between infinities of series resonant range is reduced in ratio $2/\pi$ arctan ρ^{-2}, while reactance slope is increased in ratio $(\rho+1)/2$.
(b) Reactance curves of the equivalent 2.5 λ transmission line. Note the excessive number of unwanted zeros of the reactance characteristic.

$$Z_S = jZ_O \tan K\pi/2\left[\frac{1+\rho^{-1}}{\rho^{-1} - \tan^2 K\pi/2}\right].$$

This is a series resonant circuit with $Z_S=0$ at $K=0$. As the reactance of a $\lambda/2$ S.C. transmission line at $100K$ per cent above resonance is equal to $jZ_O \tan K\pi$ and is the best that can be done with a single element, the reactance scaling factor of ERSER is substantially equal to $(\rho+1)/2$; and infinities of Z_S occur when $\tan K\pi/2 = \rho^{-1/2}$ [Figs. 2(a) and 2(b)].

The step up of the current in the S.C. end of Z_{O_1} in the ratio of ρ compared with the input line would appear to condemn the device on the basis of insertion loss; however, it will be shown that it is superior in all practical cases to the only alternative, the $(\rho+1)/2$ of $\lambda/2$ S.C. transmission line.

If for convenience $(\rho+1)/2$ is considered integral and the unit of loss is that on $\lambda/4$ of T.L. of C.I. Z_O, then the loss of

$$\left[\frac{\rho+1}{2} \text{ of } \lambda/2 \text{ T.L. of C.I. } Z_O\right] : \text{ERSER}$$

$$::(1+\rho):\rho^2\left[1+\left(\frac{b}{a}\right)^{-1/\rho}\Big/\ 1 + \left(\frac{b}{a}\right)\right]+1$$

when allowance is made for the $\rho:1$ current step up in the outer $\lambda/4$ line (Fig. 3).

Plotting this in Fig. 3, ERSER is superior to an integral number of $\lambda/2$ S.C. T.L. up to $\rho=12$, when $b/a=20$. This is a good practical figure yielding $Z_O \doteq 180$ ohms and giving a reactance scaling-up of up to 6–7:1 compared with a $\lambda/2$ S.C. T.L. for $\rho \doteq 12$.

In conclusion, ERSER shows promise as a means of conveniently extending band-pass filters using T.L. elements into higher-impedance ranges than have previously been found convenient, and is useful for the B.P. correction of antiresonant antennas.

Note: Since preparing this note the writer has discovered the "compound line section,"[1] using two $\lambda/4$ lines in cascade. This is truly the inverse problem of the one studied here, in that Z_{O_1}/Z_O is made high in order to give a low-impedance wide-band short circuit.

The author wishes to thank the Australian Department of Civil Aviation for their support.

E. O. Willoughby
Elect. Engrg. Dept.
University of Adelaide
Adelaide, South Australia

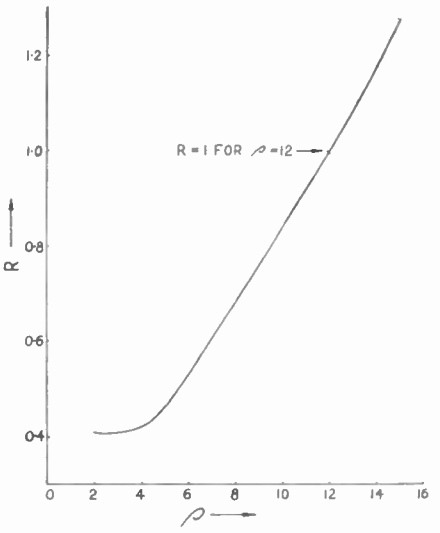

Fig. 3. R = insertion loss ratio of ERSER compared with the 0.5 $(\rho+1)$ λ/2 long short-circuited transmission line.

* Received by the IRE, June 23, 1961.

[1] Radio Research Laboratory, Harvard University Cambridge, Mass. "Very High Frequency Techniques," McGraw-Hill Book Co., Inc., New York, N. Y., vol. 2, p. 922; 1947.

Representation of Propagation Parameters for the Plasma in a Magnetic Field*

In a recent paper the properties of a uniform plasma for the propagation of electromagnetic waves were represented by curves plotted in the complex propagation plane.[1] The effect of a dc magnetic field can be shown by extending these curves to three-dimensional models in the way described below.

The complex propagation plane is represented by coordinates $A=(c/\omega)\alpha$ and $B=(c/\omega)\beta$, where α and β are the real and imaginary parts of the complex propagation constant and (c/ω) is the ratio of the velocity of light to the frequency of propagation. In the above-mentioned paper, the parameters plotted were the normalized collision frequency $Z=\nu/\omega$ where ν is the collision frequency and the normalized electron density $X=(\omega_p/\omega)^2$, where ω_p is the plasma frequency. The equations for the curves were derived from a conformal transformation of corresponding curves in the complex dielectric plane. These equations in turn were derived from the wave equation using the dielectric coefficient for a uniform plasma.

A later communication[2] indicated that by suitably choosing the normalized parameters to include the electron-cyclotron frequency ω_b these same curves could be used for the case of a plasma in the presence of a dc magnetic field. The purpose of this note is to point out that the original curves plotted in the complex propagation plane can be extended to three-dimensional models for the case of a dc magnetic field by introducing a third coordinate $Y=\omega_b/\omega$.

Appleton's equation for the complex refractive index of a magneto-ionic medium is given by[3]

$$n^2 = 1 - \frac{X}{1 - jZ - 1/2\dfrac{Y_y^2}{1 - X - jZ} \pm \left[1/4\dfrac{Y_y^4}{(1 - X - jZ)^2} \pm Y_z^2\right]^{1/2}}, \quad (1)$$

where X and Z are the normalized parameters defined above, and where

$Y_z=\omega_z/\omega$ = the normalized cyclotron frequency in the direction of propagation, z

$Y_y=\omega_y/\omega$ = the normalized cyclotron frequency in the y direction

$\omega_z=(e/m)B\cos\theta$

$\omega_y=(e/m)B\sin\theta$

θ = angle between the magnetic field B and the direction of propagation z.

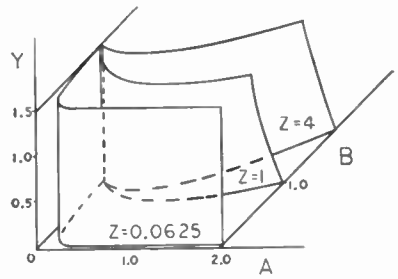

Fig. 1—Collision frequency model ordinary wave.
$A=(c/\omega)\alpha$ = normalized attenuation constant.
$B=(c/\omega)\beta$ = normalized phase-shift constant.
$Y=\omega_z/\omega$ = normalized cyclotron frequency.
$Z=\nu/\omega$ = normalized collision frequency.

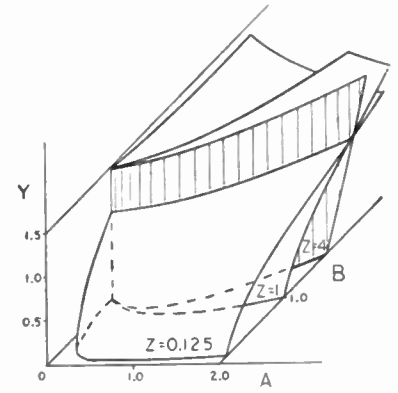

Fig. 2—Collision frequency model extraordinary wave.
$A=(c/\omega)\alpha$ = normalized attenuation constant.
$B=(c/\omega)\beta$ = normalized phase-shift constant.
$Y=\omega_z/\omega$ = normalized cyclotron frequency.
$Z=\nu/\omega$ = normalized collision frequency.

For the case of a longitudinal magnetic field, $Y_y=0$, $Y_z=Y$ and (1) reduces to

$$n^2 = 1 - \frac{X}{1 - jZ \pm Y}. \quad (2)$$

Since the square of the refractive index is equal to the dielectric coefficient, one can rationalize the right-hand side of (2) and equate the real and imaginary parts to K_r and K_i, the real and imaginary parts of the dielectric coefficient K. A conformal transformation from the complex dielectric plane to the complex propagation plane yields the following two equations for the normalized collision frequency case and for the normalized electron density case.

$$B^2 - A^2 + \frac{2AB(1 \pm Y)}{Z} = 1. \quad (3)$$

$$(A^2 + B^2)^2 - \left(2 - \frac{X}{1 \pm Y}\right)(B^2 - A^2) + \left(1 - \frac{X}{1 \pm Y}\right) = 0. \quad (4)$$

For the special case of no magnetic field these equations reduce to equations (12b) and (13b) of Bachynski.[1] They are also consistent with the redefined parameters of Bachynski.[2] Plots of (3) and (4) are shown in Figs. 1–4 where surfaces are formed for different values of Z and X. The plus sign in (3) and (4) corresponds to propagation of the ordinary wave, while the minus sign corresponds to propagation of the extraordinary wave.

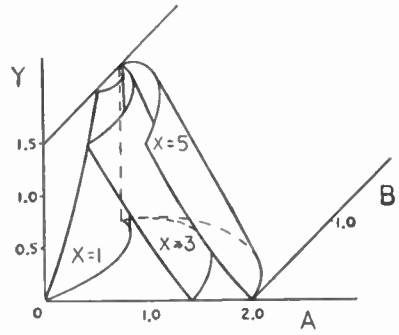

Fig. 3—Electron density model ordinary wave.
$A=(c/\omega)\alpha$ = normalized attenuation constant.
$B=(c/\omega)\beta$ = normalized phase-shift constant.
$Y=\omega_z/\omega$ = normalized cyclotron frequency.
$X=(\omega_p/\omega)^2$ = normalized electron density.

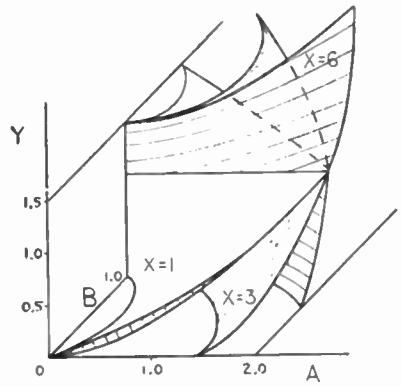

Fig. 4—Electron density model extraordinary wave.
$A=(c/\omega)\alpha$ = normalized attenuation constant.
$B=(c/\omega)\beta$ = normalized phase-shift constant.
$Y=\omega_z/\omega$ = normalized cyclotron frequency.
$X=(\omega_p/\omega)^2$ = normalized electron density.

R. E. Haskell
E. H. Holt
Rensselaer Polytechnic Institute
Troy, N. Y.

* Received by the IRE, June 30, 1961. This work was partially supported by NASA under research grant no. NsG 48-60.

[1] M. P. Bachynski, *et al.*, "Electromagnetic properties of high-temperature air," PROC. IRE, vol. 48, pp. 347–356; March, 1960.

[2] M. P. Bachynski, *et al.*, "Universal representation of electromagnetic parameters in presence of dc magnetic fields," PROC. IRE, vol. 49, pp. 354–355; January, 1961.

[3] J. A. Ratcliffe, "The Magneto-Ionic Theory and its Applications to the Ionosphere," Cambridge University Press, Cambridge, England; 1959.

Study of Electromagnetic Wave Polarization in Magneto-Plasmas by a Matrix Method of Crystal Optics*

In a series of papers Jones[1] has developed a method for treating the behavior of opti-

* Received by the IRE, June 30, 1961. This work was partially supported by NASA under research contract no. NsG 48-60.

[1] R. C. Jones, "A new calculus for the treatment of optical systems," *J. Opt. Soc. Am.*, vol. 31, pp. 488–503, July, 1941; vol. 32, pp. 486–493, August, 1942; vol. 37, pp. 107–112, February, 1947; vol. 38, pp. 671–684, August, 1948; vol. 46, pp. 126–131, February, 1956.

cal systems. We propose here a method for treating the study of electromagnetic wave propagation through magneto-plasmas by applying a modification of his method which is appropriate to the microwave region of the spectrum.

The method of Jones is based upon the assumption that the components of the electric field vector of the light wave leaving the system are linear functions of the electric field components of the wave entering the system. That is, if E_1 and E_2 are the complex components of a wave entering the system, then the output components of the wave, E_1' and E_2', are given by

$$\begin{bmatrix} E_1' \\ E_2' \end{bmatrix} = \begin{bmatrix} m_{11} & m_{12} \\ m_{21} & m_{22} \end{bmatrix} \begin{bmatrix} E_1 \\ E_2 \end{bmatrix}$$

or

$$E' = ME,$$

where M is a matrix characterizing the system.

Systems which act to alter the relationship between orthogonal components of an electromagnetic wave in the microwave region might usefully be characterized by such a matrix. A plasma in the presence of a dc magnetic field might be considered as such a system.

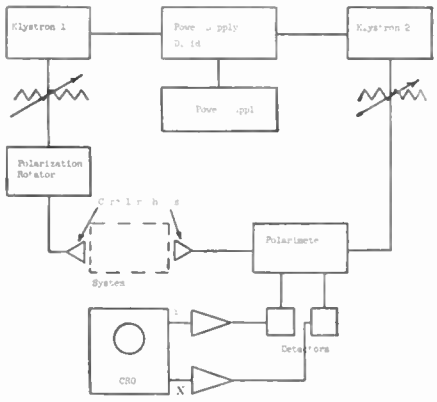

Fig. 1—Polarimeter microwave circuit.

A method for measuring the matrix has been proposed[2] for application in the optical regions. The ease with which the components of the electric field can be separated in a microwave circuit makes the measurement of the matrix M simpler at microwave frequencies.

By factoring out m_{22} three polarization measurements using a microwave polarimeter[3] will determine the matrix M to within the complex constant m_{22}. These measurements consist of measuring the output polarization for three differently oriented linearly polarized input signals. A block diagram of the microwave circuit is shown in Fig. 1. The complex constant m_{22} can be determined from a conventional attenuation and phase-shift measurement. This is done by orienting the rectangular guide of the receiving horn such that only the E_2' component is received when the input signal to the system is linearly polarized in the X_2 direction. In this way the matrix M can be uniquely determined.

R. E. Haskell
E. H. Holt
Rensselaer Polytechnic Institute
Troy, New York

[2] *Ibid.*, see vol. 37.
[3] P. J. Allen and R. D. Tompkins, "An instantaneous microwave polarimeter," Proc. IRE, vol. 47, pp. 1231–1237; July, 1959.

A Decoding Procedure for Double-Error Correcting Bose-Ray-Chaudhuri Codes*

A two-error correcting Bose-Ray-Chaudhuri Code[1] with m information bits has as Syndromes corresponding to a single error in the $(r+1)$th bit position the vector (x^r, x^{3r}), where x is the primitive element of the $GF(2^m)$ field. A double-error would give rise to the syndrome $(x^r+x^s, x^{3r}+x^{3s})$. If we call the two components of this vector m and n respectively, we have

$$n = (x^r + x^s)(x^{2r} + x^{r+s} + x^{2s})$$

$$m^3 = (x^r + x^s)(x^{2r} + x^{2s}),$$

or

$$1 + \frac{n}{m^3} = \frac{x^{r+s}}{x^{2r} + x^{2s}} = \frac{x^{2r+(s-r)}}{x^{2r}(1 + x^{2(s-r)})}$$

$$= \frac{x^{s-r}}{1 + x^{2(s-r)}} = f(s - r) \text{ (say)}.$$

It will be noticed that

$$f(s - r) = f(2^m - 1 - s + r),$$

so that a table containing only $2^{m-1}-1$ entries would set up a one-to-one correspondence between $1+(n/m^3)$ and $s-r$.

Also, $m=x^r(1+x^{s-r})$, so that the error positions r and s can both be obtained by the given manipulation of m and n.

As an example, the double-error correcting (15, 7) Bose-Ray-Chaudhuri code has as single error syndromes,

	1000 (1)	1000 (1)
	0100 (x)	0001 (x^3)
	0010 (x^2)	0011 (x^6)
*	0001 (x^3)	0101 (x^9)
	1100 (x^4)	1111 (x^{12})
	0110 (x^5)	1000 (1)
	0011 (x^6)	0001 (x^3)
*	1101 (x^7)	0011 (x^6)
	1010 (x^8)	0101 (x^9)
	0101 (x^9)	1111 (x^{12})
	1110 (x^{10})	1000 (1)
	0111 (x^{11})	0001 (x^3)
	1111 (x^{12})	0011 (x^6)
	1011 (x^{13})	0101 (x^9)
	1001 (x^{14})	1111 (x^{12})

and the correspondence between $s-r$ and $x^{s-r}/1+x^{2(s-r)}$ is as follows:

$s-r$	$\frac{x^{s-r}}{1+x^{2(s-r)}}$
1	x^8
2	x
3	x^5
4	x^2
5	1
6	x^{10}
7	x^4

Let there be an error in the positions shown by asterisks in the syndrome matrix so that the resulting syndrome, being the sum of the corresponding rows, is

$$1100(m = x^4)0110(n = x^5),$$

yielding

$$1 + \frac{n}{m^3} = 1 + \frac{x^5}{x^{12}} = 1 + x^8 = x^2,$$

whence we have from the table of correspondence $s-r=4$, *i.e.*, there is a distance of four bits between the error positions.

Again,

$$x^r = \frac{m}{1 + x^4} = \frac{x^4}{x} = x^3,$$

that is, $r=3$ yielding the error positions as 4 and 8.

In the case of single errors, $1+(n/m^3)$ will yield 0, so that the position of the error can be found from m above.

Unlike the Peterson Decoding Method,[2] this method cannot be easily generalized to a larger number of errors. However, in the special case of double-error correcting codes, the method is advantageous in involving no successive trials.

R. B. Banerji
Case Institute of Technology
Cleveland, Ohio

[2] W. W. Peterson, "Error Correcting Codes," Mass. Inst. Tech. Press, Cambridge, and John Wiley and Sons, Inc., New York, N. Y.; 1961.

Nonrealizability of the Complex Transformer*

In these Proceedings Carlin[1] has given a passive (and real) realization for the complex transformer at a single real frequency, $p_0=j\omega_0$. The question arises if such a transformer can be realized at a single complex frequency p_0 with Re $p_0>0$. This question is of importance because of the recent uses of such a device in the various branches of electrical engineering. In this connection

* Received by the IRE, July 17, 1961.
[1] R. C. Bose and D. K. Ray-Chaudhuri, "On a class of error correcting binary group codes," *Information and Control*, vol. 3, pp. 68–79; 1960.

* Received by the IRE, July 10, 1961.
[1] H. J. Carlin, "On the physical realizability of linear non-reciprocal networks," Proc. IRE, vol. 43, pp. 608–616; May, 1955. (See p. 611.)

Edelmann[2] has used them for visualizing the various transformations of power engineering. Bello[3] has used them to interpret the energy functions of nonreciprocal systems, and Belevitch[4] has incorporated them in an ingenious extension of the Brune synthesis to nonreciprocal networks. We will show that *Carlin's result does not extend to p_0 with* Re $p_0>0$.

Let a superscript asterisk denote complex conjugation and a superscript tilde denote matrix transposition. A device described by

$$V_2 = NV_1$$
$$I_1 = -\tilde{N}^* I_2, \qquad (1)$$

with the V's and I's n-vectors and N an $n\times n$ complex constant matrix, is called a complex transformer $2n$-port (here we assume that N is not real). By properly loading such a device by an n-port of admittance matrix Y_2, we can obtain an input admittance of

$$Y_1 = \tilde{N}^* Y_2 N. \qquad (2)$$

Further we have for the complex transformer itself

$$\tilde{V}_2^* I_2 + \tilde{V}_1^* I_1 = 0. \qquad (3)$$

Interpreting the components of the V's and I's as phasors, this last equation states that the average power input in the sinusoidal steady state is zero. Thus, the complex transformer has several of the useful properties of the real transformer.

We can now apply the result of Desoer and Kuh[5] which states that a network is passive at p_0 with Re $p_0\geq 0$, if and only if, $q_-(p_0)\geq 0$. For our purposes it is more convenient to use a generalization of q_- defined by

$$Q_-(V, I, p) = \begin{cases} 1/2[\tilde{V}^* I + \tilde{I}^* V] & \\ -(\sigma/|p|)|\tilde{V} I| & \text{if } \omega \neq 0 \\ 1/2[\tilde{V}^* I + \tilde{I}^* V] & \text{if } \omega = 0. \end{cases} \qquad (4)$$

Here $|\ |$ denotes the absolute value. In Newcomb,[6] it is shown that the inequality $Q_-(V, I, p_0)\geq 0$ must hold for every V and I if the network is to be passive at p_0. By using (3) and its complex conjugate transpose, we obtain for the complex transformer

$$Q_-(V, I, p) = \begin{cases} -(\sigma/|p|)|\tilde{V} I| & \text{if } \omega \neq 0 \\ 0 & \text{if } \omega = 0. \end{cases} \qquad (5)$$

Clearly, if $\sigma_0>0$, $\omega_0\neq 0$, then $Q_-(V, I, p_0)<0$ and the network is not passive at p_0. As a consequence the complex transformer can't be realized at p_0 by passive, real elements.

It should be observed that $Q_-(V, I, j\omega)=0$ which, because of the synthesis method of Newcomb,[7] coincides with Carlin's result. Further for $\sigma_0>0$, but $\omega=0$, the device doesn't have real elements and can't be realized at a fixed frequency $p_0=\sigma_0$ even though $Q_-(V, I, \sigma_0)=0$. An alternate derivation of the "activity" of the complex transformer is found in Newcomb.[8]

The author is indebted to the National Science Foundation for the support of this work and Profs. Kuh and Desoer for their interest and guidance.

R. W. Newcomb
Dept. of Elec. Engrg.
Stanford University
Stanford, Calif.

[2] H. Edelmann, "Über die Anwendung von Übertragermatrizen in untersuchungen auf dem Netzmodell," *Arch. elekt. Übertragung*, vol. 11, pp. 149–158; April, 1957.
[3] P. Bello, "Extension of Brune's energy function approach to the study of LLF networks," IRE Trans. on Circuit Theory, vol. CT-7, pp. 270–280; September, 1960. (See p. 273.)
[4] V. Belevitch, "On the Brune process for n-ports," IRE Trans. on Circuit Theory, vol. CT-7, pp. 280–296; September, 1960. (See p. 284.)
[5] C. A. Desoer and E. S. Kuh, "Bounds on natural frequencies of linear active networks," *Proc. of the Polytechnic Inst. of Brooklyn Symp.*, vol. X, pp. 415–436; 1960. (See p. 425.)
[6] R. W. Newcomb, "Synthesis of Networks Passive at p_0," University of California, Berkeley, ERL Rept., Series 60, Issue No. 317; September, 1960. (See p. 2.)
[7] *Ibid.*, p. 26.
[8] *Ibid.*, p. 25.

Tunnel-Diode Super-Regenerative Parametric Motor*

In an effort to harness the stimulance of a diode into rotary motion while maintaining the contact-free operation of the parametric motor, the author has carried out measurements on tunnel diodes and built a number of electro-mechanical devices.[1–3] The basic case of resistive load and maintained stability is shown in Fig. 1(a). If the load consists of a tuned circuit of proper inductance and capacitance, and if the dissipation of the system is sufficiently reduced, supersonic or high audio-frequency oscillations can be obtained, provided that the bias voltage is made to exceed the peak-point value V_p, but not the valley-point value V_v. The circuitry with diode and load in series connection is then largely that shown in Fig. 1(b), for which the steady-state frequency to a first approximation may be written

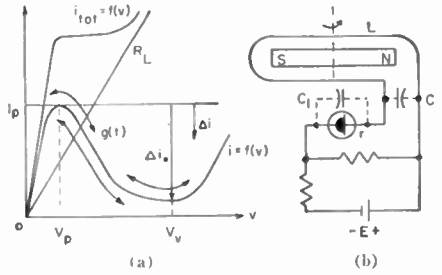

Fig. 1—(a) Tunnel-diode characteristics with possible variational bias ranges. (b) A simple scheme for turning tunnel-diode stimulance into rotary motion.

$$f_0 \doteq \frac{1}{2\pi}\sqrt{\frac{1}{LC'} - \frac{g^2}{C_1 C'}}, \qquad (1)$$

where $C'=C+C_1$. If we now make the bias voltage variational and periodic around a chosen point, such as the peak point or the valley point, the tunnel diode will never settle down to the value f_0 in (1); on the contrary, it produces a Fourier spectrum of frequencies. Swinging into the negative-slope region in Fig. 1(a), we encounter a growing transient wave train with an instantaneous amplitude associated with the downwards current deflection Δi. The wave-train instantaneous amplitude $i(t)$ is in the interval of interest almost proportional to Δi, so that we may write to a first approximation $i(t)\doteq K[1-\exp(-t/T)]$, where T is the time constant pertaining to the supersonic wave-train envelope. We observe that the generated stimulance is far from constant, taking the form of the time function

$$g(t) = g + \sum_{p=1}^{\infty} g_{p\max}\cos(p2\pi ft + \phi_p). \qquad (2)$$

The net effect of a periodic bias voltage is a varying negative conductance, going through a maximum, the subsequent quenching action that makes the magnetic field appear and vanish in a periodic fashion, and the ensuing supersonic growing and decaying wave train of variational frequency. Utilizing these facts for the accomplishment of rotary motion, we may now formulate a simple question: how can we make an alternating field in an inductor do mechanical work in such a manner that a periodic induced EMF and bias voltage results, all within the realms of the source power, secured from the negative-conductance slope of the tunnel diode? The simple answer appears in Fig. 1(b). If here the inductor contains a spinning magnet NS, the pulses of magnetic field will maintain the magnet in rotation, with the induced EMF of the spinning magnet providing the periodic bias voltage. This new electric motor has only three essential parts: the inductor L with its winding capacitance C, the rotor-magnet NS, and the tunnel diode.[4] The speed of the motor is governed by the time constant T of the wave-train envelope, and the speed is therefore quite constant. Due to the quenching action the operation is said to be superregenerative; the response on a CRO is quite typical for that of a super-regenerative device.

Parametric action appears in more than one respect. For an elementary system that may be represented by a single mesh with inductance and capacitance, loss resistance R, and slope-achieved stimulance R_N, there is a considerable change in inductance due to the rotation of the magnet, as is partly evident from the extensive change in pitch of the supersonic oscillation. A first approach integro-differential equation may therefore be written in the form

$$L\frac{di}{dt} + \left(\frac{dL}{dt} + R_n + R\right)i + \Gamma\int idt = e(t). \qquad (3)$$

* Received by the IRE, July 20, 1961.
[1] H. E. Stockman, "Parametric oscillatory and rotary motion," Proc. IRE (Correspondence), vol. 48, pp. 1157–1158; June, 1960.
[2] H. E. Stockman, "Parametric variable-capacitor motor," Proc. IRE (Correspondence), vol. 49, pp. 970–971; May, 1961.
[3] H. E. Stockman, "Electric field motor" and "Tunnel diode electromechanical movement," U. S. Patent applications of January 26, 1961, and July 12, 1961.
[4] Made by Sine-Ser Co., Waltham, Mass.

We may here rely on dL/dt and R_Y to cancel R, but in a different mode of operation we may rely on R_Y alone to cancel the sum of dL/dt and R. The peculiar modes and the mode-switching of this motor leads to rather intricate equations in any effort of analyzing the motor operation.

This is probably the world's simplest dc motor and electronics motor, but it is essentially of interest because of its constant speed and "indestructible" design. One can actually make the speed increase slightly as the battery ages. The tunnel diode is almost independent of nuclear radiation; a fact of interest in space applications. Generally the motor then has small power requirements, and may be operated from thermoelectric generators, atomic batteries, and solar cells of the type used in space vehicles. If a restoring force is applied to the moving magnet, pendulum oscillations result. These are of theoretical interest since they start to build up from building-noise level.

HARRY E. STOCKMAN
Elec. Engrg. Dept.
Lowell Technological Institute
Lowell, Mass.

An Adaptive Communications Filter*

Considerable interest has been expressed recently in the application of adaptive filters to communication problems.[1] The literature has described techniques that allow a matched filter for an unknown repetitive signal to be synthesized using information obtained from measurements of the signal and noise. Perhaps a more useful filter might be one which is optimum for a completely random communication signal (such as a random telegraph wave). Here the problem is not "optimum detection" as in a matched filter problem, but "optimum filtering."

Such a filter is described in this note. It is one of several known techniques that attempt to adjust for minimum mean-square error. Assume that the filter is to be of the form shown in Fig. 1. It is desired to adjust the potentiometers, a_i, to give minimum mean-square error. The number of taps, k_0, is fixed. The transfer function of the filter is

$$G(Z) = \sum_0^{k_0} a_n Z^{-n} \tag{1}$$

The equation for the mean-square error may be obtained from the block diagram of Fig. 2. This equation is well known and is[2]

$$\overline{e^2} = R_S(0) + \frac{T}{2\pi j}\oint_\Gamma \cdot \left\{S_{ii}(Z)\left[\sum_0^{k_0} a_n Z^{-n}\sum_0^{k_0} a_n Z^{n}\right] - \sum_0^{k_0} a_n(Z^{-n}+Z^{n})S_{ss}(Z)\right\}\frac{dZ}{Z} \tag{2}$$

where $R_S(\tau)$ is the signal autocorrelation function, $S_{ii}(Z)$ is the sampled noise plus signal spectrum, $S_{ss}(Z)$ is the sampled signal spectrum, and the integration is around the unit circle. Uncorrelated signal and noise is assumed.

The optimum setting for a_i may be found by setting the partial of $\overline{e^2}$ with respect to a_i equal to zero and solving for a_i:

$$\frac{\partial\overline{e^2}}{\partial a_i} = \frac{T}{2\pi j}\oint_\Gamma \frac{dZ}{Z}\left\{S_{ii}(Z)\left[Z^{i}\sum_0^{k_0} a_n Z^{-n} + Z^{-i}\sum_0^{k_0} a_n Z^{n}\right] - S_{ss}(Z)\left[Z^{i}+Z^{-i}\right]\right\}$$

$$= \frac{T}{2\pi j}\oint_\Gamma \frac{dZ}{Z}\left\{S_{ii}(Z)Z^{i}\left[\sum_0^{k_0} a_n Z^{-n} - \frac{S_{ss}(Z)}{S_{ii}(Z)}\right]\right\} + \frac{T}{2\pi j}\oint_\Gamma \frac{dZ}{Z}\left\{S_{ii}(Z)Z^{-i}\left[\sum_0^{k_0} a_n Z^{n} - \frac{S_{ss}(Z)}{S_{ii}(Z)}\right]\right\} = 0. \tag{3}$$

Parseval's theorem for discrete systems is

$$\frac{1}{2\pi j}\oint_\Gamma F_1(Z)F_2(Z^{-1})\frac{dZ}{Z} = \frac{1}{2\pi j}\oint_\Gamma F_1(Z^{-1})F_2(Z)\frac{dZ}{Z} = \sum_{-\infty}^{+\infty} f_1(nT)f_2(nT). \tag{4}$$

Then a solution to (3) is

$$\frac{1}{2\pi j}\oint_\Gamma \frac{dZ}{Z}\left\{S_{ii}(Z)Z^{i}\left[\sum_0^{k_0} a_n Z^{-n} - \frac{S_{ss}(Z)}{S_{ii}(Z)}\right]\right\} = \frac{1}{2\pi j}\oint_\Gamma \frac{dZ}{Z}S_{ii}(Z)\sum_0^{k_0} a_n Z^{i-n} - \frac{1}{2\pi j}\oint_\Gamma S_{ss}(Z)Z^{i}\frac{dZ}{Z} = 0. \tag{5}$$

Again using Parseval's theorem

$$\frac{1}{2\pi j}\oint_\Gamma \frac{dZ}{Z}S_{ii}(Z)\sum_0^{k_0} a_n Z^{i-n} = \sum_{n=0}^{k_0} R_{S+N}[(n-i)T]\frac{a_n}{T}. \tag{6}$$

$R_{S+N}(T)$ is the signal-plus-noise autocorrelation function. Taking the inverse,

$$\frac{1}{2\pi j}\oint_\Gamma S_{ss}(Z)Z^{i}\frac{dZ}{Z} = \frac{R_S(iT)}{T}. \tag{7}$$

Thus, we have (k_0+1) equations of the form

$$\sum_{n=0}^{k_0} a_n R_{S+N}[(n-i)T] = R_S(iT). \tag{8}$$

Expressed in matrix form this is

$$\begin{bmatrix} R_{S+N}(0) & R_{S+N}(T) & R_{S+N}(2T) & \cdots & R_{S+N}(k_0T) \\ R_{S+N}(T) & R_{S+N}(0) & R_{S+N}(T) & & \cdot \\ R_{S+N}(2T) & R_{S+N}(T) & R_{S+N}(0) & & \cdot \\ \cdot & \cdot & & \cdot & \cdot \\ \cdot & \cdot & & \cdot & \cdot \\ \cdot & & & \cdot & \cdot \\ R_{S+N}(k_0T) & \cdots & \cdots & \cdots & R_{S+N}(0) \end{bmatrix}\begin{bmatrix} a_0 \\ a_1 \\ a_2 \\ \cdot \\ \cdot \\ \cdot \\ a_{k_0} \end{bmatrix} = \begin{bmatrix} R_S(0) \\ R_S(T) \\ R_S(2T) \\ \cdot \\ \cdot \\ \cdot \\ R_S(k_0T) \end{bmatrix} \tag{9}$$

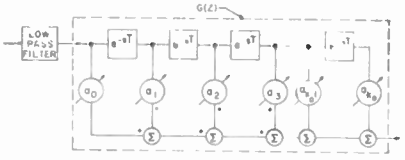

Fig. 1—A tapped delay-line filter.

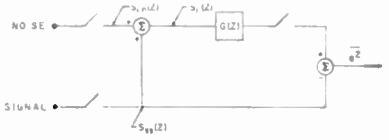

Fig. 2—The mean-squared error.

Eq. (9) shows that for a tapped delay line filter of length k_0T with no feedback, no autocorrelation for τ greater than k_0T is needed. The converse is not true, however. Even if the autocorrelations are zero for $\tau < k_1T$, the longer the length of the delay line, in general, the better the results. Eqs. (9) may be modified for some other operations on the signal. For example, if prediction is desired, $R_S(iT)$ should be replaced with $R_S[(m+i)T]$, where mT is the prediction time.

The block diagram for measuring the autocorrelation functions is shown in Fig. 3. The tapped delay line could also serve as the line used in the synthesis of the filter. Uncorrelated additive signal and noise are assumed. It is further assumed that the noise is stationary, or that its time-varying autocorrelation is known. This is a valid

* Received by the IRE, July 7, 1961.

[1] E. M. Glaser, "Signal detection by adaptive filters," IRE TRANS. ON INFORMATION THEORY, vol. IT-7, pp. 87–88; April, 1961.

[2] J. R. Ragazzini and G. F. Franklin, "Sampled-Data Control Systems," McGraw-Hill Book Co., Inc., New York, N. Y., ch. 10; 1958.

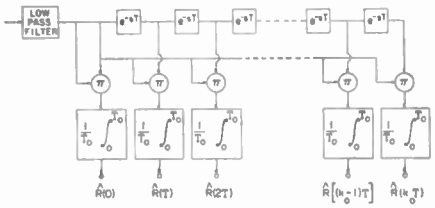

Fig. 3—Measuring the autocorrelation functions.

assumption under most practical circumstances. In fact the low-pass filter of Fig. 1 can usually be adjusted to give a noise autocorrelation that is zero for $\tau = nT$; $n \neq 0$. If the noise is stationary and no signal is present, $R_N(nT)$ is estimated and this information is stored. Then continuous estimates of $R_{S+N}(nT)$ are made. $R_S(nT)$ is

$$\hat{R}_S(nT) = \hat{R}_{S+N}(nT) - \hat{R}_N(nT). \quad (10)$$

Of course, if the signal is stationary, T_0 can be made very large and good estimates of $R_S(nT)$ will be available.

If the low-pass filter cuts off at W cps, then T, the delay between taps, should be less than $1/2W$. For a small number of taps, conceptually, the complete filter could be built on an analog computer. However, a useful filter most likely will always be constructed on a digital computer. Routines are available for easily solving 100 linear simultaneous equations, and a 100-tap delay line makes possible a complicated $G(z)$.

If $f(nT)$ is the sampled input to the computer, and $C(nT)$ is to be the sampled filter output, the $C(nT)$ and $f(nT)$ are related by the simple difference equation:

$$C(nT) = a_0 f(nT) + a_1 f[(n-1)T] + a_2 f[(n-2)T] + \cdots + a_{k_0} f[(n-k_0)T]. \quad (11)$$

This is the digital computer simulation of $G(Z)$. The sampling theorem shows

$$\frac{1}{T_0}\int_0^{T_0} f(t+nT)f(t)dt = \frac{1}{2WT_0}\sum_{m=0}^{2WT_0} f(mT)f[(m+n)T]. \quad (12)$$

Therefore, the operations of Fig. 3 can easily be simulated digitally. A low-pass filter of bandwidth W should precede the analog-to-digital converter.

In rare cases, the square matrix of (9) could be singular. For example, if a no-noise signal were periodic exactly at the sampling frequency, two rows of the matrix would be identical. These situations should be of no practical interest.

ACKNOWLEDGMENT

Special thanks are due R. Lawhorn and Dr. G. Franklin for their very helpful conversations and criticisms.

C. S. WEAVER
Philco Corp.
Western Dev. Labs.
Palo Alto, Calif.

Contributors

William Ross Aiken (S'46–A–48–M'55) was born on Maui, Hawaii, on February 19, 1919. He received the B.S.E.E. degree from the University of California, Berkeley, in 1946.

W. R. AIKEN

During World War II he supervised electronic activities at the Kaiser Shipyards, Richmond, Calif. After the war he organized the Ross Radio Corporation, Los Altos Hills, Calif., which specializes in custom-made radios, television sets, and industrial electronics. In 1948 he joined the staff of the University of California Radiation Laboratory, Berkeley, where he developed electronic controls for large nuclear accelerators. He participated in a classified project for the Atomic Energy Commission overseas as a Group Leader in 1951. Upon his return he assumed charge of the Special Problems Group at the Radiation Laboratory. He is the inventor of the Kaiser-Aiken thin cathode-ray tube. He has held his present position as Director of Research for the Kaiser Aircraft and Electronics Corporation, West Coast Electronics Laboratory, Palo Alto, Calif., since 1953.

Knut Endresen was born in Tönsberg, Norway, on February 26, 1927. He received the degree of sivilingeniör (M.Sc.) in telecommunication engineering from the Technical University of Norway, Trondheim, in 1950.

K. ENDRESEN

He was employed as a Science Assistant in telecommunications at the Technical University of Norway until 1951. Since 1951 he has been with the Norwegian Defence Research Establishment, Division for Telecommunication, Lillestrom, Norway. He spent the year 1954–1955 as a postgraduate student at the Imperial College, London, England. He is now a Senior Research Engineer. His field of work is military electronics where his main activity is in radio and radar interference problems.

Mr. Endresen is an Avionics Panel member of the NATO Advisory Group for Aeronautical Research and Development.

❖

Rolf Hedemark (A'60) was born in Bærum, Norway, on July 30, 1934. He received the degree of sivilingeniör (M.Sc.) in telecommunication engineering from the Technical University of Norway, Trondheim, in 1957.

R. HEDEMARK

He joined the Norwegian Defence Research Establishment, Division for Telecommunication, Lillestrom, Norway, in 1957 as a Research Engineer. He is active in the field of military electronics, particularly interference problems, such as the behavior of linear and nonlinear communication and radar systems subjected to heavy interference of various types.

❖

John C. Helmer was born in Evanston, Ill., on November 18, 1926. He received the B.S. degree in mathematics from Lawrence College, Appleton, Wis., in 1950, and the M.S. degree in physics from the California Institute of Technology, Pasadena, in 1952. In 1957 he was awarded the Ph.D. degree in electrical engineering from Stanford University, Stanford, Calif.

From 1951 to 1952 he worked on com-

puter circuit design at Northrop Aircraft Company, Los Angeles, Calif. In 1953 he was engaged in microwave relay research at the Bell Telephone Laboratories, Murray Hill, N. J. From 1953 to 1956 he was a Research Assistant in microwave physics at Stanford. Since 1956 he has been doing research in physical electronics at the Central Research Department of Varian Associates, Palo Alto, Calif.

J. C. HELMER

Dr. Helmer is a member of Phi Beta Kappa, Tau Beta Pi, Sigma Xi, and the American Physical Society.

❖

Leonard R. Kahn (S'46–M'51–SM'54) was born in New York, N. Y., on June 16, 1926. He received the B.E.E. degree from the Polytechnic Institute of Brooklyn, Brooklyn, N. Y., in 1951. He also studied at the Engineering School of Syracuse University, Syracuse, N. Y., and at New York University Law School. Since 1953 he has been a member of the Associated Teaching Staff of the Electrical Engineering Department of the Polytechnic Institute of Brooklyn, where he is presently an Adjunct Professor of electrical engineering.

L. R. KAHN

From 1944 to 1946 he served in the U. S. Army Signal Corps, and from 1947 to 1950 he was employed by RCA Communications, Inc., and was loaned to RCA laboratories during the last year of employment. From 1950 to 1952 he was employed by Crosby Laboratories, Inc. In 1952 he organized the Kahn Research Laboratories, where he is now President and Research Director.

He has conducted research and development on a number of original communication techniques, including single-side band transmission systems, tone converters, and other communications and television equipment. He has also served as Consultant to the Voice of America, Radio Free Europe, Willys Motors, Grumman Aircraft and Electronics, and Fairchild Engine and Airplane Corporation. He has a number of inventions in the communications field, including the ratio-squarer diversity system and television and communications transmitters.

Mr. Kahn is an associate member of the AIEE, a member of Tau Beta Pi, Eta Kappa Nu, Sigma Xi, and the AAAS, and a Fellow of the Radio Club of America.

❖

Kurt Schlesinger (A'41–SM'51–F'54) was born in Berlin, Germany, on April 20, 1906. He received the Diplom-Ingenieur degree in 1928 and the Doctor of Engineering degree in 1929, both from the Technische Hochschule in Berlin.

K. SCHLESINGER

For the next ten years he was active in television research in Europe. From 1941 to 1944 he was with RCA Laboratories, Purdue University, Lafayette, Ind., and from 1944 through 1947 he was Consulting Engineer in color television for CBS. He was head of a TV research department at Motorola, Inc., Chicago, Ill., from 1947 to 1958. At present he is Consulting Engineer for the Cathode Ray Tube Department of the General Electric Company, Syracuse, N. Y.

Dr. Schlesinger has served on NTSC committees charged with studies of dot interlace and color. He was a visiting Lecturer at Northwestern University, Evanston, Ill., in 1957.

❖

Charles Süsskind (S'47–A'52–M'53–SM'54) was born in Prague, Czechoslovakia, on August 19, 1921. He obtained his secondary eduction in that country and in Great Britain. He received the B.S. degree from the California Institute of Technology, Pasadena, in 1948, and the M.Eng. and Ph.D. degrees from Yale University, New Haven, Conn., in 1949 and 1951, respectively.

C. SÜSSKIND

His interest in the microwave field led to a doctoral dissertation on artificial dielectrics. An article based on this dissertation, published by the *Journal of the British IRE*, earned him the Clerk-Maxwell Premium for "the most outstanding paper published in the Institution's Journal" in 1952.

During the war, he served with the 8th Air Force in Europe as an airborne-radar specialist. From 1951 to 1955 he was a Research Associate at Stanford University, Stanford, Calif., and from 1953 to 1955 he was Assistant to the Director of Stanford's Microwave Laboratory and Lecturer in the Department of Electrical Engineering. In 1955 he joined the faculty of the University of California, Berkeley, where he is now Associate Professor of electrical engineering.

Dr. Süsskind is an associate member of the British IRE, and a member of the American Physical Society, the ASEE, The History of Science Society, the Society for the History of Technology, Sigma Xi, and Tau Beta Pi.

❖

Lofti A. Zadeh (S'45–A'47–SM'56–F'58) was born in Baku, Russia, on February 4, 1921. He attended the American College, Teheran, Iran, and received the B.S. degree in electrical engineering from the University of Teheran in 1942. He came to the United States in 1944 and entered the Massachusetts Institute of Technology, Cambridge, where he received the M.S. degree in 1946.

L. A. ZADEH

He joined the staff of Columbia University as an Instructor in electrical engineering and received the Ph.D. degree in 1949. He was promoted to Assistant Professor in 1950, Associate Professor in 1953, and became a full Professor in 1957. In 1956 he was a member of the Institute for Advanced Study, Princeton, N. J. At present he is Professor of electrical engineering at the University of California, Berkeley.

He has published papers on the subjects of time-varying networks, optimal filters, and nonlinear systems, with emphasis on the general principles underlying the transformation of signals and the characterization of input-output relationships. His main interest at present is in system theory.

Dr. Zadeh is Chairman of U. S. Commission VI and the International Scientific Radio Union, and a member of the AIEE, the American Mathematical Society, the American Physical Society, the Institute of Mathematical Statistics, the ACM, the Society for Industrial and Applied Mathematics, Tau Beta Pi, Eta Kappa Nu, and Sigma Xi.

Books

Wave Propagation in a Turbulent Medium, by V. I. Tatarski

Published (1961) by McGraw-Hill Book Co., Inc., 330 W. 42 St., N. Y. 36, N. Y. 257 pages+xiv pages+6 bibliography pages+2 appendix pages+22 pages notes and remarks. Illus. 7¼×10. $9.75.

In this extensive monograph the author not only has collected in one place the dispersed theories describing various aspects of wave propagation through irregular media; he also has attempted to relate these theories to physical processes that would likely be responsible for such irregularities of refractive index in the atmosphere. It is this tie between wave theory, on the one hand, and atmospheric physics, on the other, that will be especially valuable to research workers who must make observations in or through the atmosphere or who are interested in the structure of the atmosphere itself.

As is evident from the title, the author has singled out turbulence and turbulent processes for detailed analysis; and, though there may be some disagreement with the implications of this restriction, a thorough study of turbulent mechanisms and of the relation they bear to wave propagation phenomena is an important and valuable contribution.

Structure function methods and corresponding spectral analysis are employed throughout, as are the concepts of statistical turbulence theory. In fact, on the basis of referenced evidence, almost all of which is of Russian origin and which it is claimed provides convincing substantiation of the Kolmogoroff theory of locally isotropic turbulence, the author proceeds to relate each wave propagation process to the isotropic irregularity structure that he associates with such turbulence.

The book is divided into four parts: I. a review of statistical turbulence theory; II. scattering of electromagnetic and acoustic waves; III. detailed analysis of line-of-sight propagation, both by the method of geometrical optics and by the method of small perturbations; and IV. a comparison of theoretical results and experimental data. In Part II the standard single-scattering (Born) approximation is employed to calculate the scattered fields, which are expressed in terms of the spectral representation of the refractivity irregularities. Similarly in Part III solutions are developed for the usual logarithmic amplitude and phase functions and the intensity and structure of these variables are, in turn, evaluated through the spectral distribution of the refractivity. In both parts the results are generalized to include the important case of locally homogeneous fields.

Although Parts II and III contain much useful information and many important results, in the eyes of this reviewer it is Parts I and IV that give this book its true value. The detailed introduction to the theory of homogeneous and locally homogeneous random fields, the review of the statistical theory of turbulence and the discussion of its role in the study of atmospheric processes, and the development of a model for the turbulent mixing of passive, scalar quantities, such as moisture vapor, all of which are included in Part I, will be especially helpful to the worker with little or no background in turbulence. The empirical results presented and analyzed in Part IV, pertaining both to wind and temperature fluctuations in the atmosphere and to the structure of received acoustic and electromagnetic fields in actual propagation experiments, will provide the investigator with valuable insight that no amount of purely theoretical analysis could supplant.

In spite of its many strong features, this work is open to criticism for the manner in which problems of atmospheric turbulence have been oversimplified. The author appears to consider Kolmogoroff's theory of locally isotropic turbulence the panacea for all problems in which turbulence plays a role. He does not seem squarely to face the fact that, in the analysis of any real situation, one must clearly and carefully relate the small scale structure, which may perhaps be accurately described by that model, to the large scale anisotropic structure, which certainly cannot be properly represented in that way. He criticizes other authors for using phenomenological models of turbulence processes yet falls back on them himself, without comment, when in Chapter 10 he finally attempts to relate the large and small scale structures. One does not find fault with the author's analysis but rather with the manner in which he has approached it and with the impression he has thereby created that all the pertinent turbulence problems are solved by the Kolmogoroff theory, and that all that remains is the application of the results to various wave propagation situations.

This review could not close without brief comment on the translation. Dr. Silverman and the publisher have done another fine job in transcribing this work into English. It reads clearly and smoothly, a number of helpful explanatory comments have been added, and a minimum number of mechanical and editorial errors have been allowed to survive to final production. All in all, this is a valuable contribution, especially since it makes this otherwise inaccessible material, and an extensive bibliography on the subject, readily available to the Western scientific community.

Ralph Bolgiano, Jr.
School of Elec. Engrg.
Cornell University
Ithaca, N. Y.

Semiconductor Devices and Applications, by R. A. Greiner

Published (1961) by McGraw-Hill Book Co., Inc., 330 W. 42 St., New York 36, N. Y. 405 pages+5 index pages+xiv pages+12 references pages+43 appendix pages+5 pages postface. Illus. 6×9¼. $12.50.

This is another in the growing list of books which attempt to cover both semiconductor device principles and circuit applications. The book is almost equally divided between these two areas. The first half is devoted to a review of modern physics, semiconductors, conduction in semiconductors, semiconductor materials preparation, contacts, junctions, diodes, and transistors; the latter half is devoted to small signal and power amplifiers, dc amplifiers, oscillators, and switching and logic circuits. The treatment is roughly at the junior or senior level and is commendable in that the author attempts to interject device understanding into circuit understanding. The author's writing style is facile and his book easy to read.

Relative to the large number of very comprehensive books already available on semiconductors, semiconductor devices, and circuit applications of semiconductor devices, the book under review possesses a number of shortcomings. The first chapter on modern physics is too brief to be worth much to a student unacquainted with modern physics, and is unnecessary for the properly prepared student. In terms of modern device practice, a chapter entirely devoted to metal-semiconductor contacts is wasted and takes space needed for other topics. A number of statements in the first half of the book are either in error or give the wrong emphasis. For example, silicon has greater importance than germanium but not necessarily or completely because of its greater abundance and higher operating temperature; with silicon becoming more widely used than germanium, the most common method to measure lifetime is not the one stated; and a diffused impurity profile is not generally exponential. In places throughout the book strange terminology (strange to a student) is introduced without explanation or any references. Some concepts or formulas are presented without explanation or references and cannot but confuse the student or make him wonder why he doesn't grasp "the obvious." Unfortunately, many of the more powerful concepts introduced by Shockley in analyzing junctions are not included and apparently must be supplied by the classroom instructor. As mentioned, considerable space is given to metal-semiconductor contacts, and important matters such as minority carrier lifetime are not fully developed. In spite of the generality of the title, hardly any devices besides junction diodes and transistors are considered in the text proper.

Despite the limitations of this book, it should be found useful as an aid in instructing students unfamiliar with semiconductor devices and who quite likely intend to specialize in circuit applications. The experienced instructor will know what to add, what to delete, and what to correct, including misspellings of the well-known names Stirling and Hankel.

Nick Holonyak, Jr.
Semiconductor Products Dept.
General Electric Co.
Syracuse, N. Y.

Philosophical Impact of Contemporary Physics, by Milič Čapek

Published (1961) by D. Van Nostrand Co., Inc., 120 Alexander St., Princeton, N. J. 399 pages+15 index pages+vxii pages. 6×9¼. $7.50.

The primary purpose of this book is to bring into full focus the contrast between the classical and modern conceptual frameworks of physics. The book begins with a systematic examination of the fundamental classical concepts of space, time, matter, motion, and causality. These concepts and their mutual relations are discussed, and their connection with the philosophical thought of the period are expounded. The radical differences between the new concepts and their classical counterparts are explained, and misinterpretations due to the survival of the classical habits of thought are criticized.

The author of this book is well versed in both philosophy and physics, and is eminently qualified for the rather difficult interdisciplinary task which he has set himself. Currently, Professor of Philosophy at Carleton College in Northfield, Minn., the author formerly taught physics at Doane College, the University of Nebraska, and the University of Olmutz (Olomouc) in Czechoslovakia.

In principle, this book is intended both for students of philosophy interested in learning more about physics, and students of physics interested in gaining a deeper appreciation of the philosophical implications of their subject. In practice, the book will probably appeal more to the former group than to the latter, since it is written with a strong philosophical orientation. While the present reviewer found this book most worthwhile, he did not find it as incisive or illuminating as other books on the same general subject, such as Margenau's "The Nature of Physical Reality." Nevertheless, he feels the present author has made a significant contribution to the borderline area of physics and philosophy.

Frank Herman
RCA Labs.
Princeton, N. J.

Microwave Ferrites, by P. J. B. Clarricoats

Published (1961) by John Wiley and Sons, Inc., 440 Park Avenue S., New York 16, N. Y. 253 pages+4 index pages+xi pages+references by chapter. Illus. 6¼×10. $8.00.

This book contains an introductory chapter on general properties of ferrites, chapters on microwave behavior of ferrites and loss mechanisms in ferrites, a long chapter on propagation in media containing ferrites and a chapter describing briefly some microwave ferrite devices. The material in the first three chapters mentioned above may well be the most useful, although about forty percent of the book is the propagation chapter which discusses the boundary value problems involved in various configurations. It is good to have this material brought together in one place with a consistent notation, although the components designers for whom the book is intended have generally used empirical methods because of the complexity of the analytical results. In this connection, the use of mathematical appendixes makes the text of the book relatively easy to read.

In a book such as this, one might have hoped to find a discussion of nonlinear effects, but the subject is mentioned only briefly in connection with loss mechanisms.

Workers in the field are forced to adapt themselves to a mixture of cgs units and mks units, and the author has chosen to go along with the usual mixture. Two chapters on ferrite properties use cgs units, and the rest of the book uses mks units except that magnetic field strength is quoted in oersteds, and occasionally such terms as db per inch are used.

This book is definitely not intended as a designer's handbook. The emphasis on the analytical results makes it rather specialized. However, the exposition is clear and workers in the area of microwave ferrites should look at the book and may well want to own it.

E. H. Turner
Bell Telephone Labs., Inc.
Holmdel N. J.

Foundation for Electric Network Theory, by Myril B. Reed

Published (1961) by Prentice-Hall, Inc., Englewood Cliffs, N. J. 323 pages+5 index pages+xii pages +28 appendix pages. Illus. 6¼×9¼. $13.00.

Professor Reed approaches resistive networks by way of linear graph theory. He states in the preface: " . . . this book may be used as a beginning course at the sophomore level or as an elective junior or senior course. It can also be used as supplementary or reference material for senior courses, graduate courses, and self or formal training of engineers in industry."

The first major division of the book, Chapters 2 through 8, deals with linear graph theory as the foundation for formulating a set of linear simultaneous equations relating the voltage variables and current variables in a graph by Kirchhoff's laws. The second major part, Chapters 10 through 14, uses the results of the first part to derive properties of resistive networks. Chapter 1 gives some introductory material; Chapter 9 discusses such topics as energy, power, rms, and average; and the appendix presents an introduction to matrix algebra.

Within the domain of material selected, the arrangement is logical and, with the help of many illustrative examples, the explanations are very clear. There are many problems at the end of every chapter, including the appendix, to enable the student to digest the material.

Although Professor Reed claims to operate from a "near-rigorous basis," so as to give the students the solidest possible foundation, many theorems are listed as properties and presented without proof, on the ground that a "working knowledge" is being presented. In the reviewer's opinion, this leaves the students with many unexplained mysteries. Therefore, it is doubtful whether it really is worthwhile to go into the detailed properties of linear graphs at length, as is done in this book, instead of introducing just a few of the necessary concepts to enable the student to apply Kirchhoff's laws to networks as is done in Professor Guillemin's book "Introductory Circuit Theory." It is true that a student using Professor Guillemin's book has to accept, without a "rigorous" proof, that the set of equations obtained is independent. It is equally true, however, that a student using Professor Reed's book would have to take for granted that the coefficient matrices in equations (6.3.1) and (6.3.2) are non-singular.

There are some minor criticisms:

1) It is rather disappointing that Professor Reed does not include a discussion of node-pair analysis based on cut-set matrices.
2) Because of the number of symbols used in the book, a list of symbols at the end would be very helpful.
3) In the appendix, a matrix is defined as an array of entries of quite general nature, *viz.*, symbols, operators, etc. But later, in the proofs of the various properties of associativity, commutativity, and distributivity of matrix operations, nothing is mentioned about the necessary assumptions on the operations of the individual entries.
4) According to definition 1.11.2, a negative resistor would be classified as a passive element.
5) Although the statements about reciprocity (properties 10.4.1 and 10.4.2) implicitly exclude so-called controlled sources from the network, the nonreciprocal nature of vacuum tube and transistor circuits are not specifically mentioned.
6) It is somewhat confusing that, in Chapter 1, lower case letters a and b are used both to describe meter readings made on an element and to designate the terminals of an element.

In conclusion, it is the opinion of this reviewer that if this book is to be used fruitfully as a sophomore text, much guidance from the instructor is needed.

Bede Liu
Bell Telephone Labs.
Murray Hill, N. J.

Plasma Acceleration—The Fourth Lockheed Symposium on Magnetohydrodynamics, Sidney W Kash, Ed.

Published (1960) by Stanford University Press, Stanford, Calif. 117 pages+vii pages+bibliography by chapter. Illus. 6¼×9¼. $4.25.

The book is a compilation of nine papers presented at the Fourth Symposium on Magnetohydrodynamics at the Lockheed Missile and Space Division on December 2, 1959. The first two papers discuss steady-state acceleration of plasma by crossed electric and magnetic fields. In one system, the magnetic field is derived by currents in the plasma; and, in the other, it is externally applied. In the third paper are derived scaling relations for devices employing fully ionized gases. In the fourth paper, plasma acceleration by a continuous train of transverse magnetic waves in an electrodeless rectangular duct is investigated. The next four papers deal with the pulsed plasma accelerators which utilize the energy obtained in the discharge of high energy capacitors. The last paper discusses the acceleration of

ionized material by purely electrostatic means; a novel electrode arrangement is presented and problems in the design of the electrostatic accelerator are analyzed.

The book will be of interest to physicists and electronic engineers who are concerned with space vehicle propulsion or laboratory test "tunnels."

CONRAD H. HOEPPNER
Electronetics Corp.
Melbourne, Fla.

Transmission of Information, by Robert M. Fano

Published (1961) by The Technology Press, Mass. Inst. Tech., Cambridge, and John Wiley and Sons, Inc., 440 Park Ave. South, New York 16, N. Y. 340 pages +3 index pages +x pages +43 appendix pages. Illus. 6×9¼. $7.50.

The author has been active in the field of information theory since its very beginnings and has taught a graduate course on the subject over the past ten years at the Massachusetts Institute of Technology. This book is an outgrowth of his lecture notes.

The scope of the book is indicated by the following list of chapter headings and a brief description of their content. The first chapter, "The Transmission of Information," is in fact an introduction. Communication systems are defined; and related problems, which form the subject of information theory, are outlined. The major result, existence and meaning of the channel capacity, is stated at this point in advance of a proof. Chapter 2, "A Measure of Information," introduces the concepts of mutual information, self-information and, by averaging over ensembles of events, the various entropies. The nomenclature used is in conformance with the IRE Standard on Information Theory.[1] In these Standards, however, "self-information" is also called "information content," and "mutual information" is called "transinformation." In Chapter 3, "Simple Message Ensembles," the encoding of an ensemble of messages is discussed. Optimum codes, which minimize the average length of the coded message, are constructed. In Chapter 4, "Discrete Stochastic Sources," *i.e.*, sequences of messages specified by some statistical properties, are considered. Encoding is used to define their rates. The important case of Markov sources is discussed in some detail. The next chapter, "Transmission Channels," describes and classifies simple models of channels and defines their capacity as the maximum mutual information per event between the input and the output, when the probability of the input events is varied. It is computed for discrete channels and time-discrete continuous channels with additive noise. Gaussian noise and band-limited channels are considered. In Chapter 6, "Channel Encoding and Decoding," it is shown that, for some channels, the capacity defined by means of the mutual information is also the upper limit to the rates of transmission that can be approached with an arbitrary small probability of error. Conversely, a rate of transmission larger than the capacity implies a finite rate of error. The three remaining chapters treat of encoding and decoding for transmission through discrete constant channels. Chapter 7 is "Encoding for Binary Symmetric Channels," and Chapter 9, "Encoding for Discrete Constant Channels." In Chapter 8, "Multinomial Distributions," special mathematical techniques (tilted distributions) are introduced to solve the problems of upper and lower bounds for the probabilities of error in the last chapter.

The text is reproduced by photo-offset. Errors, beside those mentioned in the errata sheet, are very minor ones: in formula 7.63, p. 233, the exponent of $(1-p)$ should be $n-k$, and on page 355, problem 6.8 should be numbered 4.8. The index also is not quite complete since ergodic and tilting, for example, are not listed.

The last chapter contains original material recently developed by the author and some unpublished results of C. E. Shannon.

On the whole, the subject is presented clearly and simply. The book should be an excellent text for a first course on the subject. The mathematical background of the reader does not have to include more than the fundamentals of probability theory and of Fourier analysis. A set of 80 problems should help the student assimilate the material and appreciate some of its practical applications.

The question of the usefulness of information theory is sometimes raised in engineering circles. The author, certainly aware of this, gives an answer in the summary of the first chapter and in the conclusion of the last one. It is, in essence, that "communication engineering is at the threshold of a major technical revolution." In this revolution, data processing will play an important role, and a deep understanding of the foundations of the theory will be necessary. "Transmission of Information" will certainly contribute to this understanding.

GEORGES A. DESCHAMPS
University of Illinois
Urbana, Ill.

[1] "IRE Standard on Information Theory: Definition of Terms, 1958," PROC. IRE, pp. 1646–1648, September, 1958.

Digital Applications of Magnetic Devices, Albert J. Meyerhoff, Ed.

Published (1960) by John Wiley and Sons, Inc., 440 Fourth Ave., New York 16, N. Y. 569 pages +14 index pages +xix pages +bibliography by chapter +11 appendix pages +7 glossary pages. Illus. 6×9¼. $14.00.

This book, which could serve either as a text or reference handbook, covers a large number of digital logic and memory circuits whose operation is based on the use of magnetic components or magnetic interactions. Many of the devices presented appear in a book for the first time. The subject matter is, for the most part, covered in a very comprehensive manner.

The first seven chapters of this 604 page book serve as an introduction to the circuits described in subsequent chapters. An elementary introduction to magnetism is given. The properties of magnetic cores, diodes, and transistors are discussed. The parameters and units to be used are defined.

The next fourteen chapters, or approximately one-half of the book, are concerned with core-diode circuits. These circuits have been classified into three basic types. They are: 1) parallel magnetic-pulse amplifiers, 2) delay parallel magnetic-pulse amplifiers, and 3) series magnetic-pulse amplifiers. The treatment is rather extensive and complete.

Memories suitable for high-speed digital systems are described in the following five chapters. Coincident-current and linear-selection memories are described. Following a discussion of the general principles, specific designs are presented. Thin magnetic film, twistor, and superconductive memory elements are treated briefly. Three chapters are then devoted to the design and application of regenerative transistor-core circuits. The final chapters concern carrier magnetic amplifiers and multiaperture core circuits.

With the exception of the introductory material on ferromagnetism and core properties, most of the material presented is covered in sufficient detail and is handled well. The book would have been given better balance if the sections on core-diode and core-transistor circuits were substantially shortened and the introductory material expanded. The use of mirror symbols to simplify core circuit presentations would also have been helpful.

It is understandable that the twenty-five authors would concentrate on material with which they had firsthand experience. The final result, though, has both a lack of continuity and an omission of many useful devices. An example of this would be the parametron which logically belongs in the section on carrier magnetic amplifiers. It is hoped that this will be remedied in future editions.

In spite of the lack of balance, this book will definitely serve a useful purpose in a rapidly growing field.

A. H. BOBECK
Bell Telephone Labs., Inc.
Murray Hill, N. J.

Scanning the Transactions

Majority rule, which in various forms governs much of the affairs of man, is also governing the operation of more and more of his machines and equipment. The theory is that several heads, or parts, are often more reliable than one. The use of parallel redundant circuits to improve the reliability of electronic equipment is already a familiar technique. The majority rule idea carries this technique a step further by adding a vote-taking element to the system which polls the outputs of the redundant parts of the system to determine, on the basis of a simple majority vote, which output is correct. Thus, each redundant part assumes more than the role of a stand-by and becomes a full-time performer that has equal billing with its counterpart. It has recently been proposed that the reliability of a system could be further improved if decisions were based on a weighted vote which took into account the past voting record of each redundant part, rather than on a simple majority vote. To accomplish this, an adaptive vote-taker has been proposed which is able to reduce the significance it gives to the outputs from those parts which past experience shows are apt to make mistakes. Thus the vote-taker acts as an automatic repairman by gradually eliminating defective parts from the operations of the system. The heart of the proposed adaptive vote-taker is an element that provides variable gain with memory. A variable resistor with memory, called a memistor, has been successfully applied to this function. It is believed that, with the application of adaptive techniques to redundant systems, the dependability and life expectancy of a system can actually be made to exceed that of its component parts. (B. Widrow, *et al.*, "Birth, life, and death in microelectronic systems," IRE TRANS. ON MILITARY ELECTRONICS, July, 1961.)

The alphabet has played a greater role in the progress of mankind than many of us realize. The ancients who devised the letters of the alphabet deserve more credit for their contributions to many modern-day developments. In the electronics field, for example, it is difficult to envision what life would be like if there were no A-scopes, F-layers, G-string transmission lines, J-scans, X-rays, or z-transforms. Even filters have their Q's. More remarkable, however, is how those living centuries ago anticipated the physical shapes of things to come. It seems clear that in designing the characters of the alphabet they foresaw that today we would need such things as I-beams and S-curves, and would frown on such things as U-turns. Their foresight even carried into electronics where we find such examples as H-guides and magic T's. Whether they foresaw the new surface-wave structure that was recently developed is perhaps open to question. In any event, another worthy member has been added to the alphabetic list which is called a V-line. It is a wedge-shaped structure consisting of two conducting plates which form the sides and a dielectric medium contained within the V which supports the propagation of surface waves. A noteworthy feature is that the application of biasing potentials between the conducting plates may provide a convenient means of electronically controlling the propagation characteristics. The V-line thus makes an interesting addition to the transmission line family. (P. Diament, *et al.*, "A dielectric surface-wave structure: the V-line," IRE TRANS. ON MICROWAVE THEORY AND TECHNIQUES, July, 1961.)

How to supply the L in RLC is posing a problem today. The general trend toward microminiaturization has placed increasing emphasis on the use of semiconductor circuits. Unfortunately, it is difficult to produce useful inductance in semiconductor materials. The alternative of using wire-wound inductors is unattractive because coils are bulky and hard to microminiaturize. How, then, do we expect to obtain microminiature versions of RLC filter circuits? The answer lies in the development of inductive semiconductor elements. Although the going is not easy, some progress has been made in this direction. Forward-biased junction diodes, for example, can be made to behave like inductive elements. Unfortunately, they exhibit a low Q. Coupling them with negative resistance devices has been tried in order to increase the Q, but serious temperature and stability problems have arisen. Better success has been achieved by combining a transistor with a 90° phase-shift network to make the circuit appear inductive to an external source, but again only a moderate Q is obtainable because of the low input impedance of the transistor. A recent evaluation of these and other possibilities indicates that at the present state of the art the most promising approach lies in operating a transistor in the alpha cutoff region to produce an "inductive transistor." The problem is an important one and further progress will be watched with interest. (H. G. Dill, "Inductive semiconductor elements and their application in bandpass amplifiers," IRE TRANS. ON MILITARY ELECTRONICS, July, 1961.)

Abstracts of IRE Transactions

The following issues of TRANSACTIONS have recently been published, and are now available from The Institute of Radio Engineers, Inc., 1 East 79 Street, New York 21, N. Y., at the following prices. The contents of each issue and, where available, abstracts of technical papers are given below.

Sponsoring Group	Publication	IRE Members	Libraries and Colleges	Non-Members
Aerospace and Navigational Electronics	ANE-8, No. 2	$2.25	$3.25	$4.50
Electron Devices	ED-8, No. 4	2.25	3.25	4.50
Microwave Theory and Techniques	MTT-9. No. 4	2.25	3.25	4.50
Military Electronics	MIL-5, No. 3	2.25	3.25	4.50
Nuclear Science	NS-8, No. 3	2.25	3.25	4.50

Aerospace and Navigational Electronics

VOL. ANE-8, NO. 2, JUNE, 1961

Control Concepts of the AN/GSN-11 Terminal Air Traffic Control System—S. D. Moxley, Jr. (p. 51)

Capabilities of a newly completed terminal-area air traffic control system are discussed, in terms of recent theories of flow control. Adaptability of the system to gain the benefits of early arrival scheduling, time separation, sequencing, schedule resolution, shortest common path, dual and crossing runways is described. The author defends close-control vectoring as the only means to achieving both improved safety and increased traffic rate and discusses the system's philosophy of increasing precision with decreasing range. Getting back to the pilot, means by which the system simplifies approach procedures, reduces congestion aloft, and provides continuous radar tracking are also discussed.

Logarithmic Navigation for Precise Guidance of Space Vehicles—W. G. Green (p. 59)

The principles of logarithmic guidance are derived and their application to various space-flight guidance problems is discussed. Logarithmic guidance is shown to be ideal during the terminus of control where considerations of minimum fuel, minimum heating etc., can be subordinated to precise matching of vehicle kinematics to the desired trajectory. This precise trajectory control is achieved utilizing velocity and position measurements to govern the vehicle deceleration. Multidimensional effects are considered and it is shown that various "degrees of control" of velocity vector magnitude and angle, time of arrival, accelerations, geographical or inertial directions of approach, etc., can be achieved.

The tolerance of logarithmic guidance to instrumentation errors and parameter variations are confirmed by error analyses of these guidance principles applied to the control of the velocity vector during the deceleration process.

Optimization of a Generalized Velocity-Inertial System—W. A. Porter and L. F. Kazda (p. 72)

In this paper the variational calculus techniques of the Wiener-Kolmogoroff optimum filter theory are employed to develop the statistically optimum form of a generalized hybrid velocity-inertial system. A velocity-inertial system is considered which is general in both form and application. The form of the system encompasses pure inertial, pure Doppler, and a large family of Doppler-inertial hybrid systems including the present-day second- and third-order Doppler inertial navigation and stabilization systems. The system may be used for a wide range of applications including any linear combination of acceleration, velocity, or vertical-reference sensing.

The general system form is developed by employing an unspecified filter to mix the inertially derived signal with the signal from the auxiliary velocity sensor. As a result of utilizing this general system form, a single general error equation is found which represents the system error for each of the above system forms and applications. Using a linear analysis and the minimum mean-square error criteria, an optimum system form is found for the complete range of possible system applications.

Electron Devices

VOL. ED-8, NO. 4, JULY, 1961

On the Heating of Output Windows of Microwave Tubes by Electron Bombardment—D. H. Preist and R. C. Talcott (p. 243)

An account is given of an experimental investigation of the behavior of output windows, the particular type chosen for study being the cylindrical type in a cavity resonator. By feeding microwave power into the cavity and measuring electric field and the heat dissipated in the window and in the metal walls, a non-linear window-heating effect was discovered above a certain critical field strength. In this condition, watts dissipated at the window vary as the fifth or higher power of the electric field strength and the resulting thermal stresses may easily destroy it. Further experiments were performed on various modifications of the original structure in order to isolate and study the phenomena responsible for the heating. Some of these tests were made using an axial magnetic field.

It was found that there are two distinct mechanisms of heating, one requiring the presence of the magnetic field and the other one not requiring it. Both involve energy exchange between the electric field and the window by free electrons which dance on the window surface synchronously with the alternating field and multiply by a secondary emission or multipactor process above a certain field strength. The critical field strength may be greatly reduced by the presence of contaminating films on the dielectric surface, and may be greatly increased by suitable surface treatment.

It is shown that these effects are not restricted to cylindrical windows but will tend to occur at any dielectric surface in vacuum if the tangential RF field is strong enough.

The Spacistor—J. M. Lavine, W. Rindner, B. Nost, and R. F. Nelson (p. 252)

A brief description is given of several Spacistor structures and the techniques of fabrication. Detailed measurements of the four-pole parameters are reported and described with the aid of physical models. The mutual conductance is shown to depend upon injector-modulator spacing, injector current and modulator bias, with little variation to 25 Mc. Improvement in both g_m and shielding is shown to occur when the modulator is injecting charge. Values of g_m of the order of several hundred micromhos have been observed. The input resistance depends upon the characteristics of the modulator contact in the space-charge region and upon the dc bias. Under forward-biased modulator conditions (optimum g_m) values of input resistance of the order of several hundred thousand ohms are obtained. Under zero-bias or reverse-bias conditions (somewhat reduced g_m), values of several megohms are obtained. Values of output resistance ranging to several hundred thousand ohms have been observed with possibilities of larger values being obtained with improved design. Low frequency voltage gain of the order of 10 and power gain of the order of several hundred have been exhibited. The reduction of power gain at 25 Mc is attributed mostly to the array of contact and device resistances, and device and header capacities, some of which may be reduced by appropriate design. These prevented the elimination of shunting capacities and precluded higher frequency measurements.

Preparation and Properties of Electroluminescent Phosphors for Display Devices—H. F. Ivey and W. A. Thornton (p. 265)

Electroluminescent phosphors for use in some electronic display devices should have brightness-voltage characteristics differing from those used in light sources, for example. The various factors of phosphor preparation and of cell construction which affect these characteristics have been studied. Special phosphor powders with unusually high or unusually low values of "discrimination ratio" (a quantity related to the change in output as the applied voltage is varied) have been developed and their performance described. It has also been shown that thin phosphor films afford extremely high values of discrimination ratio,

particularly if operated on dc. The use of nonlinear materials (especially zinc oxide) as auxiliary layers to increase the discrimination ratio obtained with a given phosphor has been studied.

N-Beam Nonlinear Traveling-Wave Amplifier Analysis—J. E. Rowe (p. 279)

In large-diameter electron stream traveling-wave amplifiers there is a significant variation of the circuit electric field across the stream. Most analyses neglect the effects of these field variations. An approximate method has been used to study the effect of transverse field variations on the gain and efficiency of large-signal traveling-wave amplifiers. The annular electron stream is subdivided into a number of annular rings each containing an equal fraction of the total current. It is assumed that the circuit field varies over the stream cross section and that each segment has a different coupling to the circuit. The space-charge field is assumed independent of radius. The effect on gain and efficiency is calculated for a stream diameter of $B = 1$ and it is found that a subdivision of the stream into two segments with different couplings to the circuit gives a lower saturation efficiency but that further subdivision does not appreciably change the results.

Traveling-Wave Tubes with Ferrite Attenuators—F. K. Mullen (p. 284)

In order to determine the efficacy of ferrite isolators used as internal attenuators in traveling-wave tubes, two TWT's incorporating such isolators were developed, one using orthodox magnetic focusing, the other using electrostatic focusing. The results of the experimentation indicate that the ferrite can, in some cases, offer improvement in gain and efficiency over reciprocal attenuators. The limitations of this device are discussed together with some particular advantages it may offer for special applications.

Design criteria for such isolators and the effects of the ferrite as a circuit element in TWT's, are also investigated.

The Reflex Klystron as a Regenerative Mixer—B. G. Whitford (p. 289)

A simple receiver using a single reflex klystron as a mixer and local oscillator is described. Experimental data show typical performance, and a theory based on reflex-klystron and transmission-line theory is proposed which explains the observed behavior. The S- and X-band tangential sensitivities are about 15 db better than can be realized with a low-level crystal video detector and it is thought that this figure may be exceeded at the higher microwave frequencies where crystal sensitivity is relatively poor.

A Ladder Structure for Millimeter Waves—E. A. Ash and A. C. Studd (p. 294)

A planar structure, closely related to the stub-supported ring and bar structure, is analyzed using Fletcher's method. The computed dispersion characteristics and interaction impedances show that it should prove useful in millimeter generators. Experiments at X band have shown that oscillation bands of over 1.7:1 are possible working on a backward mode. Forward-mode operation with higher output powers, but with a more restricted bandwidth can also be realized.

Some High-Power Window Failures—J. R. M. Vaughan (p. 302)

Two types of RF window failure in a high-power magnetron are investigated. Cracking is shown to depend on electrostatic charging of an evaporated metallic deposit on the window. Punctures were investigated by observations of X-ray stereo-autograms, and are shown to result from an internal multi-pactor discharge, which in turn is enabled to function at high voltages by the stray magnetic field. Methods for curing both types of defect are given, with evidence that they are successful. The methods are applicable to other high-power microwave tubes, both magnetrons and klystrons.

Crossed-Field Electron Interaction of the Distributed-Emission Space-Charge-Limited Type—J. F. Hull (p. 309)

A semitheoretical, semiheuristic analysis is given of crossed-field electron interaction of the distributed-emission type. The emphasis of this paper is on the over-all picture of this complex type of interaction, rather than on mathematical exactness. The results are given in terms of five equations from which can be calculated the amount of dc applied power which is converted to real and reactive RF power under given conditions of frequency, RF potential, and magnetic-field strength. These equations are applied to the magnetron oscillator to predict power delivered to the anode by the electron bunches, frequency-pushing characteristics, V-I characteristics, and Rieke Diagrams. The agreement of the experimental data with the calculations over this wide range of characteristics confirms the validity of the analysis.

Some Experiments with a New Type of Crossed-Field Gun—T. A. Midford and G. S. Kino (p. 344)

The construction and testing of a crossed-field gun based on an exact space-charge flow solution will be described. All the characteristic parameters of a gun of this type may be obtained analytically. Experimentally the gun was found to perform essentially as predicted. This gun has a moderately high convergence and produces a beam whose gross features give a very good approximation to planar Brillouin flow. Work by Anderson has indicated that crossed-field beams produced by a gun of this type may be somewhat less noisy than similar beams produced by other types of guns.

High-Frequency Behavior of the Crossed-Field Potential Minimum—T. Van Duzer and J. R. Whinnery (p. 331)

A time-domain analysis of the high-frequency currents in a crossed-field potential minimum is presented. The distinctions between ordinary and crossed-field potential minimums are discussed and a one-dimensional model for the crossed-field case is described. The general form of the solution is given as an infinite array of coupled integral equations and the required expressions for the coefficients are developed. A reduced array of equations is used for a numerical analysis of a diode with a 100-gauss transverse magnetic field. The numerical analysis revealed only a minor modification of the current fluctuations as a result of the transverse magnetic field, although experiments have shown excess-energy crossed-field currents related to the potential minimum with magnetic fields lower than this.

Contributors—(p. 342)

Microwave Theory and Techniques

Vol. MTT-9, No. 4, July, 1961

Report on Advances in Microwave Theory and Techniques—1960—R. C. Hansen and M. T. Weiss (p. 278)

The Short Pulse Behavior of Lossy Tapered Transmission Lines—R. Stapelfeldt and F. J. Young (p. 290)

An analytic method is given which allows the design engineer to assess rapidly the short pulse characteristics of any given tapered-transmission-line type of pulse transformer. The method allows inclusion of both skin-effect losses and losses which are independent of frequency. The effects of mismatching at either end are shown to be as important as the taper function of the line itself. The results of this approximate method are expressed as simple integrals and matching terms to which it is easy to attach physical significance.

The method is applied to the analysis of two tapered-line pulse transformers which are geometrically uniform coaxial structures with tapered dielectric constants. The line whose nominal characteristic impedance is an exponential function of electrical position is shown to have a good rise time and tilt distortion characteristics.

A Waveguide Quadruplexer System—P. Foldes and T. B. Thomson (p. 297)

Practical design considerations are presented for a relatively simple four-channel waveguide branching system. The most important electrical characteristic of this system is an extremely low pass-band reflection coefficient (better than 1.5 per cent in 30-Mc band) which has only very small variations with the environmental conditions.

Some Recent Findings in Microwave Storage—J. D. Kellett (p. 306)

This paper describes an experimental investigation of frequency memory in a recirculating amplifier storage device. The objective of the investigation was to determine what mechanism caused injected energy to shift to preferred storage frequencies. Using fast-acting crystal switches, the output energy was selectively viewed, and it was found that the energy in any circulation when viewed separately was of the input frequency. The spectrum photographs which are included in the paper show that the recirculating amplifier when operating with an open loop gain greater than unity does not oscillate at preferred frequencies.

Excess Noise in Microwave Detector Diodes—J. J. Faris and J. M. Richardson (p. 312)

The dependence of available excess noise in type 1N26 microwave crystal-diode rectifiers on applied microwave power was measured. This may be approximated by a power law with constants characteristic of the particular crystal. As a consequence of the dependence of both excess noise and dc rectified power on input-power level, there is a level which minimizes the ratio of these quantities. Similarly, in the case of a modulated microwave carrier there is an input level which minimizes the ratio of excess noise to demodulated power, and so provides optimum detection of small modulation.

Quantum Fluctuations in Microwave Radiometry—L. P. Bolgiano, Jr. (p. 315).

This paper assesses the possible significance of the quantum nature of electromagnetic radiation in limiting the measurement accuracy attainable with a microwave radiometer. Analogies are shown to exist between the form of a formula describing fluctuations in the radiometer output, and both a formula describing the radiometer input signal, and also, a formula describing the output of a photocell detector. Detailed quantum mechanical consideration of the processes of amplification and detection are circumvented by considering how the formula for fluctuations in the radiometer output might be modified so as to make it consistent with the measurement precision implied by these other formulas. A modified formula is suggested which includes a quantum fluctuation whose magnitude depends on signal power.

On the Resolution of a Class of Waveguide Discontinuity Problems by the Use of Singular Integral Equations—L. Lewin (p. 321)

It is shown that a considerable number of solutions of rectangular waveguide problems appearing in the literature are all special cases of a general treatment focused around the known solution of a singular integral equation. In terms of this a number of typical results are re-examined. The method is then applied to four new configurations, and the range of application and the limitations are examined.

A Dielectric Surface-Wave Structure: the V-Line—P. Diament, S. P. Schlesinger, and A. Vigants (p. 332)

Properties of the V-line, a wedge-shaped surface-wave structure comprising a cylindrical dielectric binding medium of sectorial cross section supported by two conducting plates, are considered in terms of its higher-order hybrid modes of propagation. Practical modifications of the ideal structure are emphasized.

Design curves and equations are presented to determine various propagation parameters and their significance is discussed. Experimental verification of the theory is described.

Wave Propagation in a Medium with a Progressive Sinusoidal Disturbance—A. Hessel and A. A. Oliner (p. 337)

A recent paper by Simon derives approximate results, employing only three space harmonics, for the propagation characteristics of an electromagnetic wave traveling in a medium possessing a progressive sinusoidal disturbance. A rigorous result is presented here for this same problem, taking into account all of the space harmonics; also, a sufficiency condition for the convergence of this solution is discussed. This sufficiency condition is not satisfied in a particular case treated by Simon. It is shown that his analysis of this case is in error, and that the total field is singular there. The singular nature of the field is associated with "supersonic" effects in the medium containing the progressive disturbance.

A New Broad-Band Absorption Modulator for Rapid Switching of Microwave Power—F. Reggia (p. 343)

This paper describes a new technique for obtaining a broad-band absorption modulator for high-speed switching or amplitude modulation of microwave power. This ferrite modulator, an outgrowth of the longitudinal-field rectangular-waveguide phase shifter, has electrical characteristics particularly desirable in a microwave switch. These include a zero-field insertion loss of approximately 0.5 db in the ON state, an isolation of greater than 60 db in the OFF state which is nearly independent of the magnetic control field in this state, and a nearly matched input impedance for all values of applied field. These electrical characteristics are nearly constant over a 30 per cent bandwidth at X band. Also, it is possible to design the amplitude modulator to have negligible phase shift at the desired operating frequency.

Other characteristics of this ferrite modulator include small physical size, magnetic control fields of less than 50 oersteds, operating temperatures up to 150°C, and a capability of less than one μsec switching time.

Rectangular Waveguide Theoretical CW Average Power Rating—H. E. King (p. 349)

A theoretical CW average power rating, limitation imposed by a temperature rise resulting from power dissipation within the rectangular waveguide walls, can be determined by predicting the rise in temperature. Formulas for the evaluation of the CW average power rating have been developed and are presented here, and the power rating curves are given for the WR-2300 waveguide (320 Mc) through the WR-19 waveguide (60 kMc).

Localized hot spots, associated with a standing wave on a mismatched waveguide, require a derating factor. The axial flow of heat from these high current spots has been considered in calculating and plotting this derating factor.

Military Electronics

VOL. MIL-5, NO. 3, JULY, 1961

Birth, Life and Death in Microelectronic Systems—B. Widrow, W. H. Pierce, and J. B. Angell (p. 191)

In order to exploit the technological promises of microelectronics, electronic system techniques must be developed so that defective portions of a system can be tolerated without system malfunction. Such defects might be introduced during manufacture (at birth), or cause errors during operation (life). The number of permanent failures which could be endured by a system before it fails completely will determine its lifetime (death).

In this paper, an adaptive vote-taker is proposed which compares the outputs of paralleled (redundant) system parts in a binary system and determines the most probable answer based on past performance of the separate parts. Initially, the vote-taker assigns equal significance to each redundant part, and (in a binary system) requires that a simple majority of the parts be correct. With experience, the vote-taker continually reduces the weight (significance) of the outputs from those parts that make mistakes, thereby gradually eliminating the defective parts. Thus the vote-takers (which also may be paralleled if they are unreliable) act as automatic repairmen which delete defective parts of a system. System dependability and life expectancy can be made to exceed the dependability and average life expectancy of the component parts.

The heart of an adaptive vote-taker is an element providing variable gain with memory. A variable resistor with memory (memistor), which uses electrochemical deposition or removal of copper to achieve the variable memory, has been successfully applied to this function.

Use of Passive Redundancy in Electronic Systems—J. J. Suran (p. 202)

Circuit design predicated solely upon the premise of providing circuits with greater and greater immunity against component tolerances at some point results in an increase in catastrophic failure rates. Thus, circuits which are overdesigned to provide maximum protection against drift failures may actually contribute to a lower system reliability than do those circuits which are designed to operate with tighter component tolerances. These considerations lead to the conclusion that as systems grow in complexity or as reliability requirements are significantly increased for current equipment, a point is reached where further improvement in design procedures will not necessarily lead to further increases in system reliability. A way out of this dilemma appears to be the introduction of some form of redundancy on the component or circuit level in order to overcome the effects of the inevitable occurrence of catastrophic component failures. This paper discusses the application of redundancy techniques, of a nonadaptive and passive nature, to electronic circuits and systems.

Power Dissipation in Microelectronic Transmission Circuits—J. D. Meindl (p. 209)

The interrelationship of power dissipation, gain, stability, terminal impedance values, dynamic range and efficiency is investigated for small-signal amplifiers in the middle range of frequencies. Utilizing a novel circuit-design theory which treats a transistor along with its biasing resistors as a single entity, amplifier designs are derived which combine optimum ac performance and minimum dc power dissipation. The product of ac power gain and dc-to-ac efficiency is found to be a useful figure of merit for microelectronic transmission circuits.

A Thermal Design Approach for Solid-State Encapsulated High-Density Computer Circuits—A. E. Rosenberg and T. C. Taylor (p. 216)

This paper considers the thermal problems associated with the design of high component-density encapsulated circuits, constructed with small solid-state components. The thermal resistance to the dissipation of component-generated heat is shown to consist of that of the encapsulating medium, plus that of the external circuit cooling process. Because the external cooling becomes more difficult as the size of an encapsulated circuit is reduced, a method of constructing such circuits is proposed which minimizes the thermal resistance due to the encapsulating medium. This construction makes a large fraction of the allowable component temperature rise available for use in the external heat dissipation process by providing high thermal conductance paths for the transfer of heat from the surfaces of the components to one surface of the circuit structure. Analytical models are developed for the most important heat transfer processes in the proposed circuit structure. The equations based on these models are arranged in a form suitable for design use, and example designs are presented.

Integration of Microcircuitry into Microassemblies—R. A. Gerhold (p. 227)

The necessity to hybridize newer microcircuitry techniques with existing design capabilities to achieve efficient equipment designs is established. An analysis is presented of the net size and weight advantages calculated for several components of a typical weapons system, as first the micromodule and then, progressively, thin-film and solid-circuit techniques are integrated into the system design. The diminishing returns on the introduction of microcircuitry into many areas of the system emphasize the need for high efficiency in the integration of new techniques. The potential capabilities of an advanced type micromodule, which still retains the standardized microelement dimensions and assembly procedures, are explored. A further advanced modular interconnection of microcircuitry wafers into a projected microassembly is then described. 0.002×0.010-inch copper ribbon conductors are welded to the metallized edge terminations of stacked substrate wafers by an electron beam technique. Interconnection requirement is 1600 terminations per square inch. Sample illustrated showed 2000 terminations per square inch, or 80,000 terminations per cubic inch. Termination capability is increased three times, and effective useful module volume is doubled compared to existing micromodule. Details of materials and processes for the micro-connections are described together with a summary of the statistical reliability evaluation. The latter confirms the high reliability objective for this connection.

A Family of Semiconductor Devices for Microelectronic Applications—E. E. Maiden and W. F. Schnepple (p. 233)

A variety of approaches to microminiaturization is now being widely explored by electronic systems designers. Among the approaches taken, continued reliance is being placed upon discrete active components that can be used in module, welded, thin-film, or hybrid types of microcircuits. By the use of discrete elements, maximum circuit flexibility is retained, tight component tolerances are possible, and production shrinkage of complete circuit functions is minimized, as compared with the solid-state circuit approach. Moreover, "throw-away" maintenance costs are low.

A series of microminiature silicon diodes and transistors has been developed and produced for use in applications where stringent size and weight limitations, and high reliability requirements, exist. Through the use of extremely simple mechanical constructions, surface passivation techniques and impervious

glass-like coatings, low cost can be achieved in mass production without sacrificing reliability. By use of appropriate fabrication processes, alloyed or diffused diodes and transistors can be formed in mesa or planar configurations, and an extension to epitaxial structures can be employed. Electrical characteristics are comparable to, or better than those of existing conventional types of diodes and transistors. At 25°C, failure rates below 0.01 per cent per thousand hours have been substantiated.

This paper begins with an outline of the theory underlying surface protection techniques used, describes the construction and characteristics of several devices in the family, and presents test information proving a high degree of reliability.

Inductive Semiconductor Elements and Their Application in Band Pass Amplifiers—H. G. Dill (p. 239)

Filter circuits using wire-wound inductors are hard to microminiaturize because coils are rather bulky. This paper discusses different inductive semiconductor devices which may replace coils where space is a problem.

Forward-biased diodes, properly designed, behave like very lossy inductances. Combining them with negative-resistance devices increases the Q but creates serious temperature and stability problems.

Relatively temperature-stable inductance elements are possible by combination of a phase shift network with a transistor. The principle, well-known in tube circuitry, gives high inductances with only a moderate Q because of the low input impedance of the transistor.

Promising results have been demonstrated with a transistor operating in the α cutoff region. The device is dc stable, and has a moderate temperature sensitivity which might be partly compensated if necessary. Avalanche multiplication is used to reduce the damping resistance of the inductive transistor.

Simple band-pass amplifier circuits are presented in the last section to demonstrate how to use the inductive transistor in practice.

Fabrication of Microminiaturized Core Memories by Plastic Encapsulation Techniques—G. R. Henderson, W. C. Earl and C. G. Kyratzis (p. 250)

Plastic encapsulation of nonlinear ferrites, and the effect of this encapsulation on the magnetic characteristics of the ferrites, is discussed in this paper. This technique provides greater immunity to shock and vibration damage than conventional core frames and provides bit densities in excess of one million per cubic foot.

Chemical deposition and photographic techniques may be used to form a portion of the wiring matrix. Through-hole plating of ferrites having a 15-mil diameter hole is possible.

Small-evaluation memories have been fabricated, using both toroids and transfluxors. Temperature tests on these memories show that encapsulation causes a slight increase in switching speed and a small decrease on output for a given drive current. These changes remain almost constant over the temperature range. No significant changes have been noted in the noise output.

Techniques outlined are presently being used in the fabrication of microminiaturized, nondestructive memories for missile and satellite application.

MIST Module Electronics—I. Maloff and V. Lally (p. 256)

The MIST module is a proposed building block for electronic telemetry systems for use with weather balloons, providing a minimum hazard to fast-flying aircraft. This electronic telemetry system may be spread in two dimensions while having a minimum build-up or structure in the third dimension. MInimum STructure modules (MIST modules) are a proposed answer to such a requirement. MIST modules have been built on an experimental basis and the brief experimental experience with working modules indicates that they will meet the requirements and provide electronic systems which can be safely floated in the air lanes.

Nuclear Science

Vol. NS-8, No. 3, July, 1961

A Digital Start-up Control Unit for Nuclear Reactors—J. D. Schmidt, B. K. Eriksen, and W. Peil (p. 1)

The use of digital circuits for control of a nuclear reactor in the start-up range was proposed in a paper given by S. N. Lehr and V. P. Mathes at the Nuclear Engineering and Science Conference in 1959. A control of this type eliminates the many periodic adjustments that are required with linear circuits and results in a more accurate, reliable, and maintenance free unit. This paper describes the design and development of such a unit which computes and displays digitally the reactor level and period over nine decades of power. The level of the reactor is obtained from a discriminator and binary counter which resolve 2.5 m.v. pulses spaced as little as one microsecond apart. A time modulation technique incorporating binary counters for comparison and read-out is used to compute the period with a short term memory employed to provide statistical smoothing.

Use of Entrance Hodoscope for Particle Identification in Very-High-Energy Bubble Chamber Experiments—W. Selove, H. Brody, E. Leboy and R. Fullwood (p. 13)

At energies of 10 Bev and higher, it is not easy to obtain physically separated beams of π and K mesons. We have constructed a hodoscope system which will register the identity of of each of 20 particles entering a bubble chamber over a 100 microsecond time interval. Particles are localized by a scintillator hodoscope with matrix elements 1 cm square. Particle identity is determined with Cerenkov counters. The combined information is displayed on an oscilloscope and photographed at each bubble chamber expansion.

The Log Count Rate Period Meter Used with Safety Circuits—H. Christensen and R. B. Stanfield (p. 22)

Equations are presented that give the probable rate of spurious reactor scrams due to counter noise in the period circuits commonly used at low reactor power. It is shown how a filter introduced to reduce the spurious scram rate, will delay the circuit response in the case of true emergencies. A numerical example shows that a compromise can be reached that gives a very satisfactory circuit.

Proportional Control and Pressurizer Parameter Study of a Pressure Tube Reactor—D. E. Rathbone (p. 27)

An investigation of the transient behavior of a pressure tube reactor indicated a definite need for external control to handle even normal load perturbations. Three proportional controllers were developed which were effective in containing the transients of the system for changes in load. A comparison of the three controllers indicated little preference between them with regard to variations in reactor power, primary loop temperature or system pressure. The final selection of a controller was thus an economic consideration. The result of the parameter study of the pressurizer indicated that a pressurizer size of 30 cubic feet, $\frac{1}{5}$ of the total volume of the primary coolant, was adequate for the containment of the pressure and volume surge transients.

Electronic Parts in a Hypernuclear Environment—L. B. Gardner and A. B. Kaufman (p. 35)

A Double-Delay-Line Clipped Linear Amplifier—R. L. Chase and V. Svelto (p. 45)

A compact transistorized linear amplifier has been designed that is suitable for many radiation counting applications. The amplifier delivers symmetrical double-delay-line differentiated output pulses, up to ± 10 volts in amplitude with a differential non-linearity of $\pm 1\%$. It tolerates input signals 400 times full scale without producing spurious output pulses. Both a prompt output and one delayed by two microseconds are available. The clipping lines and the signal delay line are all terminated at both ends so that physically small, relatively imperfect delay lines can be employed. Five amplifiers occupy only $12\frac{1}{4}$ inches in a standard 19 inch relay rack.

A Digital Data Handler for Pulse Particle Accelerators—W. A. Higinbotham and D. W. Potter (p. 51)

This paper described a digital data handler for storing information in a magnetic core memory during the pulse of a synchroton and transferring it to a slow memory during the dead time. Digital measurements of trajectory, pulse height, time of flight, run number, etc., are typical data. The magnetic core memory provides capacity for storing 32 words (events) of 96 bits during a burst. The information contained in the core memory is then transferred to one inch magnetic tape during the dead time of the accelerator. Thence the information may be fed to a computer for future study. For economy, the data handler has one buffer which serves as the input, output and shift register.

Abstracts and References

Compiled by the Radio Research Organization of the Department of Scientific and Industrial Research, London, England, and Published by Arrangement with that Department and the *Electronic Technology* Dorset House, Stamford St., London S.E. 1, England

NOTE: The Institute of Radio Engineers does not have available copies of the publications mentioned in these pages, nor does it have reprints of the articles abstracted. Correspondence regarding these articles and requests for their procurement should be addressed to the individual publications, not to the IRE.

The number in heavy type at the upper left of each Abstract is its Universal Decimal Classification number. The number in heavy type at the top right is the serial number of the Abstract. DC numbers marked with a dagger (†) must be regarded as provisional.

UDC NUMBERS

Certain changes and extensions in UDC numbers, as published in PE Notes up to an including PE 666, will be introduced in this and subsequent issues. The main changes are:

Artificial satellites:	551.507.362.2	(PE 657)
Semiconductor devices:	621.382	(PE 657)
Velocity-control tubes, klystrons, etc.:	621.385.6	(PE 634)
Quality of received signal, propagation conditions, etc.:	621.391.8	(PE 651)
Color television:	621.397.132	(PE 650)

The "Extensions and Corrections to the UDC," Ser. 3 No. 6, August, 1959, contains details of PE Notes 598–658. This and other UDC publications, including individual PE Notes, are obtainable from The International Federation for Documentation, Willem Witsenplein 6, The Hague, Netherlands or from The British Standards Institution, 2 Park Street, London W. 1, England.

ACOUSTICS AND AUDIO FREQUENCIES

534.112–8:621.374.5 2827

Mode Coupling Occurring in the Propagation of Elastic Pulses in Wires—A. H. Meitzler. (*J. Acoust. Soc. Am.*, vol. 33, pp. 435–445; April, 1961.) Longitudinal and flexural ultrasonic pulses in a stretched wire show considerable distortion because of mode coupling at certain critical frequencies. Phase velocity calculations based on the real roots of the Pochhammer equations can be used to predict these critical frequencies for any isotropic elastic material.

534.2(204) 2828

Long-Range Sound Propagation in the Deep Ocean—F. E. Hale. (*J. Acoust. Soc. Am.*, vol. 33, pp. 456–464; April, 1961.) Information available from laboratory reports and unclassified literature on long-range convergence zone-propagation is discussed.

534.231 2829

Acoustic Intensity Anomalies introduced by Constant Velocity Gradients—M. A. Pedersen. (*J. Acoust. Soc. Am.*, vol. 33, pp. 465–474; April, 1961.) Spurious caustics can arise in ray-theory calculations of intensity based on constant-gradient layers. The use of curved-line segments preserving continuity of velocity and slope in the profile approximation is considered.

534.232:537.228.1 2830

Transient Performance of a Piezoelectric Transducer—M. Redwood. (*J. Acoust. Soc. Am.*, vol. 33, pp. 527–536; April, 1961.) Electrical and mechanical outputs due to step input signals are discussed and analyses made with reference to the exact transmission-line equivalent circuit of a transducer.

534.232–8 2831

Hypersonic Resonance of Quartz at 3500 Mc/s—J. L. Stewart and E. S. Stewart. (*J. Acoust. Soc. Am.*, vol. 33, p. 538; April, 1961.) Pure thickness-mode oscillations in the range 2950–3600 Mc were observed in X-cut crystals 0.1 mm thick. The damping effect of a thin layer of water was detected.

534.232.089.6 2832

Cylindrical-Wave Reciprocity Parameter—R. J. Bobber and G. A. Sabin. (*J. Acoust. Soc. Am.*, vol. 33, pp. 446–451; April, 1961.) A parameter $J_c=(2/\rho c)(R\lambda)^{\frac{1}{2}}L$ for use in standard reciprocity calibration is derived from network theory and from wave propagation theory and its validity is confirmed by experiment.

534.522.1 2833

Diffraction of Light by Very-High-Frequency Ultrasonic Waves—B. R. Rao and J. S. Murty. (*Proc. Phys. Soc. (London)*, vol. 77, pp. 958–964; May 1, 1961.) The investigation was carried out using ultrasonic waves in water in the range 50–230 Mc.

534.846 2834

The Problem of Acoustic Field Conditions in Recording Studios and their Representation in Rooms used for Reproduction—L. Keibs. (*Tech. Mitt. BRF, Berlin*, vol. 4, pp. 125–129; December, 1960.) Theoretical investigations of the relation between direct and indirect sound at different time intervals in rectangular rooms of volume 10,000 m³ and 100 m³ where sound is recorded are the basis of considerations of how these conditions can best be reproduced.

534.88:534.417 2835

Comparison Analysis on Four Directional-Receiver Correlators—M. J. Jacobson and R. J. Talham. (*J. Acoust. Soc. Am.*, vol. 33, pp. 518–526; April, 1961.) Four systems are analyzed and their SNR's are computed and compared. An examination is also made of their main lobes for various steering directions.

621.395.61.089.6 2836

Reciprocity Calibration of Microphones in a Diffuse Sound Field—H. G. Diestel. (*J. Acoust. Soc. Am.*, vol. 33, pp. 514–518; April, 1961.) The reciprocity parameter for a diffuse sound field follows from that for free space by replacing the distance by the "diffuse-field distance" of a point source. Hence the diffuse-field voltage response can be derived. See 1397 of May.

ANTENNAS AND TRANSMISSION LINES

621.315.212:621.372.2 2837

On the Theory of the Coaxial Cable—P. Poincelot. (*C.R. Acad. Sci. (Paris)*, vol. 251, pp. 1623–1624; October 17, 1960.) Propagation along a coaxial line is studied in terms of Maxwell's equations without introducing transmission-line constants. The method is applicable to all symmetric coaxial structures.

621.315.212:621.372.852.32 2838

A Magnetically Variable Coaxial Attenuator with Low Basic Attenuation—J. Deutsch and M. Offner. (*Frequenz*, vol. 14, pp. 344–347; October, 1960.) The type of attenuator considered uses a gyromagnetic material with an applied dc magnetic field which is variable. In the range 6–8 Gc, such an attenuator can provide maximum attenuation >12 db and a minimum of <0.9 db.

621.315 212.1:621.397.743 2839

Recent Developments in Coaxial Cables for Television Distribution—J. D. S. Hinchliffe. (*J. Brit. IRE*, vol. 21, pp. 457–462; May, 1961.) Constructional improvements incorporated in newly developed cables are discussed. Details are given of methods of testing, and cable characteristics are compared.

The Index to the Abstracts and References published in the PROC. IRE from February, 1960 through January, 1961 is published by the PROC. IRE, May, 1961, Part II. It is also published by *Electronic Technology* and included in the March, 1961 issue of that Journal. Included with the Index is a selected list of journals scanned for abstracting with publishers' addresses.

A list of organizations which have available English translations of Russian journals in the electronics and allied fields appears each June and December at the end of the Abstracts and References section.

621.372.2:621.373.421 2840
Tapered Distributed *RC* Lines or Phase-Shift Oscillators—W. A. Edson. (PROC. IRE, vol. 49, pp. 1021–1024; June, 1961.) The behavior of tapered transmission lines of distributed capacitance and inductance is examined, and summarized in the form of a set of normalized curves.

621.372.8.029.65 2841
Waveguide Equipment for 2-mm Microwaves: Parts 1 and 2—C. W. van Es, M. Gevers, and F. C. de Ronde. (*Philips Tech. Rev.*, vol. 22, pp. 113–125 and 181–189; February 16 and March 14, 1961.)

621.372.821 2842
Design Notes for Strip-Transmission-Line Tuners—G. T. Orefice. (*Electronic Ind.*, vol. 20, pp. 104–105; March 1961.) Equations are given for the design of a shorted-line piston-capacitor tuner. They are applied to the case of a resonator with a frequency range of 500–1000 mc.

621.372.823:621.372.831.1 2843
The Excitation of Higher Modes by the Fundamental at an Off-Set Junction of Two Circular Waveguides—K. Schnetzler. (*Arch. elekt. Übertragung*, vol. 14, pp. 421–424; October, 1960.) The mode conversion occurring at slightly displaced flange couplings is calculated using formulas given by Solymar (1111 of 1960) with some corrections.

621.372.823:621.396.65 2844
Circular Waveguide for Wide-Band Radio-Link Systems—E. Gillitzer and R. Herz. (*Frequenz*, vol. 14, pp. 347–357; October, 1960.) The properties and characteristics of circular waveguide are discussed and compared with those of rectangular waveguide, with particular reference to their use as antenna feeders in 4-Gc radio-link installations.

621.372.826 2845
TwoWire- Millimetre-Wave Surface Transmission—K. Ishii J. B. Y. Tsui, J. D. Horgan. (PROC. IRE vol. 49, p. 1076; June, 1961.) Experimental results are given relating to propagation on a two-wire line at 58 Gc. Attenuation was much reduced compared with a single-wire line; the spread of the fields appeared to be much smaller.

621.372.831 2846
The Excitation of Higher Modes at Waveguide Junctions—K. Schnetzler. (*Arch. elekt. Übertragung*, vol. 14, pp. 425–431; October, 1960.) Formulas are derived for calculating the spurious modes generated in a gradual transition between different waveguide, including the case in which the spurious mode is propagated only in part of the transition. See also 1726 of June and 2843 above.

621.372.852.1 2847
Design Relations for Resonant Post Waveguide Filters—R. D. Wanselow. (*J. Franklin Inst.*, vol. 271, pp. 94–107; February, 1961.) The procedures and graphs given for the design of waveguide filters with *Q*-factors under load ranging from 4 to 200 are shown to be adequate for most engineering applications.

621.372.852.21 2848
A Microwave Phase-Shifter with Dielectric Prisms—R. Tremblay. (*Canad. J. Phys.*, vol. 39, pp. 409–418; March, 1961. In French.) Two identical prisms in opposition form a dielectric plate in a rectangular waveguide. The displacement of one relative to the other along the hypotenuse changes the effective length of the plate.

621.372.852.323 2849
Resonance Isolators for Millimetre Waves—H. G. Beljers. (*Philips Tech. Rev.*, vol. 22, pp. 11–15; November 4, 1960.) Compact isolators for 35 and 70 Gc using crystal-oriented anisotropic ferrites are described.

621.396.67:624.97.042 2850
Load Specification for Aerial Supports—F. Staiger. (*Rundfunktech. Mitt.*, vol. 4, pp. 253–257; December, 1960.) The problem in load calculations of allowing for ice formation on antenna masts is considered in order to achieve greater uniformity in design specifications.

621.396.67.095.1 2851
Generating a Rotating Polarization—S. R. Penstone and A. W. Adey. (PROC. IRE, vol. 49, p. 1089; June, 1961.) A method is described of generating an electromotive wave whose plane of polarization rotates at 80 cps, for use in rocket determinations of the electron density in the ionosphere. See also 2645 of 1960 (Allen).

621.396.677.029.6 2852
Investigations on Endfire Aerials in the Microwave Region—T. Heller. (*Nachrtech. Z.*, vol. 13, pp. 529–533; November, 1960.) The antennas considered are dielectric-rod radiators of helical-line and Yagi structure, and the zig-zag antenna [2848 of 1959 (Sengupta)]. The Hansen-Woodyard conditions for optimum directivity are determined, and practical measures for improving antenna efficiency are mentioned.

621.396.677.3:621.396.43:551.507.362.2 2853
Communications Satellites using Arrays—M. H. Hansen. (See 3189.)

621.396.677.3:621.397.61 2854
Dipole Arrays for Transmitter Antennas for Television Bands IV/V—H. Laub. (*Frequenz*, vol. 14, pp. 327–334; October, 1960.) Problems of electrical and mechanical design of antenna arrays for the frequency range 470–790 Mc are discussed; a number of arrays are illustrated and examples of polar diagrams are given.

621.396.677.71 2855
Hybrid H-Guide Feeds Flush-Mounted Antennas—G. N. Voronoff. *Electronics*, vol. 34 pp. 54–57; March 31, 1961.) A two-dimensional array of slot radiators can be excited in this way.

621.396.677.73 2856
Horn Radiators as Gain Standards—K. E. Müller and J. Göller. *Nachrtech.*, vol. 10, pp. 414–422; September, 1960.) Approximation formulas for gain and field strength are given and the design procedure is summarized, with a comparison of calculated and measured characteristics.

621.396.677.73:621.396.663 2857
Direction-Finding Aerials with High Bearing Accuracy and Wide Frequency Ranges—K. P. Lensch. (*Z. angew. Phys.*, vol. 12, pp. 557–567; December, 1960.) Report of measurements on conical radiators of differing shape and construction, in the frequency range 100–2400 Mc. Measured radiation patterns are compared with those based on calculated values; agreement is only approximate.

621.397.677.85 2858
A Microwave Lens for Rapid Scanning—A. M. Scheggi and G. Toraldo di Francia. (*Alta Frequenza*, vol. 29, pp. 438–449; October, 1960.) Description of the design and construction of a configuration lens for 360° scanning, and also of a stack of such lenses. The radiation patterns and wavefronts obtained conform to theoretical predictions.

AUTOMATIC COMPUTERS

681.142 2859
The Physics of Computer Elements—C. N. W. Litting. (*Brit. J. Appl. Phys.*, vol. 12, pp. 207–213; May. 1961.) The general principles of acoustic, electrostatic, magnetic, optical, and superconducting storage systems are discussed. Magnetic or superconducting devices show the greatest promise for future high-speed applications.

681.142 2860
Control-Pulse Generation for a Digital Differential Analyser—P. L. Owen, M. F. Partridge, and T. R. H. Sizer. (*Electronic Eng.*, vol. 33, pp. 364–371; June, 1961.) Circuit details are given of a transistorized unit which generates control pulses by a pulse-division method involving some unusual processes.

681.142:539.23 2861
Thin Films as Elements for Automatic Computers—W. E. Proebster. (*Elektrotech. Z., Edn. A.*, vol. 81, pp. 913–920; December 5, 1960.) A review is given covering the application of thin-film storage devices, including the cryotron, to data-processing techniques. Thirty-three references.

681.142:621.382.23 2862
High-Speed Logic Circuits using Diode Logical Networks and Current-Switching Amplifiers—R. J. Miles. (*Mullard Tech. Commun.*, vol. 5, pp. 286–294; March, 1961.) The use of diode networks as an alternative to transistors in logical networks is considered. The circuits are versatile and economical, but require associated amplifiers and are likely to have a limiting switching time of about 10 nsec.

681.142:621.382.23 2863
Output-Coupling Networks for Use with Logical Circuits of the Emitter-Current Switching Type—R. J. Miles. (*Mullard Tech. Commun.* vol. 5, pp. 295–300; March, 1961.) Zener-diode coupling networks required to transfer the collector-voltage swing in emitter-current switching circuits to earth level are considered. The disadvantage of low-coupling efficiency of passive output coupling networks is considered in comparison with the versatility which they give to standard logical elements.

CIRCUITS AND CIRCUIT ELEMENTS

621.3.004.6 2864
Reliability of Electronic Components—(*Nachrtech. Z.*, vol. 13, pp. 505–528; November, 1960.) Four papers based on contributions to a discussion meeting on circuit components and materials held by the Nachrichtentechnische Gesellschaft in Stuttgart, May 5–6, 1960.

1) **Technological Measures for Improving the Reliability of Components**—K. H. J. Rottgardt (pp. 505–512).

2) **Lifetime Investigations on Capacitors**—W. Ackmann (pp. 513–518).

3) **The Effect of Humidity on the Electrical Characteristics of Capacitors**—H. Veith (pp. 519–523).

4) **The Unreliability of Electronic Equipment and its Causes**—H. J. Frundt (pp. 524–528).

621.3.049.7 2865
Recent Advances in Microminiaturization, Reliable Components and Cooling Techniques—G. W. A. Dummer. (*Solid-State Electronics*, vol. 2, pp. 18–34; January, 1961.)

621.3.049.75:621.382 2866
Silicon Epitaxial Microcircuit—W. Glendinning, C. Marlett, J. Allegretti, and D. Shombert. (PROC. IRE, vol. 49, pp. 1087–1088; June, 1961.) A Si microcircuit formed by vapor-phase deposition techniques is described. An eight-layered epitaxial structure was formed which

was capable of oscillation in different modes. Shunting capacitive and resistive leakage effects are discussed.

621.314.224.029.4 2867
The Design and Performance of High-Precision Audio-Frequency Current Transformers—J. J. Hill and A. P. Miller. (*Proc. IEE*, pt. B, vol. 108, pp. 327–332; May, 1961. Discussion, pp. 337–338.) Conventional multilayer current transformers are found to have large high-frequency errors. Details are given of precision single-layer transformers which cover the range 50 cps–30 kc.

621.316.5 2868
Application of Boolean Notation to the Maintenance of Switching Circuits—S. Alexander. (*Electronic Eng.*, vol. 33, pp. 372–374; June, 1961.) Concise notation by Boolean algebra of the operations in the maintenance schedules of complex switching circuits is used to simplify testing and fault location.

621.318.132 2869
High-Stability Ferrite Pot Cores—W. A. Everden. (*J. Brit. IRE*, vol. 21, pp. 409–414; May, 1961.) Describes a range of assemblies for laboratory use and for bulk production of stable inductors.

621.318.57:538.221:621.318.134 2870
Analysis of Ferrite-Core Switching for Practical Applications—P. A. Neeteson. (*Electronic Applic.*, vol. 20, pp. 133–152; February, 1961.) An analytical expression describing the switching process is derived which is suitable for practical circuit design. Measurements confirm the results of calculations.

621.318.57:621.375.3 2871
Core Matrix Driver employing Magnetic Amplifiers—J. Yamato and Y. Suzuki. (*Rev. Elect. Commun. Lab., Japan*, vol. 9, pp. 43–49; January/February, 1961.) A high-frequency magnetic amplifier with high efficiency, good SNR and high-output power has been developed.

621.319.4:621.372.54 2872
Low-Impedance Capacitor Design with Special Application to Filters—C. W. McCutchen and I. D. Howard. (*Electronic Eng.*, vol. 33, pp. 349–353; June, 1961.) Methods of reducing series inductance of conventional capacitors are investigated. Measurements of capacitor characteristics are discussed and an improved method of connection for filter capacitors is described.

621.372.44 2873
The Reactive Behaviour of Nonlinear Negative Differential Resistors—V. Cimagalli. (*Alta Frequenza*, vol. 29, pp. 548–554; October, 1960.) Nonlinear negative-resistance two-poles may have a reactive component when forming part of a given relaxation oscillator circuit

621.372.44 2874
A General Steady-State Analysis of Power /Frequency Relations in Time-Varying Reactances—R. G. Smart. (Proc. IRE, vol. 49, pp. 1051–1058; June, 1961.) This analysis produces the Manley-Rowe results as special cases. An "energy coefficient" is derived which specifies the behavior of an individual frequency transformation. The modes in which an individual transformation can operate are described and related to a wide range of varying-reactance devices.

621.372.5:621.382.3:517.945 2875
The Calculus of Deviations applied to Transistor Circuit and Network Analysis—T. R. Nisbet and W. W. Happ. *J. Brit. IRE*, vol. 21, pp. 437–450; May 1961.) Network analysis is simplified by the method described; rules are given for solving various transistor problems including the distributed-parameter network.

621.372.54 2876
Some Considerations on Optimum Filters—F. Pandarese. (*Note Recensioni Notiz.*, vol. 9, pp. 1043–1051; November/December, 1960.) An explicit formula is derived which gives the pulse response of a filter for signal detection in noise, where the known signal is expressed in the form of a trigonometric polynomial.

621.372.54 2877
The Design of All-Pass, Low-Pass and Band-Pass Filters with a Tchebycheff-Type Approximation of Constant Group Delay—E. Ulbrich and H. Piloty. (*Arch. elekt. Übertragung*, vol. 14, pp. 451–467; October, 1960.)

621.372.54 2878
Replacement of a Cascade of *n* Unequal Asymmetric Quadripoles of Equal Iterative Impedance by One Quadripole—W. Herzog. (*Nachrtech. Z.*, vol. 13, pp. 475–477; October, 1960.)

621.372.54 2879
The Cascade Connection of Nonreversible Quadripoles—W. Herzog. (*Nachrtech. Z.* vol. 13, pp. 477–478; October, 1960.)

621.372.54:621.372.57 2880
The Synthesis of Active and Passive Filters by the Root Locus Method—A. Susini. (*Alta Frequenza*, vol. 29, pp. 555–573; October, 1960.)

621.372.54:621.375.4 2881
Active Filter Element and its Application to a Fourier Comb—F. T. May and R. A. Dandl. (*Rev. Sci. Instr.*, vol. 32, pp. 387–391; April, 1961.) A theoretical analysis is given and constructional data are presented for a variable-Q variable-frequency band-pass filter using transistor amplifiers. Stable-Q operation is possible over a Q-factor range of 10–250 for frequencies up to 4 kc.

621.372.57:621.317.361.018.756 2882
The Applicability of Active Filters to the Measurements of the Frequency Spectra of Pulses—H. G. Jungmeister. (*Arch. elekt. Übertragung*, vol. 14, pp. 432–434; October, 1960.) The use in frequency analyzers of active filters comprising amplifiers with double-T type RC networks, results in higher Q-values at low frequencies than is possible with stagger-tuned LC circuits. The error assessment given by Seeger and Stäblein (1497 of 1958) is also applicable to this type of circuit.

621.372.6 2883
Synthesis of Transformerless Active *n*-Port Networks—I. W. Sandberg. (*Bell Sys. Tech. J.*, vol. 40, pp. 761–783; May, 1961.)

621.373.431.1:621.382.23 2884
A Circuit with Several Stable States using Tunnel Diodes—Y. Hazoni. (*Nuclear Instr. Meth.*, vol. 10, pp. 229–230; March, 1961. In French.) The circuit has four stable states, the time required for a change of state being of the order of 10^{-8} sec. It can serve as a fast prestorage device for a multichannel analyzer or as the basic unit of an associated address scaler.

621.374:621.382.23 2885
A Tunnel-Diode Univibrator and Pulse Height Discriminator—Y. Hazoni. (*Nuclear Instr. Meth.*, vol. 10, pp. 231–233; March, 1961.) An adaptation of the tunnel-diode oscillator circuit (2884 above) and its operation in conjunction with a biased backward diode [see 1959 WESCON Convention Record, pt. 3, pp. 9–31 (Lesk, *et al.*)] are described. Applications in pulse shaping and fast coincidence technique are noted.

621.374.3 2886
A Fast Amplitude Discriminator—A. Sarazin, J. Samueli, and G. Bougnot. (*Nuclear Instr. Meth.*, vol. 10 pp. 202–204; March, 1961. In French) The circuit has a discrimination range of 1–30 v, with a threshold stability within ±0.1 v. The output is a positive pulse 1.5 v in amplitude, with rise time <10 nsec and duration of 200 nsec.

621.374.3:621.382.3 2887
New Ways to Trigger Avalanche Pulse Circuits—H. G. Dill. (Proc. IRE, vol. 49, p. 1093; June, 1961.)

621.374.32 2888
Reversible Decimal Counters—J. L. Goldberg. (*Electronic Tech.* vol. 38, pp. 234–245; July, 1961.) Circuit design for both binary and bi-quinary scales of notation is discussed.

621.374.32:621.382.23 2889
Tunnel-Diode Binary Counter Circuit—H. Ur. (Proc. IRE, vol. 49, pp. 1092–1093; June, 1961.)

621.375.127 2890
Investigation of the Single-Ended Push-Pull Amplifier—F. Cervellati and P. Schiaffino. (*Alta Frequenza*, vol. 29, pp. 512–547; October, 1960.) Theoretical and practical design aspects of various versions of this type of AF amplifier are considered.

621.375.4 2891
A Quick Method for Calculating Transistor Amplifier Circuits—R. R. Vierhout and A. J. H. Vendraik. (*Electronic Eng.*, vol. 33, pp. 375–381; June, 1961.) By neglecting the parameter h_{12} calculations on transistor amplifiers can be greatly simplified. This is applied in calculations of feedback, temperature stability and noise.

621.375.4:621.372.632 2892
Calculation of Mixing Processes in Transistor Stages at Low Frequencies on the Basis of the Equivalent Circuit Diagram—J. S. Vogel and M. J. O. Strutt. (*Arch. elekt. Übertragung*, vol. 14, pp. 435–440; October, 1960.) The theory given in 2516 of August is extended to transistor mixer circuits and to distortion effects in them.

621.375.4.018.783 2893
Nonlinear Distortion of Transistorized Amplifiers—H. H. van Abbe and G. C. van Slagmaat. (*Electronic Appl.*, vol. 20, pp. 159–168; February, 1961.) Sources of distortion are examined and methods are suggested for minimizing their effects.

621.375.432 2894
Designing Amplifiers with Nonlinear Feedback—J. C. Looney. (*Electronics*, vol. 34, pp. 46–49; March 31, 1961.) Design criteria for the use of a nonlinear feedback loop with a transistor amplifier are given. Increase of dynamic range and an exponential response can be obtained.

621.375.9 2895
Design Theory of Optimum Negative-Resistance Amplifiers—E. S. Kuh and J. D. Patterson. (Proc. IRE vol. 49 pp. 1043–1050; June 1961.) An examination is made of amplifiers obtained by imbedding a linear active one-port device in arbitrary three-port devices. The optimum gain-bandwidth formula synthesis procedure and design curves are given for this and other amplifier configurations.

621.375.9:538.569.4 2896
Amplification through Stimulated Emission —the Maser—R. A. Smith. (*Brit. J. Appl. Phys.* vol. 12, pp. 197–206; May, 1961.) An account of the physical principles underlying two- and three-level maser action is given, and expressions for noise factor are derived. Recent maser applications in radio astronomy systems are noted.

621.375.9:538.569.4 2897
General Analysis of Optical, Infrared, and Microwave Maser Oscillator Emission—J. R. Singer and S. Wang. (*Phys. Rev. Lett.*, vol. 6, pp. 351–354; April, 1961.) The equations governing coherent emission are generalized. Amplitude modulation of the signal is to be expected and this can be used for communication purposes.

621.375.9:538.569.4:538.222 2898
Cross-Doping Agents for Rutile Masers—P. F. Chester. (*J. Appl. Phys.*, vol. 32, pp. 866–868; May, 1961.) The electron paramagnetic resonance spectra of rutile doped with Ta, Nb and Ce have been examined at liquid-helium temperatures. Ta and Nb appear to be suitable for securing a short spin-lattice relaxation time.

621.375.9:621.372.2 2899
A New Microwave Power Amplifier—P. A. Clavier. (Proc. IRE, vol. 49, pp. 1083–1084; June, 1961.) A method is suggested in which one electrode of a Lecher or coaxial line is made electron-emissive. A signal propagated down the line produces an amplified current in the anode.

621.375.9:621.372.44 2900
Nonreciprocal Parametric Amplifier Circuits—L. D. Baldwin. (Proc. IRE, vol. 49, p. 1075; June, 1961.) Two circuit configurations are given which do not use a circulator but which have similar properties to the single-port reflection amplifier with a three-port circulator.

621.375.9:621.372.44 2901
Staggered Operation of Doubly Resonant Parametric Amplifiers—S. Hamada and H. Mukai. (*Rev. Elect. Commun. Lab., Japan*, vol. 9, pp. 20–25; January/February, 1961.) A broad bandwidth is achieved by staggered operation of doubly resonant variable-capacitance parametric amplifiers in the 6-Gc band.

621.375.9:621.372.44:621.318.435 2902
On Parametric Excitation with Current-Saturable Inductances—N. S. Prywes. (*J. Franklin Inst.*, vol. 270, pp. 468–491; December, 1960.) A parametric-amplifier circuit with an abrupt nonlinearity is described. A method of analysis of "relaxation oscillations" leads to a physical understanding of the cycle of oscillations and quantitative relations. The stability problem is also solved.

621.375.9:621.372.44:621.382.23 2903
Minimum Noise Figure of the Variable-Capacitance Amplifier—K. Kurokawa and M. Uenohara. (*Bell Sys. Tech. J.*, vol. 40, pp. 695–722; May, 1961.) A discussion of the minimum noise figure of variable-capacitance diode amplifiers, on the assumption that the series resistance is the only parasitic element. Some experimental figures are given for DSB operation at 6 Gc and universal curves are included which illustrate the effect of changing network parameters and component temperatures.

621.375.9:621.372.44:621.382.23 2904
A Solid-State Analogue to a Travelling-Wave Amplifier—G. H. Heilmeier. (Proc. IRE, vol. 49, pp. 1079–1080; June, 1961.) An attempt to improve the dispersive properties of multidiode parametric amplifiers was made by placing stacks of varactor diodes inside an L-band helix. Bandwidths of 15–25 per cent and and a noise figure of 9.8 db were obtained.

621.375.9:621.372.44:621.385.6 2905
A Low-Noise Microwave Quadripole Amplifier—M. Ashkin. (See 3199.)

621.375.9:621.372.44:621.385.63 2906
Travelling-Wave Analysis of a Class of Parametric Amplifiers Based upon the Hill Equation—Fredricks. (See 3205.)

GENERAL PHYSICS

537.226 2907
Electric Fields and Currents in Dielectrics—É. I. Adirovich. (*Fiz. Tverdogo Tela*, vol. 2, pp. 1410–1422; July, 1960.) A general solution is given for the distribution of electric field and charge-carrier concentration in a dielectric between two metallic contacts when field-emission and thermionic currents flow from the cathode.

537.311.5 2908
Potentials in a Conductor of Varying Cross-Section—R. Jaggi. (*Phys. Rev.*, vol. 122, pp. 448–449; April 15, 1961.) The importance of the eigen-Hall effect [see 1497 of 1954 (Busch and Jaggi)] in masking the Bernoulli voltage in experimental measurements is pointed out.

537.525:538.69:621.314.6 2909
Rectification Effect in Gaseous Discharges in Crossed Magnetic and Electric Fields—G. Boucher and O. Doehler. (*C.R. Acad. Sci., Paris*), vol. 251, pp. 59–61; July 4, 1960.) Description of an experimental crossed-field diode consisting of two coaxial electrodes of stainless-steel tube, the inner electrode being filled with a ferrite stack separated by pieces of soft iron. Results obtained with a hydrogen-filled tube under a pressure of 10^{-4} Torr. show that the system is more efficient if the magnetic field is localized near the inner electrode in this manner.

537.533.8 2910
The Theory of Secondary-Electron Emission of Metals: Part 1—G. Bimschas. (*Z. Phys.*, vol. 161, pp. 190–204; December 16, 1960.)

537.56+537.311.33 2911
Complex Conductivity of some Plasmas and Semiconductors—P. H. Fang. (*Appl. Sci. Res.*, vol. B9, no. 1, pp. 51–64; 1961.) "The complex conductivities of plasmas and semiconductors have been calculated for several cases where the collision frequency can be expressed as a power function of the energy. From the result, some characteristic parameters of the plasma originally investigated by Spitzer are estimated. The problem of determining the relaxation time from a nonsymmetrical dispersion is discussed."

537.56 2912
Couette Flow of a Fully Ionized Gas, considered as a Two-Component Fluid—L. A. Peletier and L. van Wijngaarden. (*Appl. Sci. Res.*, vol. B9, no. 2, pp. 141–150; 1961.)

537.56 2913
Experimental Study of the Dimagnetism of Gaseous Plasmas with Electron and Nuclear Spin Resonance Techniques—T. C. Marshall and L. Goldstein. (*Phys. Rev.*, vol. 122, pp. 367–376; April 15, 1961.)

537.56:538.56 2914
Energy Conversion Mechanism in a Bounded Magnetized Current-Carrying Plasma—G. H. Joshi. (*Phys. Rev. Lett.*, vol. 6, pp. 339–341; April 1, 1961.) For a finite plasma, coupling exists between quasi-transverse electromotive waves and quasi-longitudinal space-charge waves. This can lead to an energy transfer between the kinetic energy of drifting plasma and electromotive energy. This mechanism may be useful for heating a thermonuclear plasma using the "runaway electrons." Certain types of VLF radio noise can also be explained.

537.56:538.561.029.65/.66 2915
Emission of Submillimetre Electromagnetic Radiation from Hot Plasma in ZETA—G. N. Harding, M. F. Kimmitt, J. H. Ludlow, P. Porteous, A. C. Prior, and V. Roberts. (*Proc. Phys. Soc. (London)*, vol. 77, pp. 1069–1075; May 1, 1961.) The first results are reported of experiments using spectroscopy in the far infrared (0.1–1.6 mm).

537.56:538.6 2916
Oscillations of a Plasma in a Static Magnetic Field—N. Anderson. (*Proc. Phys. Soc. (London)*, vol. 77, pp. 971–979; May 1, 1961.) The dielectric tensor is calculated and used together with the solutions to the propagation problem at zero temperature to allow for thermal effects.

537.56:538.69 2917
The Theory of Plasmas in the Presence of Magnetic Fields—J. Friedrich. (*Z. Phys.*, vol. 160, pp. 494–503; November 22, 1960.) On the basis of Boltzmann's equation the complete theory of a stationary cylindrical plasma is obtained allowing for the presence of the intrinsic magnetic field and of an additional logitudinal magnetic field.

538.221 2918
Statistical Mechanics of Ferromagnetism; Spherical Model as High-Density Limit—R. Brout. (*Phys. Rev.*, vol. 122, pp. 469–474; April 15, 1961.) The conjecture of the validity of the spherical model (3789 of 1960) is examined and justified.

538.56:621.396.677.8 2919
Measurements on Resonators formed from Circular Plane and Confocal Paraboloidal Mirrors—E. H. Scheibe. (Proc. IRE, vol. 49, p. 1079; June, 1961.) A measured Q of 260,000 at 3.2 cm λ was obtained, and results were in agreement with those of Fox and Li relating to optical masers (*ibid.*, vol. 48, pp. 1904–1905; November, 1960).

538.561:537.533 2920
Cherenkov Radiation in a Dielectric Tube Waveguide—B. W. Hakki and P. D. Coleman. (Proc. IRE, vol. 49 pp. 1084–1085; June, 1961.) An experimental arrangement for measuring the radiation is described and results are given. High interaction resistances can be obtained at the expense of physical size and mode interference.

538.566:535.43 2921
Shift of the Shadow Boundary and Scattering Cross-Section of an Opaque Object—S. I. Rubinow and J. B. Keller. (*J. Appl. Phys.*, vol. 32, pp. 814–820; May 1961.)

538.566:535.43 2922
Near-Zone Back-Scattering from Large Spheres—V. H. Weston. (*Appl. Sci. Res.* vol. B9, pp. 107–116; 1961.) Backscatter from a perfectly conducting sphere for short wavelengths is theoretically treated. The back-scatter cross section is modified considerably as the receiver approaches to within a few radii, and becomes the cross section of a flat plate for a receiver very near the sphere.

538.566:539.23 2923
Reflection and Transmission of Conductive Films—M. V. Schneider. (Proc. IRE, vol. 49, pp. 1090–1091; June, 1961.) A more general relation for the reflection and transmission co-

efficients is given for the case of oblique incidence, and perturbations due to frequency dependence and displacement currents are considered. A formula is also derived for thick films. See also 4197 of 1960 (Koide).

538.569.4:537.525 2924
Microwave Zeeman Effect of Free Hydroxyl Radicals—H. E. Radford. (*Phys. Rev.* vol. 122, pp. 114–130; April 1, 1961.) The theory of the Zeeman effect in $^2\Pi$ levels of light diatomic radicals is extended to the general intermediate coupling case and used for detailed analysis of observed paramagnetic resonance absorption spectra, at 3 cm λ, of the products of an electric discharge in low-pressure H_2O and D_2O vapor.

538.569.4:538.222 2925
On the Theory of Cross-Relaxation in Maser Materials—M. Hirono. (*J. Radio Res. Labs, Japan* vol. 8, pp. 1–15; January, 1961.) The cross-relaxation rate is calculated by the method of moments, taking into account the effect of the crystalline electric field.

538.569.4:621.375.9 2926
Phonon Masers and the Phonon Bottleneck—C. Kittel. (*Phys. Rev. Lett.*, vol. 6, p. 449; May 1, 1961.) A calculation shows that the transfer of energy from the electron spin system can set up a stimulated phonon emission leading to maser action.

538.691 2927
'Corkscrew'—a Device for Changing the Magnetic Moment of Charged Particles in a Magnetic Field—R. C. Wingerson. (*Phys. Rev. Lett.*, vol. 6, pp. 446–448; May 1, 1961.) A helical field source is described which produces a monotonic increase or decrease in the transverse energy of a particle moving initially in the uniform field along the helix axis.

539.2 2928
Higher Random-Phase Approximations in the Many-Body Problem—H. Suhl and N. R. Werthamer. (*Phys. Rev.*, vol. 122, pp. 359–366; April 15, 1961.) "The usual random phase approximation combined with an equations-of-motion technique for the many-electron problem is extended yielding many of the known results of series summation methods in a straightforward manner. The method should apply to other types of many-body problems as well."

539.2:538.2 2929
A Variational Approach to Correlation in an Electron Gas—W. H. Young. (*Phil. Mag.*, vol. 6, pp. 371–377; March, 1961.) A periodic electron density is allowed, and it is proved that there exist one-particle states energetically more favorable than the usual plane-wave orbitals.

GEOPHYSICAL AND EXTRATERRESTRIAL PHENOMENA

523.164:621.317.794 2930
Digital Radiometer—Weinreb. (See 3115.)

523.164.3 2931
Radio Emission from the Cygnus Loop—D. S. Mathewson, M. I. Large, and C. G. T. Haslam. (*Monthly Notices Roy Astron. Soc.*, vol. 121 no. 6, pp. 543–550; 1960.) A high-resolution study of the Cygnus Loop has been made at 408 Mc and the results are compared with the optical features. Estimates of the thermal and nonthermal radio emissions are made.

523.164.3 2932
Secular Variation of the Flux Density of the Radio Source Cassiopeia A—D. S. Heeschen and B. L. Meredith. (*Nature*, vol. 190, pp. 705–706; May 20, 1961.) Observations at 1400 Mc support the evidence of Hogbom and Shakeshaft (1492 of May) of a decrease of about 1 per cent per annum in the flux density of Cassiopeia A over the last 12 years.

523.164.3:523.42 2933
The Microwave Temperature of Venus—D. E. Jones. (*Planet. Space Sci.*, vol. 5, pp. 166–167; June, 1961.) Solar corpuscular radiation may maintain an ionosphere on Venus, and the variation in observed brightness temperature may consequently be a function of zenith angle.

523.164.3:523.45 2934
The Source of Radiation from Jupiter at Decimetre Wavelengths: Part 3—Time Dependence of Cyclotron Radiation—G. B. Field. (*J. Geophys. Res.*, vol. 66, pp. 1395–1405; May, 1961.) Part 2: 3471 of 1960.

523.164.4 2935
Radio Emission from the Perseus Cluster—P. R. R. Leslie and B. Elsmore. (*Observatory*, vol. 81, pp. 14–16; February, 1961.) Two small components of the Perseus cluster separated by 350 kc have been identified. They may be physically related in a similar manner to that of the two emitting regions in Cygnus-A.

523.165 2936
The Effects of Betatron Accelerat ons upon the Intensity and Energy Spectrum of Magnetically Trapped Particles—P. J. Coleman, Jr. (*J. Geophys. Res.*, vol. 66, pp. 1351–1361; May, 1961.) The effects of change of magnetic field on the energy spectrum are calculated.

523.165 2937
Characteristics and Fine Structure of the Large Cosmic-Ray Fluctuations in November 1960—J. F. Steljes H., Carmichael, and K. G. McCracken. (*J. Geophys. Res.* vo. 66, pp. 1363–1377; May, 1961.) Report and discussion of observations of solar cosmic-ray increases on November 12 and 15, the former occurring at a time of a sharp Forbush decrease.

523.165 2938
Balloon Observations of Auroral-Zone X Rays—R. R. Brown. (*J. Geophys. Res.*, vol. 66, pp. 1379–1388; May, 1961.) X rays are detectable about 10 per cent of the time; large increases occur during geomagnetic disturbances.

523.165 2939
Seasonal Variations of Cosmic-Ray Intensity in Polar Regions—K. Maeda and V. L. Patel. (*J. Geophys. Res.*, vol. 66, pp. 1389–1393; May, 1961.)

523.5:621.396.96 2940
Analysis of a Type of Rough-Trail Meteor Echo—B. A. McIntosh. (*Canad. J. Phys.*, vol. 39, pp. 437–444; March, 1961.) The characteristics of *b*-type echoes are examined in detail (see also 2226 of 1959). The rough trail may be due to fragmentation of the dust-ball type of meteoroid.

523.5:621.393.96 2941
The Height Variation of the Ambipolar Diffusion Coefficient for Meteor Trails—J. S. Greenhow and J. E. Hall. (*Planet. Space Sci.*, vol. 5, pp. 109–114; June, 1961.) Both the two-station and the split-beam measuring techniques were used. It was concluded that the atmospheric scale height during winter at a height of 98 km above Jodrell Bank (53° 14′ N) is 8.0 km.

523.75:523.165 2942
Delayed Propagation of Solar Cosmic Rays on September 3, 1960—J. R. Winckler, P. D. Bhavsar, A. J. Masley, and T. C. May. (*Phys. Rev. Lett.*, vol. 6, pp. 488–491; May 1, 1961.) An analysis of balloon, rocket and ground-level observations reveals that the delay between the flare and the arrival of solar protons increases with decrease in proton energy.

523.75:523.165 2943
Rocket Observations of Solar Protons on September 3, 1960—L. R. Davis, C. E. Fichtel, D. E. Guss, and K. W. Ogilvie. (*Phys. Rev. Lett.*, vol. 6, pp. 492–494; May 1, 1961.) The results of nuclear-emulsion and G-M counter observations are used to derive the integral and differential spectra for protons of energy 10–200 Mev arriving at the top of the atmosphere.

550.385.4 2944
Magnetic Disturbances and the Earth's Magnetic Field—J. S. Chatterjee. (*J. Geophys. Res.*, vol. 66, pp. 1535–1546; May, 1961.) Storm-time changes in the earth's magnetic field could induce currents in the earth's core which interact with the steady field. This produces a nett unidirectional current at the end of the disturbance which penetrates gradually down to the core and has a decay time of a million years. This current could be responsible for maintaining the steady field.

550.385.4 2945
Solar Corpuscular Showers and Families of Geomagnetic Storms—V. I. Afanas'eva. (*Dokl. Akad. Nauk SSSR*, vol. 135, pp. 1120–1122; December 11, 1960.) Investigation of the effect of corpuscular showers in producing 1) magnetic storms and 2) magnetic disturbances during which the corpuscular showers pass near the earth without enveloping it.

550.385.4:523.165 2946
The Ring Current, Geomagnetic Disturbance, and the Van Allen Radiation Belts—S. I. Akasofu and S. Chapman. (*J. Geophys. Res.*, vol. 66, pp. 1321–1350; May, 1961.) The negative phase of a magnetic storm is ascribed to the formation of a ring current at a distance about four earth's radii from the earth's centre. The magnetic field due to the current is calculated and compared with observational results.

551.507.362.1:523.165 2947
Radiation Measurements during the Flight of the Third Space Rocket—S. N. Vernov, A. E. Chudakov, P. V. Vakulov, E. V. Gorchakov, Yu. I. Logachev, and A. G. Nikolaev. (*Dokl. Akad. Nauk SSSR*, vol. 136, pp. 322–324; January 11, 1961.) Preliminary analysis of results of instrument recordings made during the flight of the rocket between the 4th and 18th of October, 1959.

551.507.362.2 2948
Secondary-Electron Emission and the Satellite Ionization Phenomenon—D. B. Medved. (PROC. IRE, vol. 49, pp. 1077–1078; June, 1961.) Electron emission from a satellite and the electron density variation near it due to bombardment by neutral particles are considered.

551.507.362.2 2949
Sputtering as a Possible Mechanism for Increase of Ionization in the Vicinity of Low-Altitude Satellites—G. D. Magnuson and D. B. Medved. (*Planet. Space Sci.*, vol. 5, pp. 115–121; June, 1961.) An increase in ionization above ambient may occur at distances of up to 1 mean path from the satellite. Ionization potentials of the injected atoms are ¼ to ½ those of the ambient species. The probability of any collision leading to ionization should exceed 10^{-6} with the model proposed, for the mechanism to be of interest.

551.507.362.2 2950

The Effect of Atmospheric Rotation on the Orbital Plane of a Near-Earth Satellite—G. E. Cook and R. N. A. Plimmer. (*Proc. Roy. Soc.* (*London*) *A*, vol. 258, pp. 517–528; November, 1960.) Theoretical formulas are derived for the rotation of the orbital plane and change in orbital inclination of a near-earth satellite due to the influence of the atmosphere.

551.507.362.2:523.165 2951

Satellite Determination of Heavy Primary Cosmic-Ray Spectrum—M. A. Pomerantz, S. P. Agrawal, P. Schwed and H. Hanson. (*Phys. Rev. Lett.*, vol. 6, pp. 362–364; April 1, 1961.) A preliminary report of the heavy-nuclei cosmic-ray flux observed aboard Explorer VII is given.

551.507.362.2:621 391.812.5 2952

Drop-Out Phenomenon Observed in the Satellite 1958 δ_2 Transmissions—L. Liszka. (*J. Geophys. Res.*, vol. 66, pp. 1573–1577; May, 1961.) Irradiation of the quartz oscillator in 1958 δ_2 during passage through the horns of the outer Van Allen belt may explain "drop-outs"—sudden decreases of observed signal strength.

551.507.362.2+523.3 :621.396.96 2953

Sideband Correlation of Lunar and Echo Satellite Reflection Signals in the 900-Mc/s Range—R. E. Anderson. (PROC. IRE, vol. 49, pp. 1081–1082; June, 1961.) Measurements are described and records of signal variation are illustrated. With lunar reflections a correlation of 0.1 was obtained between sidebands with 4 kc separation: the correlation of signals reflected from Echo balloon with 20-kc sideband separation was better than that of lunar reflections with 500-cps separation.

551.510.53 2954

Production of Carbon in the Upper Atmosphere—K. P. Chopra. (*Planet. Space Sci.*, vol. 5, pp. 164–166; June, 1961.) Before decaying, very fast neutrons originating from disintegrations by high energy cosmic ray particles may collide with nitrogen atoms to produce ${}_5B^{11}$ and ${}_6C^{14}$. This "neutron-capture" should result in carbon and boron atoms and traces of cyanogen gas being present in the upper atmosphere, while by-products of the mechanism may contribute significantly to the formation of the inner radiation belt.

551.510.535 2955

Studies of the *E* Layer of the Ionosphere: Part 2—Electromagnetic Perturbations and Other Anomalies—E. V. Appleton and A. J. Lyon. (*J. Atmos. Terr. Phys.*, vol. 21, pp. 73–99; June, 1961.) Departures from the predictions of simple theory in observed *E*-layer behavior are attributed to perturbations arising from the motor effect of the S_q system of currents flowing there. The main effect is to raise f_0E near noon in low latitudes and reduce it in high latitudes. The departure of f_0E from proportionality to $(\cos\chi)^{\frac{1}{2}}$, and other anomalies are also discussed. Part 1: 1432 of 1957.

551.510.535 2956

Note on the Role of Small Layers with Irregular Surfaces in the Formation of Sporadic-E Layers—J. Voge. (*Ann. Télécommun.*, vol. 16, pp. 62–63; January/February, 1961.) In earlier work by du Castel *et al.* (*ibid.*, vol. 15, pp. 38–47 and 107–142; January/February and May/June, 1960) irregularities in the refractive index of the troposphere have been represented by a model which has now been adapted to the E_s layer. The reflection coefficients calculated using the model are of the right order of magnitude.

551.510.535 2957

Irregularities in the E_s Layer of the Ionosphere—G. F. Fooks. (*Nature*, vol. 190, p. 707–708; May 20, 1961.) Correlation analysis shows no systematic elongation at Cambridge (52°N, 0°E) in contrast to the E-W elongation of auroral, and N-S elongation of equatorial type of E_s. There is a wide range of sizes in the scale of the irregularities in the diffraction pattern on the ground.

551.510.535 2958

Consideration of the F_1 Layer in the Ionosphere—S. Ishikawa and S. Hiidome. (*J. Radio Res. Labs., Japan*, vol. 8, pp. 29–40; January, 1961.) A graphical statistical description of the diurnal, seasonal and annual variations of f_0F_1 at Kokobunji and information on the relation between f_0F_1 and f_0F_2.

551.510.535 2959

Diurnal Variation of F_1-Region Drifts at Waltair—E. B. Rao and B. R. Rao (*Curr. Sci.*, vol. 30, pp. 9–10; January, 1961.) The results of F_1-region drift measurements for the four seasons in the years 1956–1958 are given. See also 2242 of 1959.

551.510.535 2960

Equatorial Spread-F at Ibadan, Nigeria—A. J. Lyon, N. J. Skinner, and R. W. Wright. (*J. Atmos. Terr. Phys.*, vol. 21, pp. 100–119; June, 1961.) Spread-F characteristics are closely related to the height of the layer; the irregularities may be due to hydromagnetic disturbances, which are increasingly attenuated at lower heights. See also 879 of March.

551.510.535 2961

Variation in Height of Anisotropy and Random Drift Velocity of the Irregularities in the Ionosphere—B. R. Rao and K. V. V. Ramana. (*Nature*, vol. 190, no. 4777, pp. 706–707; May, 1961.) Correlation analysis shows that the axial ratio of the anisotropy ellipse and the random change factor $(V_C)_r/V$ are both greatest for waves reflected from heights of 270–290 km.

551.510.535 2962

Possible Identification of Atmospheric Waves Associated with Ionospheric Storms—M. D. Wright. (*Nature*, vol. 190, no. 4779, pp. 898–899; June, 1961.) The onset time of an ionospheric storm is defined as the time of first increase at $h'F$ and the velocity is determined by measuring the time delay at Godley Head, 1105 km north of Campbell Island. The mean northward velocity for eight well-defined storms was found to be in the range 406–691 m/sec and may correspond to the velocity of a neutral gaseous wave as indicated by the Johnston Island nuclear explosion disturbance, *i.e.*, 470 m/sec.

551.510.535 2963

A Method of Calculation of N(h) Profiles from Ionospheric $h'(f)$ Curves—H. Hojo. (*J. Radio Res. Labs., Japan*, vol. 8, pp. 41–57; January, 1961.) See 1509 of May.

551.510.535 2964

A New Method for the Analysis of Ionospheric $h'(f)$ Records—J. E. Titheridge. (*J. Atmos. Terr. Phys.*, vol. 21, pp. 1–12, April, 1961.) A method is given for calculating the real heights of reflection in the ionosphere, from the observed virtual heights. The real height is assumed to be a polynomial in the plasm. frequency.

551.510.535 2965

General Expression for the Group Refractive Index of the Ionosphere—Y. S. N. Murty and S. R. Khastgir. (*J. Atmos. Terr. Phys.*, vol. 21, pp. 65–69; April, 1961.) A general expression for the group refractive index of the ionosphere is found in which wave frequency, electron density and collision frequency, magnetic field and direction of propagation are variables. See also 2001 of 1960.

551.510.535:517.64 2966

A Solution of the Integral Equation $h'(f) = \int \mu'(f; f_0)dz(f_0)$—H. Unz. (*J. Atmos. Terr. Phys.*, vol. 21, pp. 40–45; April, 1961.) A method involving power series expansions is given for solving the integral equation. One advantage of the method is the use of a set of master curves which applies for all stations.

551.510.535:523.745 2967

A Study of the Variations in a Daily Ionospheric Index of Solar Activity—G. H. Bazzard. (*J. Atmos. Terr. Phys.*, vol. 21, pp. 193–202; June, 1961.) A table of daily values of J_E/I_E^4 sec χ at Slough is given for 1959. The short term variations in J_E from July 1957–December, 1959 are examined by statistical methods and it is shown that these variations are related to changes in the sun.

551.510.535:523.746 2968

A Long-Term Variation in the Relationship of Sunspot Numbers to *E*-Region Character Figures—R. Naismith, H. C. Bevan and P. A. Smith. (*J. Atmos. Terr. Phys.*, vol. 21, pp. 167–173; June, 1961.) The statistical relation between sunspot number and month mean values of $Ch_E = f_E^4$ sec χ at Slough suggests that from 1933 onwards, there has been a decrease in the value of Ch_E corresponding to a given sunspot number.

551.510.535:523.75 2969

Solar Flare Effects in the *F* Region of the Ionosphere—R. W. Knecht and K. Davies. (*Nature*, vol. 190, no. 4778, pp. 797–798; May, 1961.) Increases in f_0F_2 were observed during flares in 1949 and 1956 which were accomplnied by increases in sea-level cosmic-ray intensity. Similar increases in f_0F_2 are reported in November, 1960, at two stations and simultaneous falls in isoionic heights of 10–20 km were also observed.

551.510.535:539.16 2970

Sporadic-*E* Phenomena associated with the High-Altitude Nuclear Explosions over Johnston Island—L. Thomas and R. E. Taylor. (*J. Atmos. Terr. Phys.*, vol. 21, pp. 205–208; June, 1961.) Marked increases in E_s occurred near latitudes 60° N and S and are attributed to the explosions.

551.510.535:550.385.2 2971

Magnetic Effects in the *F* Region of the Ionosphere—J. W. King (*J. Atmos. Terr. Phys.*, vol. 21, pp. 26–34; April, 1961.) Nighttime values of f_0F_2 at stations in the south of Africa are found to decrease with increasing values of the equivalent planetary daily amplitude A_p. The magnetic control of nighttime ionization could account for the day-to-day correlation of f_0F_2 values. The relation of ionospherically and magnetically quiet days is discussed.

551.510.535:621.3.085 2972

Automatic Ionogram Scaler—M. Onoye, F. Ochi, N. Omiya and K. Arai. (*J. Radio Res. Labs, Japan*, vol. 8, pp. 59–63; January, 1961.) An instrument has been designed which projects an ionogram onto a screen. The parameters which are read off are recorded simultaneously on punched tapes and in typewritten form. The tape can be used to produce punched cards if required.

551.510.535:621.3.087.4 2973

Active High-Frequency Spectrometers for Ionospheric Sounding: Part 3—Determination

of True Height from the Virtual Height of Reflection—A. K. Paul. (*Arch. elekt. Übertragung*, vol. 14, pp. 468–476; October, 1960.) A new method for determining true height is described (see also 2591 of August) and its application to daytime and nighttime soundings discussed. Part 2: 2597 of August (Rawer).

551.510.535:621.3.087.4 2974
A New Type of Ionospheric Drift Recorder.—B. R. Rao and R. R. Rao. (*J. Atmos. Terr. Phys.*, vol. 21, pp. 208–210; June, 1961.) A method of eliminating photographic and pen recording of fading signals and the laborious calculations. A tape recorder is used to introduce a variable time delay into one antenna feed. When this delay equals that of the received signals a minimum is obtained. Delays of 0.07–1.5 sec have been measured.

551.510.535:621.391.812.63 2975
Day-to-Day and Station-to-Station Correlation of Ionospheric F-Region Critical Frequencies—J. W. King. (*J. Atmos. Terr. Phys.*, vol. 21, pp. 35–39; April, 1961.) The correlation of simultaneous f_0F_2 values at stations separated by 1700 km in a north-south direction is found to have a semi-diurnal variation, the phase of which varies with season. Results at a single station show an important autocorrelation for values at the same time on consecutive days, and this is ascribed to magnetic effects.

551.510.535:621.391.812.63 2976
Year-to-Year Changes in the Winter Anomaly in Ionospheric Absorption—L. Thomas. (*J. Atmos. Terr. Phys.*, vol. 21, pp. 215–217; June, 1961.) The mean anomalous component in a given winter is linearly related to the mean magnetic *C* figure for the same winter.

551.510.535(98):523.75 2977
Some Characteristics of Solar Corpuscular Radiations which Excite Abnormal Ionization in the Polar Upper Atmosphere—K. Sinno. (*J. Radio Res. Labs. Japan*, vol. 8, pp. 17–28; January, 1961.) Statistical data on the time delay from the occurrence of a major flare until the onset of polar absorption have been studied. It is suggested that particles ejected from the sun may be trapped in a corpuscular cloud which may later intersect a magnetic line of force along which particles can travel to reach the earth.

551.510.536 2978
The Coupling between the Protonosphere and the Normal F Region—W. B. Hanson and I. B. Ortenburger. (*J. Geophys. Res.*, vol. 66, pp. 1425–1435; May 1961.) In the protonosphere, above about 900 km, the distribution of protons is determined by diffusion rather than chemical processes: this region is independent of diurnal changes in the ionosphere.

551.510.62 2979
Continuous Recordings for the Determination of the Vertical Gradient of the Refractive Index in the Free Atmosphere—H. P. Barthelt and A. Rossbach. (*Nachrtech. Z.*, vol. 13, pp. 462–464; October, 1960.) Report on measurements made by equipment mounted at six different levels on a 160-m tower to determine the correlation between the refractive-index gradient and field-strength fluctuations over a 250-km radio-link path.

551.510.62 2980
The Radio Refractive Index Gradient over the British Isles—J. A. Lane. (*J. Atmos. Terr. Phys.*, vol. 21, pp. 157–166; June, 1961.) Airborne microwave refractometer measurements made in the British Isles confirm that the quantity $(n-1)$ varies exponentially with height. The variations in the parameters are less than those in the U. S. There is a high correlation between the surface value of $(n-1)$ and the average decrease in the refractive index in the first kilometre in altitude.

551.594.21 2981
A Criterion for Thunderstorm Theories—J. A. Chalmers. (*J. Atmos. Terr. Phys.*, vol. 21, pp. 174–176; June, 1961.) Results on the charging and external currents of the same storm favor the classical theory rather than the convection theories. See 165 of 1960.

551.594.5 2982
Aurora and Airglow from Colour Film Observations—B. P. Sandford. (*J. Atmos. Terr. Phys.*, vol. 21, pp. 177–181; June 1961.) Summary of experience using color film records.

551.594.5:621.396.96 2983
Investigation of Auroral Echoes: Part 2.—L. Harang and J. Tröim. (*Planet Space Sci.*, vol. 5, pp. 105–108; June, 1961.) Ratios of measured echo signal strength at 40 and 80, and 40 and 120 Mc showed that the frequency dependence of the reflection coefficient is qualitatively explained by either an inverse λ^2 law (partial reflection from large surfaces) or an exp $(-k/\lambda^2)$ law (scattering from field-aligned irregularities) Part 1: 1175 of April.

551.594.6 2984
Narrow-Band Atmospherics from Two Local Thunderstorms—F. Horner. (*J. Atmos. Terr. Phys.*, vol. 21, pp. 13–25; April, 1961.) Atmospherics from two storms were studied. Reception frequencies of 11 Mc and 6 kc were used with power bandwidths in the range 200–300 cps. Duration, peak amplitude, mean field strength and mean power flux were calculated. Results conflict with some theories of the origin of atmospherics.

551.594.6 2985
On the Extremely-Low-Frequency Spectrum of Earth-Ionosphere Cavity Response to Electrical Storms—H. R. Raemer. (*J. Geophys. Res.*, vol. 66, pp. 1580–1583; May, 1961.) A comparison of the observed and calculated spectra in the range 5–33 cps.

551.594.6 2986
Simultaneous Observations of V.L.F. Noise ('Hiss') at Hobart and Macquarie Island—R. L. Dowden. (*J. Geophys., Res.*, vol. 66, pp. 1587–1588; May, 1961.) The noise sources seem to be small in size and to have different locations at 4 and 9 kc.

551.594.6 2987
Dispersions of Multiple-Stroke Whistlers—N. D. Clarence and P. A. O'Brien. (*Nature*, vol. 190, pp. 1096–1097; June 17, 1961.) Analysis of I.G.Y. records at Durban indicates a 4–6 per cent increase in the dispersion of successive components of multiple-stroke short whistlers which supports the current-jet hypothesis of whistler generation.

LOCATION AND AIDS TO NAVIGATION

621.396.663.089.6 2988
Problems of Calibration of Two-Channel Cathode-Ray Direction Finders—G. Kattner and W. Rohrbeck. (*Nachrtech.*, vol. 10, pp. 392–397; September, 1960.) Methods of calibrating and checking the calibration of direction finders are outlined, including one for periodically interchanging the two channels.

621 396.932.2:627.95 2989
Marine Distress Beacon—K. Jirsa. (*Telefunken Ztg.*, vol. 33, pp. 290–294; December, 1960.) Description of a floating distress beacon operating at 2.182 Mc using battery-driven transistor circuits and the ferrite-rod antenna detailed in 4223 of 1959 (Baur and Ziehm).

621.396.963+534.88 2990
Video Integration in Radar and Sonar Systems—D. C. Cooper and J. W. R. Griffiths. (*J. Brit. IRE*, vol. 21, pp. 421–433; May, 1961.) The performance of ideal and practical systems, including the influence of antenna beamwidth, is examined. A new double delay-loop integrator giving a small improvement in threshold detection and having some practical advantages is described.

621.396.963.325 2991
Nonlinear Effects in Rotating-Coil P.P.I. Displays—R. H. C. Morgan . (*Mullard Tech. Commun.*, vol. 5, pp. 252–258; March, 1961.) "Nonlinearity effects of the three coaxial deflection coils in a PPI display system and methods to minimize them by means of careful coil design and adjustment, are discussed."

MATERIALS AND SUBSIDIARY TECHNIQUES

535.215 2992
Theory of the Photomagnetic effect in Cubic Anisotropic Crystals—A. A. Grinberg. (*Fiz. Tverdogo Tela*, vol. 2, pp. 1361–1367; July, 1960.)

535.215:537.311.33 2993
Determination of Recombination Contents from the Spectral Characteristics of a Photocell with a *p-n* Junction: Part 2—G. B. Dubrovskil and V. K. Subashiev. (*Fiz. Tverdogo Tela*, vol. 2, pp. 1562–1571; July, 1960.) The analysis of Part 1 [1871 of June (Subashiev)] is applied to photocells obtained by diffusion of donor impurities in *p*-type Si.

535.215:539.23 2994
Photoconductivity of Sulphur Layers Treated with Mercury Vapour—M. I. Korsunskil, N. S. Pastushuk, and G. D. Mokhov. (*Fiz. Tverdogo Tela*, vol. 2, pp. 1581–1583; July, 1960.) Treated layers of resistance $\ll 10^6\ \Omega$, showed simultaneous positive and negative photoconductivity of large inertia. In the short-wavelength region ($\lambda = 453\ m\mu$) negative photoconductivity predominated; in the long-wavelength region ($\lambda = 645\ m\mu$) only positive photoconductivity was observed.

535.215:546.47'221 2995
An Investigation of the Induced Conductivity in Thin Zinc Sulphide Layers—A. A. Didenko, Yu. A. Nemilov, and V. I. Fomina. (*Fiz. Tverdogo Tela*, vol. 2, pp. 1434–1440; July, 1960.)

535.215:546.48'221 2996
The Contribution of Ions to the Current through CdS at High Temperature—K. W. Böer and H. Gutjahr. (*Mber. Dtsch. Akad. Wiss. Berlin*, vol. 2, no. 6, pp. 324–327; 1960.) Experimental investigations indicate that up to a temperature of 430°C, the ion current is less than 0.1 per cent. See also 2241 of July (Böer, *et al.*).

535.215:546.48'221 2997
An Investigation of the Lux/Ampere Characteristics of CdS Single Crystals—E. A. Sal'kov and G. A. Fedorus. (*Fiz. Tverdogo Tela*, vol. 2, pp. 1576–1580; July, 1960.) Results of photocurrent measurements are at variance with theory [see, *e.g.*, 768 of 1956 (Rose) and 3102 of 1958 (Bube)].

535.215:546.48'221 2998
Intermittent-Light Method for the Measurement of Capture Cross-Sections for Traps in Cadmium Sulphide—E. A. Niekisch. (*Z.*

Phys., vol. 161, pp. 38–45; December 1, 1960.) The method described in 2972 of 1955 is used to determine capture cross-sections for shallow traps near the conduction band in CdS crystals.

535.215.546.48'221 2999
Current Noise and Distributed Traps in Cadmium Sulphide—J. J. Brophy. (*Phys. Rev.*, vol. 122, pp. 26–30; April 1, 1961.) Measurements of noise as a function of frequency in a single crystal, at different temperatures and levels of illumination, give a $1/f$ trapping noise spectrum of the form $(1/\omega)$ arc tan $\omega\tau$. Values of τ are obtained from the low-frequency turnover point, and give trap depths which are in good agreement with discrete trapping levels determined from other measurements.

535.215:546.48'221 3000
Fine Structure and Magneto-optic Effects in the Exciton Spectrum of Cadmium Sulphide—J. J. Hopfield and D. G. Thomas. (*Phys. Rev.* vol. 122, pp. 35–52; April 1, 1961.) Detailed experimental study of the magneto-optic absorption spectrum of direct excitons formed from the top valence band and the conduction band, and theoretical interpretation of results. See also 1641 of 1960 (Thomas and Hopfield).

535.215:546.48'241 3001
The Optical Properties of Cadmium Telluride in the Far Infrared Region—A. Mitsuishi. (*J. Phys. Soc., Japan*, vol. 16, pp. 533–537; March, 1961.)

535.37:546.47'221:535.215 3002
Impedance Changes Induced by Light in ZnS Phosphors—I. Uchida and K. Satake. (*J. Phys. Soc. Japan*, vol. 16, p. 573; March, 1961.) The impedance change of a capacitor containing a phosphor is interpreted in terms of an equivalent circuit and used to derive the photoconductivity.

535.376 3003
A New Electroluminescence Effect in Black Carborundum—A. G. Gol'dman. (*Dokl. Akad. Nauk SSSR*, vol. 135, no. 5, pp. 1108–1110; December, 1960.) Samples are prepared by applying the p-type material a sensitive n-type layer. When acted upon by current in the forward direction a luminescence is produced at the p-n junction.

535.376 3004
The Field Enhancement of ZnS.CdS-Mn Phosphors with X-Ray Excitation—H. Winkler, H. Rëppischer, and G. Wendel. (*Z. Phys.*, vol. 161, no. 3, pp. 330–338; December, 1960.) The results of experimental investigations differ to some extent from those of other authors. The "memory" effect described by Destriau (1213 of 1959) was observed as a consequence of field action alone before X-ray excitation.

535.376:546.47'221 3005
Direct-Current Electroluminescence at Low Voltages—W. A. Thornton. (*Phys. Rev.*, vol. 122, pp. 58–59; April 1, 1961.) Electroluminescence can occur at applied voltages corresponding to only about half the band gap of a ZnS phosphor; hence the acceleration-collision theory is ruled out at low voltage.

535.376:546.47–31 3006
Excitation of Zinc Oxide by Slow Electrons—P. Wachter. (*Z. Phys.*, vol. 161, pp. 62–73; December 1, 1960.) Investigations of low-energy excitation of ZnO phosphors were carried out with an electron beam of small velocity spread; a theoretical interpretation of the results is given.

537.226:546.47'221:539.23 3007
On the Dielectric Properties of Thin Films of Zinc Sulphide—R. Fuchshuber, R. Gullien, and S. Roizen. (*C.R. Acad. Sci., Paris*, vol. 251, pp. 51–53; July 4, 1960.)

537.227 3008
Dielectric Properties of Solid Solutions of Sodium Niobate-Lead Zirconate and Sodium Niobate-Lead Titanate—W. R. Bratschun and R. L. Cook. (*J. Am. Ceram. Soc.*, vol. 44, no. 3, pp. 136–140; March, 1961.)

537.227 3009
Variation of Permittivity with Electric Field in Perovskite-Like Ferroelectrics—H. Diamond. (*J. Appl. Phys.*, vol. 32, pp. 909–915; May, 1961.) Variation of incremental permittivity is shown to be associated with an induced ferroelectric state rather than being directly a property of domain processes; large variations with field must be accompanied by strong thermal sensitivity.

537.227 3010
Bismuth Titanate: a Ferroelectric—L. G. Van Uitert and L. Egerton. (*J. Appl. Phys.* vol. 32, p. 959; May, 1961.) Results of measurements of dc resistivity, dielectric constant, and hysteresis loops are given.

537.227:546.431'824–31 3011
Optical Absorption and Electrical Conductivity of Reduced $BaTiO_3$ Single Crystal—S. Ikegami, I. Ueda, and Y. Ise. (*J. Phys. Soc., Japan*, vol. 16, pp. 572–573; March, 1961.)

537.227:547.476.3 3012
The Effect of a Constant Electric Field on the Hysteresis of Rochelle Salt—K. N. Karmen. (*Fiz. Tverdogo Tela*, vol. 2, pp. 1671–1675; July, 1960.) A circuit used for recording hysteresis curves during simultaneous application of steady and variable fields of different intensities is shown. Symmetric and asymmetric hysteresis loops are identified and discussed.

537.227:547.476.3:539.12.04 3013
Ferroelectric Properties of X-Ray-Damaged Rochelle Salt—K. Okada. (*J. Phys. Soc., Japan*, vol. 16, pp. 414–423; March, 1961.)

537.311.33 3014
Semiconducting Properties of the $AgFeTe_2$ Phase—E. L. Shtrum. (*Fiz. Tverdogo Tela*, vol. 2, pp. 1489–1493; July, 1960.)

537.311.33 3015
The Effect of Trapping Levels in Semiconductors on Steady-State Photoconductivity and on the Life time of Nonequilibrium Current Carriers—A. A. Grinberg, L. G. Paritskiĭ, and S. M. Ryvkin. (*Fiz. Tverdogo Tela*, vol. 2, pp. 1545–1561; July, 1960.) A quantitative investigation is made of the effects of trapping levels introduced into the crystal on carrier recombination under steady-state conditions due to the presence of other traps in the forbidden zone. The effect of the filling of trapping levels on the variation of carrier lifetimes and photoconductivity as a function of temperature and light intensity is discussed.

537.311.33 3016
Long-Range Interactions between Magnetic Moments in Semiconductors—W. Baltensperger and A. M. de Graaf. (*Helv. Phys. Acta*, vol. 33, no. 8, pp. 881–888; November, 1960.) The interaction between magnetic moments in a nondegenerate electron gas is calculated, and account is taken of the additional interaction arising from virtual excitations of the valence band in semiconductors.

537.311.33 3017
Micro-masking for Chemical Etching of Semiconductors—S. Denda. (*Solid-State Electronics*, vol. 2, pp. 69; January 1961.) A method of producing a picein mask down to 30-μ diameter.

537.311.33 3018
Theoretical Calculations of the Enthalpies and Entropies of Diffusion and Vacancy Formation in Semiconductors—R. A. Swalin. (*J. Phys. Chem. Solids*, vol. 18, pp. 290–296; March, 1961.) The covalent-bond approach is used to obtain kinetic parameters.

537.311.33 3019
One-Dimensional Overlap Functions and their Application to Auger Recombination in Semiconductors—A. R. Beattie and P. T. Landsberg. (*Proc. Roy. Soc. (London)*, vol. 258, pp. 486–495; November 8, 1960.) Certain overlap integrals, occurring as a temperature-independent parameter in a previous paper (3341 of 1959), are evaluated. Used in conjunction with the previous theory, good agreement is obtained with experimental results.

537.311.33 3020
Theory of the Auger Neutralization of Ions at the Surface of a Diamond-Type Semiconductor—H. D. Hagstrum. (*Phys. Rev.*, vol. 122, pp. 83–113; April 1, 1961.)

537.311.33 3021
Semiconducting Properties of Inorganic Amorphous Materials—H. L. Uphoff and J. H. Healy. (*J. Appl. Phys.*, vol. 32, pp. 950–954; May, 1961.) Nine materials in the systems As:Se:Te and As:S:Te were tested. Resistivity varied exponentially with temperature; the Seebeck coefficient varied linearly.

537.311.33:535.211 3022
Photothermal Effect in Semiconductors—W. W. Gärtner. (*Phys. Rev.*, vol. 122, pp. 419–424; April 15, 1961.) The establishment of a temperature distribution in a solid by optically excited diffusing and recombining carriers is called the photothermal effect. Theory is developed.

537.311.33:538.567 3023
Detection of Millimetre- and Submillimetre-Wave Radiation by Free-Carrier Absorption in a Semiconductor—B. V. Rollin. (*Proc. Phys. Soc.*, vol. 77, pp. 1102–1103; May 1, 1961.) The change in conductivity when radiation is absorbed by free carriers can be used for detection at mm and sub-mm λ. The sensitivity for n-type InSb at a temperature of about 2°K is estimated.

537.311.33:538.614 3024
Theory of Interband Faraday Rotation in Semiconductors—B. Lax and Y. Nishina. (*Phys. Rev. Lett.*, vol. 6, pp. 464–467; May 1, 1961.) The interband Faraday rotation and its dependence on frequency is examined by using a quantum-mechanics approach to calculate the rotations for the indirect and direct forbidden transitions.

537.311.33:538.63 3025
Influence of Conductivity Gradients on Galvanomagnetic Effects in Semiconductors—R. T. Bate and A. C. Beer. (*J. Appl. Phys.*, vol. 32, pp. 800–805; May, 1961.) An approximate solution is found of a boundary-value problem arising from the continuity equation in an inhomogeneous semiconductor. Experimental results indicate that transverse currents, which do not occur in the simple case discussed, do appear in general.

537.311.33:546.24 3026
Infrared Absorption and Structure of the Hole Band of Tellurium—V. M. Korsunskiĭ and M. P. Lisitsa. (*Fiz. Tverdogo Tela*, vol. 2, pp. 1619–1623; July, 1960.)

537.311.33:546.28 3027
Absorption of Infrared Radiation by Electrons in *p*-Type Silicon—V. A. Yakovlev. (*Fiz. Tverdogo Tela*, vol. 2, pp. 1624–1628; July, 1960.)

537.311.33:546.28 3028
Problems related to *p-n* Junctions in Silicon—W. Shockley. (*Solid-State Electronics*, vol. 2, pp. 35–67; January, 1961.) A simple model of the behavior of holes and electrons in the high reverse fields of *p-n* junctions is shown to account well for secondary ionization, avalanche breakdown and microplasma phenomena. Statistical spatial fluctuations of donors and acceptors are shown to have significant effects on avalanche breakdown. Typical noisy microplasma phenomena are probably associated with structural defects whose properties are specified.

537.311.33:546.28 3029
Impurity Effect upon Mobility in Heavily Doped Silicon—Y. Furukawa. (*J. Phys. Soc., Japan*, vol. 16, p. 577; March 1961.) A similar effect was obtained to that previously observed in heavily doped Ge (see 3941 of 1960).

537.311.33:546.28 3030
Some Experiments using a Vacuum-Cleaned Silicon *p-n* Junction—J. T. Law. (*J. Appl. Phys.*, vol. 32, pp. 848–855; May, 1961.) Changes in the junction characteristics during the adsorption of oxygen and hydrogen have been investigated. In the clean condition the valence band edge was 0.13–0.14 ev below the Fermi level. A large excess current across the clean junction disappeared during absorption of gas.

537.311.33:546.28:539.12.04 3031
The Effect of Fast-Electron Bombardment on the Electrical Conductivity of Silicon and the Dependence of the Rate of Defect Formation on the Orientation of a Crystal with respect to the Electron Beam—V. S. Vavilov, V. M. Patskevich, B. Ya. Yurkov, and P. Ya. Glazunov. (*Fiz. Tverdogo Tela*, vol. 2, pp. 1431–1433; July, 1960.)

537.311.33:546.289 3032
The Mechanism of Carrier Scattering in *p*-Type Germanium—M. N. Vinogradova, O. A. Golikova, B. P. Mitrenin, and L. S. Stil'bans. (*Fiz. Tverdogo Tela*, vol. 2, pp. 1428–1430; July, 1960.)

537.311.33:546.289 3033
Effect of Linear Dislocations on Charge Carrier Recombination in *p*-Type Germanium—M. I. Iglitsyn and L. I. Kolesnik. (*Fiz. Tverdogo Tela.*, vol. 2, pp. 1542–1544; July, 1960.)

537.311.33:546.289 3034
Investigation of the Kinetics of Fast Surface States on Germanium—V. G. Litovchenko and V. I. Lyashenko. (*Fiz. Tverdogo Tela.*, vol. 2, pp. 1592–1596; July, 1960.) Report of field-effect and photoconductivity measurements on high resistivity *n*- and *p*-type Ge.

537.311.33:546.289 3035
Measurements of the Anomalous Transmission Factor and of the Reflection of X Rays on Good Germanium Single Crystals for the Bragg Case of Interference: Comparison with the Dynamic Theory of X-Ray Diffraction—U. Bonse. (*Z. Phys.*, vol. 161, pp. 310–329; December 28, 1960.)

537.311.33:546.289 3036
Impurity Concentrations in the Regrown Region of In-Ge Alloyed Junctions—F. E. Roberts. (*Solid-State Electronics*, vol. 2, pp. 8–13; January, 1961.) The development of an infrared microscope for routine carrier-density measurements on small semiconducting specimens is described. The results of a study made with it of In-Ge and In-Ga-Ge recrystallized alloyed regions are given.

537.311.33:546.289 3037
Regrowth of Germanium Single Crystal from Indium Melt—M. Tomono. (*J. Phys. Soc., Japan*, vol. 16, pp. 439–453; March, 1961.)

537.311.33:546.289 3038
Hot-Electron Nonequilibrium Carrier Distribution in a Many-Valley Semiconductor—L. Gold. (*J. Phys. Soc., Japan*, vol. 16, pp. 575–576; March, 1961.) Results of a study of the contribution of nonuniform charge density to the ellipsoidal energy surfaces in Ge are given. A reasonable deviation of collinear current and voltage directions is obtained; thus measurements of this quantity may be useful in studies of effective mass and carrier density.

537.311.33:546.289 3039
Cyclotron Resonance in Germanium—R. R. Goodman. (*Phys. Rev.*, vol. 122, pp. 397–405; April 15, 1961.) A comparison is made of cyclotron resonance theory and experimental data [see 1093 of 1956 (Fletcher *et al.*)]. Values of effective mass constants which best fit the data are found.

537.311.33:546.289 3040
Generation—Recombination Noise in *p*-type Gold-Doped Germanium—L. J. Neuringer and W. Barnard. (*Phys. Rev. Lett.*, vol. 6, pp. 455–457; May 1, 1961.) A theory is developed which accounts for the noise observed in interacting two-level systems and shows good quantitative agreement with experimental observations on Au-doped Ge.

537.311.33:546.289 3041
Third-Order Elastic Moduli of Germanium—T. Bateman, W. P. Mason, and H. J. McSkimin. (*J. Appl. Phys.*, vol. 32, pp. 928–936; May, 1961.)

537.311.33:546.289:535.215 3042
A New Effect of Negative Photoconductivity in a Magnetic Field—A. A. Grinberg, S. R. Novikov, and S. M. Ryvkin. (*Dokl. Akad. Nauk SSSR*, vol. 136, pp. 329–331; January 11, 1961.) A note on effects observed in a *p*-type Ge sample illuminated in the direction of an applied magnetic field.

537.311.33:546.289:535.215 3043
Modulation of Light by means of an Electric Field—B. H. Claussen. (*Proc. Phys. Soc.*, vol. 77, pp. 1100–1101; May 1, 1961.) Experiments are noted on the modulation of light reflected at a Ge surface when the carrier density was varied by means of an applied electric field. Results show that the modulation was a function of the dielectric used as a field plate rather than a function of the Ge surface.

537.311.33:546.289:538.614 3044
Faraday Effect for Direct Magneto-optical Transitions in Germanium—M. Suffczynski. (*Proc. Phys. Soc.*, vol. 77, pp. 1042–1045; May 1, 1961.) The Faraday effect due to the interband magneto-optical transitions in Ge is calculated. The direct transitons from the upper-most Landau levels of the two light-hole ladders and two heavy-hole adders are considered. Measurement of the Faraday rotation offers a sensitive means of studying the effective masses of the levels in the presence of the magnetic field.

537.311.33:546.289:538.63 3045
Galvanomagnetic Effects in *n*-Ge in the Impurity Conduction Range—R. J. Sladek and R. W. Keyes. (*Phys. Rev.*, vol. 122, pp. 437–442; April 15, 1961.) The measured magnitude and the crystalline anisotropy of the magnetoresistance are interpreted in terms of the changes in the donor wave functions produced by the magnetic field. The field dependence of the Hall coefficient is interpreted as a magnetoresistance effect of the conduction band.

537.311.33:546.289:539.12.04 3046
The Action of Radiation on Semiconductors: Recombination Centres Introduced in Germanium by 2-MeV Electrons—P. Baruch. (*Ann. Phys.*, (*Paris*), vol. 6, pp. 21–79; January /February, 1961.)

537.311.33:546.289:539.23 3047
Textural Properties of Germanium Films—J. E. Davey. (*J. Appl. Phys.*, vol. 32, pp. 877 880; May, 1961.)

537.311.33:546.26–1 3048
Some Optical and Electrical Properties of Semiconducting Diamonds—A. Halperin and J. Nahum. (*J. Phys. Chem. Solids*, vol. 18, pp. 297–306; March, 1961.)

537.311.33:546.3–1'289'28 3049
Magnetic Susceptibility of Ge-Si Mixed Crystals—G. Busch and O. Vogt. (*Helv. Phys. Acta*, vol. 33, no. 8, pp. 889–910; November, 1960. In German.) Susceptibility was measured as a function of temperature for 34 samples in the temperature range 300–1200°K. The results are compared with those of measurements of cyclotron resonance and magnetoresistance.

537.311.33:546.3–1'289'28 3050
Lattice Thermal Conductivity of Germanium-Silicon Alloy Single Crystals at Low Temperatures—A. M. Toxen. (*Phys. Rev.*, vol 122, pp. 450–458; April 15, 1961.

537.311.33:546.431'824–31:621.316.825.2 3051
Semiconducting Bodies in the Family of Barium Titanates—O. Saburi. (*J. Amer. Ceram. Soc.*, vol. 44, pp. 54–63; February 1, 1961.) The resistivity/temperature characteristics of the semiconducting Ba titanates are examined to determine compositons suitable for the construction of positive-type thermistors.

537.311.33:546.47'241:546.48'221 3052
Some Electrical Properties of Zinc Telluride-Cadmium Sulphide Heterojunctions—M. Aven and D. M. Cook. (*J. Appl. Phys.*, vol. 32, pp. 960–961; May, 1961.) Techniques for preparing the junctions at room temperatures are described. Rectification ratios up to 5×10^4 were obtained with a CdS film and about 10^2 with a ZnTe film. The *I/V* characteristic of a CdS-film junction is given.

537.311.33:546.48'19 3053
Galvanomagnetic Properties of *n*-Type $CdAs_2$—A. S. Fischler. (*Phys. Rev.*, vol. 122, pp. 425–429; April 15, 1961.)

537.311.33:546.561–31 3054
Electrical Conductivity of Single-Crystal Cuprous Oxide at High Temperatures—R. S. Toth, R. Kilkson, and D. Trivich. (*Phys. Rev.*, vol. 122, pp. 482–488; April 15, 1961.)

537.311.33:546.681'86 3055
Optical Investigation of the Band Structure of GaSb—M. Cardona. (*Z. Phys.*, vol. 161, no. 1, pp. 99–102; December, 1960.) The reflectivity of GaSb was measured at photon energies between 0.5 and 5 ev; the structure observed is similar to that of Ge.

537.311.33:546.681'86 3056
Distribution Coefficients of Impurities in Gallium Antimonide—R. N. Hall and J. H.

Racette. (*J. Appl. Phys.*, vol. 32, p. 856; May, 1961.)

537.311.33:546.682'18 3057
Optical Studies of the Band Structure of InP—M. Cardona. (*J. Appl. Phys.*, vol. 32, p. 958; May, 1961.)

537.311.33:546.682'86 3058
Infrared Cyclotron Resonance in InSb—E. D. Palik, G. S. Picus, S. Teitler, and R. F. Wallis. (*Phys. Rev.*, vol. 122, pp. 475–481; April 15, 1961.)

537.311.33:546.682'86:538.569.4 3059
Cyclotron Resonance in Indium Antimonide at High Magnetic Fields—B. Lax, J. G. Mavroides, H. J. Zeiger, and R. J. Keyes. (*Phys. Rev.*, vol. 122, pp. 31–35; April 1, 1961.) An improved theoretical treatment is given which accounts satisfactorily for various sets of experimental data.

537.311.33:546.682'86:538.63 3060
Magnetoresistance and Hall Effect in Oriented Single-Crystal Samples of *n*-Type Indium Antimonide—C. H. Champness. (*Canad. J. Phys.*, vol. 39, pp. 452–467; March, 1961.)

537.311.33:546.682'86:538.63 3061
Influence of Magnetoconductivity Discontinuities on Galvanomagnetic Effects in Indium Antimonide—R. T. Bate, J. C. Bell, and A. C. Beer. (*J. Appl. Phys.*, vol. 32, pp. 806–814; May, 1961.) Observations are predicted qualitatively by considering a simple model consisting of a long thin specimen having a discontinuity in resistivity and Hall coefficient in the current direction. The boundary-value problem is solved for this case.

537.311.33:546.683'231 3062
Certain Properties of Thallium Selenide Single Crystals—G. A. Akhundov, G. B. Abdullaev, and G. D. Guseinov. (*Fiz. Tverdogo Tela*, vol. 2, pp. 1518–1521; July, 1960.)

537.311.33:546.873'221 3063
Some Semiconducting Properties of Bismuth Trisulphide—L. Gildart, J. M. Kline, and D. M. Mattox. (*J. Phys. Chem. Solids*, vol. 18 pp. 286–289; March 1961.) Preparation of single crystals dendrites and crystalline films is described. Data are given for the thermal energy gap of films optical energy gap resistivity carrier concentration and mobility, thermal conductivity and Seebeck coefficient for single crystals.

537.311.33:621.391.822 3064
Approximate Solution to Semiconductor Noise as a Queuing Problem—T. L. Saaty. (PROC. IRE vol. 49 p. 1095; June 1961.) An alternative treatment to that of Bell (3897 of 1958) indicating the possible usefulness of the queuing representation for low frequencies.

537.312.62 3065
The Surface Impedance of Normal and Superconducting Indium at 3000 Mc/s—P. N. Dheer. [*Proc. Roy. Soc.* (*London*) *A*, vol. 260, no. 1302 pp. 333–349; March 1961.] From impedance measurements, a value is obtained for the penetration depth λ_0, and the Fermi surface area is estimated.

537.312.62 3066
Superconducting Tunneling on Bulk Niobium—M. D. Sherrill and H. H. Edwards. (*Phys. Rev. Lett.*, vol. 6, pp. 460–461; May 1, 1961.) Measurements of tunneling current for Nb-Pb junctions are described.

537.312.62:539.23 3067
An Upper Limit for the Resistivity of a Superconducting Film—R. F. Broom. (*Nature*, vol. 190, pp. 922–933; June 10, 1961.) A persistent current was induced in a Pb-In film at 2.1°K. Hall-effect probe measurements showed the resistivity to be $<10^{-21}\Omega$.cm.

537.533.8 3068
Reflection of Slow Electrons from Tungsten Single Crystals, Clean and with Adsorbed Monolayers—P. Kisliuk. (*Phys. Rev.*, vol. 122, pp. 405–411; April 15, 1961.) Experimental results are described and considered in relation to theory and previous experimental work. The technique permits continuous recording of the change in work function as gas is adsorbed.

537.533.8:539.23 3069
Certain Regularities in the Secondary Electron Emission from Thin Metal Layers and Semiconductors—I. M. Bronshtein and B. S. Fraĭman. (*Dokl. Akad. Nauk SSSR*, vol. 135, pp. 1097–1100; December 11, 1960.) Experimental investigation of the relation between δ and η for thin layers of Ca, Be, Ba or Ti applied respectively to base layers of Be, Ca, Ti, or Ba, where δ and η are the coefficients of slow secondary emission and inelastical reflection.

538.22:538.569.4 3070
Nuclear Quadrupole Resonance in an Antiferromagnet—J. C. Burgiel, V. Jaccarino, and A. L. Schawlow. (*Phys. Rev.*, vol. 122, pp. 429–436; April 15, 1961.)

538.221 3071
The Magnetic Field above the Surface of a Plate-Shaped Domain Structure with Bloch-Wall and Surface Poles—C. Greiner. (*Mber. Dtsch. Akad. Wiss. Berlin*, vol. 2, no. 6, pp. 328–336; 1960.) The field distribution is calculated.

538.221 3072
Magnetic Properties of Fe_3P—M. C. Cadeville and A. J. P. Meyer. (*C.R. Acad. Sci.*, (*Paris*) vol. 251, pp. 1621–1622; October 17, 1960.)

538.221 3073
A Method of Analysis of the Magnetic History of Ferromagnetic Specimens by means of the Preisach Diagram—H. Seidel. (*Z. angew. Phys.* vol. 12, pp. 493–501; November, 1960.) The Preisach diagram [see, *e.g.*, 842 of 1957 (Feldtkeller and Wilde)] can be used to analyze the magnetization processes which a specimen has undergone previously. Discrepancies between theory and measurements relating to Rayleigh's constant are discussed and the use of the principle in the development of storage-type devices is indicated.

538.221 3074
The Influence of Internal Magnetic Couplings on the Shape of Preisach Functions of High-Permeability Materials—H. Girke. (*Z. angew. Phys.*, vol. 12, pp. 502–508; November, 1960.) The unsymmetrical arrangement of Preisach functions already observed are explained [3590 of 1960 (Wilde and Girke)].

538.221 3075
Effects of the Special Heat Treatment on Permalloys—S. Tomita. (*J. Phys. Soc., Japan*, vol. 16, pp. 393–396; March, 1961.) Heat treatment of mumetal and 50 per cent Ni-50 per cent Fe permalloy at temperatures from 200°C to 600°C was found to give a marked increase of maximum permeability. The effect is attributed to inhomogeneous internal structure in these materials.

538.221:538.569.4 3076
Study of the Magnetization in a Single Crystal of Silicon-Iron by Ferromagnetic Resonance—A. Coumes. (*C.R. Acad. Sci., Paris*, vol. 250, no. 21, pp. 3458–3460; May, 1960.) The theory of phases of elementary domains leads to a method of determining the true magnetization direction in a phase from the experimental resonance curve. See 978 of March.

538.221:539.23 3077
Measurements on the Magnetic Anisotropy in Evaporated Iron Films—R. Vrambout and L. De Greve. (*Appl. Sci. Res.*, vol. B9, no. 2, pp. 102–106; 1961.)

538.221:539.23:538.691 3078
The Magnetic Deflection of Electron Beams in Thin Iron Films—H. Boersch, W. Raith, and H. Weber. (*Z. Phys.*, vol. 161, pp. 1–12; December 1, 1960.) Experimental investigations of the effect of film thickness, and the internal magnetic field , on the angle of deflection of an electron beam passing through the film.

538.221:621.318.124:538.569.4 3079
Ferromagnetic-Resonance Line Width in Cobalt-Substituted Ferrites—C. W. Haas and H. B. Callen. (*Phys. Rev.*, vol. 122, pp. 59–68; April 1, 1961.)

538.221:621.318.132 3080
Possibilities of Modifying the Magnetic Properties of Permalloy Alloys—F. Pfeifer. (*Elektrotech. Z., Edn. A*, vol. 81, pp. 945–949; December 1, 1960.) Important characteristics of permalloy-type materials can be modified by high-temperature annealing and by tempering. The results of experimental investitions on various alloys are given and discussed.

538.221:621.318.134 3081
Effect of Boron on Square-Loop Cadmium Manganese Ferrites—B. R. Eichbaum. (*J. Amer. Ceram. Soc.*, vol. 44, pp. 51–54; February 1, 1961.) A ferrite toroid dipped in boron solution before heat treatment possesses much lower coercivity than an undipped core. The switching time, Curie oint and UV_2/UV_2 ratio are also reduced.

538.221:621.318.134 3082
Exchange Anisotropy in Mixed Maganites with the Hausmannite Structure—I. S. Jacobs and J. S. Kouvel. (*Phys. Rev.*, vol. 122, pp. 412–418; April 15, 1961.)

538.221:621.318.134 3083
Magnetic Torque Curves for a Single Crystal of Thulium Orthoferrite ($TmFeO_3$)—C. Kuroda T. Miyadai, A. Naemura, N. Niizeki, and H. Takata. (*Phys. Rev.*, vol. 122, pp. 446–447; April 15, 1961.) Experimental results indicate that a previously proposed model [1956 of 1959 (Sherwood *et al.*)] should be modified.

538.221:621.318.134:548.5 3084
Growth of Single-Crystal Iron Ferrites by the Czochralski Method—F. H. Horn. (*J. Appl. Phys.*, vol. 32, pp. 900–901; May, 1961.)

538.222:538.569.4 3085
Effect of Configuration Mixing and Covalency on the Energy Spectrum of Ruby—S. Sugano and M. Peter. (*Phys. Rev.*, vol. 122, pp. 381–386; April 15, 1961.)

539.23:537.533.7 3086
Hot Electrons in Metal Films: Injection and Collection—J. P. Spratt, R. F. Schwarz, and W. M. Kane. (*Phys. Rev. Lett.*, vol. 6, pp. 341–342; April 1, 1961.) A device is described in which quantum tunneling electrons are emitted into a thin metal film. The structure facilitates the separation of these hot electrons. The characteristics of the device are

given which show that it could be used as an amplifier.

548.5 3087
Radio-Frequency Technique for Pulling Oxide Crystals without employing a Crucible Susceptor—F. R. Monforte, F. W. Swanekamp, and L. G. Van Uitert. (*J. Appl. Phys.* vol. 32 pp. 959–960; May, 1961.) Details are given of a water-cooled RF induction-heating coil which keeps the center part of the charge molten and the outer part solid.

MATHEMATICS

517.512.2 3088
Simplifying the Fourier Integral by Adequate Specification—C. G. Mayo and J. W. Head. (*Brit. J. Appl. Phys.*, vol. 12, pp. 248–250; May, 1961.) Use of a limiting metrical form of definition of the impulse function is shown to be superior to the normal idealized Dirac function in removing ambiguities such as those occurring in an analysis of the voltage developed across a resistance with residual shunt capacity when a current impulse is applied.

517.64:551.510.535 3089
A Solution of the Integral Equation $h'(f)=f\mu[(f:f_0)dz(f_0)$—Unz. (See 2966.)

517.918 3090
Taylor-Cauchy Transforms for Analysis of Varying-Parameter Systems—Y. H. Ku. (PROC. IRE, vol. 49, pp. 1096–1097; June, 1961.) Six examples are given. See also 2853 of 1960 (Ku *et al.*).

518.4:621.372.5 3091
Graphs with Two Kinds of Elements—S. L. Hakimi. (*J. Franklin Inst.*, vol. 270, pp. 451–467; December, 1960.) Fundamental properties of graphs with red and black elements are studied and the procedures given are modified to find the number of poles and zeros of network functions of an *RLC* network.

519.281.2 3092
A New Technique for Increasing the Flexibility of Recursive Least-Squares Data Smoothing—N. Levine. (*Bell Sys. Tech. J.*, vol. 40, pp. 821–840; May, 1961.) Optimum, or arbitrary, weights can be assigned to the observations, and the restriction of a constant data interval can be removed without affecting the optimum weighting or recursive features.

MEASUREMENTS AND TEST GEAR

529.786:621.3.018.41(083.74) 3093
Results of a Long-Range Clock Synchronization Experiment—F. H. Reder, M. R. Winkler, and C. Bickart. (PROC. IRE, vol. 49, pp. 1028–1032; June, 1961.) Propagation and synchronization experiments are described to examine the possibility of setting up a worldwide network of synthconized atomic clocks. Original synchronization is established by using an atomic clock which is flown from the master to the slave clock and maintaining it by phase tracking a VLF signal controlled by the master clock.

537.311.33:[546.28+546.289 3094
A Rapid and Accurate Method for Measuring the Thickness of Diffused Layers in Silicon and Germanium—B. Jansen. (*Solid-State Electronics*, vol. 2, pp. 14–17; January, 1961.) A cleavage technique is described which permits accurate microscopic measurement of layer thickness.

621.3.018.41(083.7) 3095
Caesium Frequency Standards: Description and Results—P. Kartaschoff, J. Bonanomi, and J. De Prins. (*Helv. Phys. Acta*, vol. 33, no. 9, pp. 968–973; December, 1960. In French.) Brief information concerning the two standards at the Swiss Horological Research Laboratory, Neuchâtel, includes records of frequency comparisons made with other Cs standards from June to September, 1960.

621.317:621.382.3 3096
Transistors in Measurement Techniques: Properties and Application—Schneider. (See 3187.)

621.317.3:621.391.822 3097
Measuring Amplitude and Phase—N. R. Goodman. (*J. Franklin Inst.*, vol. 270, pp. 437–450; December, 1960.) The amplitude and phase of moderately wide-band noise and noise contaminated by extraneous noise can be determined from a pair of finite moving averages on the sample noise record. The method is applicable to radio-star scintillation data.

621.317.3.088 3098
Accuracy in A. C. Measurements—G. H. Rayner and A. Felton. (*J. IEE*, vol. 7, pp. 141–144; March, 1961.) Absolute values of inductance and capacitance can be obtained to an accuracy within 10–20 parts in 10^6, while calibration accuracy is within 30–100 parts in 10^6. Voltage and current at frequencies up to 50 kc can be measured to within 1 part in 10^4, and power and energy to within 5 parts in 10^4.

621.317.313:621.314.224 3099
Techniques for the Calibration of Standard Current Transformers up to 20 kc/s—J. J. Hill. (*Proc. IEE*, pt. B, vol. 108, pp. 333–336; May, 1961. Discussion, pp. 337–338.)

621.317.32:621.375.13.029.4 3100
The Design of an Audio-Frequency Amplifier for High-Precision Voltage Measurement—S. Harkness and F. J. Wilkins (*Proc. IEE*, pt. B, vol. 108, pp. 319–326; May, 1961. Discussion, pp. 337–338.) The amplifier is based on the "ring-of-three" feedback circuit and gives a number of fixed gains between 2 and 1000 in the frequency range 30 cps–30 kc.

621.317.321:537.311.33 3101
Concerning a Rapid Method of Precise Measurements of Thermal E.M.F. of Semiconductors—O. V. Emel'yanenko and F. P. Kesamanly. (*Fiz. Tverdogo Tela*, vol. 2, pp. 1494–1496; July, 1960.) Contact thermocouples with controlled heating are used.

621.317.331:537.311.33 3102
Equipment for Measuring and Recording the Resistance of Semiconductors in Coordinates $\log R=f(1/T)$—L. G. Sapogin and V. M. Ivko. (*Fiz. Tverdogo Tela*, vol. 2, pp. 1482–1488; July, 1960.) The equipment comprises a logarithmic and a hyperbolic amplifier, circuit details of which are given.

621.317.331:537.311.33 3103
An A.C. Bridge for Semiconductor Resistivity Measurements using a Four-Point Probe—M. A. Logan. (*Bell Sys. Tech. J.*, vol. 40, pp. 885–919; May, 1961.)

621.317.335 3104
Improvements in the Precision Measurement of Capacitance—G. H. Rayner and L. H. Ford. (*Proc. IEE*, pt. B, vol. 108, pp. 337–338; May, 1961. Discussion on 2123 of 1960.)

621.317.337:621.372.413 3105
The Effects of Parasitic Modulation on the Accuracy of Measurement of the Q-Factor of a Resonator—F. H. James. (*Proc. IEE*, pt. B, vol. 108, pp. 316–318; May, 1961.) An extension of a previous paper (*ibid.*, pt. B, vol. 106, pp. 489–494; September, 1959) to cover the case where parasitic modulation is found. Theoretical and experimental results in such a case are given.

621.317.343:621.315.212 3106
Impedance Measurement on Coaxial Cables by means of Pulse Echo Tester—R. Codelupi. (*Note Recensioni Notiz.*, vol. 9 pp. 1006–1033; November/December, 1960.)

621.317.361.018.756:621.372.57 3107
The Applicability of Active Filters to the Measurements of the Frequency Spectra of Pulses—Jungmeister. (See 2882.)

621.317.373:621.376.5 3108
Measuring Frequency Stability of Pulsed Signals—R. H. Holman and R. B. Shields. (*Electronics*, vol. 34, pp. 61–65; April 21, 1961.) A method of measuring the phase difference between pulses as a pulse-to-pulse rms deviation, which does not require synchronization or frequency reference from a signal source.

621.317.7:[621.382.3+621.372.5 3109
A Loss and Phase Set for Measuring Transistor Parameters and Two-Port Networks between 5 and 250 Mc/s—D. Leed and O. Kummer. (*Bell Sys. tech. J.*, vol. 40, pp. 841–884; May, 1961.) The maximum inaccuracy is 0.1 db in loss, and 0.5° in phase. The special problems of broad-band measurement on transistors are reviewed, and details are given of the experimental equipment and the results obtained.

621.317.7:621.397.6 3110
Some New Video Measurement Techniques and Apparatus—Weaver. (See 3166).

621.317.74 3111
A Transfer-Function Analyser for Linear and Nonlinear Components—A. K. Choudhury, M. S. Basu and A. K. Mahalanabis. (*Electronic Eng.*, vol. 33, pp. 382–385; June, 1961.) A method of measuring frequency response, gain and phase is described requiring only normal laboratory components.

621.317.75 3112
A Voltage Waveform Analyzer—R. Dehors and G. Seguier. (*C.R. Acad. Sci. Paris*, vol. 250, pp. 3464–3466; May 23, 1960.) A bridge method of analysis is described in which voltage measurements can be made at any point in the cycle.

621.317.75 3113
Phase Sensitive Wave Analysis—O. J. Haga and D. Midgley. (*Electronic Tech.*, vol. 38, pp. 257–261; July, 1961.) "A method of phase analysis is described in which the input waveform is applied to one input of a multiplier. The other input takes in turn reference sine and cosine waves generated locally at the harmonic frequencies. To maintain phase-coherence, operation is interrupted in alternate fundamental periods, allowing initial conditions to be reset in the reference-wave generator. Results are given for an experimental circuit with a wattmeter performing the function of multiplication."

621.317.79.029.64/.65 3114
A Microwave Interferometer with Coherent Background—A. Boivin and R. Tremblay. (*Canad. J. Phys.*, vol. 39, pp. 393–408; March, 1961. In French.) The operation of the instrument is based on the principle of coherent background. The reference signal is distributed over the whole of the image space, using suitably polarized sources and a turnstile antenna for detection. The diffraction pattern is scanned twice to determine both the real and imaginary

parts, in Cartesian form, of the distribution of complex amplitude.

621.317.794:523.164 3115
Digital Radiometer—S. Weinreb. (PROC. IRE, vol. 49, p. 1099; June, 1961.) The power spectrum of nosmic noise is measured, over a 5-Mc band, via its autocorrelation function. To eliminate the effects of gain fluctuation, the signal is amplified and limited; the autocorrelation of the resulting square waves is found by a digital technique and, assuming a Gaussian input signal, is transformed to the power spectrum. It is hoped that one can detect the galactic deuterium line.

621.317.794:621.396.62.029.65/.66 3116
Submillimetre-Wave Radiometry—Long and Rivers. (See 3143.)

OTHER APPLICATIONS OF RADIO AND ELECTRONICS

562.2:621.396.9 3117
An Electronic Distance Measurement System for Accurate Survey—(*Proc. IRE Australia*, vol. 22 pp. 22–25; January 1961.) An explanation of the principles and operation of the "Tellurometer" relating to its application in Australia. See 1980 of 1959 (Wadley) and back references.

535.376.07:537.227 3118
Ferroelectric Scanning of Electroluminescent Displays—M. Cooperman. (*RCA Rev.*, vol. 22 pp. 195–205; March 1961.) A new scanning method using a $BaTiO_3$ crystal is described.

536.587:621.382.3 3119
The Transistor as a Temperature-Sensing Device in Temperature Control Systems—J. E. Pallett. (*Electronic Eng.* vol. 33 pp. 360–363; June, 1961.) A detailed examination is made of the use of a transistor in a common-base circuit for the detection of small temperature changes.

537.533:621.9 3120
The Electron Beam as a Tool—S. Panzer and K. H. Steigerwald. (*Elektrotech. Z., Edn A*, vol. 81. pp. 925–932; December 19, 1960.) The techniques reviewed include welding, soldering, cutting, milling, drilling, alloying and vapor deposition.

621.362:621.387 3121
Calculation of the Maximum Efficiency of the Thermionic Converter—J. H. Ingold. (*J. Appl. Phys.*, vol. 32, pp. 769–772; May, 1961.)

621.362:621.387 3122
Oscillations and Saturation-Current Measurements in Thermionic Conversion Cells—R. J. Zollweg and M. Gottlieb. (*J. Appl. Phys.*, vol. 32, pp. 890–894; May, 1961.) RF oscillations in Cs-filled thermionic diodes are interpreted on the basis of a model which assumes the ions oscillate in an excess negative charge potential well outside the cathode.

621.387.462:537.311.33 3123
On the Energy Expended per Electron-Hole Pair Produced in p-n-Junction Detectors—E. Baldinger and W. Czaja. (*Nuclear Instr. Meth.*, vol. 10, pp. 237–239; March, 1961.) Previous work relating to radiation counters [see, *e.g.*, *Proc. Roy. Soc.* (*London*), *A*, vol. 224, no. 1158 pp. 362–373; July, 1954 (Erskine)] indicates that for gases, the energy loss $\epsilon = k_1 + k_2 I$, where k_1 and k_2 are constants and I is the ionization energy of the gas. A similar correlation holds for semiconductors. See also 2753 of August (Baldinger *et al.*).

PROPAGATION OF WAVES

621.391.812.62 3124
Experimental Results with Transhorizon Tropospheric Propagation—F. du Castel. (*Ann. Télécommun.*, vol. 15, pp. 255–259; November/December, 1960.) Results of experimental studies made in the period 1957–1960 are discussed.

621.391.812.62 3125
Theories of Tropospheric Propagation Beyond the Horizon—J. Voge. (*Ann. Télécommun.*, vol. 15, pp. 260–265; November/December, 1960.) A review, with 38 references.

621.391.812.62 3126
Several Aspects of Radio-Meteorology and Radio-Climatology—P. Misme. (*Ann. Télécommun.*, vol. 15, pp. 266–273; November /December, 1960.) Three aspects are considered: 1) investigation of a model atmosphere capable of sustaining transhorizon propagation, 2) refraction, 3) choice of parameters in radioclimatology.

621.391.812.62:551.510.62 3127
Radio-climatology Tests in the Congo Basin—P. Misme. (*Ann. Télécommun.*, vol. 16, pp. 28–40; January/February, 1961.) An investigation of the refractive index of the air, its gradient, the stability of the lower atmosphere and the water-vapor pressure at different heights.

621.391.812.62.029.63 3128
Some Factors Influencing 3-cm Radio-Wave Propagation Oversea Within and Beyond the Radio Horizon—F. A. Kitchen, W. R. R. Joy, and E. G. Richards. (*Proc. IEE*, pt. B, vol. 108, pp. 257–263; May, 1961.) Propagation of 10-Gc radio waves over sea did not agree with calculations based on an atmosphere of uniform refractive index gradient. Signal losses of 5–30 db often occurred within the horizon and were usually accompanied by an interference pattern.

621.391.812.62.029.64 3129
Experimental Investigation of the Instantaneous Frequency Structure of Propagation in a Heterogeneous Medium—J. Biggi, F. du Castel, J. C. Simon, A. Spizzichino, and J. Voge. (*Ann. Télécommun.*, vol. 15, pp. 274–276; November/December, 1960.) Experimental results obtained over a 300-km radio link are given. The transmitter frequency is swept over the range 3.3 3.5 Gc in 1/20 sec and the received signal analyzed as a function of either amplitude or time.

621.391.812.63 3130
The Fading of Radio Waves Weekly Scattered at Vertical Incidence from Heights near 90 km—O. Awe. (*J. Atmos. Terr. Phys.*, vol. 21, pp. 142–156; June, 1961.) At 2 3 Mc the fading rate was about 20 maxima/minutes. The echo shape is often such as would be expected from a rough screen. Appreciable energy is returned from directions well away from the vertical. The fading is due to random movements of the scattering elements whose rms velocity is about 13 m/sec.

621.391.812.63 3131
The Fading of Radio Waves Reflected from the Ionosphere at Oblique Incidence—O. Awe. (*J. Atmos. Terr. Phys.* vol. 21, pp. 120–141; June, 1961.) Pusle transmissions near 2 Mc were used. Echoes from 90 km and 120 km had fading periods near 1 minute and 6 sec respectively. Diffraction studies suggest that the irregularities near 90 km are horizontal disks while those at 120 km are spherical. Those near 300 km are elongated along the earth's field with an axial ratio of 3:1.

621.391.812.63 3132
Results of the Approximate Calculation of Space-Wave Field Strength at the Limits of the Transmission-Frequency Range—B. Beckmann. (*Nachrtech. Z.*, vol. 13 pp. 470–472; October, 1960.) Examples of the application of the formula given in 306 of 1960 are discussed.

621.391.812.63.029.45 3133
Effect of Underground Induced Polarization on E.L.F Propagation—H. Raemer. (*J. Geophys. Res.*, vol. 66, pp. 1596–1597; May, 1961.) The largest possible corrections to the mode parameters are found to be negligible.

621.391.812.63.029.45 3134
A Comparison between Theoretical Data on Phase Velocity of VLF Radio Waves—J. R. Wait. (PROC. IRE, vol. 49, pp. 1089–1090; June, 1961.) Fairly good agreement is indicated between the measured phase velocity and mode theory. The ionosphere is assumed to be sharply bounded, with its lower edge at 70 km during the day and 90 km at night.

621.391.812.63.029.45 3135
The Numerical Solution of Differential Equations governing the Reflexion of Long Radio Waves from the Ionosphere: Part 4—D. W. Barron. (*Proc. Roy. Soc.* (*London*) *A*, vol. 260, no. 1302, pp. 393–408; March, 1961.) Reflexion coefficients calculated for a series of models of the daytime ionosphere in summer by methods described previously, are compared with observed values. The model whose theoretical properties most nearly agree with experimental observations is found and suggestions are made as to how it should be changed. Sunrise and sunset transitions are also discussed and it is shown that the sharp change in reflection coefficients can be explained in terms of a low-level D layer which is only present in the daytime. Part 3: 3455 of 1959 (Barron and Budden).

621.391.812.63.029.62 3136
Studies of Ionospheric Forward Scattering using Measurements of Energy Distribution in Azimuth—W. C. Bain. (*Proc. IEE*, pt. B, vol. 108, pp. 241–252; May, 1961.) A marked diurnal variation of the mean bearing of the 37-Mc forward-scatter signal was found. This and other results suggested that the scattering process on the 1740-km link used was due mainly to meteor reflections at night but that during the day turbulent scattering was also of importance.

621.391.812.63.029.62 3137
Directional Observations on Delayed Signals on an Ionospheric Forward-Scatter Circuit—W. C. Bain. (*Proc. IEE*, pt. B, vol. 108, pp. 253–256; May, 1961.) A study was made of the mean bearing of the delayed signals arriving at Slough from Gibraltar after reception of the forward-scatter signal. Results for the first two of these to arrive at Slough are given, and also details of round-the-world echoes. See also 3136 above.

621.391.812.63.029.63 3138
The Effect of Faraday Rotation on Incoherent Back-Scatter Observations—G. H. Millman, A. J. Moceyunas, A. E. Sanders, and R. F. Wyrick. (*J. Geophys. Res.*, vol. 66, pp. 1564–1568; May, 1961.) Preliminary observations of incoherent scattering conducted at Trinidad (10.7°N, 61.6°W) with a high-power pulse radar operating at 400 Mc are described.

RECEPTION

621.376.23 3139
Certain Problems concerning the the Detection of Weak Signals—B. Picinbono. (*Ann. Télécommun.*, vol. 16, pp. 2–27; January/Feb-

ruary, 1961.) A thesis; for shorter papers on two different aspects of this work, see 1630 of May and 2763 of August.

621.391.82:621.396.73 3140
Probabilities of Interference with Mobile Field Radio Derived from a Field-Strength Survey at 59 Mc/s—D. R. W. Thomas. (*Proc. IEE*, pt. B, vol. 108, pp. 264–272; May, 1961.) The variation of field strength at 59 Mc with distance was found to agree well with calculations, its distribution at a given distance was found to be log-normal. Probabilities of interference are derived and presented graphically.

621.391.823 3141
Radio Interference from Ignition Systems—A. H. Ball and W. Nethercot. *Proc. IEE*, pt. B, vol. 108, pp. 273–278; May, 1961.) Comparison of American, German and British measuring equipment, techniques and limits. Good agreement was found between the various measuring sets.

621.391.827 3142
A Mechanism for Direct Adjacent-Channel Interference—C. L. Ruthroff. (PROC. IRE, vol. 49, pp. 1091–1092; June, 1961.) The effects of limiters can cause the modulation in a FM channel to appear as undistorted modulation in an adjacent channel.

621.396.62.029.65/.66:621.317.794 3143
Submillimetre-Wave Radiometry—M. W. Long and W. K. Rivers, Jr. (PROC. IRE, vol. 49, pp. 1024–1027; June, 1961.) Greater sensitivity in reception at sub-mm λ will result from the use of a direct detection system using a chopper, square-law detector and narrow-band amplifier than will be obtainable with a superheterodyne system.

STATIONS AND COMMUNICATION SYSTEMS

621.376.56:621.391.82 3144
Errors in Detection of R.F. Pulses Embedded in Time Crosstalk, Frequency Crosstalk, and Noise—E. A. Marcatili. (*Bell Sys. Tech. J.*, vol. 40, pp. 921–950; May, 1961.) Calculations are given of the probability of error in the detection of RF pulses in a combination of Gaussian noise, time crosstalk from two neighboring pulses, and frequency crosstalk from an adjacent channel. Criteria for the optimum design of a PCM system are discussed.

621.376.56:621.391.82 3145
Time and Frequency Crosstalk in Pulse-Modulated Systems—E. A. Marcatili. (*Bell Sys. Tech. J.*, vol. 40, pp. 951–970; May, 1961.) The time and frequency crosstalk between Gaussian RF pulses sent via adjacent frequency channels over the same transmission medium is calculated. See also 3144 above.

621.396.41 3146
A Study by means of an Analogue Computer of the Spectrum of Compatible Single-Sideband Modulation—H. Mertens. (*E.B.U. Rev.*, no. 64A, pp. 249–258; December, 1960.) Analysis of the signal spectrum produced by the Kahn system of SSB modulation (971 of 1959).

621.396.43:551.507.362.2 3147
Application of Artificial Satellites to Communications on Ultra Short Waves—M. Dolukhanov. (*Radio, Moskow*, no. 5, pp. 21–22; May, 1961.) A note on satellite period and transmitter power for heights of 1000, 2000, 3000, 4000, 5000 and 35,818 km.

621.396.43:551.507.362.2 3148
A Transatlantic Communication Experiment via Echo I Satellite—W. C. Jakes, Jr. (*Nature*, vol. 190, p. 709; May 20, 1961.) Further details are given relating to the experiment described in 1306 of April (Carru *et al.*).

621.396.43:551.507.362.2:621.396.677.3 3149
Communications Satellites Using Arrays—R. C. Hansen. (PROC. IRE, vol. 49, pp. 1066–1074; June, 1961.) Automatic angle return arrays are investigated for both passive and active systems. These Van Atta arrays return a signal in the direction of incidence and are effective over at least $\pm 45°$. Thus only partial stabilization or single axis (spin) stabilization need be used, greatly simplifying the station-keeping orbit control problem. An active Van Atta scheme has inherently high reliability since many of the distributed amplifiers can fail without serious performance degradation. The distributed structure also allows use of low-power solid-state amplifiers.

621.396.65.029.63 3150
FM120/2200: Radio-Link Installation for 120 Telephony Channels in the 2-GC/s Band—(*Telefunken Ztg.*, vol. 33, pp. 295–323; December, 1960.)

Part 1: Radio-Link System—E. Willwacher (pp. 295–302, English summary, pp. 334–335).

Part 2: Modulation Equipment—R. Heer and H. Oberbeck (pp. 302–305, English summary, p. 335).

Part 3: Radio Equipment—W. Schlotterbeck (pp. 306–309, English summary, p. 335).

Part 4: Design of Aerial Duplexers—W. Schlotterbeck and E. Willwacher (pp. 309–313, English summary, p. 336).

Part 5: Stand-By Circuit—J. Goeldner and O. Tegel (pp. 313–318, English summary, p. 336).

Part 6: Equipment for Diversity Reception—H. Weber (pp. 318–323, English summary, p. 336).

621.396.712 3151
B.B.C. Sound Broadcasting 1939–60—E. L. E. Pawley. (*Proc. IEE*, pt. B, vol. 108, pp. 279–302; May 1961.) A review of progress.

621.396.946 3152
Frequency Allocations for Space Communications—(PROC. IRE, vol. 49, pp. 1009–1015; June, 1961.) The technical aspects of space communications are examined with special attention to the use of satellites for commercial trunking purposes. The influence of system design on frequency allocation and utilization, and associated problems are discussed.

SUBSIDIARY APPARATUS

651–52 3153
Theory of Nonlinear Control—Y. H. Ku. (*J. Franklin Inst.*, vol. 271, pp. 108–144; February, 1961.) A review of work in various fields of nonlinear control (157 references).

621.311.62:621.383.292 3154
Stabilized E.H.T. Supply Unit for Photomultipliers—H. Constans and D. Vallat. (*Electronic Appl.*, vol. 20, pp. 153–158; February, 1961.) Provided the load is substantially constant, the circuit will produce an output voltage of 1000–2000v with an error not exceeding 0.5 per cent during mains fluctuations of ± 10 per cent.

621.311.69:621.383.5 3155
Spectral Response of Solar-Cell Structures—L. M. Terman. (*Solid-State Electronics*, vol. 2, pp. 1–7; January, 1961.) Measurements on Si cells with the *p-n* junction 0.6 to 5.0 μ below the surface show that the short wave response ($\lambda > 0.75$ μ) is relatively increased by making the junction close to the surface, and the long-wave response by making it deeper. Effects of rough and smooth surfaces were also studied.

621.314.63 3156
On the Electrical Parameters of some Types of Selenium Rectifier—I. Kh. Geller and P. V. Sharavskii. (*Fiz. Tverdogo Tela*, vol. 2, pp. 1441–1449; July, 1960.)

621.316.72:621.318.3 3157
Variable, Precision-Regulated, Low-Voltage High-Current Supply for Large Electromagnets—R. C. Mobley. (*Rev. Sci. Instr.*, vol. 32, pp. 432–433; April, 1961.) Circuit details are given of a power supply with combined electronic- and magnetic-amplifier control delivering currents of 5–200 A at 40v with regulation and ripple values <0.01 per cent.

TELEVISION AND PHOTOTELEGRAPHY

621.397.12:621.397.232.6 3158
A New Type of Vestigial-Sideband Facsimile System K. Kubota and K. Kobayashi. (*Rev. Elect. Commun. Lab., Japan*, vol. 9, p. 85–90; January/February, 1961.) A simple system performing homodyne detection and eliminating quadrature distortion, which does not require AFC.

621.397.13:621.395.625.3 3159
A Magnetic Wheel Store for Recording Television Signals—J. H. Wessels. (*Philips Tech. Rev.*, vol. 22, pp. 1–10; November 4, 1960.) The device described will store one or two frames of a television signal indefinitely. The recording is made on the periphery of a magnetically coated rotating wheel using a frequency-modulation technique. A useful application in radiology is mentioned.

621.397.132 3160
Comparative Investigations of Modified N.T.S.C. Colour Television Systems using Pre- or Post-correction of Gradation—K. Bernath. (*Rundfunktech. Mitt.*, vol. 4, pp. 232–237; December, 1960.) The advantages of pre-correction are established on the basis of experimental results.

621.397.132 3161
Colour Television Transmission with Simultaneous Frequency and Amplitude Modulation of the Colour Carrier (F. A. M. Method)—N. Mayer. (*Rundfunktech. Mitt.*, vol. 4, pp. 238–252; December, 1960.) The system described combines some of the advantages of the "Henri de France" (*SECAM*) system of color television (see, *e.g.*, 3660 of 1960) with those of the NTSC method. Pictures obtained on monochrome and color television receivers are reproduced.

621.397.132 3162
Trends towards a Common European Standard for Colour Television—F. Cappuccini. (*Note Recensioni Notiz.*, vol. 9, pp. 993–1005; November/December, 1960.) The problem of establishing a standard for compatible color television is related to the unification of European monochrome standards. Particular consideration is given to a 625-line standard with 8-Mc channel width.

621.397.331:621.391 3163
Television Band Compression by Contour Interpolation—D. Gabor and P. C. J. Hill. (*Proc. IEE*, pt. B, vol. 108, pp. 303–315; May, 1961.) This method of compression uses redundancies between fields and between frames. The waveband gain is 4:1 without deterioration in picture quality. The results of tests in a photomechanical model are given.

621.397.331.24 3164
Measurements of Sharpness on Picture Tubes—W. Schröder. (*Telefunken-Röhre*, no. 37, pp. 17–70; October, 1960.) A method is described which permits the measurement of fo-

cusing quality at any point on the screen of a television tube. The various factors influencing spot size are discussed with reference to the results of measurements.

621.397.334.2:778.6 3165
Electronic Reversal of Photographic Colour Negatives—K. Welland. (*Arch. elekt. Übertragung*, vol. 14, pp. 441–450; October, 1960.) An experimental flying-spot scanner with three input channels and a display unit is described. Correction and calibration methods are discussed. Color reproductions of photographically and electronically reversed test pictures are given for comparison.

621.397.6:621.317.7 3166
Some New Video Measurement Techniques and Apparatus—L. E. Weaver. (*E.B.U. Rev.*, no. 64A, pp. 242–248; December, 1960.) Description of techniques and apparatus used by the BBC, including a sine-squared pulse and bar generator, a test-waveform generator for nonlinear distortion measurements, and an outline of the spectrum method of measuring random noise (2345 of 1959). For German version see *Rundfunktech. Mitt.*, vol. 5, pp. 8–14; February, 1961.

621.397.61 3167
Methods and Limitations of Television Camera Techniques—R. Theile. (*Elektrotech. Z., Edn A*, vol. 81, pp. 895–903; December 5, 1960.) The principles underlying electron-optical image conversion are outlined and flying-spot scanning and storage-type camera-tube techniques are discussed in greater detail. Picture quality and sensitivity limits are considered in relation to results obtained by photographic means.

621.397.61:621.396.677.3 3168
Dipole Arrays for Transmitter Aerials for Television Bands IV/V—Laub. (See 2854.)

621.397.62 3169
Synchronizing and A.G.C. Circuits in TV Receivers—E. M. Cherry. (*Proc. IRE, (Australia)*, vol. 22, pp. 61–76; February, 1961.) Practical details are given for the design of a high-quality television receiver from fundamental considerations. The design is simple and noncritical.

621.397.62:616–001.26 3170
Aspects of the Emission of X Rays from Television Receivers—M. V. Callendar and D. F. White. (*J. Brit. IRE*, vol. 21, pp. 389–400; May, 1961.) Measurements made with a proportional counter of the dose rates from typical picture tubes show the radiation level is considerably less than the recommended level of 0.5 milliröntgens per hour.

621.397.62.004.6 3171
Component and Valve Reliability in Domestic Radio and Television Receivers—D. W Heightman. (*J. Brit. IRE*, vol. 21, pp. 401–407; May, 1961. Discussion.) Statistical information on the reliability of television receivers is reviewed. Some reasons for failure are examined and suggestions for improvements made.

621.397.63:621.395.625.3 3172
A Translator-Modulator-Demodulator as used in V.H.F./F.M. Techniques, for Television Tape-Recording Equipment—H. Fix and W. Habermann. (*Rundfunktech. Mitt.*, vol. 4, pp. 222–231; December, 1960.) The modification of the Ampex method of video tape recording to meet the requirements of the CCIR 625-line standard is discussed. The use of double frequency-changing overcomes most of the quality defects.

621.397.7 3173
Television Centre of Greater Moscow—(*Radio, Moskow*, no. 1, pp. 6–7; January, 1961.) Brief description of a broadcasting tower to be built in Moscow which will have a base diameter of 65 m and a height of 520 m. The station will transmit simultaneously six sound and five television programmes, one being in color, over a radius of 120–130 km.

TRANSMISSION

621.311.61:551.507.362.2 3174
Beacon Transmitters and Power Supply for Echo I—J. G. McCubbin and H. B. Goldberg. (*RCA Rev.*, vol. 22, pp. 147–161; March, 1961.) The transmitter has an output of 5–10 mw at 107.94 Mc and is mounted with Si solar cells, batteries and antenna on a printed-circuit board 10 inches in diameter.

621.396.61:621.396.662.6 3175
The Design of a Highly-Stable Short-Wave Exciter Stage with Decade Switching in the Range 1.5–30 Mc/s—H. Valdorf and R. Klinger. (*Frequenz*, vol. 14, pp. 335–343; October, 1960.) A crystal-controlled oscillator provides the standard frequency from which the output frequencies are derived by multiplication, mixing and division. Decade switching in 1-kc steps and facilities for interpolation are available in the unit described.

TUBES AND THERMIONICS

621.382.2 3176
Properties and Applications of Semiconductor Diodes—H. F. Grave. (*Elektrotech. Z., Edn A*, vol. 81, pp. 761–767; October 24, 1960.) Circuits for class-B and class-C demodulation are given, and diode applications in the field of HF and h.v. measurement, and as protective and control devices are briefly reviewed.

621.382.2 3177
Investigation of the Characteristics of Germanium Diodes—I. M. Senderikhin and P. V. Sharavskil. (*Fiz. Tverdogo Tela*, vol. 2, pp. 1497–1505; July, 1960.) Static and pulse characteristics of thermistors and Ge point-contact and junction diodes are discussed in relation to thermal effects.

621.382.2 3178
Contribution to the Theory of Thermal Breakdown of Germanium Diodes I. M. Senderikhin. (*Fiz. Tverdogo Tela*, vol. 2, pp. 1506–1517; July, 1960.) The reverse characteristics of Ge point-contact and junction diodes are analyzed and general theory of thermal breakdown is proposed. In point-contact diodes breakdown occurs earlier due to the field effect.

621.382.2 3179
Field-Effect Pinch-Off of Surface Leakage in High-Voltage Diodes—T. Kan. (*Solid-State Electronics*, vol. 2, pp. 68–69; January, 1961.) It is shown how reduced surface leakage and increased reverse-breakdown voltage can be achieved by proper geometry, so as to utilize the field-effect pinch-off.

621.382.22 3180
The Electrical Properties of Extensive Current Paths in Space-Charge Regions Close to the Surface of Semiconductors—E. Groschwitz, E. Hofmeister, and R. Ebhardt. (*Z. angew. Phys.*, vol. 12, pp. 544–557; December, 1960.) Theoretical treatment of surface currents in inversion layers, particularly relating to conditions in point-contact semiconductor diodes. See also 2799 of August.

621.382.23 3181
Construction and Characteristics of Silver-Bonded Diodes—S. Kita. (*Rev. Elect. Commun. Lab., Japan*, vol. 9, pp. 26–30; January/February, 1961.)

621.382.23 3182
High-Frequency Power in Tunnel Diodes—G. Dermit. (PROC. IRE, vol. 49, pp. 1033–1042; June, 1961.) An expression is developed for HF tunnel-diode power with a simple dissipative load and for signals confined within the nearly linear range of the diode negative resistance. Results are plotted for Ge and GaAs.

621.382.23 3183
The Equivalent Noise Current of Esaki Diodes—R. A. Pucel. (PROC. IRE, vol. 49, pp. 1080–1081; June, 1961.)

621.382.23 3184
Gallium Antimonide Esaki Diodes for High-Frequency Applications—C. A. Burrus. (PROC. IRE, vol. 49, p. 1101; June, 1961.) Diodes have been made, using both *p*- and *n*-type material, by methods similar to those applied for GaAs (*J. Appl. Phys.*, vol. 32, pp. 1031–1036; June, 1961.). They have been tested as oscillators in the 50-Gc range.

621.382.23:621.372.44 3185
Some Effects of Material Parameters on the Design of Surface-Space-Charge Varactors—D. R. Frankl. (*Solid-State Electronics*, vol. 2, pp. 71–76; January 1961.) Theoretical discussion of the effects of material parameters (semiconductor and dielectric materials and layer thicknesses) on the capacitance variation and cut-off frequency of varactor diodes.

621.382.23:621.375.9 3186
A Millimetre-Wave Esaki-Diode Amplifier—C. A. Burrus and R. Trambarulo. (PROC. IRE, vol. 49, pp. 1075–1076; June, 1961.) Amplification with Esaki diodes has been achieved in the frequency range 55–85 Gc. Gain was 20 db with 40 Mc bandwidth. Noise figure was 16–18 db, mainly due to circuit losses.

621.382.3:621.317 3187
Transistors in Measurement Techniques: Properties and Application—H. Schneider. (*Elektrotech. Z., Edn A*, vol. 81, pp. 767–773; October, 1960.) Analysis of the properties and characteristics of transistors to assess their suitability for various measurement applications; the advantages and disadvantages in comparison with relays and thermionic tubes are indicated.

621.382.3:621.318.57 3188
Storage Time of a Transistor with a Decaying Turn-Off Current—D. M. Taub. (*Proc. IEE*, pt. B, vol. 108, pp. 344–347; May, 1961.) A theoretical calculation of the storage time.

621.382.3.002.2 3189
Methods of Producing Stable Transistors—J. J. A. Ploos van Amstel. (*Philips Tech. Rev.*, vol. 22, pp. 204–214; March 14, 1961.) Very stable Ge transistors are produced by "surface forming" at 140° C, with the transistor encapsulated in a mixture of silicone grease, boracic acid and arsenic.

621.383 3190
Photoelectric Cells and Photomultipliers—J. Sharpe. (*Electronic Tech.*, vol. 38, pp. 196–201 and 248–256; June and July, 1961.) A review of the properties and applications of photoemissive cells and photomultiplier tubes.

621.383.5 3191
The Influence of the Surface Recombination Velocity and the Absorption Coefficient on the Transient Characteristics of Photodiodes—A. A. Grinberg and N. B. Strokan. (*Fiz.*

Tverdogo Tela, vol. 2, pp. 1536–1541; July, 1960.)

621.385.032.213.23 3192
Emission of Negative Ions of Oxygen from Dispenser Cathodes: Parts 1 & 2—N. A. Surplice. (*Brit. J. Appl. Phys.*, vol. 12, pp. 214–219 and 220–221; May, 1961.) Report of experimental investigations of negative-ion emission from cathodes of BaO in sintered Ni and of sintered W impregnated with Ba aluminate.

621.385.032.213.23 3193
The Emission Equation of the Oxide Cathode—J. Ruf. (*Telefunken—Röhre*, no. 37, pp. 79–132; October, 1960.) Thermionic-emission theory is reviewed and emission equations relating to various models of oxide cathode are given (46 references).

621.385.032.213.23 3194
The Evaluation of Oxide-Cathode Quality by Shot-Noise Tests—L. G. Sebestyen. (*J. Brit. IRE*, vol. 21, pp. 463–467; May, 1961.) The shot-noise test appears to be more sensitive than other methods and does not affect the cathode. Simple test equipment is described. See also 4018 of 1958 (Dahlke and Dlouhy).

621.385.2 3195
The Effect of Elastically Reflected Electrons on the Characteristics of a Thermionic Diode—K. H. V. Booth and I. A. Harris. (*Proc. Roy. Soc. (London) A*, vol. 261, no. 1304, pp. 134–152; April, 1961.) The elastic reflection of slow electrons (<2 ev) in a diode with an oxide-coated cathode has a major effect on the I/v characteristic and the electric field distribution.

621.385.3:621.396.61 3196
Calculation of Optimum Operational Data of Transmitter Valves—G. Schuster. (*Hochfrequenztech. u. Elektroakust.*, vol. 69, pp. 124–132; August, 1960.) Calculations and characteristic curves refer to the use of a power triode in induction heating equipment, but are of general application in determining optimum operating conditions.

621.385.3.029.6 3197
Applications of Microwave Triodes—J. P. M. Gieles. (*Philips Tech. Rev.*, vol. 22, pp. 16–28; November 4, 1960.) A comprehensive survey of current practice in the commercial field.

621.385.6:537.533.08 3198
Electron-Beam Analyzer using a Piezoelectric Scanner—T. Fujii. (*Rev. Sci. Instr.*, vol. 32 pp. 434 444; April, 1961.) This instrument measures transverse current density distributions of high-density electron beams using a moving pinhole target driven by a pair of $BaTiO_3$ elements. Sampling can be carried out very close to the anode aperture of an electron gun

621.385.6:621.375.9:621.372.44 3199
A Low-Noise Microwave Quadrupole Amplifier—A. Ashkin. (PROC. IRE, vol. 49 pp. 1016–1020; June, 1961.) The design of a quadrupole amplifier is discussed and experimental results using a frequency of 4137 Mc are described. At a gain of 19 db the measured double-channel noise figure is 0.79 db.

621.385.62/.63:621.391.832.4 3200
New Results on Frequency Multiplication and Nonlinear Phase Distortion in Klystrons and Travelling-Wave Tubes—F. Paschke. (*RCA Rev.*, vol. 22, pp. 162–184; March, 1961.) The nonlinear space-charge-wave equation is solved by third-order successive approximation. Phase delay and frequency multiplication effects agree well with experimental observations.

621.385.623.5 3201
Effect of Magnetic Fields upon Reflex-Klystron Characteristics—M. E. Brodwin and J. W. Davis. (*Rev. Sci. Instr.*, vol. 32, pp. 223–224; February, 1961.) Experimental results show that magnetic control of frequency is as effective as repeller control, and that the controlling elements are independent of the klystron power supply. This system should be advantageous for the stabilization of high-voltage mm-wave klystrons.

621.385.63 3202
Power Carried by the Cyclotron Waves and the Synchronous Waves on a Filamentary Electron Beam—S. Saito. PROC. IRE, vol. 49, pt. 1, pp. 969–970; May, 1961.)

621.385.63:621.373.423 3203
An Electrically Tunable Microwave Oscillator with High Efficiency and a Constant Output Level Independent of Frequency—W. Eichin and H. Heynisch. (*Nachrtech. Z.*, vol. 13, pp. 457–461; October, 1960.) The oscillator described consists of a combination of a backward-wave oscillator with a traveling-wave amplifier system in the same envelope and coupled by a common electron beam. The efficiency obtainable is that of a traveling-wave tube. Experimental results are given which were obtained with modified traveling-wave tubes containing a section of interdigital line or an eccentrically arranged helix, operating in the 4–6-Gc region.

621.385.63:621.375.9:621.372.44 3204
Excitation and Amplification of Cyclotron Waves and Thermal Orbits in the Presence of the Space Charge—R. Adler, A. Ashkin, and E. I. Gordon. (*J. Appl. Phys.*, vol. 32, pp. 672–675; April 1961.) The effect of space-charge on the motion of an electron beam and its individual electrons in the transverse fields of cyclotron-wave amplifiers is considered. The effect is such that low-field quadrupolar amplifiers do not saturate at low gains.

621.385.63:621.375.9:621.372.44 3205
Travelling-Wave Analysis of a Class of Parametric Amplifiers Based upon the Hill Equation—R. W. Fredricks. (*J. Appl. Phys.*, vol. 32, pp. 901–904, May, 1961.) Formulas are deduced for the complex wave number of beams, and conditions for growing-wave solutions are presented. The case of a sinusoidal pump field variation is treated, the optimum condition obtains when the pump frequency is twice the beam natural frequency.

621.385.632:621.391.822 3206
Noise Smoothing by Reactive Damping in Finite Multi-velocity Electron Beams—J. Berghammer. (*RCA Rev.*, vol. 22, pp. 185–194; March, 1961.) In an electron beam with rectangular velocity distribution a pair of reactively damped waves exist in addition to the Hahn-Ramo waves. Noise smoothing can result in long low-velocity beams of high density.

621.385.632.12 3207
Propagation of E.M. Waves along a Helix—R. Dingeldey and A. Cunliffe. (*Electronic Tech.*, vol. 38, pp. 262–266; July, 1961.) The introduction of an inner conductor along the axis of a helix to provide electrostatic focusing in a traveling-wave tube is considered. The inner conductor allows both slow and fast waves to be propagated corresponding respectively to the waves propagated along the helix and the conductor. Each is modified by the presence of the other. Experimental data are discussed.

621.385.69:621.372.2 3208
Distributed Amplifier Tube—T. Kojima. (*Rev. Elect. Commun. Lab., Japan*, vol. 8, pp. 343–368; July/August, 1960.) The anode and grid are helical lines with a common velocity of propagation for EM waves. Theory of amplification and measured characteristics are given for two experimental tubes, one of which has an operating range 0–150 Mc. See 1081 of 1960.

621.385.832 3209
Dynamic Deflection Sensitivity of Inclined Deflection Plates—E. Gundert. (*Telefunken—Röhre*, no. 37, pp. 5–16; October, 1960.) The deflection angle of an electron beam at the end of inclined deflection plates is calculated for frequencies at which electron transit time is no longer negligible with respect to the period of the deflection voltage. The plate length for the largest deflection angle is also calculated.

621.385.832:681.142 3210
Design of a High-Resolution Electrostatic Cathode-Ray Tube for the Flying-Spot Store—H. G. Cooper. (*Bell Sys. Tech. J.*, vol. 40, pp. 723–759; May, 1961.) The design is discussed in relation to optimum gun performance and minimum deflection focusing. A substantial reduction is effected in beam aberrations due to fringing of the deflection fields.

621.387:621.362 3211
Calculation of the Maximum Efficiency of the Thermionic Converter J. H. Ingold. (*J. Appl. Phys.*, vol. 32, pp. 769–772; May, 1961.)

621.362:621.387 3212
Oscillations and Saturation-Current Measurements in Thermionic Conversion Cells—Zollweg and Gottlieb. (See 3122.)